



UNIVERSITEIT VAN PRETORIA
UNIVERSITY OF PRETORIA
YUNIBESITHI YA PRETORIA

FACULTY OF ECONOMIC & MANAGEMENT SCIENCES

DEPARTMENT OF STATISTICS

MODELING OF GENERALIZED FAMILIES OF PROBABILITY DISTRIBUTIONS IN THE QUANTILE STATISTICAL UNIVERSE

paul j. van staden

**Submitted in fulfillment of the requirements for the
PhD in Mathematical Statistics**

Study Leaders: Dr Hermi Boraine & Dr Robert A.R. King

2013

Con todo mi amor, dedicado a Mercedes.

ABSTRACT

This thesis develops a methodology for the construction of generalized families of probability distributions in the quantile statistical universe, that is, distributions specified in terms of their quantile functions. The main benefit of the proposed methodology is that it generates quantile-based distributions with skewness-invariant measures of kurtosis. The skewness and kurtosis can therefore be identified and analyzed separately.

The key contribution of this thesis is the development of a new type of the generalized lambda distribution (GLD), using the quantile function of the generalized Pareto distribution as the basic building block (in the literature each different type of the GLD is incorrectly referred to as a parameterization of the GLD – in this thesis the term type is used). The parameters of this new type can, contrary to existing types, easily be estimated with method of L -moments estimation, since closed-form expressions are available for the estimators as well as for their asymptotic standard errors. The parameter space and the shape properties of the new type are discussed in detail, including its characterization through L -moments. A simple estimation algorithm is presented and utilization of the new type in terms of data fitting and approximation of probability distributions is illustrated.

KEYWORDS

Generalized lambda distribution; L -moment; Quantile function; Skewness-invariant measure of kurtosis

DECLARATION

I declare that this thesis, which I hereby submit for the degree PhD in Mathematical Statistics at the University of Pretoria, contains no material previously published or written by another person, except where due reference has been made in the text, and has not previously been submitted for obtaining any qualification at another tertiary institution.

Signed: *R. Staden*

Dated: 5 December 2013

TABLE OF CONTENTS

ABSTRACT	ii
KEYWORDS	ii
DECLARATION	iii
LIST OF FIGURES	viii
LIST OF TABLES	xi
ACKNOWLEDGEMENTS	xii
1. INTRODUCTION	1
1.1 AIMS AND OBJECTIVES	1
1.2 FAMILIES OF DISTRIBUTIONS	1
1.3 TUKEY’S LAMBDA FAMILY OF DISTRIBUTIONS	2
1.4 INITIAL DEVELOPMENT OF THE NEW TYPE OF THE GLD	3
1.5 OUTLINE OF THESIS	4
1.6 CONTRIBUTIONS OF THESIS	5
2. QUANTILE MODELING	7
2.1 INTRODUCTION	7
2.2 CLASSICAL AND QUANTILE STATISTICAL UNIVERSES	9
2.2.1 CLASSICAL STATISTICAL UNIVERSE	9
2.2.2 QUANTILE STATISTICAL UNIVERSE	9
2.2.3 PROBABILITY-BASED AND QUANTILE-BASED FUNCTIONS OF DISTRIBUTIONS	11
2.2.4 Q-TRANSFORMATIONS	14
2.2.5 LOCATION-SCALE AND STANDARD FORMS OF DISTRIBUTIONS	15
2.3 CONSTRUCTION RULES FOR DISTRIBUTIONAL MODEL BUILDING	16
2.3.1 UNIFORM TRANSFORMATION RULE	16
2.3.2 REFLECTION RULE	18
2.3.3 ADDITION RULE	18
2.3.4 INTERMEDIATE RULE	21
2.4 MOMENTS	24
2.5 L-MOMENTS	26

2.6	QUANTILE-BASED MEASURES OF LOCATION, SPREAD AND SHAPE	33
2.7	SKEWNESS-INVARIANT KURTOSIS MEASURES	40
2.8	PROPOSITION: QUANTILE-BASED DISTRIBUTIONS WITH SKEWNESS-INVARIANT KURTOSIS MEASURES	43
2.9	METHOD OF <i>L</i> -MOMENTS ESTIMATION	46
2.10	<i>Q-Q</i> PLOTS AND GOODNESS-OF-FIT.....	50
2.11	TAIL BEHAVIOR	52
2.12	CONCLUSION	53
2.13	DERIVATIONS	54
2.13.1	MOMENTS OF SLD	54
2.13.2	COVARIANCE MATRIX FOR METHOD OF <i>L</i> -MOMENTS ESTIMATORS OF SLD	59
2.14	APPENDIX	64
2.14.1	SPECIAL MATHEMATICAL FUNCTIONS AND RATIOS	65
2.14.2	SHIFTED LEGENDRE POLYNOMIALS.....	66
2.14.3	DISTRIBUTIONS.....	67
3.	THE GENERALIZED LAMBDA DISTRIBUTION (GLD).....	86
3.1	INTRODUCTION.....	86
3.2	TUKEY'S LAMBDA DISTRIBUTION.....	87
3.3	RAMBERG-SCHMEISER TYPE (GLD _{RS}).....	89
3.4	FREIMER-MUDHOLKAR-KOLLIA-LIN TYPE (GLD _{FMKL})	89
3.5	PARAMETER SPACE, SUPPORT AND SPECIAL CASES.....	90
3.6	MOMENTS	95
3.7	<i>L</i> -MOMENTS.....	98
3.8	QUANTILE-BASED MEASURES OF LOCATION, SPREAD AND SHAPE	102
3.9	LOCATION AND SPREAD	105
3.10	DISTRIBUTIONAL SHAPE.....	105
3.10.1	TAIL BEHAVIOR.....	106
3.10.2	SKEWNESS AND KURTOSIS	106
3.10.3	SHAPE OF THE DENSITY CURVE	109
3.11	REGIONS OF THE GLD _{RS}	112
3.11.1	REGIONS 1 AND 2	113
3.11.2	REGION 3	113
3.11.3	REGION 4	117
3.11.4	REGIONS 5 AND 6	118

3.12	CLASSES OF THE GLD_{FMKL}	119
3.12.1	CLASS I	119
3.12.2	CLASSES II AND II'	121
3.12.3	CLASS III	123
3.12.4	CLASSES IV AND IV'	123
3.12.5	CLASS V	124
3.13	PARAMETER ESTIMATION	124
3.14	MONTE CARLO SIMULATION	125
3.14.1	DISTRIBUTIONAL SHAPE	126
3.14.2	MEASURES OF SHAPE	126
3.14.3	APPROXIMATION OF DISTRIBUTIONS	127
3.14.4	ISOTONES	127
3.15	APPLICATIONS	127
3.15.1	ACTUARIAL SCIENCE	128
3.15.2	BIOCHEMISTRY	128
3.15.3	BUSINESS, ECONOMICS AND FINANCE	128
3.15.4	COMPUTER SCIENCE	129
3.15.5	EPIDEMIOLOGY	129
3.15.6	FORESTRY	129
3.15.7	INVENTORY MODELING	130
3.15.8	QUEUING THEORY	130
3.15.9	SIGNAL PROCESSING	130
3.15.10	STATISTICAL PROCESS CONTROL	131
3.15.11	SUPPLY CHAIN PLANNING	131
3.16	CONCLUSION	131
3.17	DERIVATIONS	131
3.17.1	MOMENTS OF GLD_{FMKL}	132
3.17.2	<i>L</i> -MOMENTS OF GLD_{FMKL}	136
4.	A GLD TYPE WITH SKEWNESS-INVARIANT MEASURES OF KURTOSIS	138
4.1	INTRODUCTION	138
4.2	GENESIS AND SPECIAL CASES	140
4.3	PARAMETER SPACE AND SUPPORT	143
4.4	CLASSES OF THE GLD_{GPD}	143
4.4.1	CLASS I	144

4.4.2	CLASS II	144
4.4.3	CLASS III.....	145
4.4.4	CLASS IV.....	146
4.5	MOMENTS	147
4.6	<i>L</i> -MOMENTS.....	149
4.7	QUANTILE-BASED MEASURES OF LOCATION, SPREAD AND SHAPE	155
4.8	DISTRIBUTIONAL SHAPE.....	156
4.8.1	SKEWNESS.....	156
4.8.2	KURTOSIS.....	157
4.8.3	TAIL BEHAVIOR	159
4.9	METHOD OF <i>L</i> -MOMENTS ESTIMATION	161
4.10	FITTING OF THE GLD_{GPD} TO DATA.....	166
4.10.1	TOXIC GAS PEAK CONCENTRATIONS	168
4.10.2	VENICE MAXIMUM SEA-LEVELS	169
4.10.3	MCALPHA CLAN AGES AT DEATH	171
4.10.4	CORONARY HEART DISEASE (CHD) PATIENTS' AGES	173
4.11	GLD_{GPD} APPROXIMATION OF DISTRIBUTIONS.....	174
4.11.1	SYMMETRIC DISTRIBUTIONS.....	178
4.11.2	EXTREME VALUE DISTRIBUTIONS.....	179
4.11.3	GAMMA AND LOG-NORMAL DISTRIBUTIONS	180
4.11.4	GENERALIZED EXPONENTIAL AND LOGISTIC DISTRIBUTIONS.....	181
4.12	CONCLUSION	182
4.13	DERIVATIONS	182
4.13.1	MOMENTS OF GLD_{GPD}	183
4.13.2	MINIMUM VALUE OF <i>L</i> -KURTOSIS RATIO FOR GLD_{GPD}	186
4.13.3	COVARIANCE MATRIX FOR METHOD OF <i>L</i> -MOMENTS ESTIMATORS OF GLD_{GPD} ...	187
5.	CONCLUSION.....	197
5.1	CONSTRUCTION OF QUANTILE-BASED FAMILIES OF DISTRIBUTIONS	197
5.2	CONSTRUCTION OF THE GPD TYPE OF THE GLD	197
5.3	THEORETICAL DEVELOPMENT AND PRACTICAL UTILIZATION.....	198
5.4	FUTURE RESEARCH.....	199
	REFERENCES	201

LIST OF FIGURES

Figure 2.1:	The relations between the functions in the classical statistical universe and the quantile statistical universe.....	10
Figure 2.2:	Cumulative distribution and probability density functions of the uniform, exponential and logistic distributions	12
Figure 2.3:	Quantile, quantile density and density quantile functions of the uniform, exponential and logistic distributions	13
Figure 2.4:	Quantile functions of the standard uniform distribution and of the standard exponential distribution, obtained with the uniform transformation rule.....	17
Figure 2.5:	Quantile functions of the standard exponential distribution and of the standard reflected exponential distribution, obtained with the reflection rule.....	18
Figure 2.6:	Quantile and quantile density functions of the standard exponential distribution and standard reflected exponential distribution, and of the standard logistic distribution obtained with the addition rule	20
Figure 2.7:	Quantile, quantile density, density quantile and probability density functions of the standard SLD for various values of δ	23
Figure 2.8:	L -moment ratio diagrams for the two- and three-parameter distributions in Table 2.13 in Appendix 2.14	28
Figure 2.9:	L -moment ratio diagram for generalized distributions in Table 2.13 in Appendix 2.14, considered by Hosking (1986) and Hosking & Wallis (1997).....	29
Figure 2.10:	L -moment ratio diagrams for the Burr Type III and Burr Type XII distributions.....	29
Figure 2.11:	L -moment ratio diagram for the Davies distribution.....	30
Figure 2.12:	L -moment ratio diagram for the kappa distribution.....	31
Figure 2.13:	L -moment ratio diagram for Kumaraswamy's distribution.....	32
Figure 2.14:	L -moment ratio diagram for the Schmeiser-Deutsch distribution	32
Figure 2.15:	Spread-spread plot for the logistic distribution with spread function $S_G(u)$ against the uniform distribution with spread function $S_F(u)$	37
Figure 2.16:	Histogram of the peak concentrations (in percent) of toxic gas together with the probability density functions of the fitted SLD and Davies distribution	49
Figure 2.17:	Q - Q plots for the SLD and the Davies distribution fitted to the peak concentrations (in percent) of toxic gas	52
Figure 3.1:	Probability density functions of Tukey's lambda distribution for various values of λ	88
Figure 3.2:	The parameter space of the GLD_{RS} in terms of Regions 1, 2, 3, 4, 5 and 6	90
Figure 3.3:	The sub-regions (a), (c), (d), (e), (f), (g) and (h) into which Region 3 of the GLD_{RS} is divided.....	92
Figure 3.4:	The parameter space of the GLD_{FMKL} in terms of Regions 1, 2, 3 and 4	93
Figure 3.5:	The parameter space of the GLD_{FMKL} in terms of Classes I, II, III, IV, IV' and V.....	94
Figure 3.6:	L -moment ratio diagrams for Regions 3, 4, 5 and 6 of the GLD_{RS}	99
Figure 3.7:	L -moment ratio diagrams for Regions 1, 2, 3 and 4 of the GLD_{FMKL}	100
Figure 3.8:	L -moment ratio diagrams for Region 3(a) and Region 4 of the GLD_{RS} and for Class I of the GLD_{FMKL}	101
Figure 3.9:	Probability density functions of members of the GLD_{RS} with varying location and spread.....	105
Figure 3.10:	Probability density functions of members of the GLD_{RS} from Regions 3 and 4 illustrating tail behavior	107
Figure 3.11:	Probability density functions of three members of the GLD_{RS} , all with $\alpha_3 = 0$ and $\alpha_4 = 3.4$	108
Figure 3.12:	Probability density functions of three members of the GLD_{RS} , all with $\tau_3 = 0$ and $\tau_4 = \frac{1}{21}$	108
Figure 3.13:	Probability density functions of two members of the GLD_{RS} illustrating the reflection in the shape of the density curve when the values of λ_3 and λ_4 are interchanged.....	109

Figure 3.14:	Probability density functions of three members of the GLD_{RS} with zero, one and two relative extreme turning points.....	110
Figure 3.15:	The number of relative extreme turning points of the probability density function of the GLD_{RS} in terms of the values of λ_3 and λ_4	110
Figure 3.16:	The number of relative extreme turning points of the probability density function of the GLD_{FMKL} in terms of the values of λ_3 and λ_4	112
Figure 3.17:	Probability density functions of members of the GLD_{RS} from Region 1	113
Figure 3.18:	Probability density functions of members of the GLD_{RS} from Region 3(a).....	114
Figure 3.19:	Probability density functions of members of the GLD_{RS} from Region 3(c).....	115
Figure 3.20:	Probability density functions of members of the GLD_{RS} from Region 3(e).....	116
Figure 3.21:	Probability density functions of members of the GLD_{RS} from Region 3(g).....	117
Figure 3.22:	Probability density functions of members of the GLD_{RS} from Region 3(h).....	117
Figure 3.23:	Probability density functions of members of the GLD_{RS} from Region 4	118
Figure 3.24:	Probability density functions of members of the GLD_{RS} from Region 5	119
Figure 3.25:	Probability density functions of members of the GLD_{FMKL} from Region 2 in Class I.....	120
Figure 3.26:	Probability density functions of members of the GLD_{FMKL} from Region 3 in Class I.....	120
Figure 3.27:	Probability density functions of members of the GLD_{FMKL} from Region 4 in Class I.....	121
Figure 3.28:	Probability density functions of members of the GLD_{FMKL} from Region 2 in Class II.....	121
Figure 3.29:	Probability density functions of members of the GLD_{FMKL} from Region 3 in Class II	122
Figure 3.30:	Probability density functions of members of the GLD_{FMKL} from Class III	123
Figure 3.31:	Probability density functions of members of the GLD_{FMKL} from Class IV.....	124
Figure 3.32:	Probability density functions of members of the GLD_{FMKL} from Class V.....	124
Figure 4.1:	Probability density functions of the standard GPD and the standard reflected GPD for various values of λ	141
Figure 4.2:	Probability density functions of members of the GLD_{GPD} from Class I.....	144
Figure 4.3:	Probability density functions of members of the GLD_{GPD} from Class II.....	145
Figure 4.4:	Probability density functions of members of the GLD_{GPD} from Class III.....	146
Figure 4.5:	Probability density functions of members of the GLD_{GPD} from Class IV.....	147
Figure 4.6:	L -moment ratio diagrams for Classes I, II, III and IV of the GLD_{GPD}	151
Figure 4.7:	Plot of τ_4 for the GLD_{GPD} as a function of λ	152
Figure 4.8:	L -moment ratio diagrams for Regions A and B of the GLD_{GPD}	153
Figure 4.9:	Probability density functions of members of the GLD_{GPD} from Regions A and B possessing the same set of values for τ_3 and τ_4	154
Figure 4.10:	Plots of the kurtosis functionals for the GLD_{GPD} as functions of λ	157
Figure 4.11:	Spread-spread plots for members of the GLD_{GPD}	158
Figure 4.12:	The values of λ^* in Class III of the GLD_{GPD} at which the minimum kurtosis of the kurtosis functionals is obtained for $\frac{1}{2} < v < u < 1$	159
Figure 4.13:	Histogram of the peak concentrations (in percent) of toxic gas together with the probability density functions of the fitted GLD_{GPD}	168
Figure 4.14:	Q - Q plots for the GLD_{GPD} fitted to the peak concentrations (in percent) of toxic gas	168
Figure 4.15:	Histograms of the annual maximum sea-levels (in centimeters) in Venice together with the probability density functions of the fitted GLD_{GPD} and generalized extreme value (GEV) distribution.....	170
Figure 4.16:	Q - Q plots for the GLD_{GPD} and the generalized extreme value (GEV) distribution fitted to the annual maximum sea-levels (in centimeters) in Venice	170
Figure 4.17:	Histogram of the age at death (in completed years) of male members of the McAlpha clan together with the probability density functions of the fitted GLD_{GPD} and reflected exponential distribution.....	171
Figure 4.18:	Q - Q plots for the GLD_{GPD} and the reflected exponential distribution fitted to the age at death (in completed years) of male members of the McAlpha clan, excluding under-age-five mortality	172

Figure 4.19: Histogram of the age (in completed years) of patients in a coronary heart disease (CHD) study together with the probability density functions of the fitted GLD_{GPD} , logistic distribution and generalized secant hyperbolic (GSH) distribution173

Figure 4.20: *Q-Q* plots for the GLD_{GPD} , the logistic distribution and the generalized secant hyperbolic (GSH) distribution fitted to the age (in completed years) of patients in a coronary heart disease (CHD) study.....174

Figure 4.21: Probability density functions of various symmetric distributions, indicated by the solid lines, along with the probability density functions of their GLD_{GPD} approximations, indicated by the dashed lines.....178

Figure 4.22: Probability density functions of various extreme value distributions, indicated by the solid lines, along with the probability density functions of their GLD_{GPD} approximations, indicated by the dashed lines180

Figure 4.23: Probability density functions of the gamma and log-normal distributions, indicated by the solid lines, along with the probability density functions of their GLD_{GPD} approximations, indicated by the dashed lines181

Figure 4.24: Probability density functions of the generalized exponential and logistic distributions, indicated by the solid lines, along with the probability density functions of their GLD_{GPD} approximations, indicated by the dashed lines.....181

LIST OF TABLES

Table 2.1:	Functions defining the uniform, exponential and logistic distributions.....	12
Table 2.2:	Moments for the uniform, exponential and logistic distributions	24
Table 2.3:	<i>L</i> -moments for the uniform, exponential and logistic distributions	27
Table 2.4:	Quantile-based measures of location, spread and shape for the uniform, exponential and logistic distributions.....	39
Table 2.5:	Sample size, sample <i>L</i> -moment values and data range for the peak concentrations (in percent) of toxic gas	50
Table 2.6:	Parameter estimates with asymptotic standard errors for the SLD fitted to the peak concentrations (in percent) of toxic gas	50
Table 2.7:	Goodness-of-fit statistics with <i>p</i> -values for the SLD fitted to the peak concentrations (in percent) of toxic gas	52
Table 2.8:	The values approached by the density curve and the slope of the density curve of the SLD at the end-points of the tails	53
Table 2.9:	Special mathematical constants, functions and ratios.....	65
Table 2.10:	References for and parameters and support of various probability distributions	68
Table 2.11:	Functions defining various probability distributions in terms of <i>x</i>	71
Table 2.12:	Functions defining various probability distributions in terms of <i>p</i>	76
Table 2.13:	<i>L</i> -location and <i>L</i> -scale for various probability distributions	80
Table 2.14:	<i>L</i> -skewness and <i>L</i> -kurtosis ratios for various probability distributions	83
Table 3.1:	Parameter space and support of the GLD _{RS} in terms of Regions 1, 2, 3, 4, 5 and 6.....	91
Table 3.2:	Sub-regions in Region 3 of the GLD _{RS}	92
Table 3.3:	Parameter space and support of the GLD _{FMKL} in terms of Regions 1, 2, 3 and 4	92
Table 3.4:	Parameter space of the GLD _{FMKL} in terms of Classes I, II, II', III, IV, IV' and V.....	93
Table 3.5:	Number of relative extreme turning points of the probability density function of the GLD _{RS} as depicted in Figure 3.15	111
Table 3.6:	Number of relative extreme turning points of the probability density function of the GLD _{FMKL} as depicted in Figure 3.16	112
Table 4.1:	Shape parameter values for distributions contained by the GLD _{GPD}	142
Table 4.2:	Parameter space and support of the GLD _{GPD} in terms of Classes I, II, III and IV.....	143
Table 4.3:	<i>L</i> -kurtosis ratio values for the GLD _{GPD} in terms of Regions <i>A</i> and <i>B</i> and Classes I, II, III and IV.....	152
Table 4.4:	The values approached by the density curve and the slope of the density curve of the GLD _{GPD} at the end-points of the tails	160
Table 4.5:	Sample sizes, sample <i>L</i> -moment values and data ranges for the data sets in Section 4.10.....	166
Table 4.6:	Parameter estimates with asymptotic standard errors and support for the GLD _{GPD} fitted to the data sets in Section 4.10.....	167
Table 4.7:	Goodness-of-fit statistics with <i>p</i> -values as well as average scaled absolute error (ASAE) values for the GLD _{GPD} fitted to the data sets in Section 4.10	167
Table 4.8:	Parameter and <i>L</i> -moment values of various distributions, parameter estimates of these distributions' GLD _{GPD} approximations, and values for validating the quality of the GLD _{GPD} approximations	177

ACKNOWLEDGEMENTS

Alle eer kom toe aan God die Vader, die Seun en die Heilige Gees.

Gracias a mi familia con dos y cuatro patitas, especialmente a Mercedes, por concederme el tiempo y la oportunidad de conocer a otra familia, la distribución generalizada lambda de Tukey.

I thank my two supervisors, Dr Hermi Boraine and Dr Robert King, for all their patience, assistance and advice.

Thanks to Theodor Loots for his work on L -moments in 2008.

I would also like to thank my colleagues in the Department of Statistics at the University of Pretoria, especially the Head of the Department, Prof Andriette Bekker, and her predecessor, Prof Nico Crowther.

I am grateful for financial support received from the Department of Statistics, STATOMET and the Vice-Chancellor's Academic Development Grant at the University of Pretoria.

1. INTRODUCTION

1.1 AIMS AND OBJECTIVES

The main aim of this thesis is the development of a methodology for the construction of quantile-based families of distributions possessing skewness-invariant kurtosis measures. With this methodology, specified and proved in Proposition 2.8.1 in Chapter 2, the quantile function of a generalized quantile-based distribution is obtained by taking the weighted sum of the quantile function of an asymmetric distribution on bounded or half-infinite support and the quantile function of the reflection of this asymmetric distribution.

The methodology is utilized to build a new type of the generalized lambda distribution, defined in Definition 4.2.1 in Chapter 4. The parameters of this new type can, contrary to existing types, easily be estimated with method of L -moments estimation, since closed-form expressions are available for the estimators as well as for their asymptotic standard errors.

1.2 FAMILIES OF DISTRIBUTIONS

As part of the development of continuous univariate distributions, the construction of generalized families of probability distributions has featured prominently in the literature. These distributional families include, amongst others, the Pearson family (Pearson, 1895), the Burr family (Burr, 1942, 1968, 1973; Burr & Cislak, 1968) and the family of S distributions (Voit, 1992), where each of these families is defined through a differential equation. Examples of transformation-based families of distributions are the Johnson families, which include transformations to the normal distribution (Johnson, 1949), Laplace distribution (Johnson, 1954) and logistic distribution (Tadikamalla & Johnson, 1982), the kappa family of distributions (Mielke, 1973; Hosking, 1994), which include transformations from the exponential, Gumbel and logistic distributions, and Tukey's lambda family of distributions (Hastings *et al.*, 1947; Tukey, 1960, 1962; Ramberg & Schmeiser, 1972, 1974; Freimer *et al.*, 1988) obtained through transformation of the uniform distribution.

A central motivation for using these various families of distributions is their ability to explain and control extensive levels of skewness and kurtosis and, by doing so, providing approximations to a wide variety of observed distributions and data sets. The flexibility in distributional shape allowed by these families is accomplished through the inclusion of at least two shape parameters. Usually two shape parameters are sufficient, since the gain in flexibility afforded by additional shape parameters seldom warrants the increase in complexity of computation and mathematical manipulation. Hence, including also location and scale parameters for describing location and spread, each family typically possesses four parameters.

1.3 TUKEY'S LAMBDA FAMILY OF DISTRIBUTIONS

Among the distributional families listed above, Tukey's lambda family of distributions is unique in two ways. Firstly, this family is defined exclusively through its quantile function, also known as the inverse cumulative distribution function, and is therefore a quantile-based distribution. No closed-form expressions exist for either its probability density function or cumulative distribution function. Consequently exploration and utilization of this family are in some ways more challenging. However, there are also distinctive opportunities available by modeling the family through its quantile function.

Secondly, all the members from any selected type from the lambda family possess a single functional form given by that type's quantile function. In contrast, different members of the other listed families in Section 1.2 have different functional forms. A single functional form is beneficial in that one does not need to move from one function to another when exploring different distributional shapes.

Collectively the various generalizations of the lambda family are referred to as the generalized lambda distribution (GLD), where each generalization is a distinct type. Unfortunately in the literature each different type of the GLD is incorrectly referred to as a "parameterization" of the GLD. When a distribution has different parameterizations, the parameters of the one parameterization can be transformed to the parameters of the other parameterization and vice versa. For example, the uniform distribution can be parameterized by its minimum and maximum parameters, a and b , or by its location and scale parameters, $\alpha = a$ and $\beta = b - a$. With the GLD there exist no simple transformations between different "parameterizations". Therefore in this thesis the term "type" is used instead of the term "parameterization".

The two types of the GLD by Ramberg & Schmeiser (1972, 1974) and by Freimer *et al.* (1988), labeled the Ramberg-Schmeiser (RS) and the Freimer-Mudholkar-Kollia-Lin (FMKL) Types respectively, have become the types of choice in theoretical development as well as practical application. A drawback of both these types is that parameter estimation is computationally difficult. Various estimation methodologies have been proposed in the literature, but none of these methodologies yield closed-form expressions for the parameters' estimators. This is firstly due to the absence of closed-form expressions for the GLD's probability density and cumulative distribution functions, and secondly because of the complex relation between the shape parameters and the shape characteristics of the GLD (which is not unique to this family). In particular, with the RS and FMKL Types of the GLD, the two shape parameters jointly explain the skewness and kurtosis. Numerical optimization techniques are therefore required for all of the proposed estimation methods.

A key contribution of this thesis is the construction of an alternative type of the GLD for which closed-form expressions for method of L -moments estimators are available. The problem of parameter estimation is therefore approached from a different angle by, instead of developing another new estimation method, developing a type for which method of L -moments estimation yields closed-form expressions for the estimators. This new type of the GLD utilizes a linkage existing between Tukey's lambda distribution and the generalized Pareto distribution (GPD). The history of the development of this type of the GLD, labeled the GPD Type in the rest of the thesis, is briefly outlined below.

1.4 INITIAL DEVELOPMENT OF THE NEW TYPE OF THE GLD

In 2008, M.T. (Theodor) Loots completed his Honors Essay under my supervision, focusing on the theory and application of L -moments (Loots, 2008). To illustrate the interpretation of L -skewness, Loots utilized the skew logistic distribution (SLD) of Gilchrist (2000), while he used Tukey's lambda distribution (Hastings *et al.*, 1947; Tukey, 1960, 1962) to demonstrate the interpretation of L -kurtosis. The SLD has a single shape parameter controlling the L -skewness ratio and has a constant value for its L -kurtosis ratio. Tukey's lambda distribution is symmetric and its shape parameter controls the L -kurtosis ratio.

Upon noting furthermore that the expressions for the L -kurtosis ratios of Tukey's lambda distribution and the GPD are exactly the same, we realized that a new type of the GLD could be constructed from the GPD. In the resulting GPD Type of the GLD, the shape properties of both the SLD and Tukey's lambda distribution are incorporated. Specifically the L -kurtosis

ratio of the GPD Type is explained by just one of its shape parameters. As a result, the GPD Type has closed-form expressions for method of L -moments estimation. Basic results for the GPD Type of the GLD were given in van Staden & Loots (2009a).

Subsequently, exploring the distributional properties of the GPD Type in more depth, it was found that the quantile-based measures of kurtosis of this type also exhibit skewness-invariance. This led to the development of a general methodology for the construction of families of quantile-based distributions with skewness-invariant kurtosis measures. The GPD Type of the GLD is an example of such a quantile-based distribution.

1.5 OUTLINE OF THESIS

Chapter 2 explores the techniques, functions and measures used in the modeling and description of quantile-based distributions. The focus is on the building of new distributional models through the transformation of quantile functions. The measuring and description of the location, spread and shape of distributions through L -moments, developed by Hosking (1990), as well as quantile-based measures are explained. The concept of skewness-invariant measures of kurtosis is discussed and in the main result of the thesis, Proposition 2.8.1, a methodology is presented for the creation of quantile-based distributions with skewness-invariant kurtosis measures.

Chapter 3 focuses on the GLD, a well established quantile-based distribution. Specifically the functions, measures and properties of the RS and FMKL Types of the GLD are examined. Where necessary, results not appearing in the literature before, such as the characterization of the FMKL Type by L -moments, are presented.

Chapter 4 uses the model construction methodology proposed in Proposition 2.8.1 of Chapter 2 to add to the existing types of the GLD a new type which has considerably simpler expressions for its L -moments. A detailed analysis of this new type of the GLD, specified in terms of its quantile function in Definiton 4.2.1, is presented. In particular, due to the simplicity of their expressions, the new type of the GLD is characterized through its L -moments. The shape characteristics of this type of the GLD is examined, focusing on the skewness-invariance of its L -kurtosis ratio as well as its quantile-based kurtosis measures. The use of method of L -moments estimation is advocated, with an estimation algorithm for computing method of L -moments estimates presented.

Chapter 5 summarises the main findings of the thesis and provides recommendations for further development in the area of quantile modeling.

1.6 CONTRIBUTIONS OF THESIS

As indicated in Section 1.1, the main contributions of this thesis are the development of a methodology for the construction of quantile-based families of distributions possessing skewness-invariant kurtosis measures, and the utilization of this methodology to create a new type of the GLD with closed-form expressions for its parameter estimators and their standard errors. Apart from these main contributions, the other new contributions from each chapter are listed below.

Chapter 2

- A new quantile-based measure of kurtosis, named the κ -functional, is introduced in Section 2.6. The κ -functional is related to the ratio-of-spread functions, proposed by MacGillivray & Balanda (1988), but has the added advantage of being a bounded kurtosis functional, hence simplifying interpretation.
- In Section 2.7 a decomposition for the spread function governing the existence of skewness-invariant kurtosis measures is formulated.
- It is shown in Section 2.7 that the logistic-exponential distribution, introduced by Lan & Leemis (2008), has skewness-invariant kurtosis measures.
- Formulae for the moments of the SLD of Gilchrist (2000) are listed in Section 2.4, with the derivations of these formulae presented in Section 2.13.1.
- In Section 2.6 expressions for the SLD's quantile-based measures of location, spread and shape are presented. As indicated in Section 2.7, the quantile-based kurtosis measures of the SLD are skewness-invariant.
- Expressions for the SLD's L -moments are presented in Section 2.8. In Section 2.9 an estimation algorithm for method of L -moments estimation for the SLD is given. In this algorithm, closed-form expressions for the method of L -moments estimators are specified, as are closed-form expressions for their asymptotic standard errors, derived in Section 2.13.2.

Chapter 3

- The complete set of formulae for the moments of the FMKL Type of the GLD is given in Section 3.6. Formulae for the moments of the limiting cases of the FMKL Type are derived in Section 3.17.1.

- In Section 3.7 the FMKL Type is characterized through its L -moments, whose expressions are derived in Section 3.17.2.

Chapter 4

- Formulae for the moments of the GPD Type of the GLD are given in Section 4.5. These formulae are derived in Section 4.13.1.
- In Section 4.6 the GPD Type of the GLD is characterized through its L -moments.
- Expressions for the quantile-based measures of location, spread and shape for the GPD Type of the GLD are listed in Section 4.7. It is shown that the quantile-based kurtosis measures are skewness-invariant.
- In Sections 4.4 and 4.8 a comprehensive analysis of the distributional properties and shape characteristics of the GPD Type of the GLD is done.
- An estimation algorithm for method of L -moments estimation for the GPD Type of the GLD is given in Section 4.9. Closed-form expressions for the method of L -moments estimators as well as their asymptotic standard errors are presented. The expressions for the asymptotic standard errors are derived in Section 4.13.3.

2. QUANTILE MODELING

2.1 INTRODUCTION

In statistical modeling the various functions utilized for specifying the probability distributions of random variables can be divided into two distinct categories. The first category contains functions based on the classical concepts of densities and probabilities and is hence labeled the classical statistical universe. Functions based on quantiles belong to the second category and provide an alternative yet complementary view to the functions in the classical statistical universe. The second category is called the quantile statistical universe and is the focus of this thesis.

The functions in the classical statistical universe played a central role in the development of the foundations of mathematical statistics in the late 1800s and early 1900s, in which the ideas of Pearson (1894, 1895) featured prominently (thence the use of the term classical to describe their universe). These functions' properties and their use in statistical modeling are well-documented. Standard textbooks on mathematical statistics such as Bain & Engelhardt (1992), the books on probability distributions by Johnson *et al.* (1994, 1995) and Balakrishnan & Nevzorov (2003) and also the monograph of Stuart & Ord (1994) on distribution theory can be consulted for details.

Quantiles were formally introduced by Galton (1881), but their use in statistical modeling only became more prominent in the 1960s and 1970s with Parzen and Tukey the pioneers. In particular, Parzen (1979) presented a seminal discussion on the use of quantile-based functions, measures and methods in statistical modeling, incorporating and extending ideas from Tukey (1962, 1965, 1977). More recently Gilchrist (2000) presented a detailed book-length account on statistical modeling in the quantile statistical universe, which will henceforth simply be referred to as quantile modeling. Lampasi (2008) discussed the quantile-based approach to measurement activities and applications. He was the first to refer to the two categories as universes.

In this chapter procedures applicable to and utilized in the quantile statistical universe are presented. In Section 2.2 the probability-based and quantile-based functions from the respective statistical universes are given. As highlighted by Lampasi (2008), and shown in Figure 2.1, it is possible to move from one statistical universe to the other. Each statistical universe has unique strengths and weaknesses. Specifically functions from the quantile statistical universe can be used to build new distributional models with a set of construction rules discussed in Section 2.3.

While functions in terms of probabilities or quantiles are used to specify probability distributions, the description of the characteristics of probability distributions, such as location, spread, skewness and kurtosis, are done with measures, which include the well-known moments considered in Section 2.4. Alternative measures called L -moments, which are based on order statistics, and measures based on quantiles are discussed in Sections 2.5 and 2.6 respectively. It is shown that, in the quantile statistical universe, these measures are often easier to deal with than moments. A new bounded measure of kurtosis, labeled the κ -functional, is proposed in Section 2.6. The concept of skewness-invariant measures of kurtosis is explained in Section 2.7.

The main result in the thesis is presented in Proposition 2.8.1 in Section 2.8. This proposition outlines a methodology for the construction of generalized families of quantile-based distributions with skewness-invariant measures of kurtosis. Three- and four-parameter distributions constructed with this methodology possess closed-form expressions for estimation methods based upon L -moments from Section 2.5 and, in the case of three-parameter distributions, closed-form expressions for estimation methods predicated on quantile-based measures in Section 2.6.

In this thesis method of L -moments estimation is utilized. Therefore a discussion on this estimation method is given in Section 2.9. Model validation is considered in Section 2.10. In Section 2.11 it is explained how the tail behavior of quantile-based distributions is analyzed. Concluding remarks are given in Section 2.12.

Throughout Chapter 2 a special quantile-based distribution, the skew logistic distribution of Gilchrist (2000), is used to illustrate the various concepts discussed. Many of the results for the skew logistic distribution given and derived in this chapter are new, including the expressions for its moments in Example 2.4.1, its quantile-based measures for location, spread and shape in Example 2.6.1, and its L -moments in Example 2.8.1, as well as the expressions for the skew logistic distribution's method of L -moments estimators and their asymptotic standard errors presented in the estimation algorithm in Example 2.9.1. In

particular the expressions for the moments of the skew logistic distribution are derived in Section 2.13.1, while the covariance matrix for the method of L -moments estimators is derived in Section 2.13.2.

Appendix 2.14 contains information regarding mathematical functions and ratios occurring in some of the expressions and derivations in the thesis. This information is summarized in a table in Section 2.14.1. Because shifted Legendre polynomials appear prominently in the formulae of L -moments, a brief discussion on these polynomials is presented in Section 2.14.2.

In Section 2.14.3 of Appendix 2.14 an extensive set of tables summarizing the properties, functions and expressions of various probability distributions is given. Full discussions of these distributions are beyond the scope of this thesis. The set of tables is included as a reference resource and combines information collected and derived while doing literature research for the thesis.

2.2 CLASSICAL AND QUANTILE STATISTICAL UNIVERSES

As indicated in the introduction in Section 2.1, each of the functions for specifying the probability distribution of a random variable X belongs to one of two complementary statistical universes, the classical statistical universe and the quantile statistical universe.

2.2.1 CLASSICAL STATISTICAL UNIVERSE

The classical statistical universe contains probability-based functions defined in terms of x . As demonstrated in Figure 2.1, these functions include the cumulative distribution function,

$$F(x) = P(X \leq x), \quad -\infty < x < \infty,$$

and, if X has an absolutely continuous distribution, the probability density function,

$$f(x) = \frac{dF(x)}{dx}, \quad -\infty < x < \infty.$$

2.2.2 QUANTILE STATISTICAL UNIVERSE

In the quantile statistical universe the distribution of X is specified with quantile-based functions expressed in terms of p , where $0 < p < 1$. The most prominent of these functions is the quantile function, $Q(p)$, defined for a random variable X with cumulative distribution function $F(x)$ by

$$Q(p) = \inf\{x : F(x) \geq p\}, \quad 0 < p < 1.$$

The fundamental relation between the cumulative distribution function and the quantile function is that, for $-\infty < x < \infty$ and $0 < p < 1$,

$$F(x) \geq p \Leftrightarrow Q(p) \leq x. \quad (2.1)$$

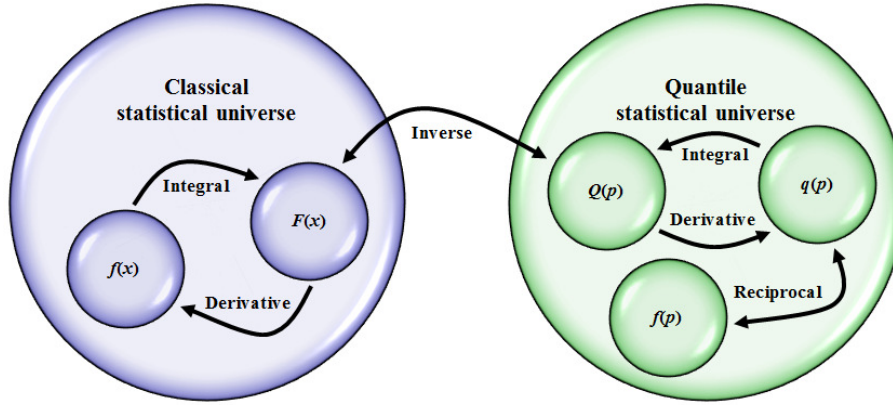


Figure 2.1: The relations between the functions in the classical statistical universe and the quantile statistical universe.

When X has an absolutely continuous distribution, then

$$Q(p) = \inf\{x : F(x) = p\}, \quad 0 < p < 1,$$

and $F(Q(p)) = p$ so that $Q(p) = F^{-1}(p)$. Thus, if X is a real-valued random variable, then the quantile function is the inverse of the cumulative distribution function and $Q(p)$ is therefore often referred to as the inverse cumulative distribution function. As illustrated in Figure 2.1, the classical and quantile statistical universes are connected through this inverse relationship between the cumulative distribution function and the quantile function.

Two other important quantile-based functions are obtained through differentiation of $Q(p)$ and of $F(Q(p)) = p$. The quantile density function is the derivative of the quantile function (see Figure 2.1),

$$q(p) = \frac{dQ(p)}{dp}, \quad 0 < p < 1.$$

Taking derivatives on both sides of $F(Q(p)) = p$ gives

$$\frac{dF(Q(p))}{dp} = f(Q(p))q(p) = f_p(p)q(p) = 1, \quad (2.2)$$

where

$$f_p(p) = f(Q(p)), \quad 0 < p < 1,$$

called the density quantile function, is the density function for the distribution of X expressed in terms of p instead of x . In effect, $f(x)$ is the density function in the classical statistical

universe, while $f_p(p)$ is the corresponding density function in the quantile statistical universe. It follows from (2.2) that

$$f_p(p) = \frac{1}{q(p)},$$

so the density quantile function and the quantile density function are reciprocals of each other (see again Figure 2.1).

Since $F(x)$ is a non-decreasing function with

$$\lim_{x \rightarrow -\infty} F(x) = 0$$

and

$$\lim_{x \rightarrow \infty} F(x) = 1,$$

$Q(p)$ is a non-decreasing function over the interval $0 < p < 1$. Consequently both $q(p)$ and $f_p(p)$ are non-negative over the interval $0 < p < 1$.

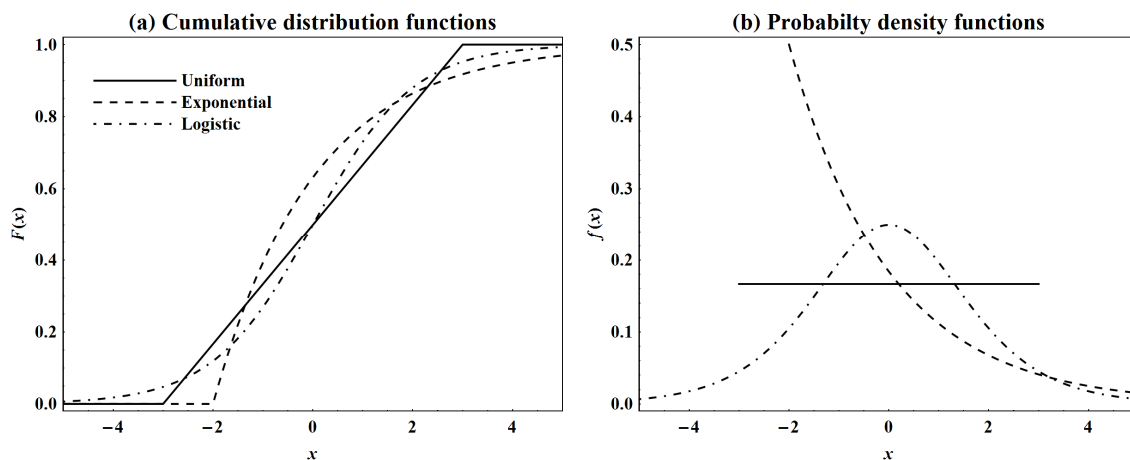
2.2.3 PROBABILITY-BASED AND QUANTILE-BASED FUNCTIONS OF DISTRIBUTIONS

All the probability-based and quantile-based functions in the two statistical universes exist for any absolutely continuous distribution. Table 2.11 and Table 2.12 in Section 2.14.3 of Appendix 2.14 present expressions for various distributions' functions from the classical statistical universe and the quantile statistical universe respectively. Details regarding the parameters and support as well as references for all the distributions covered in Tables 2.11 and 2.12 are listed in Table 2.10 in Section 2.14.3.

Table 2.1 summarizes the expressions for the probability-based and quantile-based functions of the uniform, exponential and logistic distributions, which are examples used to represent distributions with bounded, half-infinite and infinite support. The expressions are presented in location-scale form (to be explained in Section 2.2.5). The simplicity of their quantile-based functions allows these three distributions to play prominent roles in theoretical development in the quantile statistical universe. Hence, where applicable, these distributions are used in the rest of the chapter to illustrate various concepts. Figure 2.2 depicts the probability-based functions of these three distributions graphically, while their quantile-based functions are shown in Figure 2.3. In order to facilitate easy comparison in Figures 2.2 and 2.3, the location and spread of the three distributions have been made equivalent in the various graphs by setting $L_1 = 0$ and $L_2 = 1$ for all three distributions (L_1 and L_2 are respectively the L -location and L -scale to be discussed in Section 2.5).

Table 2.1: Functions defining the uniform, exponential and logistic distributions.

Function	Uniform	Exponential	Logistic
Cumulative distribution function	$F(x) = \frac{x-\alpha}{\beta}$	$F(x) = 1 - \exp\left[-\left(\frac{x-\alpha}{\beta}\right)\right]$	$F(x) = \frac{1}{1 + \exp\left[-\left(\frac{x-\alpha}{\beta}\right)\right]}$
Probability density function	$f(x) = \frac{1}{\beta}$	$f(x) = \frac{1}{\beta} \exp\left[-\left(\frac{x-\alpha}{\beta}\right)\right]$	$f(x) = \frac{1}{\beta} \frac{\exp\left[-\left(\frac{x-\alpha}{\beta}\right)\right]}{\left(1 + \exp\left[-\left(\frac{x-\alpha}{\beta}\right)\right]\right)^2}$
Quantile function	$Q(p) = \alpha + \beta p$	$Q(p) = \alpha - \beta \log[1 - p]$	$Q(p) = \alpha + \beta \log\left[\frac{p}{1-p}\right]$
Quantile density function	$q(p) = \beta$	$q(p) = \frac{\beta}{1-p}$	$q(p) = \frac{\beta}{p(1-p)}$
Density quantile function	$f_p(p) = \frac{1}{\beta}$	$f_p(p) = \frac{1-p}{\beta}$	$f_p(p) = \frac{p(1-p)}{\beta}$


Figure 2.2: Cumulative distribution and probability density functions of the uniform, exponential and logistic distributions, all with $L_1 = 0$ and $L_2 = 1$. The line types indicated in graph (a) also apply to graph (b).

The uniform, exponential and logistic distributions are examples of distributions which possess expressions for both their probability-based and quantile-based functions. This is however not the case with all distributions. In effect, although all the functions in the two statistical universes exist for any absolute continuous distribution, not all distributions possess closed-form expressions for all their functions.

Distributions such as the normal, half-normal, log-normal and gamma distributions are specified through their probability density functions. The expressions for these distributions' cumulative distribution functions contain error, gamma and other special mathematical functions, which are defined in terms of integrals (see Table 2.9 in Section 2.14.1), and hence these expressions cannot be written in closed form. As a result, the expressions for all their quantile-based functions can also not be given in closed form. Although the cumulative distribution and quantile-based functions of these distributions can be evaluated numerically

using almost any statistical software package, it is easier to work with these distributions in the classical statistical universe (through their probability density functions) than in the quantile statistical universe.

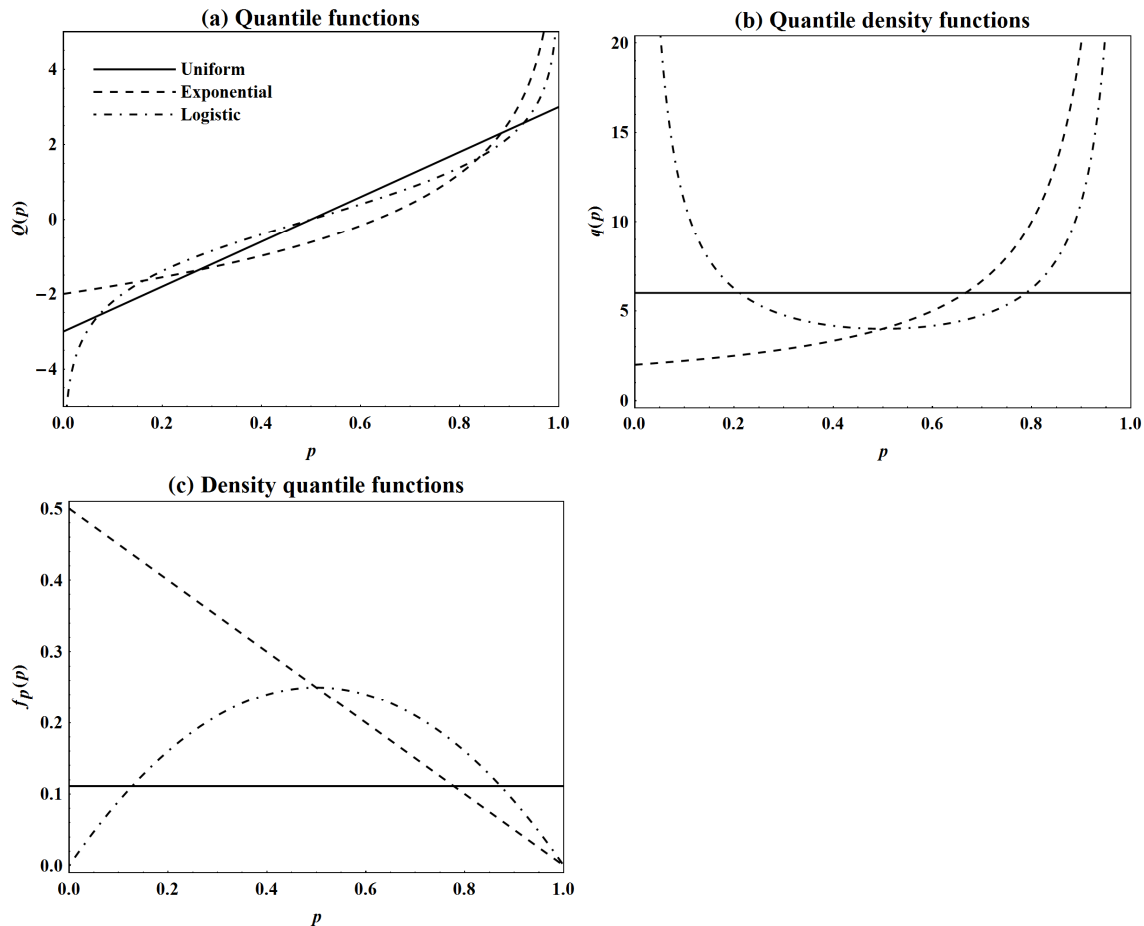


Figure 2.3: Quantile, quantile density and density quantile functions of the uniform, exponential and logistic distributions, all with $L_1 = 0$ and $L_2 = 1$. The line types indicated in graph (a) also apply to graphs (b) and (c).

Tukey's lambda distribution and its generalizations (to be discussed in detail in Chapters 2 and 3) and the Davies distribution are examples of distributions which are specified in terms of their quantile-based functions, particularly in terms of their quantile functions. No closed-form expressions exist for these distributions' functions in terms of x . It is thus not ideal to work with these quantile-based distributions in the classical statistical universe. It is however common practice to display a distribution graphically by plotting its density curve, that is, by plotting $f(x)$ against x . For quantile-based distributions, the plot of the density curve can be obtained by selecting equally spaced values of p , say $p = 0.001, 0.002, \dots, 0.999$,

evaluating $Q(p)$ and $f_p(p)$ for these chosen values of p , and plotting the points $(Q(p), f_p(p))$ to obtain a plot of the corresponding points $(x, f(x))$.

2.2.4 Q-TRANSFORMATIONS

When transformations are applied to random variables, the resulting behavior of their quantile functions plays a key role in quantile modeling. Parzen (1979) considered this important property of quantile modeling, focusing on transformations based on non-decreasing functions. Theorem 2.2.1 below deals with transformations based on non-decreasing as well as non-increasing functions. Note that the proof of Theorem 2.2.1(a) was presented by Parzen (1979). The proof of Theorem 2.2.1(b) is structured in a similar manner.

Theorem 2.2.1

Assume that X and Y are real-valued random variables related through the transformation $Y = T(X)$ and with $F_X(x)$ and $F_Y(y)$ the cumulative distribution functions and $Q_X(p)$ and $Q_Y(p)$ the quantile functions of their respective distributions.

(a) Then, if $Y = T(X)$ is a non-decreasing function of X ,

$$Q_Y(p) = T(Q_X(p)). \quad (2.3)$$

(b) In contrast, if $Y = T(X)$ is a non-increasing function of X , then

$$Q_Y(p) = T(Q_X(1-p)). \quad (2.4)$$

Proof

(a) When $Y = T(X)$ is a non-decreasing function of X ,

$$F_Y(y) = F_X(T^{-1}(y)).$$

Therefore,

$$\begin{aligned} F_Y(y) \geq p &\Leftrightarrow F_X(T^{-1}(y)) \geq p \\ &\Leftrightarrow T^{-1}(y) \geq Q_X(p) \\ &\Leftrightarrow y \geq T(Q_X(p)). \end{aligned}$$

But from (2.1) we have $F_Y(y) \geq p \Leftrightarrow y \geq Q_Y(p)$, hence (2.3) follows.

(b) When $Y = T(X)$ is a non-increasing function of X ,

$$F_Y(y) = 1 - F_X(T^{-1}(y)).$$

Then

$$\begin{aligned}
 F_Y(y) \geq p &\Leftrightarrow F_X(T^{-1}(y)) \geq 1 - p \\
 &\Leftrightarrow T^{-1}(y) \geq Q_X(1 - p) \\
 &\Leftrightarrow y \geq T(Q_X(1 - p)).
 \end{aligned}$$

Using again (2.1), that is, $F_Y(y) \geq p \Leftrightarrow y \geq Q_Y(p)$, (2.4) follows.

■

The transformations in (2.3) and (2.4) were termed Q -transformations by Gilchrist (2000). Examples of (2.3) include the logarithmic transformation, $Q_Y(p) = \log[Q_X(p)]$ if $Y = \log[X]$ for $X > 0$, and the power transformation, $Q_Y(p) = (Q_X(p))^\lambda$ if $Y = X^\lambda$ for $X > 0$ and $\lambda > 0$. The reflecting transformation, $Q_Y(p) = -Q_X(1 - p)$ if $Y = -X$, and reciprocal transformation, $Q_Y(p) = \frac{1}{Q_X(1-p)}$ if $Y = \frac{1}{X}$ for $X \neq 0$, are examples of (2.4). As will be shown in Section 2.3, Q -transformations form part of a simple quantile approach based on a set of construction rules for building new distributional models.

Another important consequence of Q -transformations is the relation between the quantile functions of the location-scale form and the standard form of a distribution. This relation is discussed in Section 2.2.5.

2.2.5 LOCATION-SCALE AND STANDARD FORMS OF DISTRIBUTIONS

The probability-based functions for all the distributions in Table 2.11 are presented in location-scale form,

$$F(x) = F_0\left(\frac{x-\alpha}{\beta}\right)$$

and

$$f(x) = \frac{1}{\beta} f_0\left(\frac{x-\alpha}{\beta}\right),$$

where α and $\beta > 0$ are respectively location and scale (spread) parameters, and $F_0\left(\frac{x-\alpha}{\beta}\right)$ and $f_0\left(\frac{x-\alpha}{\beta}\right)$ denote the cumulative distribution and probability density functions of the standard form of the distribution, in effect, the standard distribution. The corresponding representations of the quantile-based functions for the distributions in Table 2.12 are of the form

$$Q(p) = \alpha + \beta Q_0(p), \tag{2.5}$$

$$q(p) = \beta q_0(p)$$

and

$$f_p(p) = \frac{1}{\beta} f_{p;0}(p),$$

with $Q_0(p)$, $q_0(p)$ and $f_{p;0}(p)$ denoting the quantile, quantile density and density quantile functions of the standard distribution.

The linear transformation in (2.5) is a special Q -transformation controlling the relation between the location-scale form and the standard form in the quantile statistical universe. In quantile modeling it is convenient to ignore the location and the spread of distributions during the distributional model building process by applying the construction rules to the quantile functions of standard distributions. At the end of the distributional model building process, the location and scale parameters (α and β) can simply be included with the linear transformation in (2.5). This linear transformation adjusts the location and spread of the distribution while preserving its distributional shape. Therefore, if a distribution possesses any shape parameters (denoted by λ and δ for the relevant distributions in the tables in Section 2.14.3 of Appendix 2.14), both $Q(p)$ and $Q_0(p)$ will contain these parameters.

In the next section the application of Q -transformations in the distributional model building process is explained.

2.3 CONSTRUCTION RULES FOR DISTRIBUTIONAL MODEL BUILDING

An important advantage of quantile modeling, compared to statistical modeling with probability-based functions, is that new distributional models can be constructed through the addition, multiplication and transformation of quantile-based functions. This distributional model building process is guided by a set of construction rules which were outlined by Gilchrist (2000). The basic underlying condition to all these rules is that the resulting quantile function must be non-decreasing over the interval $0 < p < 1$. The rules required for the construction of specific generalized families of distributions, such as the new type of the generalized lambda distribution proposed in Chapter 4, are highlighted below.

2.3.1 UNIFORM TRANSFORMATION RULE

The standard uniform distribution is a foundation distribution in quantile modeling in that any continuous distribution can be generated from this distribution through the application of Q -transformations to its quantile function. That is, if U is a real-valued random variable having a standard uniform distribution with quantile function

$$Q_{U;0}(p) = p, \quad (2.6)$$

then, for $X = T(U)$ a non-decreasing function of U , the standard distribution of X has quantile function

$$Q_{X;0}(p) = T(Q_{U;0}(p)) = T(p),$$

while the standard distribution of X has quantile function

$$Q_{X;0}(p) = T(Q_{U;0}(1-p)) = T(1-p)$$

if $X = T(U)$ is a non-increasing function of U .

Example 2.3.1

Suppose U has a standard uniform distribution with quantile function given in (2.6). Assume that $X = T(U) = -\log[U]$ so that X is a non-increasing function of U . Then

$$\begin{aligned} Q_{X;0}(p) &= T(Q_{U;0}(1-p)) \\ &= -\log[Q_{U;0}(1-p)] \\ &= -\log[1-p], \end{aligned} \quad (2.7)$$

which is the quantile function of the standard exponential distribution. The quantile functions of the standard uniform and standard exponential distributions are shown in Figure 2.4.

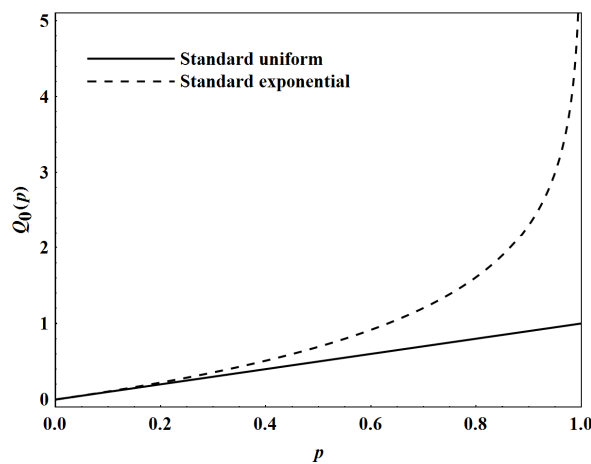


Figure 2.4: Quantile functions of the standard uniform distribution and of the standard exponential distribution, obtained with the uniform transformation rule.

This example illustrates how multiple Q -transformations can be combined to build a distributional model. In this case both the logarithmic transformation and the reflecting transformation are used in the uniform transformation rule to obtain the quantile function of the standard exponential distribution.

□

2.3.2 REFLECTION RULE

The reflecting transformation is typically applied to the quantile function of an asymmetric distribution (the reflection of a symmetric distribution is simply the distribution itself). Assume that X is a real-valued random variable with $Q_{X;0}(p)$ the quantile function of the standard distribution of X . Suppose $Y = T(X) = -X$ so that the standard distribution of Y is the reflection of the standard distribution of X about the line $x = 0$. Then, since Y is a non-increasing function of X , the quantile function of the standard distribution of Y is

$$Q_{Y;0}(p) = T(Q_{X;0}(1-p)) = -Q_{X;0}(1-p).$$

Example 2.3.2

Consider X having a standard exponential distribution with support $[0, \infty)$ and quantile function given in (2.7). Then $Y = -X$ has a standard reflected exponential distribution with support $(-\infty, 0]$ and corresponding quantile function

$$\begin{aligned} Q_{Y;0}(p) &= -Q_{X;0}(1-p) \\ &= \log[p]. \end{aligned} \tag{2.8}$$

Figure 2.5 illustrates the quantile functions of the standard exponential and the standard reflected exponential distributions.

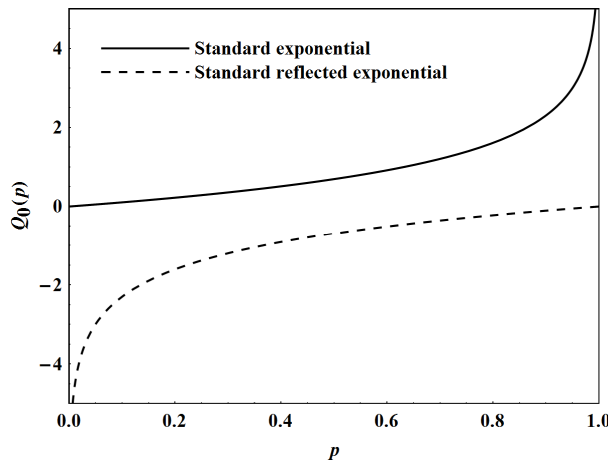


Figure 2.5: Quantile functions of the standard exponential distribution and of the standard reflected exponential distribution, obtained with the reflection rule.

□

2.3.3 ADDITION RULE

Since the sum of two non-decreasing functions is also non-decreasing, the sum of any two quantile functions is also a quantile function. So, if X and Y are two real-valued random

variables with $Q_{X;0}(p)$ and $Q_{Y;0}(p)$ the quantile functions of their standard distributions, then the quantile function of the standard distribution of another random variable, say W , can be obtained through the addition rule with

$$Q_{W;0}(p) = Q_{X;0}(p) + Q_{Y;0}(p).$$

Furthermore, because the derivative of the sum of two functions is equal to the sum of the derivatives of the functions, adding any two quantile density functions produces another quantile density function. Thus, if $q_{X;0}(p)$ and $q_{Y;0}(p)$ are the quantile density functions for the standard distributions of X and Y , then

$$q_{W;0}(p) = q_{X;0}(p) + q_{Y;0}(p)$$

is the quantile density function of the standard distribution of W .

The addition rule can of course be generalized to more than two quantile functions and quantile density functions. If $X_i : i = 1, 2, \dots, n$ are real-valued random variables with n a positive integer, and $Q_{X_i;0}(p)$ and $q_{X_i;0}(p)$ are the quantile and quantile density functions for the standard distribution of the i^{th} variable, then

$$Q_{W;0}(p) = \sum_{i=1}^n Q_{X_i;0}(p) \tag{2.9}$$

and

$$q_{W;0}(p) = \sum_{i=1}^n q_{X_i;0}(p) \tag{2.10}$$

are the quantile and quantile density functions of the standard distribution of the random variable W .

Returning to the bivariate case, $n = 2$, when adding the quantile function of an asymmetric distribution on bounded or half-infinite support to the quantile function of the reflection of this distribution, the distribution of the resulting quantile function will be symmetric. In effect, the distribution with quantile function

$$\begin{aligned} Q_{W;0}(p) &= Q_{X;0}(p) + Q_{Y;0}(p) \\ &= Q_{X;0}(p) - Q_{X;0}(1-p) \\ &= -Q_{W;0}(1-p) \end{aligned} \tag{2.11}$$

is symmetric.

Example 2.3.3

Suppose X has a standard exponential distribution, with quantile function given in (2.7). Then, as shown in Example 2.3.2, $Y = -X$ has a standard reflected exponential distribution with quantile function given in (2.8). Adding the quantile functions of the standard exponential and standard reflected exponential distributions gives

$$\begin{aligned}
 Q_{W;0}(p) &= Q_{X;0}(p) + Q_{Y;0}(p) \\
 &= -\log[1-p] + \log[p] \\
 &= \log\left[\frac{p}{1-p}\right].
 \end{aligned}
 \tag{2.12}$$

The quantile density functions of X and Y are respectively $q_{X;0}(p) = \frac{1}{1-p}$ and $q_{Y;0}(p) = \frac{1}{p}$, and the sum of these two functions is

$$\begin{aligned}
 q_{W;0}(p) &= q_{X;0}(p) + q_{Y;0}(p) \\
 &= \frac{1}{1-p} + \frac{1}{p} \\
 &= \frac{1}{p(1-p)}.
 \end{aligned}$$

$Q_{W;0}(p)$ and $q_{W;0}(p)$ are respectively the quantile function and the quantile density function of the standard logistic distribution, which is a symmetric distribution. The quantile and quantile density functions of the standard exponential, standard reflected exponential and standard logistic distributions are depicted in Figure 2.6.

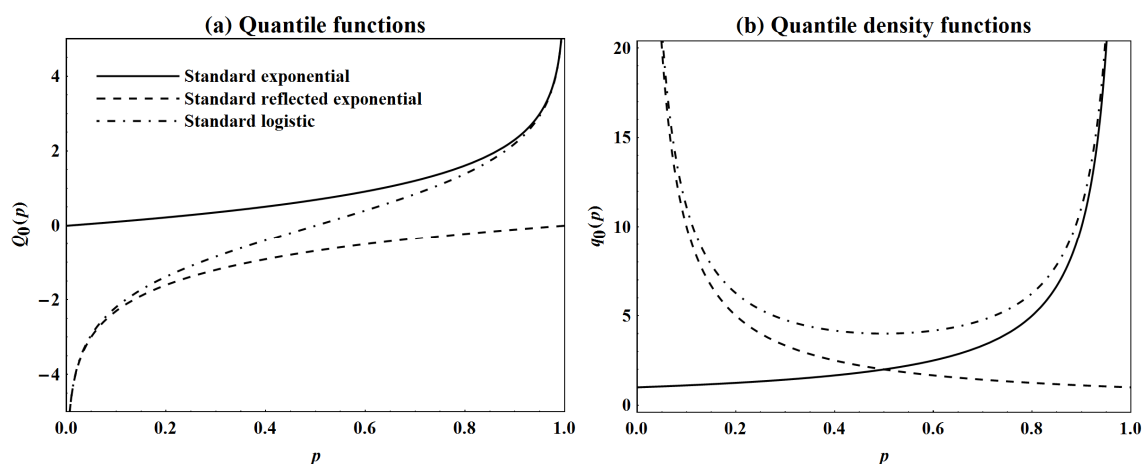


Figure 2.6: Quantile and quantile density functions of the standard exponential distribution and standard reflected exponential distribution, and of the standard logistic distribution obtained with the addition rule. The line types indicated in graph (a) also apply to graph (b).

□

2.3.4 INTERMEDIATE RULE

The addition rule for quantile functions in (2.9) and for quantile density functions in (2.10) can be further generalized by considering linear combinations of quantile functions and of quantile density functions. That is, if $c_i : i = 1, 2, \dots, n$ are non-negative constants with n a positive integer and $X_i : i = 1, 2, \dots, n$ are real-valued random variables with $Q_{X_i;0}(p)$ and $q_{X_i;0}(p)$ the quantile and quantile density functions for the standard distribution of the i^{th} variable, then

$$Q_{W;0}(p) = \sum_{i=1}^n c_i Q_{X_i;0}(p)$$

and

$$q_{W;0}(p) = \sum_{i=1}^n c_i q_{X_i;0}(p)$$

are the quantile and quantile density functions of the standard distribution of the random variable W .

A special situation arises in the bivariate case, $n = 2$, if $c_1 = \delta$ and $c_2 = 1 - \delta$ where $0 \leq \delta \leq 1$ so that $c_1 + c_2 = 1$. That is, suppose X and Y are two real-valued random variables with $Q_{X;0}(p)$ and $Q_{Y;0}(p)$ the quantile functions of their standard distributions. Consider another random variable, W , whose quantile function is defined as the weighted sum of $Q_{X;0}(p)$ and $Q_{Y;0}(p)$,

$$Q_{W;0}(p) = \delta Q_{X;0}(p) + (1 - \delta) Q_{Y;0}(p). \quad (2.13)$$

If, for a given value of p , $Q_{X;0}(p) \geq Q_{Y;0}(p)$, then $Q_{X;0}(p) \geq Q_{W;0}(p) \geq Q_{Y;0}(p)$ for that value of p . In effect, the weighted sum of two quantile functions is bounded by these two quantile functions. This result is known as the intermediate rule for quantile functions.

It was shown in Section 2.3.3 that a distribution with quantile function obtained with (2.11) is symmetric. The reason is that the percentage of weight allocated to the quantile functions of the distributions of X and Y is 50% each, in effect, equal. The transformation in (2.13) can be used to introduce skewness by taking the weighted sum of the quantile function of an asymmetric distribution on bounded or half-infinite support and the quantile function of the reflection of this distribution. That is, the distribution with quantile function

$$\begin{aligned} Q_{W;0}(p) &= \delta Q_{X;0}(p) + (1 - \delta) Q_{Y;0}(p) \\ &= \delta Q_{X;0}(p) - (1 - \delta) Q_{X;0}(1 - p), \end{aligned}$$

is an asymmetric distribution where δ can be viewed as a weight parameter which controls the level of skewness through the allocation of weight to $Q_{X;0}(p)$ and to $Q_{Y;0}(p) = -Q_{X;0}(1-p)$. In effect, δ is a shape parameter. Note that W has a symmetric distribution for $\delta = \frac{1}{2}$.

Example 2.3.4

Consider again X having a standard exponential distribution with quantile function given in (2.7) and $Y = -X$ having a standard reflected exponential distribution with quantile function given in (2.8). Then

$$\begin{aligned} Q_{W;0}(p) &= \delta Q_{X;0}(p) + (1-\delta)Q_{Y;0}(p) \\ &= -\delta \log[1-p] + (1-\delta) \log[p] \end{aligned} \quad (2.14)$$

is the quantile function of a skewed form of the standard logistic distribution with $0 \leq \delta \leq 1$ a shape parameter. Using the linear transformation in (2.5) to include location and scale parameters (α and β), the quantile function of the resulting three-parameter asymmetric distribution, aptly named the skew logistic distribution by Gilchrist (2000), is

$$Q(p) = \alpha + \beta \left((1-\delta) \log[p] - \delta \log[1-p] \right). \quad (2.15)$$

The skew logistic distribution, which will be abbreviated SLD, is symmetric for $\delta = \frac{1}{2}$, negatively skewed for $\delta < \frac{1}{2}$ and positively skewed for $\delta > \frac{1}{2}$. The reflected exponential, symmetric logistic and exponential distributions are all special cases of the SLD for $\delta = 0$, $\delta = \frac{1}{2}$ and $\delta = 1$ respectively. The SLD's quantile density and density quantile functions are

$$q(p) = \beta \left(\frac{1-\delta}{p} + \frac{\delta}{1-p} \right) = \beta \left(\frac{\delta p + (1-\delta)(1-p)}{p(1-p)} \right) \quad (2.16)$$

and

$$f_p(p) = \frac{p(1-p)}{\beta \left(\delta p + (1-\delta)(1-p) \right)}. \quad (2.17)$$

As with Tukey's lambda distribution (and its generalizations) and the Davies distribution, the probability-based functions of the SLD cannot be expressed in closed-form (except of course for its special cases mentioned above). The SLD is thus a quantile-based distribution. The quantile, quantile density, density quantile and probability density functions of the standard SLD are shown in Figure 2.7 for $\delta = 0, \frac{1}{4}, \frac{1}{2}, \frac{3}{4}, 1$.

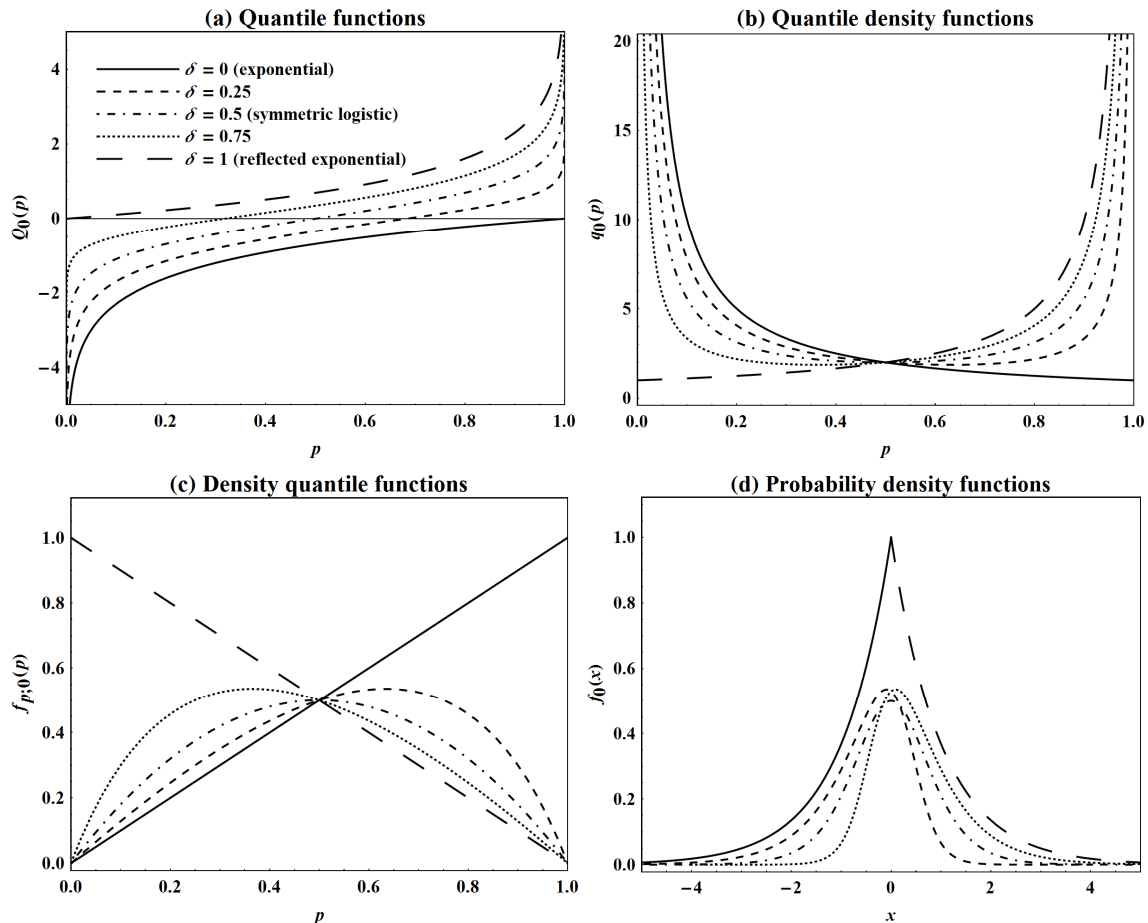


Figure 2.7: Quantile, quantile density, density quantile and probability density functions of the standard SLD for various values of δ . The line types indicated in graph (a) also apply to the other graphs.

The intermediate rule for quantile functions is evident from Figure 2.7(a), with the SLD's quantile function bounded by the quantile functions of the exponential and reflected exponential distributions. Furthermore, as can be seen in Figure 2.7(d), the SLD is J-shaped with half-infinite support for $\delta = 0$ and $\delta = 1$, and unimodal with infinite support for $0 < \delta < 1$. Note that, since no closed-form expression exists for the SLD's probability density function, Figure 2.7(d) was obtained by plotting the points $(Q_0(p), f_{p;0}(p))$ to obtain a plot of the corresponding points $(x, f_0(x))$.

□

Note that the quantile-based SLD presented in Example 2.3.4 is not the only type of skew logistic distribution in existence. Wahed & Ali (2001) and Nadarajah (2009) studied a skew logistic distribution based upon the skewing methodology introduced by Azzalini (1985, 1986), with probability density function in standard form given by

$$g_0(x) = 2f_0(x)F_0(\lambda x),$$

where $f_0(x)$ and $F_0(x)$ are the probability density and cumulative distribution functions of the standard logistic distribution and λ is a shape parameter. This density-based skew logistic distribution is in no way related to the quantile-based SLD considered in this thesis.

It was shown in Section 2.3 how probability distributions can be created through the application of model building construction rules to quantile functions. In Sections 2.4 to 2.8 measures of location, spread and shape for probability distributions are considered. Specifically it is proved in Section 2.8 that a distribution whose quantile function is given by the weighted sum of the quantile function of an asymmetric distribution on bounded or half-infinite support and the quantile function of the reflection of this asymmetric distribution possesses certain measures of kurtosis which are skewness-invariant.

2.4 MOMENTS

In the classical statistical universe it is common practice to use moments and moment ratios to describe the location, spread and shape characteristics of a probability distribution. Following conventional notation, if X is a real-valued random variable, then $\mu'_r = E[X^r]$ is the r^{th} order uncorrected (crude) moment and $\mu_r = E[(X - \mu)^r]$ is the r^{th} order corrected (central) moment, where $\mu = \mu'_1$, the first order uncorrected moment, is the mean of X and a measure of location. The second order corrected moment, $\sigma^2 = \mu_2$, is the variance of X and a measure of spread. The skewness and kurtosis moment ratios, defined as

$$\alpha_3 = \frac{\mu_3}{\sigma^3} \text{ and } \alpha_4 = \frac{\mu_4}{\sigma^4}, \quad (2.18)$$

are used to describe the shape of the distribution. Expressions and values for the mean, variance, skewness moment ratio and kurtosis moment ratio of the uniform, exponential and logistic distributions are presented in Table 2.2.

Table 2.2: Moments for the uniform, exponential and logistic distributions.

Measure	Uniform	Exponential	Logistic
Mean	$\mu = \alpha + \frac{1}{2}\beta$	$\mu = \alpha + \beta$	$\mu = \alpha$
Variance	$\sigma^2 = \frac{1}{12}\beta^2$	$\sigma^2 = \beta^2$	$\sigma^2 = \frac{\pi^2}{3}\beta^2$
Skewness moment ratio	$\alpha_3 = 0$	$\alpha_3 = 2$	$\alpha_3 = 0$
Kurtosis moment ratio	$\alpha_4 = \frac{9}{5}$	$\alpha_4 = 9$	$\alpha_4 = \frac{21}{5}$

The moments and moment ratios can also be used in the quantile statistical universe, since

$$\mu'_r = \int_0^1 (Q_X(p))^r dp$$

and

$$\mu_r = \int_0^1 (Q_X(p) - \mu)^r dp,$$

where

$$\mu = \int_0^1 Q_X(p) dp.$$

However, often the formulae obtained for the moments and moment ratios of quantile-based distributions are not straightforward, complicating the use of these measures. Therefore alternative measures of location, spread and shape are discussed in Sections 2.5 and 2.6.

Example 2.4.1

The mean, variance, skewness moment ratio and kurtosis moment ratio of the SLD are

$$\mu = \alpha + \beta(2\delta - 1), \quad (2.19)$$

$$\sigma^2 = \beta^2 \left((2\delta - 1)^2 + \frac{\pi^2}{3} \omega \right), \quad (2.20)$$

$$\alpha_3 = \frac{\beta^3}{\sigma^3} \left(2(2\delta - 1) \left(1 - \omega \left(4 - 3\zeta(3) \right) \right) \right) \quad (2.21)$$

and

$$\alpha_4 = \frac{\beta^4}{\sigma^4} \left(9 + \omega \left(2 \left((2\delta - 1)^2 \pi^2 - 4 \right) + (9\omega - 4) \left(16 - \frac{\pi^4}{15} \right) \right) \right), \quad (2.22)$$

with $\omega = \delta(1 - \delta)$ and where $\zeta(a)$ is Riemann's zeta function – see Section 2.14.1 for details. These formulae, which have not been given in the literature before, are derived in Section 2.13.1. As will be seen in subsequent sections, the formulae for other measures of location, spread and shape of the SLD are considerably simpler.

□

2.5 L-MOMENTS

The theory of L -moments was compiled by Hosking (1990). He extended and unified theoretical results and techniques described by Sillitto (1951, 1964, 1969), Downton (1966), Chan (1967), Konheim (1971), Mallows (1973) and Greenwood *et al.* (1979). L -moments are expectations of linear combinations of order statistics. Let $X_{1:n} \leq X_{2:n} \leq \dots \leq X_{n:n}$ denote the order statistics for a random sample of size n from the distribution of X . The r^{th} order L -moment of X is then defined by

$$L_r = r^{-1} \sum_{k=0}^{r-1} (-1)^k \binom{r-1}{k} E(X_{r-k:r}), \quad r = 1, 2, 3, \dots$$

Note that in the literature the r^{th} order L -moment is usually denoted by λ_r . However, the parameters of the generalized lambda distribution in Chapter 3 are also denoted by λ_r . Therefore in this thesis the r^{th} order L -moment will be denoted by L_r instead of λ_r , to avoid confusion with the parameters of the generalized lambda distribution.

Hosking (1990) showed that the r^{th} order L -moment of X can be written in terms of its quantile function as

$$L_r = \int_0^1 Q(p) P_{r-1}^*(p) dp, \quad (2.23)$$

where

$$P_r^*(p) = \sum_{k=0}^r \left((-1)^{r-k} \binom{r}{k} \binom{r+k}{k} p^k \right) \quad (2.24)$$

is the r^{th} order shifted Legendre polynomial. See Section 2.14.2 of Appendix 2.14 for a brief explanation on Legendre polynomials.

The first order L -moment, referred to as L -location, is simply the mean, $L_1 = \mu$. The second order L -moment, L_2 , is called the L -scale. L_2 is a measure of spread and is related to Gini's mean difference statistic (Gini 1913–1914). L -moment ratios are defined as

$$\tau_r = \frac{L_r}{L_2}, \quad r = 3, 4, 5, \dots \quad (2.25)$$

The L -skewness ratio, τ_3 , and L -kurtosis ratio, τ_4 , are of particular interest in that they are measures of shape. Symmetric distributions have $\tau_3 = 0$.

Compared to conventional moments, L -moments possess a number of superior characteristics. For instance, L -moment ratios are bounded, simplifying their interpretation

compared to conventional moments. Specifically, as proven by Hosking (1990) and Jones (2004), the boundaries of the L -skewness and L -kurtosis ratios are

$$-1 < \tau_3 < 1 \text{ and } \frac{1}{4}(5\tau_3^2 - 1) \leq \tau_4 < 1. \quad (2.26)$$

Furthermore, Hosking (1990) proved that, if the mean of a probability distribution exists, then all the L -moments exist and the distribution is uniquely characterized by its L -moments.

Expressions and values for the L -moments of the uniform, exponential and logistic distributions are given in Table 2.3. The expressions and values for the L -moments of these three distributions as well as for various other well-known distributions were provided by Hosking (1986, 1990, 1992) and Hosking & Wallis (1997). Other sources for expressions of the L -moments of specific distributions include Jones (2002a, 2002b, 2009) for Student's $t(2)$, the cosine and Kumaraswamy's distribution respectively, and Gupta & Kundu (2001) for the generalized exponential distribution. Table 2.13 in Section 2.14.3 of Appendix 2.14 presents expressions for the L -location and L -scale of the distributions considered in Tables 2.10 to 2.12 in this appendix, while expressions for the L -skewness and L -kurtosis ratios of these distributions are presented in Table 2.14 in Section 2.14.3.

Table 2.3: L -moments for the uniform, exponential and logistic distributions.

L -moment	Uniform	Exponential	Logistic
L -location	$L_1 = \alpha + \frac{1}{2}\beta$	$L_1 = \alpha + \beta$	$L_1 = \alpha$
L -scale	$L_2 = \frac{1}{6}\beta$	$L_2 = \frac{1}{2}\beta$	$L_2 = \beta$
L -skewness ratio	$\tau_3 = 0$	$\tau_3 = \frac{1}{3}$	$\tau_3 = 0$
L -kurtosis ratio	$\tau_4 = 0$	$\tau_4 = \frac{1}{6}$	$\tau_4 = \frac{1}{6}$

Returning to Table 2.3, the uniform and logistic distributions are symmetric, so they have $\tau_3 = 0$. It is furthermore interesting to note that the exponential distribution and the logistic distribution both have $\tau_4 = \frac{1}{6}$.

As explained by Hosking & Wallis (1997), the L -moment ratio diagram is a convenient graphical representation for the L -skewness and L -kurtosis ratios in that it indicates the (τ_3, τ_4) space attained by different distributions. No distribution's (τ_3, τ_4) space can extend beyond the boundary given by (2.26). Figures 2.8 to 2.14 depict the L -moment ratio diagrams of the distributions considered in Table 2.14 in Section 2.14.3. As can be seen in these figures, especially Figure 2.8(b), a distribution which possesses only location and scale parameters and no shape parameters appears as a single point in the L -moment ratio diagram.

A distribution with a single shape parameter, say λ , is plotted with a line, where each point on the line indicates the values of τ_3 and τ_4 obtained for the corresponding value of λ . Figure 2.8 illustrates the values of τ_3 and τ_4 obtained by the distributions with shape parameter λ from Table 2.14. Figure 2.9 presents the L -moment ratio diagram for the various generalized distributions considered by Hosking (1986) and Hosking & Wallis (1997). Note that the log-normal, generalized normal, gamma and generalized gamma distributions do not have simple expressions for their L -skewness and L -kurtosis ratios. The values of τ_3 and τ_4 for these distributions can be calculated using rational-function approximations given by Hosking & Wallis (1997).

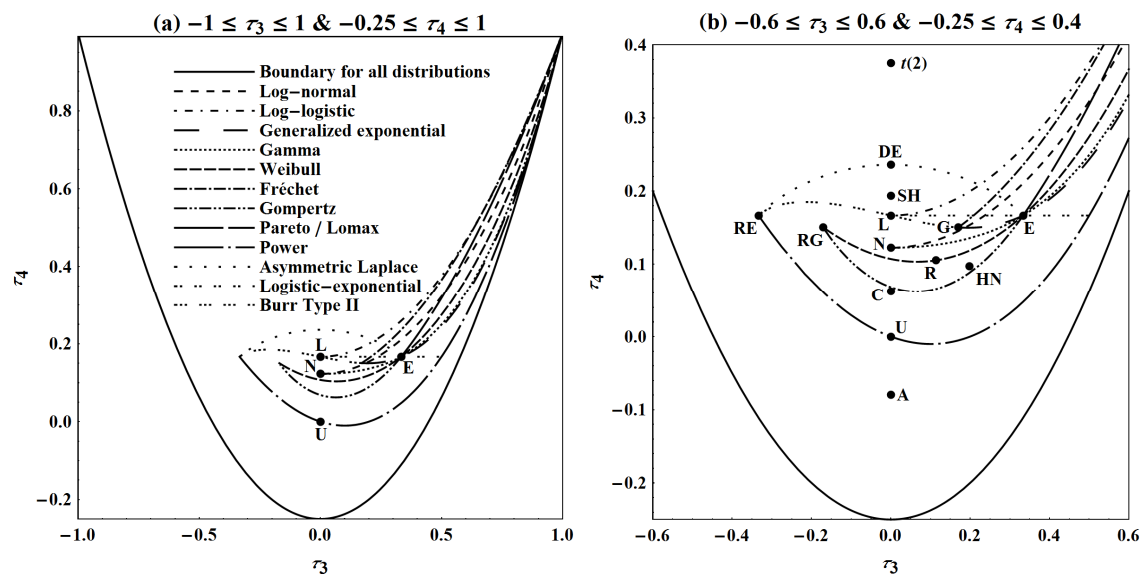


Figure 2.8: L -moment ratio diagrams for the two- and three-parameter distributions in Table 2.14 in Appendix 2.14. The line types indicated in diagram (a) also apply to diagram (b). The uniform, normal, logistic and exponential distributions are denoted in diagrams (a) and (b) by U, N, L and E respectively, while A, C, SH, DE, $t(2)$, G, HN and R, in diagram (b) denote the arcsine, cosine, secant hyperbolic, Laplace (double exponential), Student's $t(2)$, Gumbel, half-normal and Rayleigh distributions. The reflected distributions of the exponential and the Gumbel are indicated in diagram (b) with RE and RG.

Distributional families with multiple shape parameters cover areas of τ_3 and τ_4 values corresponding to the values of these shape parameters. Figures 2.10 to 2.14 show the L -moment ratio diagrams for the Burr Types III and XII distributions, the Davies distribution, the kappa distribution, Kumaraswamy's distribution and the Schmeiser-Deutsch distribution, all possessing two shape parameters, say λ and δ . Different colours are used to distinguish between the various areas of τ_3 and τ_4 values attained for the values of λ and δ as detailed in Table 2.14. Special and limiting distributions obtained by the Burr Types III and XII, Davies, kappa, Kumaraswamy's and Schmeiser-Deutsch distributions are also indicated.

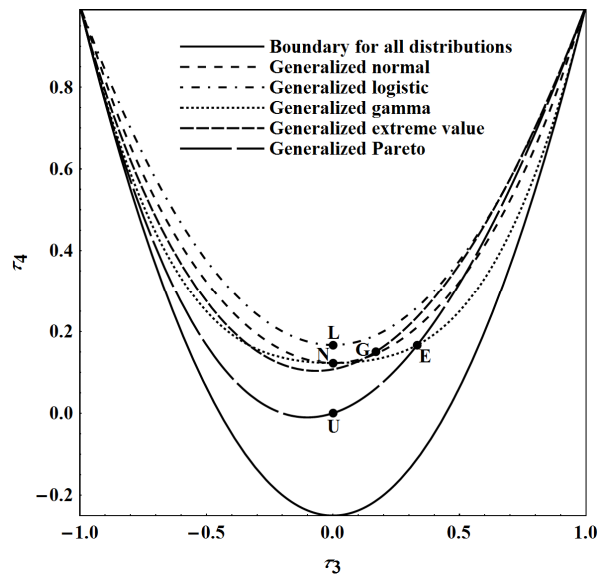


Figure 2.9: *L*-moment ratio diagram for generalized distributions in Table 2.14 in Appendix 2.14, considered by Hosking (1986) and Hosking & Wallis (1997). The uniform, normal, logistic, exponential and Gumbel distributions, which are special or limiting cases of these generalized distributions, are denoted by U, N, L, E and G respectively.

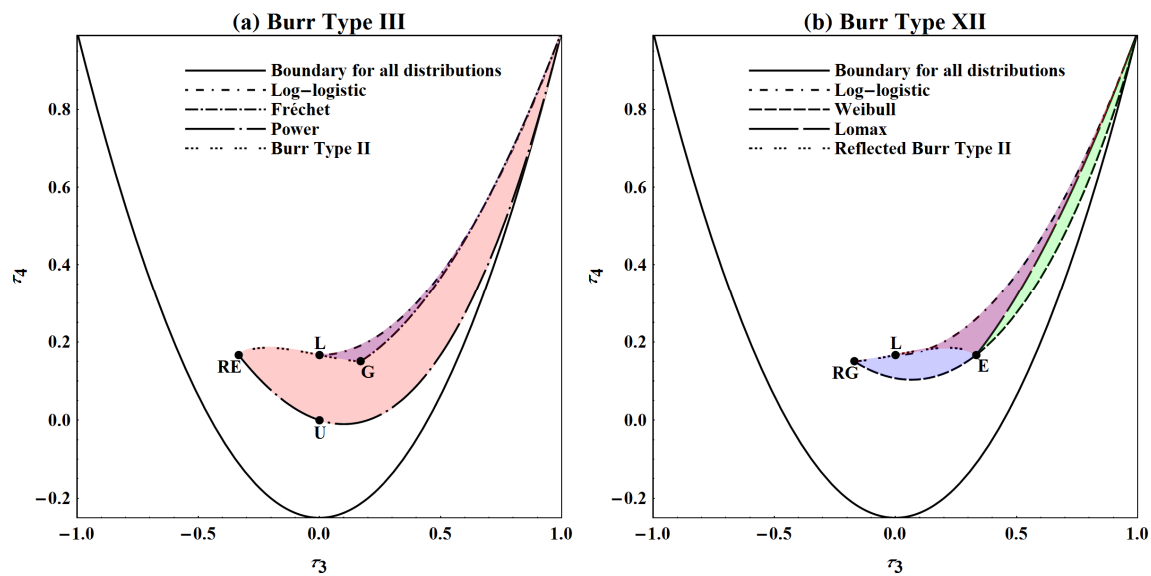


Figure 2.10: *L*-moment ratio diagrams for the Burr Type III and Burr Type XII distributions. The uniform, logistic, exponential, reflected exponential, Gumbel and reflected Gumbel distributions are indicated in diagrams (a) and (b) by U, L, E, RE, G and RG respectively. In diagram (a), the purple- and the red-shaded areas are the (τ_3, τ_4) spaces obtained by the Burr Type III distribution for $\lambda > 1$. But the purple-shaded area in diagram (a) is also obtained by the Burr Type III distribution when $\lambda < 1$. In effect, in the purple-shaded area there is not a one-to-one relation between the shape parameters of the Burr Type III distribution and the *L*-skewness and *L*-kurtosis ratios. In diagram (b), the purple- and blue-shaded areas are the (τ_3, τ_4) spaces obtained by the Burr Type XII distribution when both $\lambda < 1$ and $\delta < 1$. The purple-shaded area is also obtained by the Burr Type XII distribution for $\lambda > 1$ and $\delta < 1$. So in the purple-shaded area there is not a one-to-one relation between the shape parameters of the Burr Type XII distribution and the *L*-skewness and *L*-kurtosis ratios. When $\lambda < 1$ and $\delta > 1$, the Burr Type XII distribution attains the green-shaded area in diagram (b).

In general a distribution which covers a larger area of the (τ_3, τ_4) space is more flexible with respect to distributional shape. For instance, as indicated in Figure 2.10, the Burr Type III distribution covers a larger area compared to the Burr Type XII distribution, indicating its higher flexibility in terms of shape. This is interesting since the Burr Type XII distribution is the most popular of the Burr family of distributions – Tadikamalla (1980) made a similar observation in terms of the (α_3, α_4) space attained by the Burr Type III and Type XII distributions.

Figure 2.10 also indicates that there does not always exist a one-to-one correspondence between the shape parameters of a distribution and the distribution's L -skewness and L -kurtosis ratios. This can be problematic when L -moments are used for parameter estimation.

The coverage of the (τ_3, τ_4) space by the Davies distribution shown in Figure 2.11 is equivalent to the coverage of the (τ_3, τ_4) space by the Burr Type III distribution shown in Figure 2.10(a). But the expressions of the L -moments of the Davies distribution are considerably simpler than the expressions of the L -moments of the Burr Type III distribution – see Tables 2.13 and 2.14. This suggests that the Davies distribution could be used as a proxy for the Burr Type III distribution in studies involving L -moments.

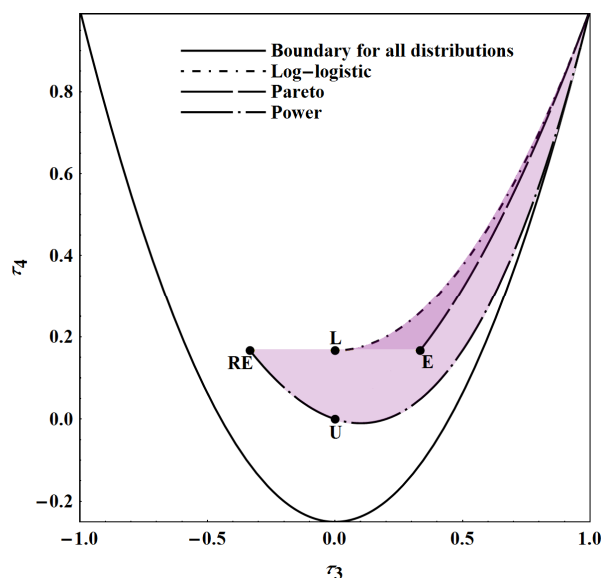


Figure 2.11: L -moment ratio diagram for the Davies distribution. The uniform, logistic, exponential and reflected exponential distributions are indicated by U, L, E and RE. In the light-shaded area there is a one-to-one relation between the shape parameters of the Davies distribution and the L -skewness and L -kurtosis ratios. In the dark-shaded area, two different pairs of values for λ and δ produce the same pair of values for the L -skewness and L -kurtosis ratios. In effect, there is not a one-to-one relation between the shape parameters and the L -skewness and L -kurtosis ratios in the dark-shaded area.

Both the kappa distribution and Kumaraswamy's distribution cover extensive areas of the (τ_3, τ_4) space as shown in Figures 2.12 and 2.13. Importantly these two distributions' coverage of the (τ_3, τ_4) space extends all the way to the lower boundary for τ_4 given by (2.26), that is,

$$\tau_4 = \frac{1}{4}(5\tau_3^2 - 1).$$

However, apart from the Schmeiser-Deutsch distribution in Figure 2.14, none of the other families of distributions considered in Figures 2.10 to 2.13 cover the area of the (τ_3, τ_4) space given by

$$-1 < \tau_3 < 1 \text{ and } \frac{1}{6}(5\tau_3^2 - 1) \leq \tau_4 < 1, \quad (2.27)$$

where the lower boundary of the excluded region of τ_4 in (2.27), in effect,

$$\tau_4 = \frac{1}{6}(5\tau_3^2 - 1),$$

is given by the generalized logistic distribution. It will be shown in Chapters 2 and 3 that the generalized lambda distribution does cover this important area of the (τ_3, τ_4) space which is representative of heavy-tailed distributions with moderate to large levels of skewness.

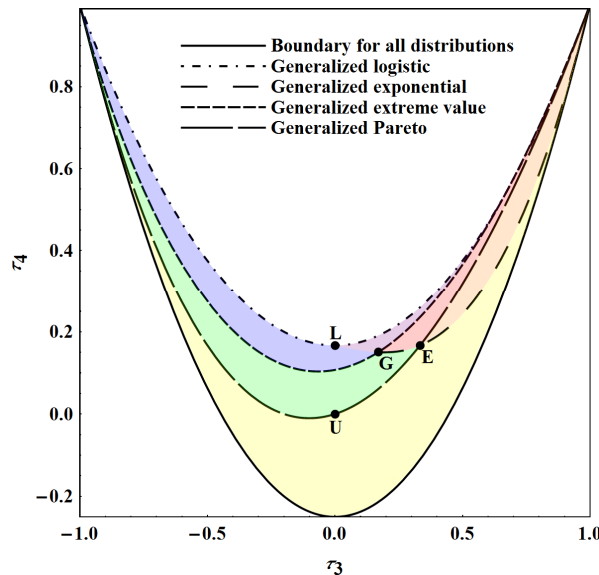


Figure 2.12: *L*-moment ratio diagram for the kappa distribution. The uniform, exponential, logistic and Gumbel distributions are indicated by U, E, L and G. The purple- and blue-shaded areas are the (τ_3, τ_4) spaces obtained for $-1 < \delta < 0$, the green- and red-shaded areas are the (τ_3, τ_4) spaces obtained for $0 < \delta < 1$, and the yellow- and orange-shaded areas are the (τ_3, τ_4) spaces attained for $\delta > 1$. In the purple-, red- and orange-shaded areas, $-1 < \lambda < 0$, while $\lambda > 0$ in the blue-, green- and yellow-shaded areas.

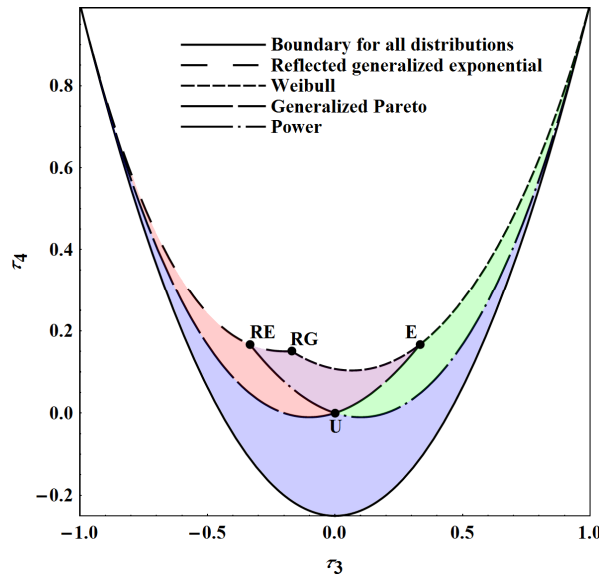


Figure 2.13: *L*-moment ratio diagram for Kumaraswamy's distribution. The uniform and exponential distributions are indicated by U and E, while RE and RG denote the reflected exponential and reflected Gumbel distributions. The purple-shaded area is the (τ_3, τ_4) space obtained for $0 < \lambda < 1$ and $0 < \delta < 1$. When both $\lambda > 1$ and $\delta > 1$, the blue-shaded area is attained. The red- and green-shaded areas are the (τ_3, τ_4) spaces covered by Kumaraswamy's distribution for $0 < \lambda < 1$ and $\delta > 1$ and for $0 < \delta < 1$ and $\lambda > 1$ respectively.

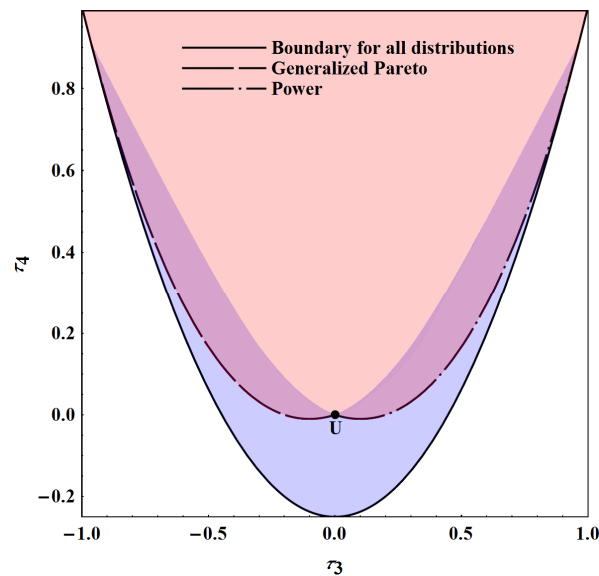


Figure 2.14: *L*-moment ratio diagram for the Schmeiser-Deutsch distribution. The uniform distribution is indicated by U. The purple- and blue-shaded areas are the (τ_3, τ_4) spaces attained for $\lambda < 1$, while the purple- and red-shaded areas are the (τ_3, τ_4) spaces attained when $\lambda > 1$. So it follows that there does not exist a one-to-one relation between the shape parameters of the Schmeiser-Deutsch distribution and the *L*-skewness and *L*-kurtosis ratios in the purple-shaded area.

Hosking (1990) provided unbiased estimators for *L*-moments. Let $x_{1:n} \leq x_{2:n} \leq \dots \leq x_{n:n}$ denote an ordered data set of sample size n . Then, based upon the theory of *U*-statistics (Hoeffding, 1948), the r^{th} order sample *L*-moment is represented by

$$\ell_r = \binom{n}{r}^{-1} \sum_{1 \leq i_1 < i_2 < \dots < i_r \leq n} \sum_{k=0}^{r-1} r^{-1} (-1)^k \binom{r-1}{k} x_{i_{r-k}:n}, \quad r = 1, 2, \dots, n, \quad (2.28)$$

while the r^{th} order sample L -moment ratio is given by

$$t_r = \frac{\ell_r}{\ell_2}, \quad r = 3, 4, \dots, n. \quad (2.29)$$

In particular the first four sample L -moments are

$$\ell_1 = \frac{1}{n} \sum_{i=1}^n x_{i:n} = \bar{x}, \quad (2.30)$$

$$\ell_2 = \frac{1}{2} \binom{n}{2}^{-1} \sum_{i>j} (x_{i:n} - x_{j:n}), \quad (2.31)$$

$$\ell_3 = \frac{1}{3} \binom{n}{3}^{-1} \sum_{i>j>k} (x_{i:n} - 2x_{j:n} + x_{k:n}), \quad (2.32)$$

and

$$\ell_4 = \frac{1}{4} \binom{n}{4}^{-1} \sum_{i>j>k>l} (x_{i:n} - 3x_{j:n} + 3x_{k:n} - x_{l:n}). \quad (2.33)$$

The interpretation of the sample L -moments is analogous to the population L -moments in that $\ell_1 = \bar{x}$, ℓ_2 , t_3 and t_4 are respectively the sample L -location (sample mean), sample L -scale, sample L -skewness ratio and sample L -kurtosis ratio. The sample L -moments can thus be used as alternatives to conventional sample moments for describing the location, spread and shape of a data set and, as will be shown in Section 2.9, they may be used to fit a distribution to the data set with method of L -moments estimation. In fact, because the sample L -moments are linear functions of the data values, they are less adversely affected by sampling variability than the conventional sample moments, Hosking (1990), and more robust to extreme values in the data. It is thus not surprising that L -moments are popular in extreme event analysis. For example, Hosking & Wallis (1997) gave a thorough account of the use of L -moments in regional frequency analysis in environmental applications.

2.6 QUANTILE-BASED MEASURES OF LOCATION, SPREAD AND SHAPE

As suggested by the name, quantile-based measures of location, spread and shape for a distribution are defined as functions of the quantiles of the distribution and are therefore ideally suited for use in the quantile statistical universe. They are of course also utilized in the classical statistical universe. If the distribution under consideration possesses a simple expression for its quantile function, the associated expressions of the quantile-based measures

will also be simple. Unlike conventional moments and L -moments, quantile-based measures exist for all parameter values of a distribution.

The 50th percentile, that is, the median,

$$me = Q\left(\frac{1}{2}\right), \quad (2.34)$$

is an obvious choice as measure of location. The spread function, introduced by MacGillivray & Balanda (1988), is given by

$$S(u) = Q(u) - Q(1-u), \quad \frac{1}{2} < u < 1. \quad (2.35)$$

From the linear transformation in (2.5) it follows immediately that

$$\begin{aligned} S(u) &= \left(\alpha + \beta Q_0(u) \right) - \left(\alpha + \beta Q_0(1-u) \right) \\ &= \beta \left(Q_0(u) - Q_0(1-u) \right), \end{aligned} \quad (2.36)$$

so the spread function is location-invariant. Furthermore, since $u > 1-u$ and hence $Q(u) > Q(1-u)$, we have $S(u) > 0$. Thus the spread function satisfies the basic requirements for measures of spread. Special cases of the spread function include the interquartile range (IQR) and interdecile range (IDR), obtained respectively for $u = \frac{3}{4}$ and $u = \frac{9}{10}$.

Several measures of shape have been proposed in the literature. These measures include location- and scale-invariant shape functionals. Analogous to the spread function, shape functionals are not just evaluated at specific quantiles, but are analyzed as functions themselves. In fact, just as the IQR and IDR are special cases of the spread function for $u = \frac{3}{4}$ and $u = \frac{9}{10}$, quantile-based measures of shape are often special cases of shape functionals, attained for selected quantiles.

As part of a study in which she compiled a skewness structure of ordering for identifying the roles of various skewness measures and for classification of the skewness properties of distributions, MacGillivray (1986) considered two skewness functionals. The first of these, the γ -functional, is given by

$$\gamma(u) = \frac{Q(u) + Q(1-u) - 2Q\left(\frac{1}{2}\right)}{Q(u) - Q(1-u)} = \frac{Q(u) + Q(1-u) - 2me}{S(u)}, \quad \frac{1}{2} < u < 1. \quad (2.37)$$

Originally suggested by David & Johnson (1956), the γ -functional can be viewed as a functional generalization of the well-known quartile-based measure of skewness attributed to Bowley (1902). Bowley's measure of skewness, referred to by some authors (Johnson *et al.*, 1994; Gilchirst, 2000) as Galton's measure of skewness, is obtained by evaluating the γ -

functional at $u = \frac{3}{4}$. The γ -functional preserves the skewness ordering \leq_2^m (MacGillivray, 1986) in that

$$F \leq_2^m G \Leftrightarrow \gamma_F(u) \leq \gamma_G(u).$$

In effect, distribution G has greater skewness to the right than distribution F if $\gamma_G(u) > \gamma_F(u)$. MacGillivray (1992) proposed

$$\sup_{\frac{1}{2} < u < 1 - \varepsilon} |\gamma(u)|$$

as a measure of overall skewness for the central $100(1 - 2\varepsilon)\%$ of a distribution.

The second skewness functional, named the η -functional by King (1999), is

$$\eta(u, v) = \frac{Q(u) + Q(1-u) - Q(v) - Q(1-v)}{Q(v) - Q(1-v)} = \frac{Q(u) + Q(1-u) - Q(v) - Q(1-v)}{S(v)}, \quad \frac{1}{2} < v < u < 1. \quad (2.38)$$

The η -functional is linked to the skewness ordering $\leq_{2, \text{star}}^m$ (MacGillivray, 1986) in that it proves

$$F \leq_{2, \text{star}}^m G \Rightarrow \eta_F(u, v) \leq \eta_G(u, v).$$

The skewness of a distribution can also be measured by comparing the relative weight allocated to the two tails of the distribution. For instance, the left-right tail-weight ratio,

$$TWR(u) = \frac{Q\left(\frac{1}{2}\right) - Q(1-u)}{Q(u) - Q\left(\frac{1}{2}\right)} = \frac{me - Q(1-u)}{Q(u) - me}, \quad \frac{1}{2} < u < 1,$$

was utilized by Karian & Dudewicz (1999) in their proposed percentile-based estimation method for the generalized lambda distribution – see Section 3.13. The tail-weight ratio can be evaluated for any $\frac{1}{2} < u < 1$ and hence it is a shape functional, but it is typically only evaluated for a specific value of u . For instance, Karian & Dudewicz (1999) promoted the use of $u = \frac{9}{10}$ in their proposed estimation method. Both the numerator and the denominator of the tail-weight ratio are positive, so $TWR(u) > 0$. Since the tail-weight ratio measures the relative tail weights of the left tail (in the numerator) to the right tail (in the denominator), $TWR(u) < 1$ indicates that the distribution is positively skewed, $TWR(u) = 1$ for a symmetric distribution, and a negatively skewed distribution has $TWR(u) > 1$.

Following van Zwet (1964a), a measure of skewness should preferably be zero for a variable with a symmetric distribution, and, if two random variables are related through

$Y = -X$, then the measures of skewness for the distributions of X and Y should only differ in terms of sign. These criteria hold for the skewness moment ratio and L -skewness ratio and also for both the γ -functional and η -functional. However, for the tail-weight ratio we have

$$TWR_X(u) = [TWR_Y(u)]^{-1},$$

that is, an inverse relation around the symmetric value of $TWR(u) = 1$. The interpretation of the tail-weight ratio is therefore more complex than for the γ -functional or the η -functional. Interpretation of skewness measures is further simplified if the measure under consideration is bounded, as is for example the L -skewness ratio – see again (2.26). Akin to the skewness moment ratio, the η -functional is not bounded, but, as proven by King (1999), the γ -functional is bounded, $-1 < \gamma(u) < 1$.

Turning to kurtosis, one of the initial quantile-based measures proposed in the literature is the measure of Kelley (1921),

$$K = \frac{\varrho\left(\frac{3}{4}\right) - \varrho\left(\frac{1}{4}\right)}{2\left(\varrho\left(\frac{9}{10}\right) - \varrho\left(\frac{1}{10}\right)\right)} = \frac{s\left(\frac{3}{4}\right)}{2s\left(\frac{9}{10}\right)} = \frac{IQR}{2IDR}. \quad (2.39)$$

Karian & Dudewicz (1999) utilized a similar measure in their percentile-based estimation method for the generalized lambda distribution,

$$TWF(u) = \frac{\varrho\left(\frac{3}{4}\right) - \varrho\left(\frac{1}{4}\right)}{\varrho(u) - \varrho(1-u)} = \frac{s\left(\frac{3}{4}\right)}{s(u)} = \frac{IQR}{s(u)}, \quad \frac{3}{4} < u < 1, \quad (2.40)$$

labeled by them the tail-weight factor. As with the tail-weight ratio, Karian & Dudewicz (1999) promoted the use of $u = \frac{9}{10}$. The tail-weight factor is then simply the ratio of the interquartile range to the interdecile range and we have

$$TWF\left(\frac{9}{10}\right) = \frac{\varrho\left(\frac{3}{4}\right) - \varrho\left(\frac{1}{4}\right)}{\varrho\left(\frac{9}{10}\right) - \varrho\left(\frac{1}{10}\right)} = \frac{s\left(\frac{3}{4}\right)}{s\left(\frac{9}{10}\right)} = \frac{IQR}{IDR} = 2K.$$

The octile-based measure of kurtosis (Moors, 1988; Moors *et al.*, 1996),

$$T = \frac{\varrho\left(\frac{7}{8}\right) - \varrho\left(\frac{5}{8}\right) + \varrho\left(\frac{3}{8}\right) - \varrho\left(\frac{1}{8}\right)}{\varrho\left(\frac{6}{8}\right) - \varrho\left(\frac{2}{8}\right)} = \frac{s\left(\frac{7}{8}\right) - s\left(\frac{5}{8}\right)}{s\left(\frac{3}{4}\right)} = \frac{s\left(\frac{7}{8}\right) - s\left(\frac{5}{8}\right)}{IQR}, \quad (2.41)$$

and the quintile-based measure of kurtosis (Jones *et al.*, 2011),

$$J = \frac{\varrho\left(\frac{4}{5}\right) - 3\varrho\left(\frac{3}{5}\right) + 3\varrho\left(\frac{2}{5}\right) - \varrho\left(\frac{1}{5}\right)}{\varrho\left(\frac{4}{5}\right) - \varrho\left(\frac{1}{5}\right)} = \frac{s\left(\frac{4}{5}\right) - 3s\left(\frac{3}{5}\right)}{s\left(\frac{4}{5}\right)}, \quad (2.42)$$

can both be viewed as natural extensions of Bowley's quartile-based measure of skewness.

A shape functional for kurtosis, the ratio-of-spread functions, was proposed by MacGillivray & Balanda (1988),

$$R(u, v) = \frac{S(u)}{S(v)}, \quad \frac{1}{2} < v < u < 1. \quad (2.43)$$

The ratio-of-spread functions, referred to as the spread-spread function by some researchers in the literature (Seier & Bonett, 2003; Kotz & Seier, 2008), is linked to the plot of $S_G(S_F)^{-1}$ for distributions F and G , called the spread-spread plot by Balanda & MacGillivray (1990). In the spread-spread plot the spread function of distribution G , $S_G(u)$, is plotted on the vertical axis against the spread function of distribution F , $S_F(u)$, on the horizontal axis. Linking the spread-spread plot to kurtosis orderings, Balanda & MacGillivray (1990) extended van Zwet's ordering \leq_S (van Zwet, 1964a, 1964b) to skewed distributions, defining

$$F \leq_S G \Leftrightarrow S_G((S_F(u))^{-1}) \text{ convex for } \frac{1}{2} < u < 1.$$

That is, if the spread-spread plot is convex for $\frac{1}{2} < u < 1$, then distribution G has greater kurtosis than distribution F . Conversely distribution F has greater kurtosis than distribution G if the spread-spread plot is concave. For example, in Figure 2.15 the spread-spread plot for the logistic distribution against the uniform distribution is convex indicating the logistic distribution's greater kurtosis compared to the uniform distribution.

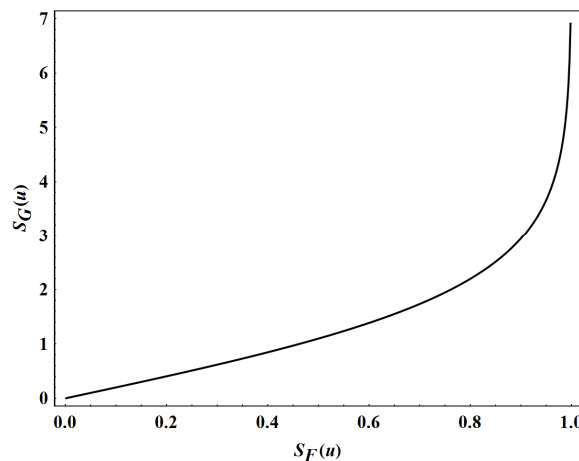


Figure 2.15: Spread-spread plot for the logistic distribution with spread function $S_G(u)$ against the uniform distribution with spread function $S_F(u)$. For both distributions the value of β is set to one in their respective spread functions, given in Table 2.4.

Because $S(u) > 0$ for any $\frac{1}{2} < u < 1$, the values obtained for Kelley's measure, the tail-weight factor, the octile-based measure of kurtosis and the ratio-of-spread functions are always positive. Furthermore, since $S(u) > S(v)$ for $\frac{1}{2} < v < u < 1$, it follows that both

Kelley's measure and the tail-weight factor are bounded above in that their values cannot exceed one. Thus $0 < K < 1$ and $0 < TWF(u) < 1$ and therefore, like the L -kurtosis ratio, these two measures are bounded measures of kurtosis – see again (2.26) for the bounds of the L -kurtosis ratio.

However, a drawback of Kelley's measure and the tail-weight factor is that they operate in an opposite direction to the other measures of kurtosis. For Kelley's measure and the tail-weight factor, smaller values (in effect, values closer to zero) are indicative of heavier tails, while larger values (that is, values closer to one) indicate shorter tails. The more intuitive interpretation delivered by the other measures of kurtosis is that an increase in the value of any of these measures signifies an increase in kurtosis.

In fact, comparing their expressions, we see that the tail-weight factor is a special case of the inverse of the ratio-of-spread functions,

$$TWF(u) = \left[R\left(u, \frac{3}{4}\right) \right]^{-1}.$$

This inverse relation between the ratio-of-spread functions and the tail-weight factor suggests a newly proposed functional for kurtosis which is bounded. Because $S(u) > S(v)$ for $\frac{1}{2} < v < u < 1$, we have $R(u, v) > 1$, and hence the inverse of the ratio-of-spread functions is bounded, in effect, $0 < [R(u, v)]^{-1} < 1$. The new functional for kurtosis, to be called the κ -functional, is then defined as one minus the inverse of the ratio-of-spread functions and given, after simplification, by

$$\kappa(u, v) = 1 - [R(u, v)]^{-1} = \frac{S(u) - S(v)}{S(u)}, \quad \frac{1}{2} < v < u < 1. \quad (2.44)$$

The κ -functional is thus a bounded functional for kurtosis, $0 < \kappa(u, v) < 1$. More importantly, the κ -functional preserves the ordering \leq_s given above and, in doing so, adheres to the directional interpretation of kurtosis delivered by the majority of measures (an increase in value implies an increase in kurtosis).

The median, the spread function, the γ -functional and η -functional, and the ratio-of-spread functions and κ -functional will be the respective quantile-based measures of location, spread, skewness and kurtosis utilized in the rest of this thesis. Table 2.4 presents the expressions (and values) for these measures for the uniform, exponential and logistic distributions.

Table 2.4: Quantile-based measures of location, spread and shape for the uniform, exponential and logistic distributions.

Measure	Uniform	Exponential	Logistic
Median	$me = \alpha + \frac{1}{2}\beta$	$me = \alpha + \beta \log[2]$	$me = \alpha$
Spread function	$S(u) = (2u - 1)\beta$	$S(u) = \beta \log\left[\frac{u}{1-u}\right]$	$S(u) = 2\beta \log\left[\frac{u}{1-u}\right]$
γ -functional	$\gamma(u) = 0$	$\gamma(u) = -\frac{\log[4u(1-u)]}{\log\left[\frac{u}{1-u}\right]}$	$\gamma(u) = 0$
η -functional	$\eta(u, v) = 0$	$\eta(u, v) = -\frac{\log\left[\frac{u(1-u)}{v(1-v)}\right]}{\log\left[\frac{v}{1-v}\right]}$	$\eta(u, v) = 0$
Ratio-of-spread functions	$R(u, v) = \frac{2u-1}{2v-1}$	$R(u, v) = \frac{\log\left[\frac{u}{1-u}\right]}{\log\left[\frac{v}{1-v}\right]}$	$R(u, v) = \frac{\log\left[\frac{u}{1-u}\right]}{\log\left[\frac{v}{1-v}\right]}$
κ -functional	$\kappa(u, v) = \frac{2(u-v)}{2u-1}$	$\kappa(u, v) = \frac{\log\left[\frac{u(1-v)}{v(1-u)}\right]}{\log\left[\frac{u}{1-u}\right]}$	$\kappa(u, v) = \frac{\log\left[\frac{u(1-v)}{v(1-u)}\right]}{\log\left[\frac{u}{1-u}\right]}$

Because they are symmetric distributions, both the uniform and logistic distributions have $\gamma(u) = \eta(u, v) = 0$. Regarding kurtosis, it is interesting to note that the ratio-of-spread functions of the exponential and logistic distributions are exactly the same, as are the κ -functional of these distributions. Recall that these two distributions are special cases of the SLD, introduced in Example 2.3.4. The SLD's quantile-based measures of location, spread and shape are considered in Example 2.6.1.

Example 2.6.1

Substituting the SLD's quantile function in (2.15) into the expressions for the median in (2.34), the spread function in (2.35), the γ -functional and η -functional in (2.37) and (2.38), and the ratio-of-spread functions and κ -functional in (2.43) and (2.44) and simplifying gives

$$me = \alpha + \beta(2\delta - 1)\log[2],$$

$$S(u) = \beta \log\left[\frac{u}{1-u}\right], \quad (2.45)$$

$$\gamma(u) = -\frac{(2\delta - 1)\log[4u(1-u)]}{\log\left[\frac{u}{1-u}\right]},$$

$$\eta(u, v) = -\frac{(2\delta - 1)\log\left[\frac{u(1-u)}{v(1-v)}\right]}{\log\left[\frac{v}{1-v}\right]},$$

$$R(u, v) = \frac{\log\left[\frac{u}{1-u}\right]}{\log\left[\frac{v}{1-v}\right]} \quad (2.46)$$

and

$$\kappa(u, v) = \frac{\log\left[\frac{u(1-v)}{v(1-u)}\right]}{\log\left[\frac{u}{1-u}\right]}, \quad (2.47)$$

where $\frac{1}{2} < v < u < 1$. The shape functionals of the SLD are location- and scale-invariant in that they are all independent of the location and scale parameters (α and β). Furthermore, the two kurtosis functionals of the SLD in (2.46) and (2.47) are independent of the shape parameter, δ . In Section 2.7 this result is explained.

□

2.7 SKEWNESS-INVARIANT KURTOSIS MEASURES

Careful examination of the various kurtosis measures discussed in Section 2.6 reveals that they are all of the general form

$$\frac{\sum_{j=1}^{n_1} a_j S(u_j)}{\sum_{k=1}^{n_2} b_k S(u_k)} = \frac{\sum_{j=1}^{n_1} a_j \left(Q(u_j) - Q(1-u_j) \right)}{\sum_{k=1}^{n_2} b_k \left(Q(u_k) - Q(1-u_k) \right)}, \quad (2.48)$$

where $a_j : j = 1, 2, \dots, n_1$ and $b_k : k = 1, 2, \dots, n_2$ are constants with n_1 and n_2 positive integers. In effect, all the kurtosis measures in (2.39) to (2.44) are defined as ratios of linear combinations of spread functions. The general form in (2.48) was considered by Jones *et al.* (2011) in a seminal discussion on skewness-invariant kurtosis measures.

Before focusing on skewness-invariance, it should be noted that all kurtosis measures of the general form (2.48) are location- and scale-invariant. It was already indicated through (2.36) that the spread function is location-invariant. Scale-invariance is imposed via ratios in that (2.48) can be rewritten as

$$\begin{aligned} \frac{\sum_{j=1}^{n_1} a_j S(u_j)}{\sum_{k=1}^{n_2} b_k S(u_k)} &= \frac{\sum_{j=1}^{n_1} a_j \beta \left(Q_0(u_j) - Q_0(1-u_j) \right)}{\sum_{k=1}^{n_2} b_k \beta \left(Q_0(u_k) - Q_0(1-u_k) \right)} \\ &= \frac{\sum_{j=1}^{n_1} a_j \left(Q_0(u_j) - Q_0(1-u_j) \right)}{\sum_{k=1}^{n_2} b_k \left(Q_0(u_k) - Q_0(1-u_k) \right)}. \end{aligned}$$

Now, suppose the distribution under consideration possesses a shape parameter, denoted in general by ζ (depending on the distribution under consideration ζ will be either λ or δ), and it is possible to express the spread function for this distribution by

$$S(u) = \beta g(\zeta)G(u). \quad (2.49)$$

That is, assume the spread function can be expressed as the product of β (the scale parameter) and two other components, where the first component, $g(\zeta)$, is a function of ζ but independent of u , and the second component, the function $G(u)$, is independent of ζ . Then the distribution will have quantile-based kurtosis measures of the general form

$$\begin{aligned} \frac{\sum_{j=1}^{n_1} a_j S(u_j)}{\sum_{k=1}^{n_2} b_k S(u_k)} &= \frac{\sum_{j=1}^{n_1} a_j \beta g(\zeta) G(u_j)}{\sum_{k=1}^{n_2} b_k \beta g(\zeta) G(u_k)} \\ &= \frac{\sum_{j=1}^{n_1} a_j G(u_j)}{\sum_{k=1}^{n_2} b_k G(u_k)}, \end{aligned}$$

which are skewness-invariant with respect to ζ .

Example 2.7.1

Comparing the spread function of the SLD in (2.45) with (2.49), it follows that $g(\zeta) = 1$, where $\zeta = \delta$ is the shape parameter, and $G(u) = \log\left[\frac{u}{1-u}\right]$ for the SLD. The SLD thus has skewness-invariant quantile-based kurtosis measures, since

$$\frac{\sum_{j=1}^{n_1} a_j G(u_j)}{\sum_{k=1}^{n_2} b_k G(u_k)} = \frac{\sum_{j=1}^{n_1} a_j \log\left[\frac{u_j}{1-u_j}\right]}{\sum_{k=1}^{n_2} b_k \log\left[\frac{u_k}{1-u_k}\right]}. \quad (2.50)$$

Examples of these skewness-invariant measures include the ratio-of-spread functions and the κ -functional, given in (2.46) and (2.47).

□

Example 2.7.2

Recently Lan & Leemis (2008) introduced the logistic-exponential distribution, a flexible survival distribution with half-infinite support, $[0, \infty)$, and quantile function given by

$$Q(p) = \frac{1}{b} \log \left[1 + \left(\frac{p}{1-p} \right)^{\frac{1}{c}} \right],$$

where $b > 0$ and $c > 0$ are respectively scale and shape parameters. For $c > 1$ the logistic-exponential distribution is unimodal and has upside-down bathtub-shaped failure rates. The distribution is J-shaped for $c \leq 1$ and reduces to the exponential distribution with a constant failure rate when $c = 1$. Bathtub-shaped failure rates are obtained for $c < 1$.

In this thesis a slight reparameterization of the logistic-exponential distribution is considered. This parameterization is obtained by letting $\beta = \frac{1}{b}$ and $\lambda = \frac{1}{c}$ and by including a location parameter, α , not restricted in sign (in effect, α may assume negative values), so that the distribution has support $[\alpha, \infty)$. The corresponding quantile function is

$$Q(p) = \alpha + \beta \log \left[1 + \left(\frac{p}{1-p} \right)^{\lambda} \right].$$

See Tables 2.10 to 2.12 in Section 2.14.3 for the distribution's other properties and functions.

The spread function of the logistic-exponential distribution for $\frac{1}{2} < u < 1$ is

$$\begin{aligned} S(u) &= Q(u) - Q(1-u) \\ &= \left(\alpha + \beta \log \left[1 + \left(\frac{u}{1-u} \right)^{\lambda} \right] \right) - \left(\alpha + \beta \log \left[1 + \left(\frac{1-u}{u} \right)^{\lambda} \right] \right) \\ &= \beta \log \left[\frac{1 + \left(\frac{u}{1-u} \right)^{\lambda}}{1 + \left(\frac{1-u}{u} \right)^{\lambda}} \right] \\ &= \beta \log \left[\left(\frac{u}{1-u} \right)^{\lambda} \right] \quad \text{since } \frac{1+z}{1+z^{-1}} = z \text{ for } z \neq 0 \\ &= \beta \lambda \log \left[\frac{u}{1-u} \right]. \end{aligned}$$

It follows that $g(\zeta) = g(\lambda) = \lambda$, with $\zeta = \lambda$ the shape parameter, and $G(u) = \log \left[\frac{u}{1-u} \right]$. Thus

$$\frac{\sum_{j=1}^{n_1} a_j G(u_j)}{\sum_{k=1}^{n_2} b_k G(u_k)} = \frac{\sum_{j=1}^{n_1} a_j \log \left[\frac{u_j}{1-u_j} \right]}{\sum_{k=1}^{n_2} b_k \log \left[\frac{u_k}{1-u_k} \right]}$$

and the quantile-based kurtosis measures of the logistic-exponential distribution are hence skewness-invariant. Furthermore, as indicated in Table 2.14 and illustrated in Figure 2.8, the L -kurtosis ratio of the logistic-exponential distribution is $\tau_4 = \frac{1}{6}$ and hence also skewness-invariant with respect to the shape parameter.

□

2.8 PROPOSITION: QUANTILE-BASED DISTRIBUTIONS WITH SKEWNESS-INVARIANT KURTOSIS MEASURES

In this section the main proposition in the thesis is presented. This proposition provides a methodology for the construction of quantile-based families of distributions possessing skewness-invariant measures of kurtosis.

Proposition 2.8.1

Assume that X is a real-valued random variable with an asymmetric distribution on bounded or half-infinite support and with r^{th} order L -moment and r^{th} order L -moment ratio denoted by $L_{X;r}$ and $\tau_{X;r}$. Let $Q_{X;0}(p)$ denote the quantile function of the standard distribution of X . Suppose $Y = -X$ so that the standard distribution of Y is the reflection of the standard distribution of X about the line $x = 0$ with quantile function $Q_{Y;0}(p) = -Q_{X;0}(1-p)$. Consider a random variable W with quantile function

$$Q_W(p) = \alpha + \beta \left(\delta Q_{X;0}(p) - (1-\delta) Q_{X;0}(1-p) \right), \quad (2.51)$$

where α is a location parameter, $\beta > 0$ is a scale parameter and $0 \leq \delta \leq 1$ is a weight parameter.

(a) The first order L -moment of W is

$$L_{W;1} = \alpha + \beta(2\delta - 1)L_{X;1}, \quad (2.52)$$

its r^{th} order L -moment for $r > 1$ is

$$L_{W;r} = \beta(2\delta - 1)^{r \bmod 2} L_{X;r}, \quad (2.53)$$

and its r^{th} order L -moment ratio for $r > 2$ is

$$\tau_{W;r} = (2\delta - 1)^{r \bmod 2} \tau_{X;r}. \quad (2.54)$$

(b) The L -skewness ratio of W is bounded by $-\tau_{X;3} \leq \tau_{W;3} \leq \tau_{X;3}$.

(c) The L -kurtosis ratio of W , $\tau_{W;4}$, is skewness-invariant with respect to δ .

(d) The spread function of W is

$$S_W(u) = \beta \left(Q_{X;0}(u) - Q_{X;0}(1-u) \right), \quad \frac{1}{2} < u < 1,$$

so that W has quantile-based kurtosis measures which are skewness-invariant with respect to δ , given in general form by

$$\frac{\sum_{j=1}^{n_1} a_j S_W(u_j)}{\sum_{k=1}^{n_2} b_k S_W(u_k)} = \frac{\sum_{j=1}^{n_1} a_j \left(Q_{X;0}(u_j) - Q_{X;0}(1-u_j) \right)}{\sum_{k=1}^{n_2} b_k \left(Q_{X;0}(u_k) - Q_{X;0}(1-u_k) \right)}, \quad (2.55)$$

where $a_j : j = 1, 2, \dots, n_1$ and $b_k : k = 1, 2, \dots, n_2$ are constants with n_1 and n_2 positive integers.

Proof

(a) Substituting (2.51) into (2.23), the r^{th} order L -moment of W can be expressed as

$$\begin{aligned} L_{W;r} &= \int_0^1 Q_W(p) P_{r-1}^*(p) dp \\ &= \alpha \int_0^1 P_{r-1}^*(p) dp + \beta \left(\delta \int_0^1 Q_{X;0}(p) P_{r-1}^*(p) dp - (1-\delta) \int_0^1 Q_{X;0}(1-p) P_{r-1}^*(p) dp \right) \\ &= \alpha^* + \beta^*. \end{aligned}$$

Using (2.93) given in Section 2.14.2,

$$\begin{aligned} \beta^* &= \beta \left(\delta \int_0^1 Q_{X;0}(p) P_{r-1}^*(p) dp - (1-\delta)(-1)^{r-1} \int_0^1 Q_{X;0}(1-p) P_{r-1}^*(1-p) dp \right) \\ &= \beta \left(\delta \int_0^1 Q_{X;0}(p) P_{r-1}^*(p) dp - (1-\delta)(-1)^{r-1} \int_0^1 Q_{X;0}(p) P_{r-1}^*(p) dp \right) \\ &= \beta(2\delta - 1)^{r \bmod 2} \int_0^1 Q_{X;0}(p) P_{r-1}^*(p) dp \\ &= \beta(2\delta - 1)^{r \bmod 2} L_{X;r}. \end{aligned}$$

From (2.94) in Section 2.14.2 we have that $\alpha^* = \alpha$ for the first order L -moment and $\alpha^* = 0$ for higher order L -moments. Using these expressions for α^* and β^* gives (2.52) and (2.53), while (2.54) follows directly from the formula for the L -moment ratio given in (2.25).

- (b) Since $0 \leq \delta \leq 1$, it follows from (2.54) that, in general for r odd, the r^{th} order L -moment ratio of W is bounded by $-\tau_{X;r} \leq \tau_{W;r} \leq \tau_{X;r}$. The L -skewness ratio of W is therefore bounded by $-\tau_{X;3} \leq \tau_{W;3} \leq \tau_{X;3}$.
- (c) From (2.54) it follows that, in general for r even, $\tau_{W;r} = \tau_{X;r}$. Specifically $\tau_{W;4} = \tau_{X;4}$ and the L -kurtosis ratio of W is hence independent of δ and skewness-invariant.

(d) The spread function of W is obtained by substituting the quantile function of W , given in (2.51), into the expression for the spread function in (2.35) and simplifying. The general form of the quantile-based kurtosis measures in (2.55) follows directly.

■

Example 2.8.1

Consider X having a standard exponential distribution with, as given for example by Hosking (1986), $L_{X;1} = 1$, $L_{X;r} = \frac{1}{r(r-1)}$ for $r > 1$ and $\tau_{X;r} = \frac{2}{r(r-1)}$ for $r > 2$, and hence $L_{X;2} = \frac{1}{2}$, $\tau_{X;3} = \frac{1}{3}$ and $\tau_{X;4} = \frac{1}{6}$. Using (2.52), (2.53) and (2.54), the SLD then has

$$L_1 = \alpha + \beta(2\delta - 1), \quad (2.56)$$

$$L_r = \frac{\beta(2\delta - 1)^{r \bmod 2}}{r(r-1)}, \quad r > 1, \quad (2.57)$$

and

$$\tau_r = \frac{2(2\delta - 1)^{r \bmod 2}}{r(r-1)}, \quad r > 2. \quad (2.58)$$

In particular the L -scale, L -skewness ratio and L -kurtosis ratio of the SLD are

$$L_2 = \frac{1}{2}\beta, \quad (2.59)$$

$$\tau_3 = \frac{1}{3}(2\delta - 1) \quad (2.60)$$

and

$$\tau_4 = \frac{1}{6}. \quad (2.61)$$

So, as with the SLD's quantile-based kurtosis measures in (2.50), the L -kurtosis ratio of the SLD in (2.61) is skewness-invariant with respect to δ . Note furthermore that, because $0 \leq \delta \leq 1$, the SLD has $-\frac{1}{3} \leq \tau_3 \leq \frac{1}{3}$.

Comparing the L -moments of the SLD in (2.56), (2.59), (2.60) and (2.61) with its conventional moments in (2.19) to (2.22), it is evident that it is more expedient to characterize the SLD with its L -moments than with its moments, since the expressions for the L -moments are much simpler than the corresponding expressions for the moments. Also, simple general expressions exist for the SLD's r th order L -moment, (2.57), and r th order L -moment ratio, (2.58). There are no such general expressions for the SLD's moments or moment ratios.

□

2.9 METHOD OF L -MOMENTS ESTIMATION

The fitting of a probability distribution to an observed data set is a common problem in statistical modeling. Hosking (1986, 1990) proposed that, given that the data set under consideration is assumed to be a random sample of size n from the distribution to be fitted and this distribution has finite variance and contains m unknown parameters, the parameters of the distribution be estimated through method of L -moments estimation. With method of L -moments estimation the first m sample L -moments are equated to the corresponding population L -moments. That is, if the parameters $\theta_r : r = 1, 2, \dots, m$ and the L -moments $L_r : r = 1, 2, \dots, m$ of a probability distribution are related by

$$\theta_r = g(L_1, L_2, \dots, L_m), \quad r = 1, 2, \dots, m,$$

then the estimators obtained with method of L -moments estimation are given by

$$\hat{\theta}_r = g(\ell_1, \ell_2, \dots, \ell_m), \quad r = 1, 2, \dots, m,$$

where $\ell_r : r = 1, 2, \dots, m$ are the sample L -moments calculated from the random sample with (2.28).

Hosking (1986) and Hosking & Wallis (1997) presented method of L -moments estimators for various well-known distributions. As with other estimation methods, the method of L -moments estimators do not possess closed-form expressions for all distributions. However, if a quantile-based distribution is constructed using Proposition 2.8.1 and possesses at most two shape parameters, so that its quantile function is of the form (2.51) where one of the shape parameters is a weight parameter, $0 \leq \delta \leq 1$, then closed-form expressions will be available for the method of L -moments estimators. This is illustrated in Example 2.9.1 for the SLD.

As pointed out by Hosking (1986, 1990), in general it is difficult to derive exact sampling distributions of sample L -moments and, as a result, exact distributions for the method of L -moments estimators. Therefore asymptotic distribution theory must be utilized. Using asymptotic theory for linear combinations of order statistics, developed by Chernoff *et al.* (1967), Moore (1968) and Stigler (1974, 1979), Hosking (1986) proved that, if X is a real-valued random variable and the probability distribution of X has cumulative distribution function $F(x)$, quantile density function $q(p)$ and finite variance, then, as $n \rightarrow \infty$,

$$n^{\frac{1}{2}}(\ell_r - L_r), \quad r = 1, 2, \dots, m,$$

converge in distribution to the multivariate normal distribution, $N(0, \Lambda)$, with $\Lambda_{r,s} : r, s = 1, 2, \dots, m$ the elements of the covariance matrix Λ given by

$$\begin{aligned}
 \Lambda_{r,s} &= \lim_{n \rightarrow \infty} n \operatorname{cov}(\ell_r, \ell_s) \\
 &= \iint_{x < y} \left(P_{r-1}^*(F(x))P_{s-1}^*(F(y)) + P_{s-1}^*(F(x))P_{r-1}^*(F(y)) \right) F(x)(1-F(y)) dx dy \quad (2.62) \\
 &= \iint_{0 \ 0}^{1 \ 1} \left(P_{r-1}^*(u)P_{s-1}^*(v) + P_{s-1}^*(u)P_{r-1}^*(v) \right) u(1-v)q(u)q(v) dudv,
 \end{aligned}$$

where $P_r^*(p)$ is the r^{th} order shifted Legendre polynomial given in (2.24). Consequently, as $n \rightarrow \infty$,

$$n^{\frac{1}{2}}(\hat{\theta}_r - \theta_r), \quad r = 1, 2, \dots, m,$$

converge in distribution to the multivariate normal distribution, $N(0, \Theta)$, where

$\Theta_{r,s} : r, s = 1, 2, \dots, m$ are the elements of the covariance matrix $\Theta = G\Lambda G^T$, given by

$$\Theta_{r,s} = \sum_{t=1}^m \sum_{u=1}^m G_{r,t} \Lambda_{t,u} G_{s,u}$$

with

$$G_{r,s} = \frac{\partial \theta_r}{\partial L_s}. \quad (2.63)$$

That is, the asymptotic variances of and covariances between the method of L -moments estimators, $\hat{\theta}_r : r = 1, 2, \dots, m$, can be obtained with

$$n \operatorname{var} \begin{bmatrix} \hat{\theta}_1 \\ \hat{\theta}_2 \\ \vdots \\ \hat{\theta}_m \end{bmatrix} \approx \begin{bmatrix} \Theta_{1,1} & \Theta_{1,2} & \cdots & \Theta_{1,m} \\ \Theta_{2,1} & \Theta_{2,2} & \cdots & \Theta_{2,m} \\ \vdots & \vdots & \ddots & \vdots \\ \Theta_{m,1} & \Theta_{m,2} & \cdots & \Theta_{m,m} \end{bmatrix}.$$

Note that both Λ and Θ are symmetric matrices with $\Lambda_{r,s} = \Lambda_{s,r}$ and $\Theta_{r,s} = \Theta_{s,r}$.

Example 2.9.1

Because the SLD has three parameters to be estimated, $\theta_1 = \alpha$, $\theta_2 = \beta$, and $\theta_3 = \delta$, the first three L -moments of the SLD are utilized in method of L -moments estimation. The method of L -moments estimates for the SLD and their asymptotic standard errors can be computed using the following simple estimation algorithm:

Step 1

Use (2.30), (2.31) and (2.32) to calculate the first three sample L -moments, ℓ_1 , ℓ_2 and ℓ_3 , and then (2.29) to calculate the sample L -skewness ratio, t_3 . Since the SLD has $-\frac{1}{3} \leq \tau_3 \leq \frac{1}{3}$, check whether $-\frac{1}{3} \leq t_3 \leq \frac{1}{3}$. If so, proceed with Step 2. If not, the SLD cannot be fitted to the data.

Step 2

The method of L -moments estimators for δ and β are obtained by inverting (2.60) and (2.59), giving

$$\begin{aligned}\hat{\delta} &= \frac{1}{2}(1 + 3t_3) \\ &= \frac{1}{2}\left(1 + 3\frac{\ell_3}{\ell_2}\right)\end{aligned}\tag{2.64}$$

and

$$\hat{\beta} = 2\ell_2.\tag{2.65}$$

From (2.56) it follows that the location parameter is estimated with

$$\begin{aligned}\hat{\alpha} &= \ell_1 - \hat{\beta}(2\hat{\delta} - 1) \\ &= \ell_1 - 6\ell_3,\end{aligned}\tag{2.66}$$

where the final result is obtained by substituting the expressions for $\hat{\beta}$ in (2.65) and $\hat{\delta}$ in (2.64) into (2.66) and simplifying.

Step 3

Finally the asymptotic standard errors of the method of L -moments estimators for the SLD's parameters can be calculated with

$$\text{s.e.}[\hat{\alpha}] = \beta \sqrt{\frac{1}{15n} \left(57 + (125\pi^2 - 1308)\omega \right)},\tag{2.67}$$

$$\text{s.e.}[\hat{\beta}] = \beta \sqrt{\frac{4}{3n} \left(1 - (\pi^2 - 8)\omega \right)}\tag{2.68}$$

and

$$\text{s.e.}[\hat{\delta}] = \sqrt{\frac{1}{15n} \left(8 - \omega \left(397 + 160\omega - 20\pi^2(\omega + 2) \right) \right)},\tag{2.69}$$

where $\omega = \delta(1 - \delta)$. The derivation of these expressions for the standard errors is done in Section 2.13.2.

■

Note that, even though ℓ_4 is not used in the estimation of any of the parameters of the SLD in Step 2, one can calculate its value with (2.33) and then use it to calculate the value of the sample L -kurtosis ratio, t_4 , with (2.29). Because the SLD has $\tau_4 = \frac{1}{6}$, the value of t_4 gives an indication whether the SLD is a plausible distribution for the data. If the value of t_4 deviates drastically from $\tau_4 = \frac{1}{6}$, one can expect that the SLD will not fit the data well. Formal methods for distribution validation are presented in Section 2.10.

To illustrate the estimation algorithm for the SLD, consider a data set consisting of the peak concentrations (in percent) of toxic gas released in a series of atmospheric diffusion experiments carried out by Hall (1991). Hankin & Lee (2006) fitted the Davies distribution to this data set using both maximum likelihood estimation and a logged regression estimation method.

Figure 2.16 shows a histogram for the data set. The sample L -moment and L -moment ratio values for the data set, consisting of $n = 100$ observations, are given in Table 2.5. Since $-\frac{1}{3} \leq t_3 \leq \frac{1}{3}$, the SLD can be fitted to the data set. Note furthermore that the value of t_4 is reasonably close to $\tau_4 = \frac{1}{6}$.

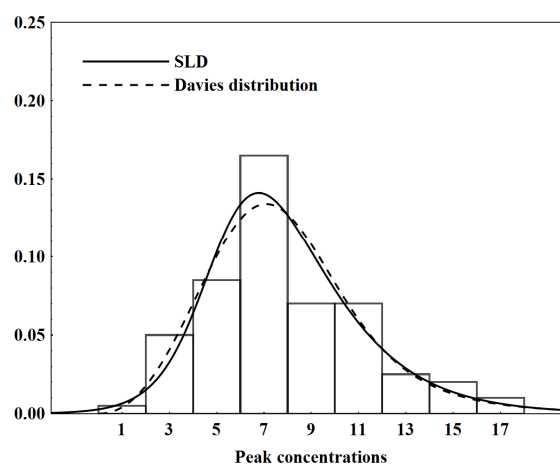


Figure 2.16: Histogram of the peak concentrations (in percent) of toxic gas together with the probability density functions of the fitted SLD and Davies distribution.

Table 2.5: Sample size, sample L -moment values and data range for the peak concentrations (in percent) of toxic gas.

n	ℓ_1	ℓ_2	t_3	t_4	Data range
100	7.9384	1.8432	0.1293	0.1451	[1.701, 16.910]

Table 2.6 presents the parameter estimates of the SLD obtained with method of L -moments estimation. The standard error of each estimate is given in parentheses below the estimate. In Figure 2.16 the density curve of the fitted SLD is superimposed on the histogram, as is, for comparison purposes, the density curve of the Davies distribution fitted with maximum likelihood estimation by Hankin & Lee (2006).

Table 2.6: Parameter estimates with asymptotic standard errors* for the SLD fitted to the peak concentrations (in percent) of toxic gas.

$\hat{\alpha}$	$\hat{\beta}$	$\hat{\delta}$
6.5085 (0.6111)	3.6863 (0.3305)	0.6940 (0.0784)

* Standard errors given in parentheses.

□

2.10 Q-Q PLOTS AND GOODNESS-OF-FIT

Model validation for quantile-based distributions proceeds as for other distributions. Apart from histograms of the data with density curve(s) of the fitted distribution(s) overlaid (as for example in Figure 2.16), graphical displays include quantile-quantile ($Q-Q$) plots of the points $\hat{Q}(p_{i:n})$ versus $x_{i:n}$ for $i=1, 2, \dots, n$, where $\hat{Q}(p_{i:n})$ denotes the empirical quantile function of the fitted distribution and $x_{i:n}$ is the i^{th} value in the ordered data set $x_{1:n} \leq x_{2:n} \leq \dots \leq x_{n:n}$. A number of different plotting positions, $p_{i:n}$, have been suggested in the statistical literature – see Thas (2010). The general form proposed by Blom (1958) is

$$p_{i:n} = \frac{i-c}{n+1-2c}.$$

In this thesis $c = \frac{1}{3}$ is used, giving

$$p_{i:n} = \frac{i - \frac{1}{3}}{n + \frac{1}{3}}, \quad (2.70)$$

which provides the ideal depth of the i^{th} order statistic from a sample of size n as suggested by Hoaglin (1983) in that, for any continuous distribution, this choice of $p_{i:n}$ very closely approximates the median of the distribution of the i^{th} order statistic.

Goodness-of-fit can further be assessed by using classical tests such as the Kolmogorov-Smirnov D_n statistic, the Anderson-Darling A_n statistic and the Cramér-von Mises W_n statistic. For a detailed account of these three tests, see Thas (2010). These tests are all based on the empirical distribution function, $\hat{F}(x_{i:n})$. A slight complication for quantile-based distributions is that, because closed-form expressions for their cumulative distribution functions are not available, $\hat{F}(x_{i:n})$ must be calculated numerically by the reverse transformation.

The parametric bootstrap can be used to estimate p -values for D_n , A_n and W_n (see Appendix B of Thas (2010) for details). In this thesis $N = 10\,000$ bootstrap samples will be used. When sampling from a fitted quantile-based distribution, bootstrap samples may be obtained for which the distribution cannot be refitted due to the values of t_3 and t_4 for these samples lying outside the (τ_3, τ_4) space attained by the distribution. The number of valid bootstrap samples will be denoted N_V .

The abovementioned graphical displays and tests are useful for verifying whether a fitted distribution adequately explains the observed data set. To compare the fit of various distributions and find the “best” of these fits, the average scaled absolute error (ASAE) introduced by Castillo & Hadi (1997),

$$\text{ASAE} = \frac{1}{n} \sum_{i=1}^n \frac{|x_{i:n} - \hat{Q}(p_{i:n})|}{x_{n:n} - x_{1:n}},$$

can be used. Smaller ASAE values are indicative of better fits. See Castillo *et al.* (2005) for its application in extreme value modeling. Note that $p_{i:n}$ as given by (2.70) is used in this thesis, whereas Castillo & Hadi (1997) and Castillo *et al.* (2005) used $p_{i:n} = \frac{i}{n+1}$, that is, $p_{i:n}$ with $c = 0$.

Example 2.10.1

Figure 2.17 depicts Q - Q plots for the SLD fitted to the peak concentrations (in percent) of toxic gas in Example 2.9.1 with method of L -moments estimation, and for the Davies distribution fitted by Hankin & Lee (2006) with maximum likelihood estimation. These plots indicate that the SLD fits the data slightly better in the upper tail, while the Davies distribution provides a slightly better fit in the lower tail.

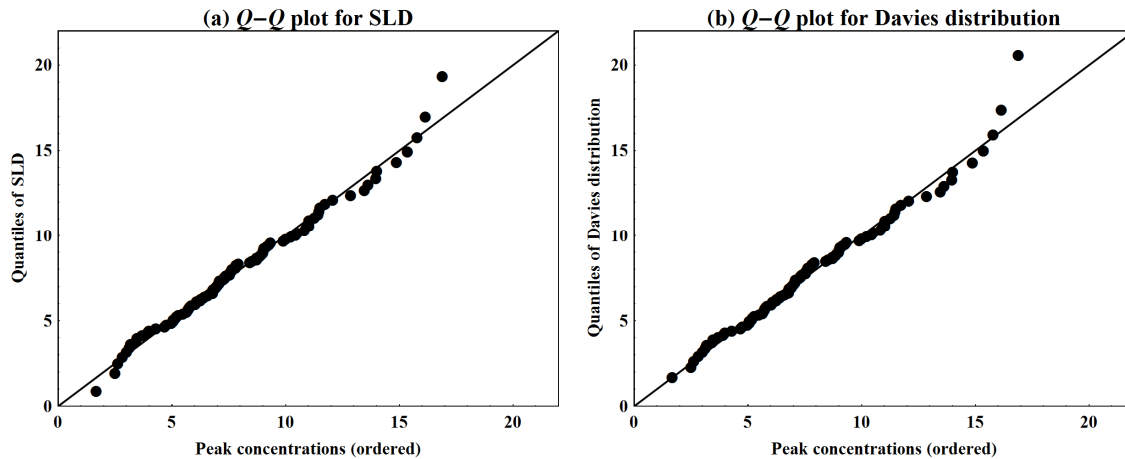


Figure 2.17: $Q-Q$ plots for the SLD and the Davies distribution fitted to the peak concentrations (in percent) of toxic gas.

To calculate p -values for goodness-of-fit tests, tabulated in Table 2.7 along with the goodness-of-fit statistics, $N = N_V = 10\,000$ bootstrap samples were used. In effect, the SLD could be refitted to all generated bootstrap samples. All three goodness-of-fit tests suggest that the SLD provides an adequate fit to the data. The fitted SLD has an ASAE value of 0.0154, which is lower than the ASAE value of 0.0166 attained for the Davies distribution fitted by Hankin & Lee (2006) with maximum likelihood estimation.

Table 2.7: Goodness-of-fit statistics with p -values* for the SLD fitted to the peak concentrations (in percent) of toxic gas.

D_n	A_n	W_n
0.4892 (0.5251)	0.2489 (0.5868)	0.0351 (0.6092)

* p -values given in parentheses.

□

2.11 TAIL BEHAVIOR

The tail behavior of the density curve of a distribution is usually analyzed through the probability density function, $f(x)$, of the distribution. But, as explained in Section 2.2.3, no closed-form expression exists for the probability density function of a quantile-based distribution. The density quantile function, $f_p(p)$, must therefore be utilized. To determine the values which the density curve approaches at the end points of the left tail and the right tail respectively, one has to compute $\lim_{p \rightarrow 0} f_p(p)$ and $\lim_{p \rightarrow 1} f_p(p)$. The value which the slope

of the density curve approaches at the end point of each tail can be obtained by computing $\lim_{p \rightarrow 0} \xi(p)$ and $\lim_{p \rightarrow 1} \xi(p)$, where

$$\xi(p) = -\frac{dq(p)}{dp} \frac{1}{(q(p))^3}, \quad (2.71)$$

derived by King (1999), is the derivative of the probability density function expressed in terms of p instead of x . In effect, $\xi(p)$ represents $\frac{df(x)}{dx}$ in the quantile statistical universe.

Example 2.11.1

For the SLD, the values which its density curve as well as the slope of its density curve approach at the end point of each tail are determined using the SLD's density quantile function, given in (2.17), and the function

$$\xi(p) = -\frac{p(1-p)\left(\delta p^2 - (1-\delta)(1-p)^2\right)}{\beta^2\left(\delta p + (1-\delta)(1-p)\right)^3}.$$

The values obtained are summarized in Table 2.8. For $\delta = 1$ the values given are for the exponential distribution, while the values for $\delta = 0$ are for the reflected exponential distribution. For $0 < \delta < 1$, the density curve and the slope of the density curve approach zero at both tails, which is equivalent to the tail behavior of the logistic distribution (in effect, the SLD with $\delta = \frac{1}{2}$).

Table 2.8: The values approached by the density curve and the slope of the density curve of the SLD at the end-points of the tails.

Shape parameter values	Density curve		Slope of density curve	
	Left tail	Right tail	Left tail	Right tail
$\delta = 0$	0	$\frac{1}{\beta}$	0	$\frac{1}{\beta^2}$
$0 < \delta < 1$	0	0	0	0
$\delta = 1$	$\frac{1}{\beta}$	0	$-\frac{1}{\beta^2}$	0

□

2.12 CONCLUSION

In this chapter functions, methods and measures for quantile modeling were presented. It was shown how quantile-based distributions can be developed with a set of construction rules based on Q -transformations.

Specifically Proposition 2.8.1 outlined a quantile-based methodology for obtaining distributions with skewness-invariant measures of kurtosis and, as a result, closed-form expressions for the distributions' method of L -moments estimators and their asymptotic standard errors. The methodology was illustrated with the SLD.

In Chapter 4 the methodology outlined in Proposition 2.8.1 is used to derive a special type of the generalized lambda distribution, of which the SLD is a limiting case. Before doing so, the properties of two existing types of the generalized lambda distribution are presented in Chapter 3.

2.13 DERIVATIONS

In Section 2.13.1 below formulae for the moments of the SLD are derived. The covariance matrix for the method of L -moments estimators of the SLD is derived in Section 2.13.2.

2.13.1 MOMENTS OF SLD

Lemma 2.13.1

The integral

$$\Psi(j, k) = \int_0^1 (\log[p])^j (\log[1-p])^k dp, \quad j, k = 0, 1, 2, \dots \quad (2.72)$$

is encountered in the derivation of the formulae for the moments of the SLD. Since

$$(\log[p])^j = \frac{\partial^j}{\partial u^j} (p^u) \Big|_{u=0}, \quad j = 0, 1, 2, \dots$$

and

$$(\log[1-p])^k = \frac{\partial^k}{\partial v^k} ((1-p)^v) \Big|_{v=0}, \quad k = 0, 1, 2, \dots,$$

the integral in (2.72) can be solved using

$$\begin{aligned} \Psi(j, k) &= \frac{\partial^{j+k}}{\partial u^j \partial v^k} \left(\int_0^1 p^u (1-p)^v dp \right) \Big|_{u=v=0} \\ &= \frac{\partial^{j+k}}{\partial u^j \partial v^k} (\mathbf{B}(u+1, v+1)) \Big|_{u=v=0}, \end{aligned}$$

where $\mathbf{B}(a, b) = \frac{\Gamma(a)\Gamma(b)}{\Gamma(a+b)}$ is the beta function with $\Gamma(a)$ the gamma function (see Section 2.14.1). In particular, to derive the formulae for the first four moments of the SLD, $\Psi(i, 0) = \Psi(0, i)$ for $i = 1, 2, 3, 4$ and $\Psi(j, k)$ for $j = 0, 1, 2, 3$ and $k = 0, 1, 2, 3$ are used.

Note that $\frac{d}{da}\Gamma(a) = \Gamma(a)\psi(a)$ where $\psi(a)$ is the psi function (see Section 2.14.1).

Therefore the first partial derivative of the beta function with respect to u is

$$\begin{aligned}
 \frac{\partial}{\partial u} \mathbf{B}(u+1, v+1) &= \frac{\partial}{\partial u} \frac{\Gamma(u+1)\Gamma(v+1)}{\Gamma(u+v+2)} \\
 &= \frac{\Gamma(v+1)}{(\Gamma(u+v+2))^2} \left(\Gamma(u+v+2) \frac{\partial}{\partial u} \Gamma(u+1) - \Gamma(u+1) \frac{\partial}{\partial u} \Gamma(u+v+2) \right) \\
 &= \frac{\Gamma(v+1)}{(\Gamma(u+v+2))^2} \left(\Gamma(u+v+2)\Gamma(u+1)\psi(u+1) \right. \\
 &\quad \left. - \Gamma(u+1)\Gamma(u+v+2)\psi(u+v+2) \right) \\
 &= \mathbf{B}(u+1, v+1) \left(\psi(u+1) - \psi(u+v+2) \right),
 \end{aligned}$$

and likewise it can be shown that the first partial derivative of the beta function with respect to v is

$$\frac{\partial}{\partial v} \mathbf{B}(u+1, v+1) = \mathbf{B}(u+1, v+1) \left(\psi(v+1) - \psi(u+v+2) \right).$$

Because $\Gamma(a) = (a-1)!$, it follows that $\mathbf{B}(1,1) = \frac{\Gamma(1)\Gamma(1)}{\Gamma(2)} = 1$. From Gradshteyn & Ryzhik (2007, 8.366.1) we have $\psi(1) = -C$, where C is Euler's constant given in Section 2.14.1. Furthermore, using Gradshteyn & Ryzhik (2007, 8.365.4), $\psi(2) = 1 - C$. Hence

$$\Psi(1,0) = \Psi(0,1) = -1.$$

The second partial derivative of the beta function with respect to u is

$$\begin{aligned}
 \frac{\partial^2}{\partial u^2} \mathbf{B}(u+1, v+1) &= \frac{\partial}{\partial u} \left(\mathbf{B}(u+1, v+1) \left(\psi(u+1) - \psi(u+v+2) \right) \right) \\
 &= \left(\psi(u+1) - \psi(u+v+2) \right) \frac{\partial}{\partial u} \mathbf{B}(u+1, v+1) \\
 &\quad + \mathbf{B}(u+1, v+1) \frac{\partial}{\partial u} \left(\psi(u+1) - \psi(u+v+2) \right) \\
 &= \mathbf{B}(u+1, v+1) \left(\left(\psi(u+1) - \psi(u+v+2) \right)^2 \right. \\
 &\quad \left. + \left(\psi^{(1)}(u+1) - \psi^{(1)}(u+v+2) \right) \right),
 \end{aligned}$$

where $\psi^{(1)}(a)$ is the first derivative of the psi function (see again Section 2.14.1). Similarly the second partial derivative of the beta function with respect to v is

$$\begin{aligned} \frac{\partial^2}{\partial v^2} \mathbf{B}(u+1, v+1) &= \mathbf{B}(u+1, v+1) \left(\left(\psi(v+1) - \psi(u+v+2) \right)^2 \right. \\ &\quad \left. + \left(\psi^{(1)}(v+1) - \psi^{(1)}(u+v+2) \right) \right). \end{aligned}$$

Also,

$$\begin{aligned} \frac{\partial^2}{\partial u \partial v} \mathbf{B}(u+1, v+1) &= \frac{\partial}{\partial v} \left(\mathbf{B}(u+1, v+1) \left(\psi(u+1) - \psi(u+v+2) \right) \right) \\ &= \left(\psi(u+1) - \psi(u+v+2) \right) \frac{\partial}{\partial v} \mathbf{B}(u+1, v+1) \\ &\quad - \mathbf{B}(u+1, v+1) \psi^{(1)}(u+v+2) \\ &= \mathbf{B}(u+1, v+1) \left(\left(\psi(u+1) - \psi(u+v+2) \right) \left(\psi(v+1) - \psi(u+v+2) \right) \right. \\ &\quad \left. - \psi^{(1)}(u+v+2) \right). \end{aligned}$$

Then, since $\psi^{(1)}(1) = \frac{\pi^2}{6}$ from Gradshteyn & Ryzhik (2007, 8.366.8) and $\psi^{(1)}(2) = \frac{\pi^2}{6} - 1$ from Gradshteyn & Ryzhik (2007, 8.366.11),

$$\Psi(2,0) = \Psi(0,2) = 2$$

and

$$\Psi(1,1) = 2 - \frac{\pi^2}{6}.$$

Continuing this way, the higher-order partial derivatives of the beta function and the resulting expressions for $\Psi(i,0) = \Psi(0,i)$ and $\Psi(j,k)$ can be obtained. In general

$$\Psi(i,0) = \Psi(0,i) = (-1)^i i!$$

so that

$$\Psi(3,0) = \Psi(0,3) = -6$$

and

$$\Psi(4,0) = \Psi(0,4) = 24.$$

Also,

$$\Psi(2,1) = \Psi(1,2) = \frac{\pi^2}{3} + 2\zeta(3) - 6,$$

$$\Psi(2,2) = 24 - \frac{4\pi^2}{3} - \frac{\pi^4}{90} - 8\zeta(3)$$

and

$$\Psi(3,1) = \Psi(1,3) = 24 - \pi^2 - \frac{\pi^4}{15} - 6\zeta(3),$$

where $\zeta(a)$ is Riemann's zeta function (see again Section 2.14.1).

■

Theorem 2.13.1

Let X be a real-valued random variable which has a skew logistic distribution, denoted $X \sim \text{SLD}(\alpha, \beta, \delta)$, where α is the location parameter, $\beta > 0$ is the scale parameter and $0 \leq \delta \leq 1$ is the shape parameter. The mean, variance, skewness moment ratio and kurtosis moment ratio of X are then given by (2.19) to (2.22).

Proof

Let $Z = \frac{X-\alpha}{\beta} \sim \text{SLD}(0, 1, \delta)$ with quantile function given in (2.14). That is, consider the standard SLD with location parameter and scale parameter set to zero and one respectively. Then, for example, the fourth order uncorrected moment of Z is given by

$$\begin{aligned} E[Z^4] &= \int_0^1 (Q_{Z;0}(p))^4 dp \\ &= \int_0^1 \left((1-\delta) \log[p] - \delta \log[1-p] \right)^4 dp \\ &= (1-\delta)^4 \int_0^1 (\log[p])^4 dp - 4(1-\delta)^3 \delta \int_0^1 (\log[p])^3 \log[1-p] dp \\ &\quad + 6(1-\delta)^2 \delta^2 \int_0^1 (\log[p])^2 (\log[1-p])^2 dp \\ &\quad - 4(1-\delta) \delta^3 \int_0^1 \log[p] (\log[1-p])^3 dp + \delta^4 \int_0^1 (\log[1-p])^4 dp \\ &= (1-\delta)^4 \Psi(4,0) - 4(1-\delta)^3 \delta \Psi(3,1) + 6(1-\delta)^2 \delta^2 \Psi(2,2) - 4(1-\delta) \delta^3 \Psi(1,3) \\ &\quad + \delta^4 \Psi(0,4) \\ &= 2 \left(12\phi_4 - 2\omega\phi_2 \left(24 - \pi^2 - \frac{\pi^4}{15} - 6\zeta(3) \right) + 3\omega^2 \left(24 - \frac{4\pi^2}{3} - \frac{\pi^4}{90} - 8\zeta(3) \right) \right), \end{aligned}$$

where $\omega = \delta(1-\delta)$ and $\phi_k = \left((1-\delta)^k + (-1)^k \delta^k \right)$. Likewise it can be shown that

$$E[Z] = -\phi_1,$$

$$E[Z^2] = 2 \left(\phi_2 - \omega \left(2 - \frac{\pi^2}{6} \right) \right)$$

and

$$E[Z^3] = -3 \left(2\phi_3 + \omega \phi_1 \left(\frac{\pi^2}{3} + 2\zeta(3) - 6 \right) \right).$$

Since $X = \alpha + \beta Z$, the first four uncorrected moments of X are

$$\begin{aligned} \mu'_1 &= E[X] \\ &= \alpha + \beta E[Z] \\ &= \alpha - \beta \phi_1, \end{aligned} \tag{2.73}$$

$$\begin{aligned} \mu'_2 &= E[X^2] \\ &= \alpha^2 + 2\alpha\beta E[Z] + \beta^2 E[Z^2] \\ &= \alpha^2 - 2\alpha\beta\phi_1 + 2\beta^2 \left(\phi_2 - \omega \left(2 - \frac{\pi^2}{6} \right) \right), \end{aligned}$$

$$\begin{aligned} \mu'_3 &= E[X^3] \\ &= \alpha^3 + 3\alpha^2\beta E[Z] + 3\alpha\beta^2 E[Z^2] + \beta^3 E[Z^3] \\ &= \alpha^3 - 3\alpha^2\beta\phi_1 + 6\alpha\beta^2 \left(\phi_2 - \omega \left(2 - \frac{\pi^2}{6} \right) \right) - 3\beta^3 \left(2\phi_3 + \omega \phi_1 \left(\frac{\pi^2}{3} + 2\zeta(3) - 6 \right) \right), \end{aligned}$$

and

$$\begin{aligned} \mu'_4 &= E[X^4] \\ &= \alpha^4 + 4\alpha^3\beta E[Z] + 6\alpha^2\beta^2 E[Z^2] + 4\alpha\beta^3 E[Z^3] + \beta^4 E[Z^4] \\ &= \alpha^4 - 4\alpha^3\beta\phi_1 + 12\alpha^2\beta^2 \left(\phi_2 - \omega \left(2 - \frac{\pi^2}{6} \right) \right) - 12\alpha\beta^3 \left(2\phi_3 + \omega \phi_1 \left(\frac{\pi^2}{3} + 2\zeta(3) - 6 \right) \right) \\ &\quad + 2\beta^4 \left(12\phi_4 - 2\omega\phi_2 \left(24 - \pi^2 - \frac{\pi^4}{15} - 6\zeta(3) \right) + 3\omega^2 \left(24 - \frac{4\pi^2}{3} - \frac{\pi^4}{90} - 8\zeta(3) \right) \right). \end{aligned}$$

The first four corrected moments of X are then

$$\begin{aligned} \mu_1 &= E[X - E[X]] = 0, \\ \mu_2 &= E[(X - E[X])^2] \\ &= \mu'_2 - (\mu'_1)^2 \\ &= \beta^2 \left(\phi_1^2 + \frac{\pi^2}{3} \omega \right), \end{aligned} \tag{2.74}$$

$$\begin{aligned}
 \mu_3 &= E[(X - E[X])^3] \\
 &= \mu'_3 - 3\mu'_2\mu'_1 + 2(\mu'_1)^3 \\
 &= \beta^3 \left(2\phi_1 \left(\omega \left(4 - 3\zeta(3) \right) - 1 \right) \right),
 \end{aligned} \tag{2.75}$$

and

$$\begin{aligned}
 \mu_4 &= E[(X - E[X])^4] \\
 &= \mu'_4 - 4\mu'_3\mu'_1 + 6\mu'_2(\mu'_1)^2 - 3(\mu'_1)^4 \\
 &= \beta^4 \left(9 + \omega \left(2 \left(\phi_1^2 \pi^2 - 4 \right) + (9\omega - 4) \left(16 - \frac{\pi^4}{15} \right) \right) \right),
 \end{aligned} \tag{2.76}$$

where each moment's final expression is found after extensive simplification. The mean and variance of X in (2.19) and (2.20) are respectively given by $\mu = \mu'_1$ in (2.73) and $\sigma^2 = \mu_2$ in (2.74), and the skewness and kurtosis moment ratios of X in (2.21) and (2.22) are obtained by substituting the expressions for μ_3 in (2.75) and μ_4 in (2.76) into (2.18). Note that $\phi_1 = -(2\delta - 1)$ in (2.19) to (2.22).

■

2.13.2 COVARIANCE MATRIX FOR METHOD OF L -MOMENTS ESTIMATORS OF SLD

Lemma 2.13.2

In the derivation of the covariance matrix for the method of L -moments estimators of the SLD, the double integral

$$\begin{aligned}
 \Xi(j, k) &= \int_0^1 v^k \int_0^v u^{j-1} (1-u)^{-1} du dv \\
 &= \int_0^1 v^k B_v(j, 0) dv,
 \end{aligned} \tag{2.77}$$

where $B_z(a, b)$ is the incomplete beta function (see Section 2.14.1), must be solved for $j = 2, 3, 4$ and $k = -1, 0, 1, 2$. Now,

$$\begin{aligned}
 B_v(j, 0) &= \frac{v^j}{j} F(j, 1; j+1; v) \\
 &= v^j \varphi(v, 1, j) \\
 &= \sum_{i=0}^{\infty} \frac{v^{i+j}}{i+j},
 \end{aligned} \tag{2.78}$$

where $F(a, b; c; z)$ and $\varphi(z, a, b)$ are respectively the hypergeometric series and the Lerch function (see Section 2.14.1). The relation between the incomplete beta function and the hypergeometric series in (2.78) is given by Gradshteyn & Ryzhik (2007, 8.391), while the relation between the hypergeometric series and the Lerch function is given by Gradshteyn & Ryzhik (2007, 9.559).

Setting $m = i + j$ in (2.78) and simplifying gives

$$\begin{aligned}
 B_v(j, 0) &= \sum_{m=j}^{\infty} \frac{v^m}{m} \\
 &= \sum_{m=1}^{\infty} \frac{v^m}{m} - \sum_{m=1}^{j-1} \frac{v^m}{m} \\
 &= -\ln[1-v] - \sum_{m=1}^{j-1} \frac{v^m}{m},
 \end{aligned} \tag{2.79}$$

where Gradshteyn & Ryzhik (2007, 1.513.4) is used in the final result in (2.79). Then, substituting (2.79) into (2.77) gives

$$\begin{aligned}
 \Xi(j, k) &= \int_0^1 v^k \left(-\ln[1-v] - \sum_{m=1}^{j-1} \frac{v^m}{m} \right) dv \\
 &= -\int_0^1 v^k \ln[1-v] dv - \sum_{m=1}^{j-1} \frac{1}{m(m+k+1)}.
 \end{aligned}$$

From Gradshteyn & Ryzhik (2007, 4.291.4) we get

$$\Xi(j, -1) = \frac{\pi^2}{6} - \sum_{m=1}^{j-1} \frac{1}{m^2},$$

while from Gradshteyn & Ryzhik (2007, 4.293.8)

$$\Xi(j, k) = \frac{1}{k+1} \left(\psi(k+2) + C \right) - \sum_{m=1}^{j-1} \frac{1}{m(m+k+1)}, \quad k > -1,$$

where $\psi(a)$ is the psi function and C is Euler's constant (see again Section 2.14.1). In particular, using Gradshteyn & Ryzhik (2007, 8.365.4),

$$\Xi(j, 0) = 1 - \sum_{m=1}^{j-1} \frac{1}{m(m+1)},$$

$$\Xi(j, 1) = \frac{3}{4} - \sum_{m=1}^{j-1} \frac{1}{m(m+2)}$$

and

$$\mathbb{E}(j, 2) = \frac{11}{18} - \sum_{m=1}^{j-1} \frac{1}{m(m+3)}.$$

■

Theorem 2.13.2

Let X be a real-valued random variable which has a skew logistic distribution, $X \sim \text{SLD}(\alpha, \beta, \delta)$, with method of L -moments estimators for the location parameter, α , the scale parameter, $\beta > 0$, and the shape parameter, $0 \leq \delta \leq 1$, given respectively by $\hat{\alpha}$ in (2.66), $\hat{\beta}$ in (2.65) and $\hat{\delta}$ in (2.64). The asymptotic variances of $\hat{\alpha}$, $\hat{\beta}$ and $\hat{\delta}$ are obtained with

$$n \text{ var} \begin{bmatrix} \hat{\alpha} \\ \hat{\beta} \\ \hat{\delta} \end{bmatrix} \approx \begin{bmatrix} \Theta_{1,1} & \Theta_{1,2} & \Theta_{1,3} \\ \Theta_{2,1} & \Theta_{2,2} & \Theta_{2,3} \\ \Theta_{3,1} & \Theta_{3,2} & \Theta_{3,3} \end{bmatrix},$$

where

$$\Theta_{1,1} = \frac{1}{15} \beta^2 \left(57 + (125\pi^2 - 1308)\omega \right), \quad (2.80)$$

$$\Theta_{1,2} = \Theta_{2,1} = -\beta^2 (2\delta - 1), \quad (2.81)$$

$$\Theta_{1,3} = \Theta_{3,1} = -\frac{1}{5} \beta \left(7 + (25\pi^2 - 253)\omega \right), \quad (2.82)$$

$$\Theta_{2,2} = \frac{4}{3} \beta^2 \left(1 - (\pi^2 - 8)\omega \right), \quad (2.83)$$

$$\Theta_{2,3} = \Theta_{3,2} = \frac{1}{3} \beta (2\delta - 1) \left(1 + 2(\pi^2 - 8)\omega \right) \quad (2.84)$$

and

$$\Theta_{3,3} = \frac{1}{15} \left(8 - \omega \left(397 + 160\omega - 20\pi^2(\omega + 2) \right) \right), \quad (2.85)$$

with $\omega = \delta(1 - \delta)$. Specifically the asymptotic standard errors of $\hat{\alpha}$, $\hat{\beta}$ and $\hat{\delta}$ are given by (2.67), (2.68) and (2.69).

Proof

We must derive the covariance matrix $\Theta = G\Lambda G^T$. Consider first the matrix G , whose elements, as indicated in (2.63), are given by the partial derivatives of the parameters with respect to the L -moments. Thus, for the SLD with $\theta_1 = \alpha$, $\theta_2 = \beta$, and $\theta_3 = \delta$,

$$\begin{aligned}
 G &= \begin{bmatrix} \frac{\partial \alpha}{\partial L_1} & \frac{\partial \alpha}{\partial L_2} & \frac{\partial \alpha}{\partial L_3} \\ \frac{\partial \beta}{\partial L_1} & \frac{\partial \beta}{\partial L_2} & \frac{\partial \beta}{\partial L_3} \\ \frac{\partial \delta}{\partial L_1} & \frac{\partial \delta}{\partial L_2} & \frac{\partial \delta}{\partial L_3} \end{bmatrix} \\
 &= \begin{bmatrix} 1 & 0 & -6 \\ 0 & 2 & 0 \\ 0 & -\frac{3L_3}{2L_2^2} & \frac{3}{2L_2} \end{bmatrix} \\
 &= \begin{bmatrix} 1 & 0 & -6 \\ 0 & 2 & 0 \\ 0 & -\frac{2\delta-1}{\beta} & \frac{3}{\beta} \end{bmatrix},
 \end{aligned}$$

where the final result is obtained using (2.59) and (2.60) and simplifying.

Consider next the symmetric matrix

$$\Lambda = \begin{bmatrix} \Lambda_{1,1} & \Lambda_{1,2} & \Lambda_{1,3} \\ \Lambda_{2,1} & \Lambda_{2,2} & \Lambda_{2,3} \\ \Lambda_{3,1} & \Lambda_{3,2} & \Lambda_{3,3} \end{bmatrix},$$

whose elements are obtained with (2.62) using the quantile density function of the SLD given in (2.16) and the shifted Legendre polynomials $P_0^*(x)$, $P_1^*(x)$ and $P_2^*(x)$ given in (2.89), (2.90) and (2.91). For example,

$$\begin{aligned}
 \Lambda_{3,3} &= \int_0^1 \int_0^v \left(P_2^*(u)P_2^*(v) + P_2^*(u)P_2^*(v) \right) u(1-v)q(u)q(v)dudv \\
 &= 2 \int_0^1 \int_0^v \left(6u^2 - 6u + 1 \right) \left(6v^2 - 6v + 1 \right) u(1-v) \beta \left(\frac{1-\delta}{u} + \frac{\delta}{1-u} \right) \beta \left(\frac{1-\delta}{v} + \frac{\delta}{1-v} \right) dudv \\
 &= 2\beta^2 \int_0^1 \left(\left((1-\delta) \left(-6v^2 + 12v - 7 + v^{-1} \right) + \delta \left(6v^2 - 6v + 1 \right) \right) \right. \\
 &\quad \left. \times \int_0^v \left((1-\delta) \left(6u^2 - 6u + 1 \right) + \delta \left(6u^3 - 6u^2 + u \right) (1-u)^{-1} \right) du \right) dv \\
 &= 2\beta^2 \int_0^1 \left(\left((1-\delta) \left(-6v^2 + 12v - 7 + v^{-1} \right) + \delta \left(6v^2 - 6v + 1 \right) \right) \right. \\
 &\quad \left. \times \left((1-\delta) \left(2v^3 - 3v^2 + v \right) + \delta \left(6B_v(4,0) - 6B_v(3,0) + B_v(2,0) \right) \right) \right) dv \\
 &= 2\beta^2 \left((1-\delta)^2 \int_0^1 \left(-12v^5 + 42v^4 - 56v^3 + 35v^2 - 10v + 1 \right) dv \right. \\
 &\quad \left. + \omega \int_0^1 \left(12v^5 - 30v^4 + 26v^3 - 9v^2 + v \right) dv \right. \\
 &\quad \left. + \omega \left(-36\Xi(4,2) + 72\Xi(4,1) - 42\Xi(4,0) + 6\Xi(4,-1) \right. \right. \\
 &\quad \left. \left. + 36\Xi(3,2) - 72\Xi(3,1) + 42\Xi(3,0) - 6\Xi(3,-1) \right. \right. \\
 &\quad \left. \left. - 6\Xi(2,2) + 12\Xi(2,1) - 7\Xi(2,0) + \Xi(2,-1) \right) \right. \\
 &\quad \left. + \delta^2 \left(36\Xi(4,2) - 36\Xi(4,1) + 6\Xi(4,0) - 36\Xi(3,2) + 36\Xi(3,1) - 6\Xi(3,0) \right. \right. \\
 &\quad \left. \left. + 6\Xi(2,2) - 6\Xi(2,1) + \Xi(2,0) \right) \right) \\
 &= \frac{1}{15} \beta^2 \left(2 + \omega(5\pi^2 - 53) \right),
 \end{aligned}$$

with $\omega = \delta(1-\delta)$ and where the final expression is obtained after substantial simplification.

Likewise it can be shown that

$$\Lambda_{1,1} = \frac{1}{3} \beta^2 \left(3 + \omega(\pi^2 - 12) \right),$$

$$\Lambda_{2,2} = \frac{1}{3} \beta^2 \left(1 - \omega(\pi^2 - 8) \right),$$

$$\Lambda_{1,2} = \Lambda_{2,1} = \frac{1}{2} \beta^2 (2\delta - 1),$$

$$\Lambda_{1,3} = \Lambda_{3,1} = \frac{1}{6} \beta^2 \left(1 + \omega(\pi^2 - 11) \right)$$

and

$$\Lambda_{2,3} = \Lambda_{3,2} = \frac{1}{6} \beta^2 (2\delta - 1).$$

Finally, since

$$\begin{aligned} \Theta &= G\Lambda G^T \\ &= \begin{bmatrix} 1 & 0 & -6 \\ 0 & 2 & 0 \\ 0 & -\frac{2\delta-1}{\beta} & \frac{3}{\beta} \end{bmatrix} \begin{bmatrix} \Lambda_{1,1} & \Lambda_{1,2} & \Lambda_{1,3} \\ \Lambda_{1,2} & \Lambda_{2,2} & \Lambda_{2,3} \\ \Lambda_{1,3} & \Lambda_{2,3} & \Lambda_{3,3} \end{bmatrix} \begin{bmatrix} 1 & 0 & 0 \\ 0 & 2 & -\frac{2\delta-1}{\beta} \\ -6 & 0 & \frac{3}{\beta} \end{bmatrix}, \end{aligned}$$

the expressions for the elements of Θ in (2.80) to (2.85) are obtained with

$$\Theta_{1,1} = \Lambda_{1,1} - 12(\Lambda_{1,3} - 3\Lambda_{3,3}),$$

$$\Theta_{1,2} = \Theta_{2,1} = 2(\Lambda_{1,2} - 6\Lambda_{3,3}),$$

$$\Theta_{1,3} = \Theta_{3,1} = \frac{1}{\beta} \left(3(\Lambda_{1,3} - 6\Lambda_{3,3}) - (2\delta - 1)(\Lambda_{1,2} - 6\Lambda_{2,3}) \right),$$

$$\Theta_{2,2} = 4\Lambda_{2,2},$$

$$\Theta_{2,3} = \Theta_{3,2} = \frac{2}{\beta} (3\Lambda_{2,3} - (2\delta - 1)\Lambda_{2,2})$$

and

$$\Theta_{3,3} = \frac{1}{\beta^2} \left((2\delta - 1)^2 \Lambda_{2,2} - 6(2\delta - 1)\Lambda_{2,3} + 9\Lambda_{3,3} \right).$$

■

2.14 APPENDIX

Section 2.14.1 contains information on special mathematical constants, functions and ratios used in the thesis. The properties of shifted Legendre polynomials, which appear in the formulae of L -moments, are briefly given in Section 2.14.2. Tables with expressions for probability-based functions, quantile-based functions and L -moments for various probability distributions are presented in Section 2.14.3.

2.1.4.1 SPECIAL MATHEMATICAL FUNCTIONS AND RATIOS

The mathematical constants, functions and ratios listed in Table 2.9 are utilized throughout the thesis. Where applicable, full details regarding these constants, functions and ratios are available from Gradshteyn & Ryzhik (2007).

Table 2.9: Special mathematical constants, functions and ratios.

Name	Expression	Reference
Error function	$\operatorname{erf}(z) = \frac{2}{\sqrt{\pi}} \int_0^z \exp[-t^2] dt$	Gradshteyn & Ryzhik (2007, 8.25)
Inverse error function	$\operatorname{erf}^{-1}(s)$	
Standard normal density function	$\phi(z) = \frac{1}{\sqrt{2\pi}} \exp\left[-\frac{1}{2}z^2\right], \quad -\infty < z < \infty$	
Standard normal distribution function	$\Phi(z) = \int_{-\infty}^z \phi(t) dt = \frac{1}{2} \left(1 + \operatorname{erf}\left[\frac{1}{\sqrt{2}}z\right] \right), \quad -\infty < z < \infty$	
Euler gamma function	$\Gamma(a) = \int_0^{\infty} t^{a-1} \exp[-t] dt, \quad \operatorname{Re}(a) > 0$	Gradshteyn & Ryzhik (2007, 8.31)
Incomplete gamma function	$\gamma(a, z) = \int_0^z t^{a-1} \exp[-t] dt, \quad \operatorname{Re}(a) > 0$	Gradshteyn & Ryzhik (2007, 8.35)
Regularized incomplete gamma function	$G(a, z) = \frac{\gamma(a, z)}{\Gamma(a)}$	
Inverse of regularized incomplete gamma function	$G^{-1}(a, s)$	
Euler beta function	$B(a, b) = \frac{\Gamma(a)\Gamma(b)}{\Gamma(a+b)} = \int_0^1 t^{a-1} (1-t)^{b-1} dt, \quad \operatorname{Re}(a) > 0, \operatorname{Re}(b) > 0$	Gradshteyn & Ryzhik (2007, 8.38)
Incomplete beta function	$B_z(a, b) = \int_0^z t^{a-1} (1-t)^{b-1} dt, \quad \operatorname{Re}(a) > 0, \operatorname{Re}(b) < 1$	Gradshteyn & Ryzhik (2007, 8.391)
Regularized incomplete beta function ratio	$I_z(a, b) = \frac{B_z(a, b)}{B(a, b)}$	Gradshteyn & Ryzhik (2007, 8.392)
Hypergeometric series	$F(a, b; c; z) = \sum_{k=0}^{\infty} \frac{(a)_k (b)_k z^k}{(c)_k k!}$	Gradshteyn & Ryzhik (2007, 9.1)
Riemann zeta function	$\zeta(a) = \sum_{k=1}^{\infty} \frac{1}{k^a}, \quad \operatorname{Re}(a) > 1$	Gradshteyn & Ryzhik (2007, 9.5)
Euler's constant	$C = \lim_{n \rightarrow \infty} \left(\sum_{k=1}^n \frac{1}{k} - \log[n] \right) = \lim_{z \rightarrow 1} \left(\zeta(z) - \frac{1}{z-1} \right) = 0.5772156649\dots$	Gradshteyn & Ryzhik (2007, 8.367)
Euler psi function	$\psi(a) = \frac{1}{\Gamma(a)} \frac{d}{da} \Gamma(a) = \frac{d}{da} \log[\Gamma(a)] = \int_0^1 \frac{t^{a-1}-1}{t-1} dt - C, \quad \operatorname{Re}(a) > 0$	Gradshteyn & Ryzhik (2007, 8.36)
r^{th} derivative of Euler psi function	$\psi^{(r)}(a) = \frac{d^r}{da^r} \psi(a) = (-1)^{r+1} r! \sum_{k=0}^{\infty} \frac{1}{(a+k)^{r+1}}, \quad \operatorname{Re}(a) > 0$	Gradshteyn & Ryzhik (2007, 8.363.8)
Lerch function	$\phi(z, a, b) = \sum_{k=0}^{\infty} \frac{z^k}{(b+k)^a}, \quad -1 < \operatorname{Re}(z) < 1, b \neq 0, -1, \dots$	Gradshteyn & Ryzhik (2007, 9.55)
Exponential integral function	$\operatorname{Ei}(z) = \operatorname{PV} \int_{-\infty}^z \frac{\exp[t]}{t} dt$ where PV denotes principal value of integral	Gradshteyn & Ryzhik (2007, 8.21)

2.1.4.2 SHIFTED LEGENDRE POLYNOMIALS

The sequence of polynomials,

$$P_r(x) = \sum_{k=0}^r P_{r,k} x^k, \quad r = 0, 1, 2, \dots,$$

satisfying the differential equation

$$(1-x^2) \frac{d^2 z}{dx^2} - 2x \frac{dz}{dx} + r(r+1)z = 0$$

and the orthogonality relation

$$\int_{-1}^1 P_r(x) P_s(x) dx = 0, \quad r \neq s, \quad (2.86)$$

are called Legendre polynomials. As indicated by Gradshteyn & Ryzhik (2007, 8.910.2), the r^{th} order Legendre polynomial is given by

$$P_r(x) = \frac{1}{2^r r!} \frac{d^r}{dx^r} (x^2 - 1)^r.$$

Shifted Legendre polynomials,

$$P_r^*(x) = \sum_{k=0}^r P_{r,k}^* x^k, \quad r = 0, 1, 2, \dots, \quad (2.87)$$

satisfy the orthogonality relation

$$\int_0^1 P_r^*(x) P_s^*(x) dx = 0, \quad r \neq s. \quad (2.88)$$

In effect, the interval over which the polynomials are orthogonal is shifted from $[-1, 1]$ for the Legendre polynomials in (2.86) to $[0, 1]$ in (2.88) for the shifted Legendre polynomials. Thus, as indicated by Hosking (1986), the Legendre and shifted Legendre polynomials are related through

$$P_r(x) = P_r^*(2x - 1),$$

so that the r^{th} order shifted Legendre polynomial is given by

$$P_r^*(x) = \frac{(-1)^r}{r!} \frac{d^r}{dx^r} (x(1-x))^r.$$

The coefficients of the shifted Legendre polynomials in (2.87) are then

$$P_{r,k}^* = \frac{(-1)^{r-k} (r+k)!}{(k!)^2 (r-k)!} = (-1)^{r-k} \binom{r}{k} \binom{r+k}{k}.$$

To obtain expressions for the first four L -moments, the shifted Legendre polynomials up to the third order are needed and they are

$$P_0^*(x) = 1, \quad (2.89)$$

$$P_1^*(x) = 2x - 1, \quad (2.90)$$

$$P_2^*(x) = 6x^2 - 6x + 1, \quad (2.91)$$

$$P_3^*(x) = 20x^3 - 30x^2 + 12x - 1. \quad (2.92)$$

Two additional results used in the proofs of Proposition 2.8.1 and Theorem 3.17.2 are

$$P_r^*(x) = (-1)^r P_r^*(1-x) \quad (2.93)$$

and

$$\int_0^1 P_r^*(x) dx = \begin{cases} 1, & r=0, \\ 0, & r>0. \end{cases} \quad (2.94)$$

Further details regarding Legendre polynomials are available from Gradshteyn & Ryzhik (2007, 8.91) and Hosking (1986).

2.1.4.3 DISTRIBUTIONS

In this section tables summarizing the properties, functions and expressions of various probability distributions are presented. Within each table the distributions are divided into three groups. The first group consists of distributions with location parameter, α , and scale parameter, $\beta > 0$, but no shape parameters. Apart from location and shape parameters, the distributions in the second group each has a single shape parameter, λ , while the distributions in the third group each possesses two shape parameters, λ and δ . The distributions within each group are sorted alphabetically in each of the tables.

Table 2.10 provides information regarding the parameters and support of the various distributions. References for each distribution are also given. The books on probability distributions by Johnson *et al.* (1994, 1995) and Balakrishnan & Nevzorov (2003) contain details for all the well-known distributions. For distributions not covered in these books as well as newer distributions, the relevant articles are given in Table 2.10. Also, where applicable, original references are listed in Table 2.10.

Table 2.11 and Table 2.12 respectively give expressions for the probability-based functions and the quantile-based functions of the various distributions. Expressions and values for the distributions' L -location and L -scale are presented in Table 2.13, while Table 2.14 provides expressions and values for the distributions' L -skewness and the L -kurtosis ratios.

Table 2.10: References for and parameters and support of various probability distributions.

Distribution	References	Parameters	Support
Distributions with location parameter α and scale parameter β			
Arcsine	Balakrishnan & Nevzorov (2003, Chapter 17)	α and $\beta > 0$	$[\alpha, \alpha + \beta]$
Cauchy	Cauchy (1853) Johnson <i>et al.</i> (1994, Chapter 16) Balakrishnan & Nevzorov (2003, Chapter 12)	α and $\beta > 0$	$(-\infty, \infty)$
Cosine	Jones (2002b)	α and $\beta > 0$	$[\alpha, \alpha + \beta]$
Exponential	Johnson <i>et al.</i> (1994, Chapter 19) Balakrishnan & Basu (1995) Balakrishnan & Nevzorov (2003, Chapter 18) Ahsanullah & Hamedani (2010)	α and $\beta > 0$	$[\alpha, \infty)$
Gumbel	Gumbel (1954, 1958) Johnson <i>et al.</i> (1995, Chapter 22) Coles (2001) Balakrishnan & Nevzorov (2003, Chapter 21) Castillo <i>et al.</i> (2005)	α and $\beta > 0$	$(-\infty, \infty)$
Half-normal	Johnson <i>et al.</i> (1994, Chapter 18)	α and $\beta > 0$	$[\alpha, \infty)$
Laplace	Laplace (1774) Johnson <i>et al.</i> (1995, Chapter 24) Kotz <i>et al.</i> (2001) Balakrishnan & Nevzorov (2003, Chapter 19)	α and $\beta > 0$	$(-\infty, \infty)$
Logistic	Balakrishnan (1992) Johnson <i>et al.</i> (1995, Chapter 23) Balakrishnan & Nevzorov (2003, Chapter 22)	α and $\beta > 0$	$(-\infty, \infty)$
Normal	Gauss (1809, 1816) Johnson <i>et al.</i> (1994, Chapter 13) Patel & Read (1997) Balakrishnan & Nevzorov (2003, Chapter 23)	α and $\beta > 0$	$(-\infty, \infty)$
Rayleigh	Rayleigh (1880, 1919) Johnson <i>et al.</i> (1994, Chapter 18)	α and $\beta > 0$	$[\alpha, \infty)$
Secant hyperbolic	Johnson <i>et al.</i> (1995, Chapter 23) Vaughan (2002)	α and $\beta > 0$	$(-\infty, \infty)$
Student's $t(2)$	Student (1908) Jones (2002a)	α and $\beta > 0$	$(-\infty, \infty)$
Uniform	Johnson <i>et al.</i> (1995, Chapter 26) Balakrishnan & Nevzorov (2003, Chapter 11)	α and $\beta > 0$	$[\alpha, \alpha + \beta]$

Table 2.10: continues...

Distribution	References	Parameters	Support
Distributions with location parameter α , scale parameter β and shape parameter λ			
Asymmetric Laplace	Kotz <i>et al.</i> (2001) Yu & Zhang (2005)	$\alpha, \beta > 0$ and $0 < \lambda < 1$	$(-\infty, \infty)$
Burr Type II	Burr (1942)	$\alpha, \beta > 0$ and $\lambda > 0$	$(-\infty, \infty)$
Fréchet	Fréchet (1927) Johnson <i>et al.</i> (1995, Chapter 22) Coles (2001) Balakrishnan & Nevzorov (2003, Chapter 21) Castillo <i>et al.</i> (2005)	$\alpha, \beta > 0$ and $\lambda > 0$	$[\alpha, \infty)$
Gamma	Johnson <i>et al.</i> (1994, Chapter 17) Balakrishnan & Nevzorov (2003, Chapter 20) Kleiber & Kotz (2003, Chapter 5)	$\alpha, \beta > 0$ and $\lambda > 0$	$[\alpha, \infty)$
Generalized exponential	Gupta & Kundu (1999, 2007)	$\alpha, \beta > 0$ and $\lambda > 0$	$[\alpha, \infty)$
Generalized extreme value	Jenkinson (1955) Johnson <i>et al.</i> (1995, Chapter 22) Coles (2001) Balakrishnan & Nevzorov (2003, Chapter 21) Castillo <i>et al.</i> (2005)	$\alpha, \beta > 0$ and λ	$\left[\alpha + \frac{\beta}{\lambda}, \infty\right), \lambda < 0$ $(-\infty, \infty), \lambda = 0$ $\left(-\infty, \alpha + \frac{\beta}{\lambda}\right], \lambda > 0$
Generalized gamma	Hosking & Wallis (1997)	$\alpha, \beta > 0$ and $\lambda = \frac{1}{4}\alpha_3^2 \geq 0$	$(-\infty, \alpha], \alpha_3 < 0$ $(-\infty, \infty), \alpha_3 = 0$ $[\alpha, \infty), \alpha_3 > 0$
Generalized logistic	Hosking (1986)	$\alpha, \beta > 0$ and λ	$\left[\alpha + \frac{\beta}{\lambda}, \infty\right), \lambda < 0$ $(-\infty, \infty), \lambda = 0$ $\left(-\infty, \alpha + \frac{\beta}{\lambda}\right], \lambda > 0$
Generalized normal	Hosking (1986)	$\alpha, \beta > 0$ and λ	$\left[\alpha + \frac{\beta}{\lambda}, \infty\right), \lambda < 0$ $(-\infty, \infty), \lambda = 0$ $\left(-\infty, \alpha + \frac{\beta}{\lambda}\right], \lambda > 0$

Table 2.10: continues...

Distribution	References	Parameters	Support
Generalized Pareto	Pickands (1975) Coles (2001) Castillo <i>et al.</i> (2005)	$\alpha, \beta > 0$ and λ	$[\alpha, \infty), \lambda \leq 0$ $[\alpha, \alpha + \frac{\beta}{\lambda}], \lambda > 0$
Generalized secant hyperbolic	Vaughan (2002)	$\alpha, \beta > 0$ and $\lambda > -\pi$	$(-\infty, \infty)$
Gompertz	Gompertz (1825) Johnson <i>et al.</i> (1995, Chapter 22)	$\alpha, \beta > 0$ and $\lambda > 0$	$[\alpha, \infty)$
Logistic-exponential	Lan & Leemis (2008)	$\alpha, \beta > 0$ and $\lambda > 0$	$[\alpha, \infty)$
Log-logistic	Kleiber & Kotz (2003, Chapter 6)	$\alpha, \beta > 0$ and $\lambda > 0$	$[\alpha, \infty)$
Log-normal	Crow & Shimizu (1988) Johnson <i>et al.</i> (1994, Chapter 14) Kleiber & Kotz (2003, Chapter 4)	$\alpha, \beta > 0$ and $\lambda > 0$	(α, ∞)
Lomax	Lomax (1954) Arnold (1983) Johnson <i>et al.</i> (1994, Chapter 20) Kleiber & Kotz (2003, Chapter 6)	$\alpha, \beta > 0$ and $\lambda > 0$	$[\alpha, \infty)$
Pareto	Pareto (1896, 1897) Arnold (1983) Johnson <i>et al.</i> (1994, Chapter 20) Balakrishnan & Nevzorov (2003, Chapter 15) Kleiber & Kotz (2003, Chapter 3)	$\alpha, \beta > 0$ and $\lambda > 0$	$[\alpha + \beta, \infty)$
Power	Balakrishnan & Nevzorov (2003, Chapter 14)	$\alpha, \beta > 0$ and $\lambda > 0$	$[\alpha, \alpha + \beta]$
Tukey's lambda	Hastings <i>et al.</i> (1947) Tukey (1960, 1962) Tukey & McLaughlin (1963)	$\alpha, \beta > 0$ and λ	$(-\infty, \infty), \lambda \leq 0$ $[\alpha - \frac{\beta}{\lambda}, \alpha + \frac{\beta}{\lambda}], \lambda > 0$
Weibull	Weibull (1939a, 1939b) Johnson <i>et al.</i> (1994, Chapter 21) Kleiber & Kotz (2003, Chapter 5) Rinne (2009)	$\alpha, \beta > 0$ and $\lambda > 0$	$[\alpha, \infty)$
Distributions with location parameter α , scale parameter β and shape parameters λ and δ			
Burr Type III	Burr (1942, 1968, 1973) Tadikamalla (1980)	$\alpha, \beta > 0, \lambda > 0$ and $\delta > 0$	$[\alpha, \infty)$
Burr Type XII	Burr (1942, 1968, 1973) Burr & Cislak (1968) Rodriguez (1977) Tadikamalla (1980)	$\alpha, \beta > 0, \lambda > 0$ and $\delta > 0$	$[\alpha, \infty)$

Table 2.10: continues...

Distribution	References	Parameters	Support
Davies	Gilchrist (2000) Hankin & Lee (2006)	$\alpha, \beta > 0, \lambda \geq 0, \delta \geq 0$ and $\lambda + \delta > 0$	$[\alpha, \infty)$
Kappa	Hosking (1994) Mielke (1973) Karian & Dudewicz (2010, Chapter 17)	$\alpha, \beta > 0, \lambda$ and δ	$\left[\alpha + \frac{\beta}{\lambda}, \infty\right), \quad \lambda < 0, \delta \leq 0$ $\left[\alpha + \frac{\beta}{\lambda}(1 - \delta^{-\lambda}), \infty\right), \quad \lambda < 0, \delta > 0$ $(-\infty, \infty), \quad \lambda = 0, \delta \leq 0$ $[\alpha + \beta \log[\delta], \infty), \quad \lambda = 0, \delta > 0$ $\left(-\infty, \alpha + \frac{\beta}{\lambda}\right], \quad \lambda > 0, \delta \leq 0$ $\left[\alpha + \frac{\beta}{\lambda}(1 - \delta^{-\lambda}), \alpha + \frac{\beta}{\lambda}\right], \quad \lambda > 0, \delta > 0$
Kumaraswamy	Kumaraswamy (1980) Jones (2009)	$\alpha, \beta > 0, \lambda > 0$ and $\delta > 0$	$[\alpha, \alpha + \beta]$
Schmeiser-Deutsch	Schmeiser & Deutsch (1977)	$\alpha, \beta > 0, \lambda > 0$ and $0 \leq \delta \leq 1$	$[\alpha - \beta\delta^\lambda, \alpha + \beta(1 - \delta)^\lambda]$

 Table 2.11: Functions defining various probability distributions in terms of x .

Distribution	Cumulative distribution function	Probability density function
Distributions with location parameter α and scale parameter β		
Arcsine	$F(x) = 2\pi^{-1} \arcsin\left[\sqrt{\frac{x-\alpha}{\beta}}\right]$	$f(x) = \frac{1}{\pi\beta} \frac{1}{\sqrt{\left(\frac{x-\alpha}{\beta}\right)\left(1 - \frac{x-\alpha}{\beta}\right)}}$
Cauchy	$F(x) = \frac{1}{2} + \pi^{-1} \arctan\left[\frac{x-\alpha}{\beta}\right]$	$f(x) = \frac{1}{\pi\beta} \frac{1}{1 + \left(\frac{x-\alpha}{\beta}\right)^2}$
Cosine	$F(x) = \sin\left[\frac{1}{2}\pi\left(\frac{x-\alpha}{\beta}\right)\right]^2$	$f(x) = \frac{1}{2\beta} \pi \sin\left[\pi\left(\frac{x-\alpha}{\beta}\right)\right]$
Exponential	$F(x) = 1 - \exp\left[-\left(\frac{x-\alpha}{\beta}\right)\right]$	$f(x) = \frac{1}{\beta} \exp\left[-\left(\frac{x-\alpha}{\beta}\right)\right]$

Table 2.11: continues...

Distribution	Cumulative distribution function	Probability density function
Gumbel	$F(x) = \exp\left[-\exp\left[-\left(\frac{x-\alpha}{\beta}\right)\right]\right]$	$f(x) = \frac{1}{\beta} \exp\left[-\left(\frac{x-\alpha}{\beta}\right)\right] \exp\left[-\exp\left[-\left(\frac{x-\alpha}{\beta}\right)\right]\right]$
Half-normal	$F(x) = 2\Phi\left(\frac{x-\alpha}{\beta}\right) - 1$	$f(x) = \sqrt{\frac{2}{\pi}} \frac{1}{\beta} \exp\left[-\frac{1}{2}\left(\frac{x-\alpha}{\beta}\right)^2\right]$
Laplace	$F(x) = \begin{cases} \frac{1}{2} \exp\left[-\left \frac{x-\alpha}{\beta}\right \right], & x \leq \alpha \\ 1 - \frac{1}{2} \exp\left[-\left \frac{x-\alpha}{\beta}\right \right], & x \geq \alpha \end{cases}$	$f(x) = \frac{1}{2\beta} \exp\left[-\left \frac{x-\alpha}{\beta}\right \right]$
Logistic	$F(x) = \frac{1}{1 + \exp\left[-\left(\frac{x-\alpha}{\beta}\right)\right]}$	$f(x) = \frac{1}{\beta} \frac{\exp\left[-\left(\frac{x-\alpha}{\beta}\right)\right]}{\left(1 + \exp\left[-\left(\frac{x-\alpha}{\beta}\right)\right]\right)^2}$
Normal	$F(x) = \Phi\left(\frac{x-\alpha}{\beta}\right)$	$f(x) = \frac{1}{\sqrt{2\pi}\beta} \exp\left[-\frac{1}{2}\left(\frac{x-\alpha}{\beta}\right)^2\right]$
Rayleigh	$F(x) = 1 - \exp\left[-\frac{1}{2}\left(\frac{x-\alpha}{\beta}\right)^2\right]$	$f(x) = \left(\frac{x-\alpha}{\beta^2}\right) \exp\left[-\frac{1}{2}\left(\frac{x-\alpha}{\beta}\right)^2\right]$
Secant hyperbolic	$F(x) = 2\pi^{-1} \arctan\left[\exp\left[\frac{x-\alpha}{\beta}\right]\right]$	$f(x) = \frac{2}{\pi\beta} \frac{\exp\left[-\left(\frac{x-\alpha}{\beta}\right)\right]}{1 + \exp\left[-2\left(\frac{x-\alpha}{\beta}\right)\right]}$
Student's $t(2)$	$F(x) = \frac{1}{2} \left(1 + \frac{\frac{x-\alpha}{\beta}}{\sqrt{\left(\frac{x-\alpha}{\beta}\right)^2 + 2}} \right)$	$f(x) = \frac{1}{\beta} \left(\left(\frac{x-\alpha}{\beta}\right)^2 + 2 \right)^{-\frac{3}{2}}$
Uniform	$F(x) = \frac{x-\alpha}{\beta}$	$f(x) = \frac{1}{\beta}$

Table 2.11: continues...

Distribution	Cumulative distribution function	Probability density function
Distributions with location parameter α , scale parameter β and shape parameter λ		
Asymmetric Laplace	$F(x) = \begin{cases} \lambda \exp\left[-(1-\lambda)\left \frac{x-\alpha}{\beta}\right \right], & x \leq \alpha \\ 1 - (1-\lambda) \exp\left[-\lambda\left \frac{x-\alpha}{\beta}\right \right], & x \geq \alpha \end{cases}$	$f(x) = \begin{cases} \frac{\lambda(1-\lambda)}{\beta} \exp\left[-(1-\lambda)\left \frac{x-\alpha}{\beta}\right \right], & x \leq \alpha \\ \frac{\lambda(1-\lambda)}{\beta} \exp\left[-\lambda\left \frac{x-\alpha}{\beta}\right \right], & x \geq \alpha \end{cases}$
Burr Type II	$F(x) = \left(1 + \exp\left[-\left(\frac{x-\alpha}{\beta}\right)\right]\right)^{-\frac{1}{\lambda}}$	$f(x) = \frac{1}{\beta\lambda} \exp\left[-\left(\frac{x-\alpha}{\beta}\right)\right] \left(1 + \exp\left[-\left(\frac{x-\alpha}{\beta}\right)\right]\right)^{-\frac{1}{\lambda}-1}$
Fréchet	$F(x) = \exp\left[-\left(\frac{x-\alpha}{\beta}\right)^{\frac{1}{\lambda}}\right]$	$f(x) = \frac{1}{\beta\lambda} \left(\frac{x-\alpha}{\beta}\right)^{\frac{1}{\lambda}-1} \exp\left[-\left(\frac{x-\alpha}{\beta}\right)^{\frac{1}{\lambda}}\right]$
Gamma	$F(x) = G\left(\frac{1}{\lambda}, \frac{x-\alpha}{\beta}\right)$	$f(x) = \frac{1}{\beta\Gamma\left(\frac{1}{\lambda}\right)} \left(\frac{x-\alpha}{\beta}\right)^{\frac{1}{\lambda}-1} \exp\left[-\left(\frac{x-\alpha}{\beta}\right)\right]$
Generalized exponential	$F(x) = \left(1 - \exp\left[-\left(\frac{x-\alpha}{\beta}\right)\right]\right)^{\frac{1}{\lambda}}$	$f(x) = \frac{1}{\beta\lambda} \exp\left[-\left(\frac{x-\alpha}{\beta}\right)\right] \left(1 - \exp\left[-\left(\frac{x-\alpha}{\beta}\right)\right]\right)^{\frac{1}{\lambda}-1}$
Generalized extreme value	$F(x) = \begin{cases} \exp\left[-\left(1 - \lambda\left(\frac{x-\alpha}{\beta}\right)\right)^{\frac{1}{\lambda}}\right], & \lambda \neq 0 \\ \exp\left[-\exp\left[-\left(\frac{x-\alpha}{\beta}\right)\right]\right], & \lambda = 0 \end{cases}$	$f(x) = \begin{cases} \frac{1}{\beta} \left(1 - \lambda\left(\frac{x-\alpha}{\beta}\right)\right)^{\frac{1}{\lambda}-1} \exp\left[-\left(1 - \lambda\left(\frac{x-\alpha}{\beta}\right)\right)^{\frac{1}{\lambda}}\right], & \lambda \neq 0 \\ \frac{1}{\beta} \exp\left[-\left(\frac{x-\alpha}{\beta}\right)\right] \exp\left[-\exp\left[-\left(\frac{x-\alpha}{\beta}\right)\right]\right], & \lambda = 0 \end{cases}$
Generalized gamma	$F(x) = \begin{cases} 1 - G\left(\frac{1}{\lambda}, -\frac{x-\alpha}{\beta}\right), & \alpha_3 < 0 \\ \Phi\left(\frac{x-\alpha}{\beta}\right), & \alpha_3 = 0 \\ G\left(\frac{1}{\lambda}, \frac{x-\alpha}{\beta}\right), & \alpha_3 > 0 \end{cases}$	$f(x) = \begin{cases} \frac{1}{\beta\Gamma\left(\frac{1}{\lambda}\right)} \left(-\frac{x-\alpha}{\beta}\right)^{\frac{1}{\lambda}-1} \exp\left[\frac{x-\alpha}{\beta}\right], & \alpha_3 < 0 \\ \frac{1}{\sqrt{2\pi}\beta} \exp\left[-\frac{1}{2}\left(\frac{x-\alpha}{\beta}\right)^2\right], & \alpha_3 = 0 \\ \frac{1}{\beta\Gamma\left(\frac{1}{\lambda}\right)} \left(\frac{x-\alpha}{\beta}\right)^{\frac{1}{\lambda}-1} \exp\left[-\left(\frac{x-\alpha}{\beta}\right)\right], & \alpha_3 > 0 \end{cases}$

Table 2.11: continues...

Distribution	Cumulative distribution function	Probability density function
Generalized logistic	$F(x) = \begin{cases} \frac{1}{1 + \left(1 - \lambda \left(\frac{x-\alpha}{\beta}\right)\right)^{\frac{1}{\lambda}}}, & \lambda \neq 0 \\ \frac{1}{1 + \exp\left[-\left(\frac{x-\alpha}{\beta}\right)\right]}, & \lambda = 0 \end{cases}$	$f(x) = \begin{cases} \frac{\frac{1}{\beta} \left(1 - \lambda \left(\frac{x-\alpha}{\beta}\right)\right)^{\frac{1}{\lambda}-1}}{\left(1 + \left(1 - \lambda \left(\frac{x-\alpha}{\beta}\right)\right)^{\frac{1}{\lambda}}\right)^2}, & \lambda \neq 0 \\ \frac{\frac{1}{\beta} \exp\left[-\left(\frac{x-\alpha}{\beta}\right)\right]}{\left(1 + \exp\left[-\left(\frac{x-\alpha}{\beta}\right)\right]\right)^2}, & \lambda = 0 \end{cases}$
Generalized normal	$F(x) = \begin{cases} \Phi\left(-\frac{1}{\lambda} \log\left[1 - \lambda \left(\frac{x-\alpha}{\beta}\right)\right]\right), & \lambda \neq 0 \\ \Phi\left(\frac{x-\alpha}{\beta}\right), & \lambda = 0 \end{cases}$	$f(x) = \begin{cases} \frac{\frac{1}{\sqrt{2\pi}\beta} \left(1 - \lambda \left(\frac{x-\alpha}{\beta}\right)\right) \exp\left[-\frac{1}{2} \left(\frac{1}{\lambda} \log\left[1 - \lambda \left(\frac{x-\alpha}{\beta}\right)\right]\right)^2\right]}{\left(1 - \lambda \left(\frac{x-\alpha}{\beta}\right)\right)}, & \lambda \neq 0 \\ \frac{1}{\sqrt{2\pi}\beta} \exp\left[-\frac{1}{2} \left(\frac{x-\alpha}{\beta}\right)^2\right], & \lambda = 0 \end{cases}$
Generalized Pareto	$F(x) = \begin{cases} 1 - \left(1 - \lambda \left(\frac{x-\alpha}{\beta}\right)\right)^{\frac{1}{\lambda}}, & \lambda \neq 0 \\ 1 - \exp\left[-\left(\frac{x-\alpha}{\beta}\right)\right], & \lambda = 0 \end{cases}$	$f(x) = \begin{cases} \frac{1}{\beta} \left(1 - \lambda \left(\frac{x-\alpha}{\beta}\right)\right)^{\frac{1}{\lambda}-1}, & \lambda \neq 0 \\ \frac{1}{\beta} \exp\left[-\left(\frac{x-\alpha}{\beta}\right)\right], & \lambda = 0 \end{cases}$
Generalized secant hyperbolic	$F(x) = \begin{cases} \frac{\frac{1}{\lambda} \operatorname{arccot}\left(\cot(\lambda) + \csc(\lambda) \exp\left[-\left(\frac{x-\alpha}{\beta}\right)\right]\right)}{1 + \exp\left[-\left(\frac{x-\alpha}{\beta}\right)\right]}, & -\pi < \lambda < 0 \\ \frac{1}{1 + \exp\left[-\left(\frac{x-\alpha}{\beta}\right)\right]}, & \lambda = 0 \\ \frac{\frac{1}{\lambda} \operatorname{arccoth}\left(\coth(\lambda) + \operatorname{csch}(\lambda) \exp\left[-\left(\frac{x-\alpha}{\beta}\right)\right]\right)}{1 + \exp\left[-\left(\frac{x-\alpha}{\beta}\right)\right]}, & \lambda > 0 \end{cases}$	$f(x) = \begin{cases} \frac{\frac{1}{2\beta\lambda} \frac{\sin(\lambda)}{\cos(\lambda) + \cosh\left(\frac{x-\alpha}{\beta}\right)}}{\left(1 + \exp\left[-\left(\frac{x-\alpha}{\beta}\right)\right]\right)^2}, & -\pi < \lambda < 0 \\ \frac{\frac{1}{\beta} \exp\left[-\left(\frac{x-\alpha}{\beta}\right)\right]}{\left(1 + \exp\left[-\left(\frac{x-\alpha}{\beta}\right)\right]\right)^2}, & \lambda = 0 \\ \frac{\frac{1}{2\beta\lambda} \frac{\sinh(\lambda)}{\cosh(\lambda) + \cosh\left(\frac{x-\alpha}{\beta}\right)}}{\left(1 + \exp\left[-\left(\frac{x-\alpha}{\beta}\right)\right]\right)^2}, & \lambda > 0 \end{cases}$
Gompertz	$F(x) = 1 - \exp\left[\frac{1}{\lambda} \left(1 - \exp\left[\frac{x-\alpha}{\beta}\right]\right)\right]$	$f(x) = \frac{1}{\beta\lambda} \exp\left[\frac{x-\alpha}{\beta}\right] \exp\left[\frac{1}{\lambda} \left(1 - \exp\left[\frac{x-\alpha}{\beta}\right]\right)\right]$

Table 2.11: continues...

Distribution	Cumulative distribution function	Probability density function
Logistic-exponential	$F(x) = 1 - \frac{1}{1 + \left(\exp\left[\frac{x-\alpha}{\beta}\right] - 1\right)^{\frac{1}{\lambda}}}$	$f(x) = \frac{1}{\beta\lambda} \frac{\exp\left[\frac{x-\alpha}{\beta}\right] \left(\exp\left[\frac{x-\alpha}{\beta}\right] - 1\right)^{\frac{1}{\lambda}-1}}{\left(1 + \left(\exp\left[\frac{x-\alpha}{\beta}\right] - 1\right)^{\frac{1}{\lambda}}\right)^2}$
Log-logistic	$F(x) = \frac{1}{1 + \left(\frac{x-\alpha}{\beta}\right)^{\frac{1}{\lambda}}}$	$f(x) = \frac{1}{\beta\lambda} \frac{\left(\frac{x-\alpha}{\beta}\right)^{\frac{1}{\lambda}-1}}{\left(1 + \left(\frac{x-\alpha}{\beta}\right)^{\frac{1}{\lambda}}\right)^2}$
Log-normal	$F(x) = \Phi\left(\frac{1}{\lambda} \log\left[\frac{x-\alpha}{\beta}\right]\right)$	$f(x) = \frac{1}{\sqrt{2\pi}\lambda(x-\alpha)} \exp\left[-\frac{1}{2}\left(\frac{1}{\lambda} \log\left[\frac{x-\alpha}{\beta}\right]\right)^2\right]$
Lomax	$F(x) = 1 - \left(1 + \frac{x-\alpha}{\beta}\right)^{\frac{1}{\lambda}}$	$f(x) = \frac{1}{\beta\lambda} \left(1 + \frac{x-\alpha}{\beta}\right)^{\frac{1}{\lambda}-1}$
Pareto	$F(x) = 1 - \left(\frac{x-\alpha}{\beta}\right)^{-\frac{1}{\lambda}}$	$f(x) = \frac{1}{\beta\lambda} \left(\frac{x-\alpha}{\beta}\right)^{-\frac{1}{\lambda}-1}$
Power	$F(x) = \left(\frac{x-\alpha}{\beta}\right)^{\frac{1}{\lambda}}$	$f(x) = \frac{1}{\beta\lambda} \left(\frac{x-\alpha}{\beta}\right)^{\frac{1}{\lambda}-1}$
Tukey's lambda	No closed-form expression	No closed-form expression
Weibull	$F(x) = 1 - \exp\left[-\left(\frac{x-\alpha}{\beta}\right)^{\frac{1}{\lambda}}\right]$	$f(x) = \frac{1}{\beta\lambda} \left(\frac{x-\alpha}{\beta}\right)^{\frac{1}{\lambda}-1} \exp\left[-\left(\frac{x-\alpha}{\beta}\right)^{\frac{1}{\lambda}}\right]$
Distributions with location parameter α , scale parameter β and shape parameters λ and δ		
Burr Type III	$F(x) = \left(1 + \left(\frac{x-\alpha}{\beta}\right)^{\frac{1}{\delta}}\right)^{\frac{1}{\lambda}}$	$f(x) = \frac{1}{\beta\lambda\delta} \left(\frac{x-\alpha}{\beta}\right)^{\frac{1}{\delta}-1} \left(1 + \left(\frac{x-\alpha}{\beta}\right)^{\frac{1}{\delta}}\right)^{\frac{1}{\lambda}-1}$
Burr Type XII	$F(x) = 1 - \left(1 + \left(\frac{x-\alpha}{\beta}\right)^{\frac{1}{\delta}}\right)^{-\frac{1}{\lambda}}$	$f(x) = \frac{1}{\beta\lambda\delta} \left(\frac{x-\alpha}{\beta}\right)^{\frac{1}{\delta}-1} \left(1 + \left(\frac{x-\alpha}{\beta}\right)^{\frac{1}{\delta}}\right)^{-\frac{1}{\lambda}-1}$

Table 2.11: continues...

Distribution	Cumulative distribution function	Probability density function
Davies	No closed-form expression	No closed-form expression
Kappa	$F(x) = \begin{cases} \left(1 - \delta \left(1 - \lambda \left(\frac{x-\alpha}{\beta}\right)\right)^{\frac{1}{\lambda}}\right)^{\frac{1}{\delta}}, & \lambda \neq 0, \delta \neq 0 \\ \exp\left[-\left(1 - \lambda \left(\frac{x-\alpha}{\beta}\right)\right)^{\frac{1}{\lambda}}\right], & \lambda \neq 0, \delta = 0 \\ \left(1 - \delta \exp\left[-\left(\frac{x-\alpha}{\beta}\right)\right]\right)^{\frac{1}{\delta}}, & \lambda = 0, \delta \neq 0 \\ \exp\left[-\exp\left[-\left(\frac{x-\alpha}{\beta}\right)\right]\right], & \lambda = 0, \delta = 0 \end{cases}$	$f(x) = \begin{cases} \frac{1}{\beta} \left(1 - \lambda \left(\frac{x-\alpha}{\beta}\right)\right)^{\frac{1}{\lambda}-1} \left(1 - \delta \left(1 - \lambda \left(\frac{x-\alpha}{\beta}\right)\right)^{\frac{1}{\lambda}}\right)^{\frac{1}{\delta}-1}, & \lambda \neq 0, \delta \neq 0 \\ \frac{1}{\beta} \left(1 - \lambda \left(\frac{x-\alpha}{\beta}\right)\right)^{\frac{1}{\lambda}-1} \exp\left[-\left(1 - \lambda \left(\frac{x-\alpha}{\beta}\right)\right)^{\frac{1}{\lambda}}\right], & \lambda \neq 0, \delta = 0 \\ \frac{1}{\beta} \exp\left[-\left(\frac{x-\alpha}{\beta}\right)\right] \left(1 - \delta \exp\left[-\left(\frac{x-\alpha}{\beta}\right)\right]\right)^{\frac{1}{\delta}-1}, & \lambda = 0, \delta \neq 0 \\ \frac{1}{\beta} \exp\left[-\left(\frac{x-\alpha}{\beta}\right)\right] \exp\left[-\exp\left[-\left(\frac{x-\alpha}{\beta}\right)\right]\right], & \lambda = 0, \delta = 0 \end{cases}$
Kumaraswamy	$F(x) = 1 - \left(1 - \left(\frac{x-\alpha}{\beta}\right)^{\frac{1}{\delta}}\right)^{\frac{1}{\lambda}}$	$f(x) = \frac{1}{\beta\lambda\delta} \left(\frac{x-\alpha}{\beta}\right)^{\frac{1}{\delta}-1} \left(1 - \left(\frac{x-\alpha}{\beta}\right)^{\frac{1}{\delta}}\right)^{\frac{1}{\lambda}-1}$
Schmeiser-Deutsch	$F(x) = \begin{cases} \delta - \left(-\left(\frac{x-\alpha}{\beta}\right)\right)^{\frac{1}{\lambda}}, & x \leq \alpha \\ \delta + \left(\frac{x-\alpha}{\beta}\right)^{\frac{1}{\lambda}}, & x \geq \alpha \end{cases}$	$f(x) = \frac{1}{\beta\lambda} \left -\left(\frac{x-\alpha}{\beta}\right) \right ^{\frac{1}{\lambda}-1}$

 Table 2.12: Functions defining various probability distributions in terms of p .

Distribution	Quantile function	Quantile density function	Density quantile function
Distributions with location parameter α and scale parameter β			
Arcsine	$Q(p) = \alpha + \beta \sin\left[\frac{1}{2} p\pi\right]^2$	$q(p) = \frac{1}{2} \pi\beta \sin[p\pi]$	$f_p(p) = \frac{2}{\pi\beta} \csc[p\pi]$
Cauchy	$Q(p) = \alpha + \beta \tan\left[\frac{1}{2} \pi(2p-1)\right]$	$q(p) = \pi\beta \sec\left[\frac{1}{2} \pi(2p-1)\right]^2$	$f_p(p) = \frac{1}{\pi\beta} \cos\left[\frac{1}{2} \pi(2p-1)\right]^2$

Table 2.12: continues...

Distribution	Quantile function	Quantile density function	Density quantile function
Cosine	$Q(p) = \alpha + 2\pi^{-1}\beta \arcsin[\sqrt{p}]$	$q(p) = \frac{\beta}{\pi\sqrt{p(1-p)}}$	$f_p(p) = \frac{1}{\beta}\pi\sqrt{p(1-p)}$
Exponential	$Q(p) = \alpha - \beta \log[1-p]$	$q(p) = \frac{\beta}{1-p}$	$f_p(p) = \frac{1-p}{\beta}$
Gumbel	$Q(p) = \alpha - \beta \log[-\log[p]]$	$q(p) = -\frac{\beta}{p \log[p]}$	$f_p(p) = -\frac{1}{\beta} p \log[p]$
Half-normal	$Q(p) = \alpha + \sqrt{2}\beta \operatorname{erf}^{-1}[p]$	$q(p) = \sqrt{\frac{2}{\pi}}\pi\beta \exp[-\operatorname{erf}^{-1}[p]^2]$	$f_p(p) = \sqrt{\frac{2}{\pi}}\frac{1}{\beta} \exp[-\operatorname{erf}^{-1}[p]^2]$
Laplace	$Q(p) = \begin{cases} \alpha + \beta \log[2p], & p \leq \frac{1}{2} \\ \alpha - \beta \log[2(1-p)], & p \geq \frac{1}{2} \end{cases}$	$q(p) = \begin{cases} \frac{\beta}{p}, & p \leq \frac{1}{2} \\ \frac{\beta}{1-p}, & p \geq \frac{1}{2} \end{cases}$	$f_p(p) = \begin{cases} \frac{p}{\beta}, & p \leq \frac{1}{2} \\ \frac{1-p}{\beta}, & p \geq \frac{1}{2} \end{cases}$
Logistic	$Q(p) = \alpha + \beta \log\left[\frac{p}{1-p}\right]$	$q(p) = \frac{\beta}{p(1-p)}$	$f_p(p) = \frac{p(1-p)}{\beta}$
Normal	$Q(p) = \alpha + \sqrt{2}\beta \operatorname{erf}^{-1}[2p-1]$	$q(p) = \sqrt{2\pi}\beta \exp[-\operatorname{erf}^{-1}[2p-1]^2]$	$f_p(p) = \frac{1}{\sqrt{2\pi}\beta} \exp[-\operatorname{erf}^{-1}[2p-1]^2]$
Rayleigh	$Q(p) = \alpha + \beta\sqrt{-2\log[1-p]}$	$q(p) = \frac{\beta}{(1-p)\sqrt{-2\log[1-p]}}$	$f_p(p) = \frac{1-p}{\beta}\sqrt{-2\log[1-p]}$
Secant hyperbolic	$Q(p) = \alpha + \beta \log\left[\tan\left[\frac{1}{2}p\pi\right]\right]$	$q(p) = \pi\beta \csc[p\pi]$	$f_p(p) = \frac{1}{\pi\beta} \sin[p\pi]$
Student's $t(2)$	$Q(p) = \alpha + \beta \frac{2p-1}{\sqrt{2p(1-p)}}$	$q(p) = \frac{\beta}{(2p(1-p))^{3/2}}$	$f_p(p) = \frac{1}{\beta} (2p(1-p))^{3/2}$
Uniform	$Q(p) = \alpha + \beta p$	$q(p) = \beta$	$f_p(p) = \frac{1}{\beta}$
Distributions with location parameter α , scale parameter β and shape parameter λ			
Asymmetric Laplace	$Q(p) = \begin{cases} \alpha + \frac{\beta}{1-\lambda} \log\left[\frac{p}{\lambda}\right], & p \leq \lambda, \\ \alpha - \frac{\beta}{\lambda} \log\left[\frac{1-p}{1-\lambda}\right], & p \geq \lambda, \end{cases}$	$q(p) = \begin{cases} \frac{\beta}{(1-\lambda)p}, & p \leq \lambda, \\ \frac{\beta}{\lambda(1-p)}, & p \geq \lambda, \end{cases}$	$f_p(p) = \begin{cases} \frac{(1-\lambda)p}{\beta}, & p \leq \lambda, \\ \frac{\lambda(1-p)}{\beta}, & p \geq \lambda, \end{cases}$
Burr Type II	$Q(p) = \alpha + \beta \log\left[\frac{p^\lambda}{1-p^\lambda}\right]$	$q(p) = \frac{\beta\lambda}{p(1-p^\lambda)}$	$f_p(p) = \frac{1}{\beta\lambda} p(1-p^\lambda)$
Fréchet	$Q(p) = \alpha + \beta(-\log[p])^{-\lambda}$	$q(p) = \frac{\beta\lambda}{p(-\log[p])^{\lambda+1}}$	$f_p(p) = \frac{1}{\beta\lambda} p(-\log[p])^{\lambda+1}$

Table 2.12: continues...

Distribution	Quantile function	Quantile density function	Density quantile function
Gamma	$Q(p) = \alpha + \beta G^{-1}\left(\frac{1}{\lambda}, p\right)$	$q(p) = \beta \Gamma\left(\frac{1}{\lambda}\right) \left(G^{-1}\left(\frac{1}{\lambda}, p\right)\right)^{\frac{1}{\lambda}-1} \exp\left[-G^{-1}\left(\frac{1}{\lambda}, p\right)\right]$	$f_p(p) = \frac{1}{\beta \Gamma\left(\frac{1}{\lambda}\right)} \left(G^{-1}\left(\frac{1}{\lambda}, p\right)\right)^{\frac{1}{\lambda}-1} \exp\left[-G^{-1}\left(\frac{1}{\lambda}, p\right)\right]$
Generalized exponential	$Q(p) = \alpha - \beta \log[1 - p^\lambda]$	$q(p) = \frac{\beta \lambda p^{\lambda-1}}{1 - p^\lambda}$	$f_p(p) = \frac{1 - p^\lambda}{\beta \lambda p^{\lambda-1}}$
Generalized extreme value	$Q(p) = \begin{cases} \alpha + \frac{\beta}{\lambda} (1 - (-\log[p])^\lambda), & \lambda \neq 0 \\ \alpha - \beta \log[-\log[p]], & \lambda = 0 \end{cases}$	$q(p) = \frac{\beta}{p} (-\log[p])^{\lambda-1}$	$f_p(p) = \frac{1}{\beta} p (-\log[p])^{1-\lambda}$
Generalized gamma	$Q(p) = \begin{cases} \alpha - \beta G^{-1}\left(\frac{1}{\lambda}, 1 - p\right), & \alpha_3 < 0 \\ \alpha + \sqrt{2} \beta \operatorname{erf}^{-1}[2p - 1], & \alpha_3 = 0 \\ \alpha + \beta G^{-1}\left(\frac{1}{\lambda}, p\right), & \alpha_3 > 0 \end{cases}$	$q(p) = \begin{cases} \beta \Gamma\left(\frac{1}{\lambda}\right) \left(G^{-1}\left(\frac{1}{\lambda}, 1 - p\right)\right)^{\frac{1}{\lambda}-1} \exp\left[-G^{-1}\left(\frac{1}{\lambda}, 1 - p\right)\right], & \alpha_3 < 0 \\ \sqrt{2\pi} \beta \exp\left[\operatorname{erf}^{-1}[2p - 1]^2\right], & \alpha_3 = 0 \\ \beta \Gamma\left(\frac{1}{\lambda}\right) \left(G^{-1}\left(\frac{1}{\lambda}, p\right)\right)^{\frac{1}{\lambda}-1} \exp\left[-G^{-1}\left(\frac{1}{\lambda}, p\right)\right], & \alpha_3 > 0 \end{cases}$	$f_p(p) = \begin{cases} \frac{1}{\beta \Gamma\left(\frac{1}{\lambda}\right)} \left(G^{-1}\left(\frac{1}{\lambda}, 1 - p\right)\right)^{\frac{1}{\lambda}-1} \exp\left[-G^{-1}\left(\frac{1}{\lambda}, 1 - p\right)\right], & \alpha_3 < 0 \\ \frac{1}{\sqrt{2\pi} \beta} \exp\left[-\operatorname{erf}^{-1}[2p - 1]^2\right], & \alpha_3 = 0 \\ \frac{1}{\beta \Gamma\left(\frac{1}{\lambda}\right)} \left(G^{-1}\left(\frac{1}{\lambda}, p\right)\right)^{\frac{1}{\lambda}-1} \exp\left[-G^{-1}\left(\frac{1}{\lambda}, p\right)\right], & \alpha_3 > 0 \end{cases}$
Generalized logistic	$Q(p) = \begin{cases} \alpha + \frac{\beta}{\lambda} \left(1 - \left(\frac{1-p}{p}\right)^\lambda\right), & \lambda \neq 0 \\ \alpha + \beta \log\left[\frac{p}{1-p}\right], & \lambda = 0 \end{cases}$	$q(p) = \frac{\beta(1-p)^{\lambda-1}}{p^{\lambda+1}}$	$f_p(p) = \frac{p^{\lambda+1}}{\beta(1-p)^{\lambda-1}}$
Generalized normal	$Q(p) = \begin{cases} \alpha + \frac{\beta}{\lambda} \left(1 - \exp\left[-\sqrt{2} \lambda \operatorname{erf}^{-1}[2p - 1]\right]\right), & \lambda \neq 0 \\ \alpha + \sqrt{2} \beta \operatorname{erf}^{-1}[2p - 1], & \lambda = 0 \end{cases}$	$q(p) = \sqrt{2\pi} \beta \exp\left[-\operatorname{erf}^{-1}[2p - 1] \left(\sqrt{2} \lambda - \operatorname{erf}^{-1}[2p - 1]\right)\right]$	$f_p(p) = \frac{1}{\sqrt{2\pi} \beta} \exp\left[\operatorname{erf}^{-1}[2p - 1] \left(\sqrt{2} \lambda - \operatorname{erf}^{-1}[2p - 1]\right)\right]$
Generalized Pareto	$Q(p) = \begin{cases} \alpha + \frac{\beta}{\lambda} (1 - (1 - p)^\lambda), & \lambda \neq 0 \\ \alpha - \beta \log[1 - p], & \lambda = 0 \end{cases}$	$q(p) = \beta (1 - p)^{\lambda-1}$	$f_p(p) = \frac{1}{\beta} (1 - p)^{1-\lambda}$
Generalized secant hyperbolic	$Q(p) = \begin{cases} \alpha + \beta \log\left[\frac{\sin(\lambda p)}{\sin(\lambda(1-p))}\right], & -\pi < \lambda < 0 \\ \alpha + \beta \log\left[\frac{p}{1-p}\right], & \lambda = 0 \\ \alpha + \beta \log\left[\frac{\sinh(\lambda p)}{\sinh(\lambda(1-p))}\right], & \lambda > 0 \end{cases}$	$q(p) = \begin{cases} \beta \lambda \sin(\lambda) \csc(\lambda p) \csc(\lambda(1-p)), & -\pi < \lambda < 0 \\ \frac{\beta}{p(1-p)}, & \lambda = 0 \\ \beta \lambda \sinh(\lambda) \operatorname{csch}(\lambda p) \operatorname{csch}(\lambda(1-p)), & \lambda > 0 \end{cases}$	$f_p(p) = \begin{cases} \frac{1}{\beta \lambda} \csc(\lambda) \sin(\lambda p) \sin(\lambda(1-p)), & -\pi < \lambda < 0 \\ \frac{p(1-p)}{\beta}, & \lambda = 0 \\ \frac{1}{\beta \lambda} \operatorname{csch}(\lambda) \sinh(\lambda p) \sinh(\lambda(1-p)), & \lambda > 0 \end{cases}$

Table 2.12: continues...

Distribution	Quantile function	Quantile density function	Density quantile function
Gompertz	$Q(p) = \alpha + \beta \log[1 - \lambda \log[1 - p]]$	$q(p) = \frac{\beta\lambda}{(1-p)(1-\lambda \log[1-p])}$	$f_p(p) = \frac{1}{\beta\lambda} (1-p)(1-\lambda \log[1-p])$
Logistic-exponential	$Q(p) = \alpha + \beta \log\left[1 + \left(\frac{p}{1-p}\right)^\lambda\right]$	$q(p) = \frac{\beta\lambda p^{\lambda-1}}{(1-p)^{\lambda+1}} \frac{1}{\left(1 + \left(\frac{p}{1-p}\right)^\lambda\right)}$	$f_p(p) = \frac{(1-p)^{\lambda+1}}{\beta\lambda p^{\lambda-1}} \left(1 + \left(\frac{p}{1-p}\right)^\lambda\right)$
Log-logistic	$Q(p) = \alpha + \beta \left(\frac{p}{1-p}\right)^\lambda$	$q(p) = \frac{\beta\lambda p^{\lambda-1}}{(1-p)^{\lambda+1}}$	$f_p(p) = \frac{(1-p)^{\lambda+1}}{\beta\lambda p^{\lambda-1}}$
Log-normal	$Q(p) = \alpha + \beta \exp\left[\sqrt{2}\lambda \operatorname{erf}^{-1}[2p-1]\right]$	$q(p) = \sqrt{2\pi}\beta\lambda \exp\left[\operatorname{erf}^{-1}[2p-1]\left(\sqrt{2}\lambda + \operatorname{erf}^{-1}[2p-1]\right)\right]$	$f_p(p) = \frac{1}{\sqrt{2\pi}\beta\lambda} \exp\left[-\operatorname{erf}^{-1}[2p-1]\left(\sqrt{2}\lambda + \operatorname{erf}^{-1}[2p-1]\right)\right]$
Lomax	$Q(p) = \alpha + \beta(1-p)^{-\lambda} - 1$	$q(p) = \beta\lambda(1-p)^{-\lambda-1}$	$f_p(p) = \frac{1}{\beta\lambda} (1-p)^{\lambda+1}$
Pareto	$Q(p) = \alpha + \beta(1-p)^{-\lambda}$	$q(p) = \beta\lambda(1-p)^{-\lambda-1}$	$f_p(p) = \frac{1}{\beta\lambda} (1-p)^{\lambda+1}$
Power	$Q(p) = \alpha + \beta p^\lambda$	$q(p) = \beta\lambda p^{\lambda-1}$	$f_p(p) = \frac{1}{\beta\lambda} p^{1-\lambda}$
Tukey's lambda	$Q(p) = \begin{cases} \alpha + \frac{\beta}{\lambda}(p^\lambda - (1-p)^\lambda), & \lambda \neq 0 \\ \alpha + \beta \log\left[\frac{p}{1-p}\right], & \lambda = 0 \end{cases}$	$q(p) = \beta(p^{\lambda-1} + (1-p)^{\lambda-1})$	$f_p(p) = \frac{1}{\beta(p^{\lambda-1} + (1-p)^{\lambda-1})}$
Weibull	$Q(p) = \alpha + \beta(-\log[1-p])^\lambda$	$q(p) = \frac{\beta\lambda}{1-p} (-\log[1-p])^{\lambda-1}$	$f_p(p) = \frac{1}{\beta\lambda} (1-p)(-\log[1-p])^{1-\lambda}$
Distributions with location parameter α , scale parameter β and shape parameters λ and δ			
Burr Type III	$Q(p) = \alpha + \beta \left(\frac{p^\lambda}{1-p^\lambda}\right)^\delta$	$q(p) = \frac{\beta\lambda\delta p^{\lambda\delta-1}}{(1-p^\lambda)^{\delta+1}}$	$f_p(p) = \frac{(1-p^\lambda)^{\delta+1}}{\beta\lambda\delta p^{\lambda\delta-1}}$
Burr Type XII	$Q(p) = \alpha + \beta(1-p)^{-\lambda} - 1)^\delta$	$q(p) = \frac{\beta\lambda\delta(1-p)^{-\lambda-1}}{(1-p)^{\lambda+1}} \delta^{-1}$	$f_p(p) = \frac{1}{\beta\lambda\delta} (1-p)^{\lambda+1} \left((1-p)^{-\lambda} - 1\right)^{1-\delta}$
Davies	$Q(p) = \alpha + \beta \frac{p^\lambda}{(1-p)^\delta}$	$q(p) = \frac{\beta p^{\lambda-1} (\lambda(1-p) + \delta p)}{(1-p)^{\delta+1}}$	$f_p(p) = \frac{(1-p)^{\delta+1}}{\beta p^{\lambda-1} (\lambda(1-p) + \delta p)}$

Table 2.12: continues...

Distribution	Quantile function	Quantile density function	Density quantile function
Kappa	$Q(p) = \begin{cases} \alpha + \frac{\beta}{\lambda} \left(1 - \left(\frac{1-p^\delta}{\delta} \right)^\lambda \right), & \lambda \neq 0, \delta \neq 0 \\ \alpha + \frac{\beta}{\lambda} (1 - (-\log[p])^\lambda), & \lambda \neq 0, \delta = 0 \\ \alpha - \beta \log \left[\frac{1-p^\delta}{\delta} \right], & \lambda = 0, \delta \neq 0 \\ \alpha - \beta \log[-\log[p]], & \lambda = 0, \delta = 0 \end{cases}$	$q(p) = \begin{cases} \beta p^{\delta-1} \left(\frac{1-p^\delta}{\delta} \right)^{\lambda-1}, & \delta \neq 0 \\ \frac{\beta}{p} (-\log[p])^{\lambda-1}, & \delta = 0 \end{cases}$	$f_p(p) = \begin{cases} \frac{1}{\beta} p^{1-\delta} \left(\frac{1-p^\delta}{\delta} \right)^{1-\lambda}, & \delta \neq 0 \\ \frac{1}{\beta} p (-\log[p])^{1-\lambda}, & \delta = 0 \end{cases}$
Kumaraswamy	$Q(p) = \alpha + \beta (1 - (1-p)^\lambda)^\delta$	$q(p) = \beta \lambda \delta (1-p)^{\lambda-1} (1 - (1-p)^\lambda)^{\delta-1}$	$f_p(p) = \frac{1}{\beta \lambda \delta} (1-p)^{1-\lambda} (1 - (1-p)^\lambda)^{1-\delta}$
Schmeiser-Deutsch	$Q(p) = \begin{cases} \alpha - \beta(\delta - p)^\lambda, & p \leq \delta \\ \alpha + \beta(p - \delta)^\lambda, & p \geq \delta \end{cases}$	$q(p) = \begin{cases} \beta \lambda (\delta - p)^{\lambda-1}, & p \leq \delta \\ \beta \lambda (p - \delta)^{\lambda-1}, & p \geq \delta \end{cases}$	$f_p(p) = \begin{cases} \frac{1}{\beta \lambda} (\delta - p)^{1-\lambda}, & p \leq \delta \\ \frac{1}{\beta \lambda} (p - \delta)^{1-\lambda}, & p \geq \delta \end{cases}$

Table 2.13: L -location and L -scale for various probability distributions.

Distribution	L -location	L -scale
Distributions with location parameter α and scale parameter β		
Arcsine	$L_1 = \alpha + \frac{1}{2}\beta$	$L_2 = 2\pi^{-2}\beta$
Cauchy	Does not exist	Does not exist
Cosine	$L_1 = \alpha + \frac{1}{2}\beta$	$L_2 = \frac{1}{8}\beta$
Exponential	$L_1 = \alpha + \beta$	$L_2 = \frac{1}{2}\beta$
Gumbel	$L_1 = \alpha + \beta C$	$L_2 = \beta \log[2]$
Half-normal	$L_1 = \alpha + \beta \sqrt{\frac{2}{\pi}}$	$L_2 = \frac{\beta}{\sqrt{\pi}} (2 - \sqrt{2})$
Laplace	$L_1 = \alpha$	$L_2 = \frac{3}{4}\beta$
Logistic	$L_1 = \alpha$	$L_2 = \beta$

Table 2.13: continues...

Distribution	L -location	L -scale
Normal	$L_1 = \alpha$	$L_2 = \frac{\beta}{\sqrt{\pi}}$
Rayleigh	$L_1 = \alpha + \beta\sqrt{\frac{1}{2}\pi}$	$L_2 = \frac{1}{2}\beta\sqrt{\pi}(\sqrt{2}-1)$
Secant hyperbolic	$L_1 = \alpha$	$L_2 = 7\pi^{-2}\beta\zeta(3)$
Student's $t(2)$	$L_1 = \alpha$	$L_2 = \frac{\pi\beta}{2\sqrt{2}}$
Uniform	$L_1 = \alpha + \frac{1}{2}\beta$	$L_2 = \frac{1}{6}\beta$
Distributions with location parameter α , scale parameter β and shape parameter λ		
Asymmetric Laplace	$L_1 = \alpha + \frac{\beta(1-2\lambda)}{\lambda(1-\lambda)}$	$L_2 = \frac{1}{2}\beta\left(\frac{1}{\lambda(1-\lambda)} - 1\right)$
Burr Type II	$L_1 = \alpha + \beta\left(C + \psi\left(\frac{1}{\lambda}\right)\right)$	$L_2 = \beta\left(\psi\left(\frac{2}{\lambda}\right) - \psi\left(\frac{1}{\lambda}\right)\right)$
Fréchet	$L_1 = \alpha + \beta\Gamma(1-\lambda), \quad \lambda < 1$	$L_2 = \beta(2^\lambda - 1)\Gamma(1-\lambda), \quad \lambda < 1$
Gamma	$L_1 = \alpha + \frac{\beta}{\lambda}$	$L_2 = \beta B\left(\frac{1}{\lambda}, \frac{1}{2}\right)$
Generalized exponential	$L_1 = \alpha + \beta\left(C + \psi\left(\frac{1}{\lambda}\right) + \lambda\right)$	$L_2 = \beta\left(\psi\left(\frac{2}{\lambda}\right) - \psi\left(\frac{1}{\lambda}\right) - \frac{1}{2}\lambda\right)$
Generalized extreme value	$L_1 = \alpha + \frac{\beta}{\lambda}(1 - \Gamma(\lambda+1)), \quad \lambda > -1$	$L_2 = \beta(1 - 2^{-\lambda})\Gamma(\lambda), \quad \lambda > -1$
Generalized gamma	$L_1 = \alpha + \frac{\beta}{\lambda}$	$L_2 = \beta B\left(\frac{1}{\lambda}, \frac{1}{2}\right)$
Generalized logistic	$L_1 = \alpha + \beta\left(\frac{1}{\lambda} - \pi \csc(\lambda\pi)\right), \quad -1 < \lambda < 1$	$L_2 = \beta\lambda\pi \csc(\lambda\pi), \quad -1 < \lambda < 1$
Generalized normal	$L_1 = \alpha + \frac{\beta}{\lambda}\left(1 - \exp\left[\frac{1}{2}\lambda^2\right]\right)$	$L_2 = \frac{\beta}{\lambda}\left(1 - 2\Phi\left(-\frac{\lambda}{\sqrt{2}}\right)\right)\exp\left[\frac{1}{2}\lambda^2\right]$
Generalized Pareto	$L_1 = \alpha + \frac{\beta}{\lambda+1}, \quad \lambda > -1$	$L_2 = \frac{\beta}{(\lambda+1)(\lambda+2)}, \quad \lambda > -1$
Generalized secant hyperbolic	$L_1 = \alpha$	No simple expression
Gompertz	$L_1 = \alpha - \beta \exp\left[\frac{1}{\lambda}\right] \text{Ei}\left(-\frac{1}{\lambda}\right)$	$L_2 = \beta\left(\exp\left[\frac{2}{\lambda}\right] \text{Ei}\left(-\frac{2}{\lambda}\right) - \exp\left[\frac{1}{\lambda}\right] \text{Ei}\left(-\frac{1}{\lambda}\right)\right)$

Table 2.13: continues...

Distribution	L -location	L -scale
Logistic-exponential	No simple expression	$L_2 = \frac{1}{2} \beta \lambda$
Log-logistic	$L_1 = \alpha + \beta \lambda \pi \csc(\lambda \pi), \quad \lambda < 1$	$L_2 = \beta \lambda^2 \pi \csc(\lambda \pi), \quad \lambda < 1$
Log-normal	$L_1 = \alpha + \beta \exp\left[\frac{1}{2} \lambda^2\right]$	$L_2 = \beta \left(2\Phi\left(\frac{\lambda}{\sqrt{2}}\right) - 1\right) \exp\left[\frac{1}{2} \lambda^2\right]$
Lomax	$L_1 = \alpha + \frac{\beta \lambda}{1-\lambda}, \quad \lambda < 1$	$L_2 = \frac{\beta \lambda}{(\lambda-1)(\lambda-2)}, \quad \lambda < 1$
Pareto	$L_1 = \alpha + \frac{\beta}{1-\lambda}, \quad \lambda < 1$	$L_2 = \frac{\beta \lambda}{(\lambda-1)(\lambda-2)}, \quad \lambda < 1$
Power	$L_1 = \alpha + \frac{\beta}{\lambda+1}$	$L_2 = \frac{\beta \lambda}{(\lambda+1)(\lambda+2)}$
Tukey's lambda	$L_1 = \alpha, \quad \lambda > -1$	$L_2 = \frac{2\beta}{(\lambda+1)(\lambda+2)}, \quad \lambda > -1$
Weibull	$L_1 = \alpha + \beta \Gamma(\lambda + 1)$	$L_2 = \beta(1 - 2^{-\lambda})\Gamma(\lambda + 1)$
Distributions with location parameter α , scale parameter β and shape parameters λ and δ		
Burr Type III	$L_1 = \alpha + \frac{\beta}{\lambda} B(1 - \delta, \delta + \frac{1}{\lambda}), \quad \delta < 1$	$L_2 = \frac{\beta}{\lambda} (2B(1 - \delta, \delta + \frac{2}{\lambda}) - B(1 - \delta, \delta + \frac{1}{\lambda})), \quad \delta < 1$
Burr Type XII	$L_1 = \alpha + \frac{\beta}{\lambda} B(\delta + 1, \frac{1}{\lambda} - \delta), \quad \delta < \frac{1}{\lambda}$	$L_2 = \frac{\beta}{\lambda} (B(\delta + 1, \frac{1}{\lambda} - \delta) - 2B(\delta + 1, \frac{2}{\lambda} - \delta)), \quad \delta < \frac{1}{\lambda}$
Davies	$L_1 = \alpha + \beta B(1 + \lambda, 1 - \delta), \quad \delta < 1$	$L_2 = \frac{\beta(\lambda + \delta)B(1 + \lambda, 1 - \delta)}{2 + \lambda - \delta}, \quad \delta < 1$
Kappa	$L_1 = \begin{cases} \alpha + \frac{\beta}{\lambda} \left(1 - \frac{B(\lambda + 1, -\lambda - \frac{1}{\delta})}{(-\delta)^{\lambda + 1}}\right), & \delta < 0, -1 < \lambda < -\frac{1}{\delta} \\ \alpha + \frac{\beta}{\lambda} (1 - \Gamma(\lambda + 1)), & \delta = 0, \lambda > -1 \\ \alpha + \frac{\beta}{\lambda} \left(1 - \frac{B(\lambda + 1, \frac{1}{\delta})}{\delta^{\lambda + 1}}\right), & \delta > 0, \lambda > -1 \end{cases}$	$L_2 = \begin{cases} \frac{\beta}{\lambda} \left(\frac{B(\lambda + 1, -\lambda - \frac{1}{\delta}) - 2B(\lambda + 1, -\lambda - \frac{2}{\delta})}{(-\delta)^{\lambda + 1}}\right), & \delta < 0, -1 < \lambda < -\frac{1}{\delta} \\ \beta(1 - 2^{-\lambda})\Gamma(\lambda), & \delta = 0, \lambda > -1 \\ \frac{\beta}{\lambda} \left(\frac{B(\lambda + 1, \frac{1}{\delta}) - 2B(\lambda + 1, \frac{2}{\delta})}{\delta^{\lambda + 1}}\right), & \delta > 0, \lambda > -1 \end{cases}$
Kumaraswamy	$L_1 = \alpha + \frac{\beta}{\lambda} B(\delta + 1, \frac{1}{\lambda})$	$L_2 = \frac{\beta}{\lambda} (B(\delta + 1, \frac{1}{\lambda}) - 2B(\delta + 1, \frac{2}{\lambda}))$
Schmeiser-Deutsch	$L_1 = \alpha + \frac{\beta}{\lambda + 1} ((1 - \delta)^{\lambda + 1} - \delta^{\lambda + 1})$	$L_2 = \frac{\beta}{(\lambda + 1)(\lambda + 2)} ((2\delta + \lambda)(1 - \delta)^{\lambda + 1} + (2(1 - \delta) + \lambda)\delta^{\lambda + 1})$

Table 2.14: L -skewness and L -kurtosis ratios for various probability distributions.

Distribution	L -skewness ratio	L -kurtosis ratio
Distributions with location parameter α and scale parameter β		
Arcsine	$\tau_3 = 0$	$\tau_4 = 6 - 60\pi^{-2}$
Cauchy	Does not exist	Does not exist
Cosine	$\tau_3 = 0$	$\tau_4 = \frac{1}{16}$
Exponential	$\tau_3 = \frac{1}{3}$	$\tau_4 = \frac{1}{6}$
Gumbel	$\tau_3 = \frac{\log\left[\frac{9}{8}\right]}{\log[2]}$	$\tau_4 = \frac{2\log\left[\frac{256}{243}\right]}{\log[2]}$
Half-normal	$\tau_3 = 7 + 4\sqrt{2} - 12(\sqrt{2} + 2)\pi^{-1} \arctan[\sqrt{2}]$	$\tau_4 = 180(\sqrt{2} + 2)\pi^{-1} \arctan[\sqrt{2}] - 109 - 55\sqrt{2}$
Laplace	$\tau_3 = 0$	$\tau_4 = \frac{17}{72}$
Logistic	$\tau_3 = 0$	$\tau_4 = \frac{1}{6}$
Normal	$\tau_3 = 0$	$\tau_4 = 30\pi^{-1} \arctan[\sqrt{2}] - 9$
Rayleigh	$\tau_3 = \frac{3\sqrt{2} + 2\sqrt{6} - 9}{3(\sqrt{2} - 1)}$	$\tau_4 = \frac{20\sqrt{6} - 9(\sqrt{2} + 4)}{6(\sqrt{2} - 1)}$
Secant hyperbolic	$\tau_3 = 0$	$\tau_4 = 6 - \frac{465}{7}\pi^{-2} \frac{\zeta(5)}{\zeta(3)}$
Student's $t(2)$	$\tau_3 = 0$	$\tau_4 = \frac{3}{8}$
Uniform	$\tau_3 = 0$	$\tau_4 = 0$
Distributions with location parameter α , scale parameter β and shape parameter λ		
Asymmetric Laplace	$\tau_3 = \frac{1}{3} \left(1 - \frac{2\lambda^2(2-\lambda)}{1-\lambda+\lambda^2} \right)$	$\tau_4 = \frac{1}{6} \left(1 + \frac{5\lambda^2(1-\lambda)^2}{1-\lambda+\lambda^2} \right)$
Burr Type II	$\tau_3 = \frac{2\psi\left(\frac{3}{\lambda}\right) - 3\psi\left(\frac{2}{\lambda}\right) + \psi\left(\frac{1}{\lambda}\right)}{\psi\left(\frac{2}{\lambda}\right) - \psi\left(\frac{1}{\lambda}\right)}$	$\tau_4 = \frac{5\psi\left(\frac{4}{\lambda}\right) - 10\psi\left(\frac{3}{\lambda}\right) + 6\psi\left(\frac{2}{\lambda}\right) - \psi\left(\frac{1}{\lambda}\right)}{\psi\left(\frac{2}{\lambda}\right) - \psi\left(\frac{1}{\lambda}\right)}$

Table 2.14: continues...

Distribution	L -skewness ratio	L -kurtosis ratio
Fréchet	$\tau_3 = \frac{2(3^\lambda) - 3(2^\lambda) + 1}{2^\lambda - 1}, \quad \lambda < 1$	$\tau_4 = \frac{5(4^\lambda) - 10(3^\lambda) + 6(2^\lambda) - 1}{2^\lambda - 1}, \quad \lambda < 1$
Gamma	$\tau_3 = 6I_{\frac{1}{3}}\left(\frac{1}{\lambda}, \frac{2}{\lambda}\right) - 3$	No simple expression
Generalized exponential	$\tau_3 = \frac{2\psi\left(\frac{3}{\lambda}\right) - 3\psi\left(\frac{2}{\lambda}\right) + \psi\left(\frac{1}{\lambda}\right) + \frac{\lambda}{6}}{\psi\left(\frac{2}{\lambda}\right) - \psi\left(\frac{1}{\lambda}\right) - \frac{\lambda}{2}}$	$\tau_4 = \frac{5\psi\left(\frac{4}{\lambda}\right) - 10\psi\left(\frac{3}{\lambda}\right) + 6\psi\left(\frac{2}{\lambda}\right) - \psi\left(\frac{1}{\lambda}\right) - \frac{\lambda}{12}}{\psi\left(\frac{2}{\lambda}\right) - \psi\left(\frac{1}{\lambda}\right) - \frac{\lambda}{2}}$
Generalized extreme value	$\tau_3 = \frac{-1 + 3(2^{-\lambda}) - 2(3^{-\lambda})}{1 - 2^{-\lambda}}, \quad \lambda > -1$	$\tau_4 = \frac{1 - 6(2^{-\lambda}) + 10(3^{-\lambda}) - 5(4^{-\lambda})}{1 - 2^{-\lambda}}, \quad \lambda > -1$
Generalized gamma	$\tau_3 = 6I_{\frac{1}{3}}\left(\frac{1}{\lambda}, \frac{2}{\lambda}\right) - 3$	No simple expression
Generalized logistic	$\tau_3 = -\lambda, \quad -1 < \lambda < 1$	$\tau_4 = \frac{1}{6} + \frac{5}{6}\lambda^2, \quad -1 < \lambda < 1$
Generalized normal	No simple expression	No simple expression
Generalized Pareto	$\tau_3 = \frac{1 - \lambda}{\lambda + 3}, \quad \lambda > -1$	$\tau_4 = \frac{(\lambda - 1)(\lambda - 2)}{(\lambda + 3)(\lambda + 4)}, \quad \lambda > -1$
Generalized secant hyperbolic	$\tau_3 = 0$	No simple expression
Gompertz	$\tau_3 = \frac{-2\exp\left[\frac{2}{\lambda}\right]\text{Ei}\left(-\frac{3}{\lambda}\right) + 3\exp\left[\frac{1}{\lambda}\right]\text{Ei}\left(-\frac{2}{\lambda}\right) - \text{Ei}\left(-\frac{1}{\lambda}\right)}{\exp\left[\frac{1}{\lambda}\right]\text{Ei}\left(-\frac{2}{\lambda}\right) - \text{Ei}\left(-\frac{1}{\lambda}\right)}$	$\tau_4 = \frac{5\exp\left[\frac{3}{\lambda}\right]\text{Ei}\left(-\frac{4}{\lambda}\right) - 10\exp\left[\frac{2}{\lambda}\right]\text{Ei}\left(-\frac{3}{\lambda}\right) + 6\exp\left[\frac{1}{\lambda}\right]\text{Ei}\left(-\frac{2}{\lambda}\right) - \text{Ei}\left(-\frac{1}{\lambda}\right)}{\exp\left[\frac{1}{\lambda}\right]\text{Ei}\left(-\frac{2}{\lambda}\right) - \text{Ei}\left(-\frac{1}{\lambda}\right)}$
Logistic-exponential	No simple expression	$\tau_4 = \frac{1}{6}$
Log-logistic	$\tau_3 = \lambda, \quad \lambda < 1$	$\tau_4 = \frac{1}{6} + \frac{5}{6}\lambda^2, \quad \lambda < 1$
Log-normal	No simple expression	No simple expression
Lomax	$\tau_3 = \frac{\lambda + 1}{3 - \lambda}, \quad \lambda < 1$	$\tau_4 = \frac{(\lambda + 1)(\lambda + 2)}{(\lambda - 3)(\lambda - 4)}, \quad \lambda < 1$
Pareto	$\tau_3 = \frac{\lambda + 1}{3 - \lambda}, \quad \lambda < 1$	$\tau_4 = \frac{(\lambda + 1)(\lambda + 2)}{(\lambda - 3)(\lambda - 4)}, \quad \lambda < 1$
Power	$\tau_3 = \frac{\lambda - 1}{\lambda + 3}$	$\tau_4 = \frac{(\lambda - 1)(\lambda - 2)}{(\lambda + 3)(\lambda + 4)}$
Tukey's lambda	$\tau_3 = 0, \quad \lambda > -1$	$\tau_4 = \frac{(\lambda - 1)(\lambda - 2)}{(\lambda + 3)(\lambda + 4)}, \quad \lambda > -1$

Table 2.14: continues...

Distribution	L -skewness ratio	L -kurtosis ratio
Weibull	$\tau_3 = \frac{1-3(2^{-\lambda})+2(3^{-\lambda})}{1-2^{-\lambda}}$	$\tau_4 = \frac{1-6(2^{-\lambda})+10(3^{-\lambda})-5(4^{-\lambda})}{1-2^{-\lambda}}$
Distributions with location parameter α , scale parameter β and shape parameters λ and δ		
Burr Type III	$\tau_3 = \frac{6B\left(1-\delta, \delta+\frac{3}{\lambda}\right)-6B\left(1-\delta, \delta+\frac{2}{\lambda}\right)+B\left(1-\delta, \delta+\frac{1}{\lambda}\right)}{2B\left(1-\delta, \delta+\frac{2}{\lambda}\right)-B\left(1-\delta, \delta+\frac{1}{\lambda}\right)}, \quad \delta < 1$	$\tau_4 = \frac{20B\left(1-\delta, \delta+\frac{4}{\lambda}\right)-30B\left(1-\delta, \delta+\frac{3}{\lambda}\right)+12B\left(1-\delta, \delta+\frac{2}{\lambda}\right)-B\left(1-\delta, \delta+\frac{1}{\lambda}\right)}{2B\left(1-\delta, \delta+\frac{2}{\lambda}\right)-B\left(1-\delta, \delta+\frac{1}{\lambda}\right)}, \quad \delta < 1$
Burr Type XII	$\tau_3 = \frac{B\left(\delta+1, \frac{1}{\lambda}-\delta\right)-6B\left(\delta+1, \frac{2}{\lambda}-\delta\right)+6B\left(\delta+1, \frac{3}{\lambda}-\delta\right)}{B\left(\delta+1, \frac{1}{\lambda}-\delta\right)-2B\left(\delta+1, \frac{2}{\lambda}-\delta\right)}, \quad \delta < \frac{1}{\lambda}$	$\tau_4 = \frac{B\left(\delta+1, \frac{1}{\lambda}-\delta\right)-12B\left(\delta+1, \frac{2}{\lambda}-\delta\right)+30B\left(\delta+1, \frac{3}{\lambda}-\delta\right)-20B\left(\delta+1, \frac{4}{\lambda}-\delta\right)}{B\left(\delta+1, \frac{1}{\lambda}-\delta\right)-2B\left(\delta+1, \frac{2}{\lambda}-\delta\right)}, \quad \delta < \frac{1}{\lambda}$
Davies	$\tau_3 = \frac{\lambda(\lambda-1)+4\lambda\delta+\delta(\delta+1)}{(\lambda+\delta)(3+\lambda-\delta)}, \quad \delta < 1$	$\tau_4 = \frac{\lambda(\lambda-3)+2(1+4\lambda\delta)+\delta(\delta+3)}{(3+\lambda-\delta)(4+\lambda-\delta)}, \quad \delta < 1$
Kappa	$\tau_3 = \begin{cases} \frac{-B\left(\lambda+1, -\lambda-\frac{1}{\delta}\right)+6B\left(\lambda+1, -\lambda-\frac{2}{\delta}\right)-6B\left(\lambda+1, -\lambda-\frac{3}{\delta}\right)}{B\left(\lambda+1, -\lambda-\frac{1}{\delta}\right)-2B\left(\lambda+1, -\lambda-\frac{2}{\delta}\right)}, & \delta < 0, -1 < \lambda < -\frac{1}{\delta} \\ \frac{-1+3(2^{-\lambda})-2(3^{-\lambda})}{1-2^{-\lambda}}, & \delta = 0, \lambda > -1 \\ \frac{-B\left(\lambda+1, \frac{1}{\delta}\right)+6B\left(\lambda+1, \frac{2}{\delta}\right)-6B\left(\lambda+1, \frac{3}{\delta}\right)}{B\left(\lambda+1, \frac{1}{\delta}\right)-2B\left(\lambda+1, \frac{2}{\delta}\right)}, & \delta > 0, \lambda > -1 \end{cases}$	$\tau_4 = \begin{cases} \frac{B\left(\lambda+1, -\lambda-\frac{1}{\delta}\right)-12B\left(\lambda+1, -\lambda-\frac{2}{\delta}\right)+30B\left(\lambda+1, -\lambda-\frac{3}{\delta}\right)-20B\left(\lambda+1, -\lambda-\frac{4}{\delta}\right)}{B\left(\lambda+1, -\lambda-\frac{1}{\delta}\right)-2B\left(\lambda+1, -\lambda-\frac{2}{\delta}\right)}, & \delta < 0, -1 < \lambda < -\frac{1}{\delta} \\ \frac{1-6(2^{-\lambda})+10(3^{-\lambda})-5(4^{-\lambda})}{1-2^{-\lambda}}, & \delta = 0, \lambda > -1 \\ \frac{B\left(\lambda+1, \frac{1}{\delta}\right)-12B\left(\lambda+1, \frac{2}{\delta}\right)+30B\left(\lambda+1, \frac{3}{\delta}\right)-20B\left(\lambda+1, \frac{4}{\delta}\right)}{B\left(\lambda+1, \frac{1}{\delta}\right)-2B\left(\lambda+1, \frac{2}{\delta}\right)}, & \delta > 0, \lambda > -1 \end{cases}$
Kumaraswamy	$\tau_3 = \frac{B\left(\delta+1, \frac{1}{\lambda}\right)-6B\left(\delta+1, \frac{2}{\lambda}\right)+6B\left(\delta+1, \frac{3}{\lambda}\right)}{B\left(\delta+1, \frac{1}{\lambda}\right)-2B\left(\delta+1, \frac{2}{\lambda}\right)}$	$\tau_4 = \frac{B\left(\delta+1, \frac{1}{\lambda}\right)-12B\left(\delta+1, \frac{2}{\lambda}\right)+30B\left(\delta+1, \frac{3}{\lambda}\right)-20B\left(\delta+1, \frac{4}{\lambda}\right)}{B\left(\delta+1, \frac{1}{\lambda}\right)-2B\left(\delta+1, \frac{2}{\lambda}\right)}$
Schmeiser-Deutsch	$\tau_3 = \frac{(12\delta^2+6\delta(\lambda-1)+\lambda(\lambda-1))(1-\delta)^{\lambda+1}-(12\delta^2-6\delta(\lambda+3)+(\lambda+2)(\lambda+3))\delta^{2\lambda+1}}{(\lambda+3)((2\delta+\lambda)(1-\delta)^{2\lambda+1}+(2(1-\delta)+\lambda)\delta^{2\lambda+1})}$	$\tau_4 = \frac{(120\delta^3+60\delta^2(\lambda-2)+12\delta(\lambda-1)(\lambda-2)+\lambda(\lambda-1)(\lambda-2))(1-\delta)^{\lambda+1}-(120\delta^3-60\delta^2(\lambda+4)+12\delta(\lambda+3)(\lambda+4)-(\lambda+2)(\lambda+3)(\lambda+4))\delta^{2\lambda+1}}{(\lambda+3)(\lambda+4)((2\delta+\lambda)(1-\delta)^{2\lambda+1}+(2(1-\delta)+\lambda)\delta^{2\lambda+1})}$

3. THE GENERALIZED LAMBDA DISTRIBUTION (GLD)

3.1 INTRODUCTION

In the middle of the twentieth century, Tukey, along with his research associates, introduced and studied a symmetric distribution called Tukey's lambda distribution (Hastings *et al.*, 1947; Tukey, 1960, 1962; Tukey & McLaughlin, 1963). This distribution has a single shape parameter, λ , from which the name of the distribution originates. It is the simplest example of a quantile-based distribution, that is, a distribution specified in terms of its quantile-based functions. These functions of Tukey's lambda distribution are given in Section 3.2.

Since the 1970s, various generalizations of Tukey's lambda distribution have been developed. These generalizations are collectively referred to as generalized lambda distributions (GLDs). Each generalization possesses multiple shape parameters, usually two, and can be viewed as a distinct type of the GLD. Two of these types, the Ramberg-Schmeiser (RS) Type (Ramberg & Schmeiser, 1972, 1974) and the Freimer-Mudholkar-Kollia-Lin (FMKL) Type (Freimer *et al.*, 1988), have been studied and used extensively in theoretical development and in practice, and are the focus of this chapter.

Akin to Tukey's lambda distribution, no closed-form expression exists for the cumulative distribution function, $F(x)$, of the GLD. Furthermore, the probability density function, $f(x)$, of the GLD cannot be expressed as a function of x . It is therefore more convenient to describe the GLD in quantile form using the quantile function of the type under consideration along with the type's quantile density and density quantile functions. The quantile-based functions of the RS and FMKL Types of the GLD are given in Section 3.3 and 3.4 respectively.

The parameter space of the GLD with respect to its shape parameters can be divided into regions or classes based on the distributional shapes and the support attainable in each region or class. In Section 3.5 these regions and classes are illustrated graphically and also tabulated in terms of the corresponding shape parameter values and support

Measures of location, spread and shape based on moments, L -moments and quantiles are presented for the GLD in Sections 3.6, 3.7 and 3.8 respectively. Section 3.9 briefly deals with the location and scale properties of the GLD, which are straightforward.

In contrast, the shape properties of the GLD are much more complex, specifically for the RS and FMKL Types. Hence a detailed discussion thereof is presented in Section 3.10, focusing on tail behavior in Section 3.10.1, skewness and kurtosis properties in Section 3.10.2 and the shapes attainable by the GLD's density curve in Section 3.10.3. The distributional shape and properties for each region or class of the RS and FMKL Types are further exemplified in Sections 3.11 and 3.12 respectively, highlighting the flexibility of the GLD in terms of distributional shape.

Because of the complex nature of the shape properties of the RS and FMKL Types of the GLD, parameter estimation for these types is computationally difficult. Section 3.13 gives a brief discussion on the estimation methods proposed in the literature. Utilization of the GLD is described in Sections 3.14 and 3.15, focusing on Monte Carlo simulation in Section 3.14, for which the GLD was originally developed, and applications, including the fitting of the GLD to data sets, in Section 3.15. In particular Section 3.15 lists applications of the GLD appearing in the literature since 2001. The chapter concludes in Section 3.16.

The theoretical material presented in this chapter has been compiled from various sources, most notably the books of Karian & Dudewicz (2000, 2010), which focused on the RS Type of the GLD, and the doctoral thesis of King (1999) in which both the RS and FMKL Types were covered. In general the theoretical development of the GLD in the literature has been concentrated on the RS Type. Results for the FMKL Type not given before in the literature are derived and described in this chapter.

Formulae for the moments for limiting cases of the FMKL Type, which have not appeared before in the literature, are derived in Section 3.17.1. Karvanen & Nuutinen, (2008) presented the characterization of the RS Type of the GLD by L -moments, given in Section 3.7. The corresponding characterization of the FMKL Type is also given in Section 3.7, with the expressions for the L -moments derived in Section 3.17.2.

3.2 TUKEY'S LAMBDA DISTRIBUTION

Even though Tukey's lambda distribution has a single shape parameter, λ , it produces an astounding variety of symmetric distributional shapes. As illustrated in Figure 3.1, Tukey's lambda distribution encompasses unimodal bell-shaped distributions with infinite support for $\lambda \leq 0$ and bounded support for $0 < \lambda < 1$, the uniform distribution for both $\lambda = 1$ and $\lambda = 2$, U-shaped distributions for $1 < \lambda < 2$ and unimodal truncated distributions for $\lambda > 2$.

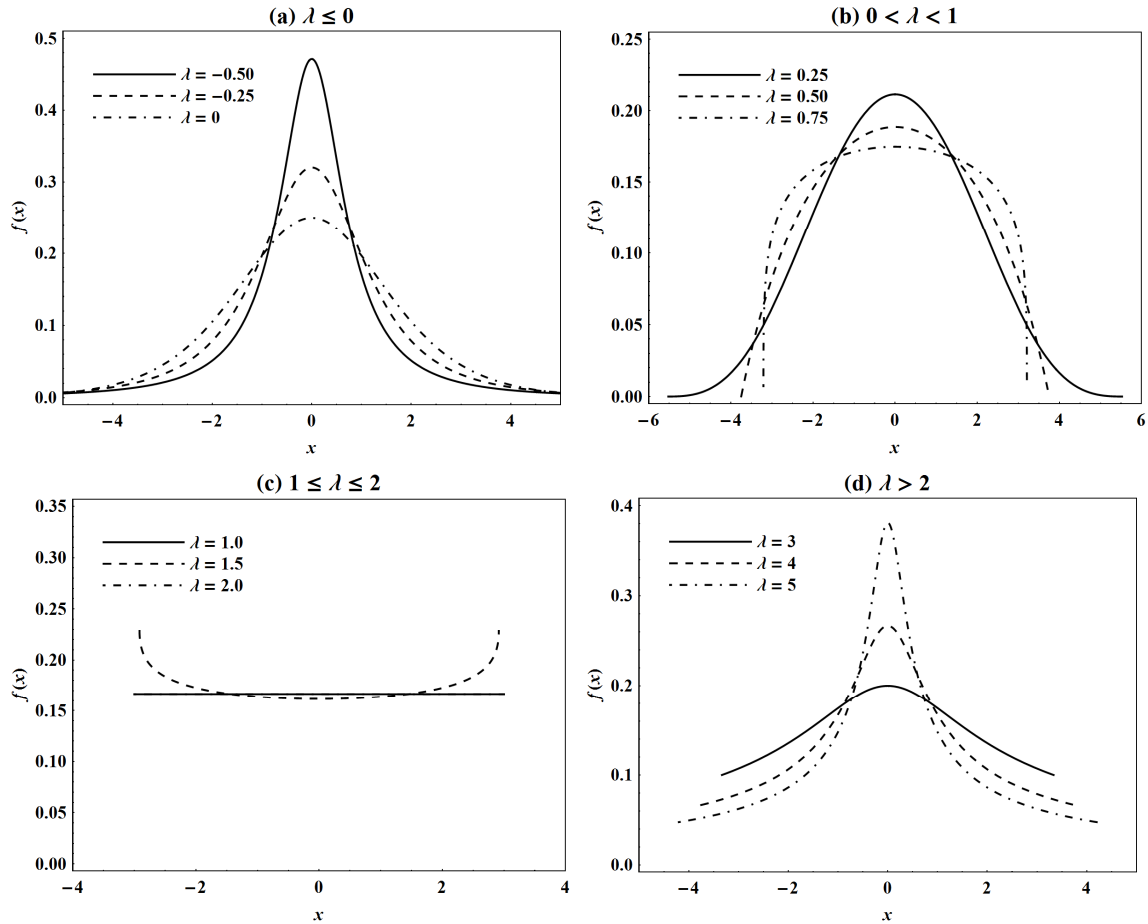


Figure 3.1: Probability density functions of Tukey's lambda distribution for various values of λ , all with $L_1 = 0$ and $L_2 = 1$. Since Tukey's lambda distribution reduces to the uniform distribution for both $\lambda = 1$ and $\lambda = 2$, the corresponding two density curves in graph (c) plot on top of each other.

The standard form of Tukey's lambda distribution is specified in terms of its quantile function by

$$Q_0(p) = \begin{cases} \frac{1}{\lambda} \left(p^\lambda - (1-p)^\lambda \right) & , \lambda \neq 0, \\ \log \left[\frac{p}{1-p} \right] & , \lambda = 0. \end{cases} \quad (3.1)$$

where the limiting case, $\lambda = 0$ in (3.1), is the quantile function of the standard logistic distribution, obtained by applying L'Hôpital's rule (de l'Hôpital, 1696). In the literature Tukey's lambda distribution is usually presented by the standard form in (3.1). Adding location and scale parameters yields the more general form,

$$Q(p) = \begin{cases} \alpha + \frac{\beta}{\lambda} \left(p^\lambda - (1-p)^\lambda \right) & , \lambda \neq 0, \\ \alpha + \beta \log \left[\frac{p}{1-p} \right] & , \lambda = 0. \end{cases} \quad (3.2)$$

The quantile density and density quantile functions of Tukey's lambda distribution are then

$$q(p) = \beta \left(p^{\lambda-1} + (1-p)^{\lambda-1} \right)$$

and

$$f_p(p) = \frac{1}{\beta \left(p^{\lambda-1} + (1-p)^{\lambda-1} \right)}.$$

3.3 RAMBERG-SCHMEISER TYPE (GLD_{RS})

The Ramberg-Schmeiser (RS) Type of the GLD was developed by Ramberg & Schmeiser (1972, 1974) in order to provide an algorithm for generating symmetric and asymmetric real-valued random variables in Monte Carlo simulations. Ramberg *et al.* (1979) extended the use of the RS Type of the GLD, henceforth denoted GLD_{RS}, by developing a system using moments and tables to fit the GLD_{RS} to data sets. The quantile function of the GLD_{RS} is

$$Q(p) = \lambda_1 + \frac{1}{\lambda_2} \left(p^{\lambda_3} - (1-p)^{\lambda_4} \right), \quad (3.3)$$

where λ_1 is a location parameter, $\lambda_2 \neq 0$ is a scale parameter and λ_3 and λ_4 are shape parameters. The quantile density and density quantile functions of the GLD_{RS} are respectively

$$q(p) = \frac{1}{\lambda_2} \left(\lambda_3 p^{\lambda_3-1} + \lambda_4 (1-p)^{\lambda_4-1} \right)$$

and

$$f_p(p) = \frac{\lambda_2}{\lambda_3 p^{\lambda_3-1} + \lambda_4 (1-p)^{\lambda_4-1}}.$$

3.4 FREIMER-MUDHOLKAR-KOLLIA-LIN TYPE (GLD_{FMKL})

The Freimer-Mudholkar-Kollia-Lin (FMKL) Type of the GLD, introduced by Freimer *et al.* (1988) and denoted GLD_{FMKL}, has quantile function

$$Q(p) = \lambda_1 + \frac{1}{\lambda_2} \left(\frac{p^{\lambda_3} - 1}{\lambda_3} - \frac{(1-p)^{\lambda_4} - 1}{\lambda_4} \right). \quad (3.4)$$

The quantile density and density quantile functions of the GLD_{FMKL} are respectively

$$q(p) = \frac{1}{\lambda_2} \left(p^{\lambda_3-1} + (1-p)^{\lambda_4-1} \right)$$

and

$$f_p(p) = \frac{\lambda_2}{p^{\lambda_3-1} + (1-p)^{\lambda_4-1}}.$$

It should be noted that the parameters as given by Freimer *et al.* (1988) were numbered differently. To avoid confusion, the parameters of the GLD_{FMKL} are numbered in the same order as the parameters of the GLD_{RS} so that they have the same interpretation. That is, λ_1 is the location parameter, $\lambda_2 \neq 0$ is the scale parameter and λ_3 and λ_4 are the shape parameters.

3.5 PARAMETER SPACE, SUPPORT AND SPECIAL CASES

Figure 3.2 illustrates the parameter space of the GLD_{RS} with respect to the two shape parameters. The parameter space is divided into six regions. Initially, as given by Ramberg & Schmeiser (1974) and Ramberg *et al.* (1979), the validity of the GLD_{RS} was restricted to the values of λ_3 and λ_4 in Regions 1, 2, 3 and 4. Karian *et al.* (1996) obtained the two additional valid regions, namely Regions 5 and 6. See Karian & Dudewicz (2000, 2010) for the complete derivation of the parameter space of the GLD_{RS} . They furthermore provided a comprehensive discussion of the characteristics of the GLD_{RS} within each region, including the support of the GLD_{RS} summarized in Table 3.1.

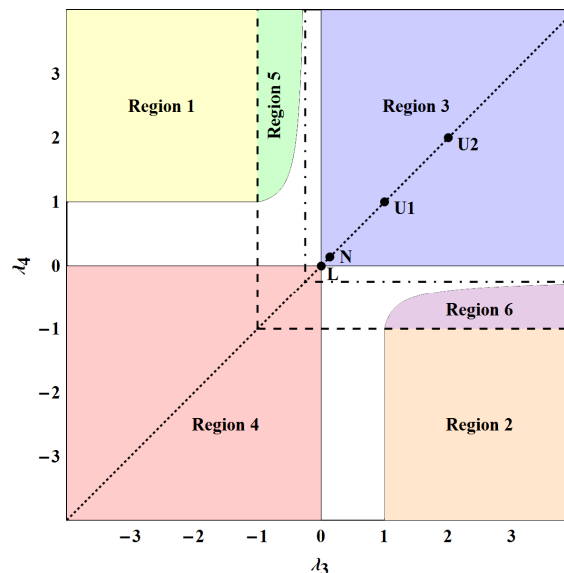


Figure 3.2: The parameter space of the GLD_{RS} in terms of Regions 1, 2, 3, 4, 5 and 6. The dotted line at $\lambda_3 = \lambda_4$ indicates symmetric distributions. U1 and U2 denote the uniform distribution at $\lambda_3 = \lambda_4 = 1$ and $\lambda_3 = \lambda_4 = 2$ respectively, while N and L denote approximations of the normal distribution and the logistic distribution by the GLD_{RS} . The first four moments and thus the mean, the variance, the skewness moment ratio and the kurtosis moment ratio exist for values of λ_3 and λ_4 to the right and above the dot-dashed lines, in effect, for $\lambda_3 > -\frac{1}{4}$ and $\lambda_4 > -\frac{1}{4}$, while all L -moments exist for values of λ_3 and λ_4 to the right and above the dashed lines, that is, for $\lambda_3 > -1$ and $\lambda_4 > -1$.

Table 3.1: Parameter space and support of the GLD_{RS} in terms of Regions 1, 2, 3, 4, 5 and 6.

Region	Shape parameter values	Support
Region 1	$\lambda_3 < -1, \lambda_4 > 1$	$\left(-\infty, \lambda_1 + \frac{1}{\lambda_2}\right]$
Region 2	$\lambda_3 > 1, \lambda_4 < -1$	$\left[\lambda_1 - \frac{1}{\lambda_2}, \infty\right)$
Region 3	$\lambda_3 = 0, \lambda_4 > 0$ $\lambda_3 > 0, \lambda_4 = 0$ $\lambda_3 > 0, \lambda_4 > 0$	$\left[\lambda_1, \lambda_1 + \frac{1}{\lambda_2}\right]$ $\left[\lambda_1 - \frac{1}{\lambda_2}, \lambda_1\right]$ $\left[\lambda_1 - \frac{1}{\lambda_2}, \lambda_1 + \frac{1}{\lambda_2}\right]$
Region 4	$\lambda_3 = 0, \lambda_4 < 0$ $\lambda_3 < 0, \lambda_4 = 0$ $\lambda_3 < 0, \lambda_4 < 0$	$[\lambda_1, \infty)$ $(-\infty, \lambda_1]$ $(-\infty, \infty)$
Region 5*	$-1 < \lambda_3 < 0, \lambda_4 > 1, u(\lambda_3, \lambda_4) < v(\lambda_3, \lambda_4)$	$\left(-\infty, \lambda_1 + \frac{1}{\lambda_2}\right]$
Region 6*	$\lambda_3 > 1, -1 < \lambda_4 < 0, u(\lambda_4, \lambda_3) < v(\lambda_4, \lambda_3)$	$\left[\lambda_1 - \frac{1}{\lambda_2}, \infty\right)$

$$* u(\lambda_i, \lambda_j) = \frac{(1 - \lambda_i)^{1 - \lambda_i} (\lambda_j - 1)^{\lambda_j - 1}}{(\lambda_j - \lambda_i)^{\lambda_j - \lambda_i}}, v(\lambda_i, \lambda_j) = -\frac{\lambda_i}{\lambda_j}$$

If $\lambda_3 = \lambda_4 = \lambda$, indicated by the dotted line in Figure 3.2, the GLD_{RS} is symmetric and reduces to Tukey's lambda distribution in (3.2) with $\lambda_1 = \alpha$ and $\lambda_2 = \frac{\lambda}{\beta}$. When both $\lambda_3 \rightarrow 0$ and $\lambda_4 \rightarrow 0$, the GLD_{RS} approximates the logistic distribution, while for $\lambda_3 = \lambda_4 \approx 0.14$, the normal distribution is approximated. Remarkably the uniform distribution can be obtained from the GLD_{RS} with four different pairs of values of λ_3 and λ_4 . The four pairs of values are $(\lambda_3, \lambda_4) = (1, 1)$, $(\lambda_3, \lambda_4) = (2, 2)$, $(\lambda_3, \lambda_4) = (1, 0)$ and $(\lambda_3, \lambda_4) = (0, 1)$.

Region 3 of the GLD_{RS} can be divided into seven sub-regions based on the diverse distributional shapes attainable in this region. These sub-regions, defined by King (1999) and labeled (a) to (h) by him, are illustrated in Figure 3.3 and listed in Table 3.2. Note that there is no sub-region (b) in Region 3. King (1999) assigned sub-region (b) to the values $-0.1359 \leq \lambda_3 < 0$ and $-0.1495 \leq \lambda_4 < 0$ in Region 4 associated with the tables provided by Ramberg *et al.* (1979) for method of moments estimation.

Similar to the GLD_{RS}, the GLD_{FMKL} possesses all three possible types of support, namely infinite support, half-infinite support and bounded support. The support attained by the GLD_{FMKL} for different values of its shape parameters, summarized in Table 3.3, suggests the division of the parameter space of the GLD_{FMKL} into four distinct regions. These four regions are illustrated graphically in Figure 3.4.

CHAPTER 3. THE GENERALIZED LAMBDA DISTRIBUTION (GLD)

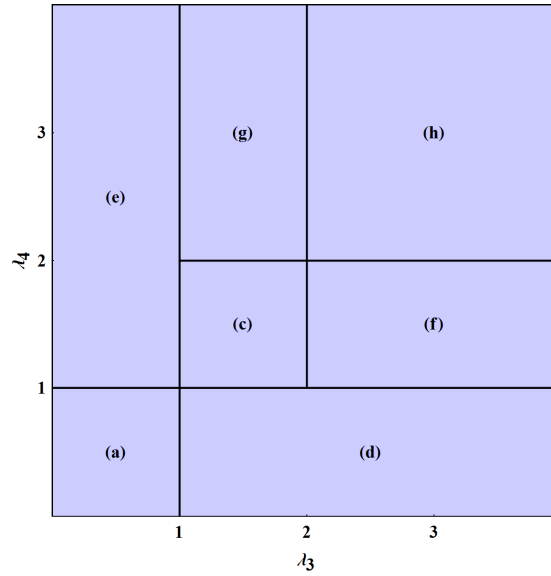


Figure 3.3: The sub-regions (a), (c), (d), (e), (f), (g) and (h) into which Region 3 of the GLD_{RS} is divided.

Table 3.2: Sub-regions in Region 3 of the GLD_{RS} .

Region	Shape parameter values
Region 3(a)	$0 \leq \lambda_3 < 1, 0 \leq \lambda_4 < 1, \lambda_3 + \lambda_4 > 0$
Region 3(c)	$1 < \lambda_3 \leq 2, 1 < \lambda_4 \leq 2$
Region 3(d)	$\lambda_3 \geq 1, 0 \leq \lambda_4 \leq 1$
Region 3(e)	$0 \leq \lambda_3 \leq 1, \lambda_4 \geq 1$
Region 3(f)	$\lambda_3 > 2, 1 < \lambda_4 < 2$
Region 3(g)	$1 < \lambda_3 < 2, \lambda_4 > 2$
Region 3(h)	$\lambda_3 \geq 2, \lambda_4 \geq 2, \lambda_3 + \lambda_4 > 4$

Table 3.3: Parameter space and support of the GLD_{FMKL} in terms of Regions 1, 2, 3 and 4.

Region	Shape parameter values	Support
Region 1	$\lambda_3 \leq 0, \lambda_4 > 0$	$\left(-\infty, \lambda_1 + \frac{1}{\lambda_2 \lambda_4}\right]$
Region 2	$\lambda_3 > 0, \lambda_4 \leq 0$	$\left[\lambda_1 - \frac{1}{\lambda_2 \lambda_3}, \infty\right)$
Region 3	$\lambda_3 > 0, \lambda_4 > 0$	$\left[\lambda_1 - \frac{1}{\lambda_2 \lambda_3}, \lambda_1 + \frac{1}{\lambda_2 \lambda_4}\right]$
Region 4	$\lambda_3 \leq 0, \lambda_4 \leq 0$	$(-\infty, \infty)$

Freimer *et al.* (1988) used a different classification scheme for the GLD_{FMKL} . They divided the parameter space of the GLD_{FMKL} into five distinct classes numbered I to V. King (1999) labeled two additional classes, Class II' and Class IV', which contain the reflection of the GLD_{FMKL} from Class II and Class IV. The seven classes are listed in Table 3.4 and

CHAPTER 3. THE GENERALIZED LAMBDA DISTRIBUTION (GLD)

indicated graphically in Figure 3.5. Comparing Figures 3.5 and 3.3, it follows that, in Region 3, the seven classes of the GLD_{FMKL} and the seven sub-regions of the GLD_{RS} are equivalent in terms of their coverage of the values of λ_3 and λ_4 .

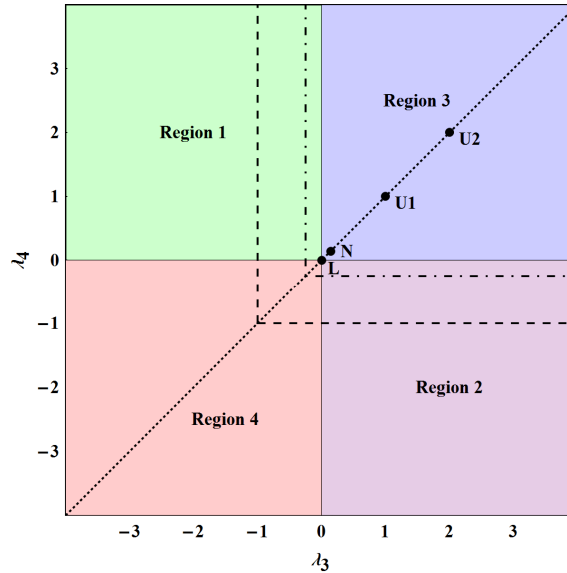


Figure 3.4: The parameter space of the GLD_{FMKL} in terms of Regions 1, 2, 3 and 4. The dotted line at $\lambda_3 = \lambda_4$ indicates symmetric distributions, U1 and U2 denote the uniform distribution at $\lambda_3 = \lambda_4 = 1$ and $\lambda_3 = \lambda_4 = 2$, L denotes the logistic distribution with $\lambda_3 = \lambda_4 = 0$, and N denotes the approximation of the normal distribution by the GLD_{FMKL} . The first four moments and hence the mean, variance and skewness and kurtosis moment ratios exist for values of λ_3 and λ_4 to the right and above the dot-dashed lines, in effect, for $\lambda_3 > -\frac{1}{4}$ and $\lambda_4 > -\frac{1}{4}$, whereas all L -moments exist for values of λ_3 and λ_4 to the right and above the dashed lines, that is, for $\lambda_3 > -1$ and $\lambda_4 > -1$.

Table 3.4: Parameter space of the GLD_{FMKL} in terms of Classes I, II, II', III, IV, IV' and V.

Class	Shape parameter values
Class I	$\lambda_3 < 1, \lambda_4 < 1$
Class II	$\lambda_3 \geq 1, \lambda_4 \leq 1$
Class II'	$\lambda_3 \leq 1, \lambda_4 \geq 1$
Class III	$1 < \lambda_3 \leq 2, 1 < \lambda_4 \leq 2$
Class IV	$\lambda_3 > 2, 1 < \lambda_4 < 2$
Class IV'	$1 < \lambda_3 < 2, \lambda_4 > 2$
Class V	$\lambda_3 \geq 2, \lambda_4 \geq 2, \lambda_3 + \lambda_4 > 4$

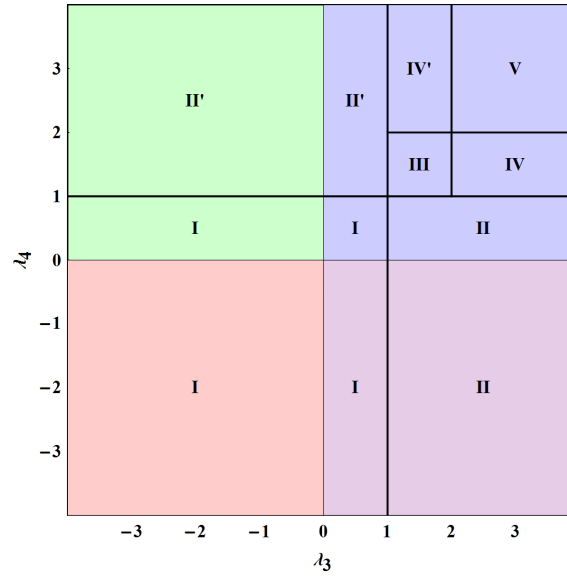


Figure 3.5: The parameter space of the GLD_{FMKL} in terms of Classes I, II, II', III, IV, IV' and V. The green-shaded, purple-shaded, blue-shaded and red-shaded areas indicate Regions 1, 2, 3 and 4 as shown in Figure 3.4.

The main difference between the parameter spaces of the GLD_{RS} and the GLD_{FMKL} is that, unlike the GLD_{RS} , the GLD_{FMKL} is a valid distribution for all values of λ_3 and λ_4 , including when these shape parameters tend to zero or infinity. The quantile functions for these limiting cases, obtained by applying L'Hôpital's rule (de l'Hôpital, 1696) and given by King (1999), are

$$Q(p) = \begin{cases} \lambda_1 + \frac{1}{\lambda_2} \log\left[\frac{p}{1-p}\right], & \lambda_3 = \lambda_4 = 0, \\ \lambda_1 + \frac{1}{\lambda_2} \left(\log[p] - \frac{(1-p)^{\lambda_4} - 1}{\lambda_4} \right), & \lambda_3 = 0, 0 < |\lambda_4| < \infty, \\ \lambda_1 + \frac{1}{\lambda_2} \log[p], & \lambda_3 = 0, \lambda_4 \rightarrow \infty, \\ \lambda_1 + \frac{1}{\lambda_2} \left(\frac{p^{\lambda_3} - 1}{\lambda_3} - \log[1-p] \right), & 0 < |\lambda_3| < \infty, \lambda_4 = 0, \\ \lambda_1 + \frac{1}{\lambda_2} \left(\frac{p^{\lambda_3} - 1}{\lambda_3} \right), & 0 < |\lambda_3| < \infty, \lambda_4 \rightarrow \infty, \\ \lambda_1 - \frac{1}{\lambda_2} \log[1-p], & \lambda_3 \rightarrow \infty, \lambda_4 = 0, \\ \lambda_1 - \frac{1}{\lambda_2} \left(\frac{(1-p)^{\lambda_4} - 1}{\lambda_4} \right), & \lambda_3 \rightarrow \infty, 0 < |\lambda_4| < \infty. \end{cases} \quad (3.5)$$

Various special and limiting cases of the GLD_{FMKL} are immediately evident from (3.5). For instance, the GLD_{FMKL} reduces to the logistic distribution for $\lambda_3 = \lambda_4 = 0$, while the exponential distribution is obtained when $\lambda_3 \rightarrow \infty$ and $\lambda_4 = 0$.

Similar to the GLD_{RS} , if $\lambda_3 = \lambda_4 = \lambda$, then the GLD_{FMKL} is symmetric, indicated by the dotted line in Figure 3.4, and simplifies to Tukey's lambda distribution in (3.2) with $\lambda_1 = \alpha$ and $\lambda_2 = \frac{1}{\beta}$. Furthermore the GLD_{FMKL} , like the GLD_{RS} , approximates the normal distribution for $\lambda_3 = \lambda_4 \approx 0.14$.

Akin to the GLD_{RS} , the uniform distribution is realized from the GLD_{FMKL} for four different pairs of values of λ_3 and λ_4 . But only two of these pairs of values, $(\lambda_3, \lambda_4) = (1, 1)$ and $(\lambda_3, \lambda_4) = (2, 2)$, are in accordance with the GLD_{RS} . The GLD_{FMKL} also simplifies to the uniform distribution for $\lambda_3 = 1$ and $\lambda_4 \rightarrow \infty$ and for $\lambda_3 \rightarrow \infty$ and $\lambda_4 = 1$, while, as indicated above, the remaining two pairs of values for which the GLD_{RS} simplifies to the uniform distribution are $(\lambda_3, \lambda_4) = (1, 0)$ and $(\lambda_3, \lambda_4) = (0, 1)$.

This disparity between the GLD_{RS} and the GLD_{FMKL} with respect to their simplifications to the uniform distribution extends to their general parameter spaces. Indeed, the GLD_{RS} and the GLD_{FMKL} are two distinct types of the GLD and not merely reparameterizations of the same distribution. The only direct functional relation between the GLD_{RS} and the GLD_{FMKL} occurs in the symmetric case with $\lambda_3 = \lambda_4$, when both types reduce to Tukey's lambda distribution.

3.6 MOMENTS

As first shown by Ramberg & Schmeiser (1974), the r^{th} order moment of the GLD_{RS} only exists if $\lambda_3 > -\frac{1}{r}$ and $\lambda_4 > -\frac{1}{r}$. So, if $\lambda_3 > -\frac{1}{4}$ and $\lambda_4 > -\frac{1}{4}$, then the mean, variance, skewness moment ratio and kurtosis moment ratio of the GLD_{RS} are

$$\mu = \lambda_1 + \frac{M_1}{\lambda_2}, \quad (3.6)$$

$$\sigma^2 = \frac{M_2 - M_1^2}{\lambda_2^2}, \quad (3.7)$$

$$\alpha_3 = \frac{M_3 - 3M_1M_2 + 2M_1^3}{(\sigma\lambda_2)^3}$$

and

$$\alpha_4 = \frac{M_4 - 4M_1M_3 + 6M_1^2M_2 - 3M_1^4}{(\sigma\lambda_2)^4},$$

where

$$M_1 = \frac{1}{\lambda_3 + 1} - \frac{1}{\lambda_4 + 1},$$

$$M_2 = \frac{1}{2\lambda_3+1} - 2B(\lambda_3 + 1, \lambda_4 + 1) + \frac{1}{2\lambda_4+1},$$

$$M_3 = \frac{1}{3\lambda_3+1} - 3B(2\lambda_3 + 1, \lambda_4 + 1) + 3B(\lambda_3 + 1, 2\lambda_4 + 1) - \frac{1}{3\lambda_4+1}$$

and

$$M_4 = \frac{1}{4\lambda_3+1} - 4B(3\lambda_3 + 1, \lambda_4 + 1) + 6B(2\lambda_3 + 1, 2\lambda_4 + 1) - 4B(\lambda_3 + 1, 3\lambda_4 + 1) + \frac{1}{4\lambda_4+1},$$

with $B(a, b)$ the beta function (see Section 2.14.1 in Chapter 2 for details).

It follows that the first four moments of the GLD_{RS} do not exist for any values of λ_3 and λ_4 in Regions 1 and 2. They do exist for all values of λ_3 and λ_4 in Region 3, but only for the small sections of Regions 4, 5 and 6 where $\lambda_3 > -\frac{1}{4}$ and $\lambda_4 > -\frac{1}{4}$.

Analogous to the GLD_{RS} , the r^{th} order moment of the GLD_{FMKL} only exists if both $\lambda_3 > -\frac{1}{r}$ and $\lambda_4 > -\frac{1}{r}$. Expressions for the mean, the variance and the skewness and kurtosis moment ratios of the GLD_{FMKL} were derived and presented by Lakhany & Mausser (2000) for $\lambda_3 \neq 0$ and $\lambda_4 \neq 0$, while their expressions for the special case where both shape parameters are zero, $\lambda_3 = \lambda_4 = 0$, are simply the expressions for the logistic distribution. However, expressions have not been given before in the literature for the special cases of the GLD_{FMKL} where just one of the shape parameters is zero, that is, for $\lambda_3 = 0$ and $\lambda_4 \neq 0$ or for $\lambda_3 \neq 0$ and $\lambda_4 = 0$. These expressions are derived in Section 3.17.1.

The complete set of expressions for the mean, the variance and the skewness and kurtosis moment ratios of the GLD_{FMKL} for $\lambda_j > -\frac{1}{4}$ and $\lambda_k > -\frac{1}{4}$, where $j = 3, 4$ and $k = 3, 4$, are

$$\mu = \begin{cases} \lambda_1 + \frac{1}{\lambda_2} \left(M_1 - \frac{(-1)^k}{\lambda_j} - \frac{(-1)^j}{\lambda_k} \right), & \lambda_j \neq 0, \lambda_k \neq 0, \lambda_j \neq \lambda_k, \\ \lambda_1 + \frac{M_1}{\lambda_2}, & \text{otherwise,} \end{cases} \quad (3.8)$$

$$\sigma^2 = \frac{M_2 - M_1^2}{\lambda_2^2}, \quad (3.9)$$

$$\alpha_3 = \frac{M_3 - 3M_1M_2 + 2M_1^3}{(\sigma\lambda_2)^3} \quad (3.10)$$

and

$$\alpha_4 = \frac{M_4 - 4M_1M_3 + 6M_1^2M_2 - 3M_1^4}{(\sigma\lambda_2)^4}, \quad (3.11)$$

with

$$M_1 = \begin{cases} \frac{(-1)^k}{\lambda_j(\lambda_j+1)} + \frac{(-1)^j}{\lambda_k(\lambda_k+1)}, & \lambda_j \neq 0, \lambda_k \neq 0, \lambda_j \neq \lambda_k, \\ \frac{(-1)^k \lambda_j}{\lambda_j+1}, & \lambda_j \neq 0, \lambda_k = 0, \\ 0, & \lambda_j = \lambda_k, \end{cases}$$

$$M_2 = \begin{cases} \frac{1}{\lambda_j^2(2\lambda_j+1)} - \frac{2B(\lambda_j+1, \lambda_k+1)}{\lambda_j \lambda_k} + \frac{1}{\lambda_k^2(2\lambda_k+1)}, & \lambda_j \neq 0, \lambda_k \neq 0, \\ \frac{2(2\lambda_j^3 + \lambda_j^2 - \lambda_j - 1)}{\lambda_j(\lambda_j+1)(2\lambda_j+1)} + \frac{2(C+\psi(\lambda_j+2))}{\lambda_j(\lambda_j+1)}, & \lambda_j \neq 0, \lambda_k = 0, \\ \frac{\pi^2}{3}, & \lambda_j = \lambda_k = 0, \end{cases}$$

$$M_3 = \begin{cases} \frac{(-1)^k}{\lambda_j^3(3\lambda_j+1)} - \frac{3(-1)^k B(2\lambda_j+1, \lambda_k+1)}{\lambda_j^2 \lambda_k} - \frac{3(-1)^j B(\lambda_j+1, 2\lambda_k+1)}{\lambda_j \lambda_k^2} \\ + \frac{(-1)^j}{\lambda_k^3(3\lambda_k+1)}, & \lambda_j \neq 0, \lambda_k \neq 0, \lambda_j \neq \lambda_k, \\ \frac{3(-1)^k (12\lambda_j^5 + 10\lambda_j^4 - 4\lambda_j^3 - \lambda_j^2 + 4\lambda_j + 1)}{\lambda_j^2(\lambda_j+1)(2\lambda_j+1)(3\lambda_j+1)} - \frac{6(-1)^k (C+\psi(\lambda_j+2))}{\lambda_j^2(\lambda_j+1)} \\ + \frac{3(-1)^k (C+\psi(2\lambda_j+2))}{\lambda_j^2(2\lambda_j+1)} + \frac{3(-1)^k \left(\frac{\pi^2}{6} + (C+\psi(\lambda_j+2))^2 - \psi^{(1)}(\lambda_j+2) \right)}{\lambda_j(\lambda_j+1)}, & \lambda_j \neq 0, \lambda_k = 0, \\ 0, & \lambda_j = \lambda_k, \end{cases}$$

and

$$M_4 = \begin{cases} \frac{1}{\lambda_j^4(4\lambda_j+1)} - \frac{4B(3\lambda_j+1, \lambda_k+1)}{\lambda_j^3 \lambda_k} + \frac{6B(2\lambda_j+1, 2\lambda_k+1)}{\lambda_j^2 \lambda_k^2} \\ - \frac{4B(\lambda_j+1, 3\lambda_k+1)}{\lambda_j \lambda_k^3} + \frac{1}{\lambda_k^4(4\lambda_k+1)}, & \lambda_j \neq 0, \lambda_k \neq 0, \\ \frac{4(144\lambda_j^7 + 156\lambda_j^6 - 18\lambda_j^5 - 24\lambda_j^4 + 7\lambda_j^3 - 11\lambda_j^2 - 7\lambda_j - 1)}{\lambda_j^3(\lambda_j+1)(2\lambda_j+1)(3\lambda_j+1)(4\lambda_j+1)} + \frac{12(C+\psi(\lambda_j+2))}{\lambda_j^3(\lambda_j+1)} \\ - \frac{12(C+\psi(2\lambda_j+2))}{\lambda_j^3(2\lambda_j+1)} + \frac{4(C+\psi(3\lambda_j+2))}{\lambda_j^3(3\lambda_j+1)} - \frac{12 \left(\frac{\pi^2}{6} + (C+\psi(\lambda_j+2))^2 - \psi^{(1)}(\lambda_j+2) \right)}{\lambda_j^2(\lambda_j+1)} \\ + \frac{6 \left(\frac{\pi^2}{6} + (C+\psi(2\lambda_j+2))^2 - \psi^{(1)}(2\lambda_j+2) \right)}{\lambda_j^2(2\lambda_j+1)} \\ + \frac{4 \left(3 \left(\frac{\pi^2}{6} - \psi^{(1)}(\lambda_j+2) \right) (C+\psi(\lambda_j+2)) + (C+\psi(\lambda_j+2))^3 + 2\zeta(3) + \psi^{(2)}(\lambda_j+2) \right)}{\lambda_j(\lambda_j+1)}, & \lambda_j \neq 0, \lambda_k = 0, \\ \frac{7\pi^4}{15}, & \lambda_j = \lambda_k = 0, \end{cases}$$

where C is Euler's constant, $\psi(a)$ is the psi function and $\psi^{(r)}(a)$ is the r^{th} derivative of the psi function (see again Section 2.14.1 in Chapter 2 for details).

3.7 L-MOMENTS

Recall from Section 2.5 that, if the mean of a probability distribution exists, then all the L -moments exist. Thus, the r^{th} order L -moment of the GLD_{RS} exists if $\lambda_3 > -1$ and $\lambda_4 > -1$. This implies that the L -moments of the GLD_{RS} exist for all values of λ_3 and λ_4 in Regions 3, 5 and 6 as well as for the section of Region 4 where $\lambda_3 > -1$ and $\lambda_4 > -1$.

Expressions for the L -moments of the GLD_{RS} have been derived and given in the literature in a variety of forms (Bergevin, 1993; Mohan, 1994; Karian & Dudewicz, 2003; Asquith, 2007; Karvanen & Nuutinen, 2008). The L -location and L -scale of the GLD_{RS} are

$$L_1 = \lambda_1 + \frac{1}{\lambda_2} \left(\frac{1}{\lambda_3+1} - \frac{1}{\lambda_4+1} \right) \quad (3.12)$$

and

$$L_2 = \frac{1}{\lambda_2} \left(\frac{\lambda_3}{(\lambda_3+1)(\lambda_3+2)} + \frac{\lambda_4}{(\lambda_4+1)(\lambda_4+2)} \right), \quad (3.13)$$

while the r^{th} order L -moment is given by

$$L_r = \frac{1}{\lambda_2} \left(\frac{\prod_{k=0}^{r-2} (\lambda_3 - k)}{\prod_{k=1}^r (\lambda_3 + k)} + (-1)^r \frac{\prod_{k=0}^{r-2} (\lambda_4 - k)}{\prod_{k=1}^r (\lambda_4 + k)} \right), \quad r = 3, 4, 5, \dots$$

The L -skewness ratio and L -kurtosis ratio for the GLD_{RS} are

$$\tau_3 = \frac{\frac{\lambda_3(\lambda_3-1)}{(\lambda_3+1)(\lambda_3+2)(\lambda_3+3)} - \frac{\lambda_4(\lambda_4-1)}{(\lambda_4+1)(\lambda_4+2)(\lambda_4+3)}}{\frac{\lambda_3}{(\lambda_3+1)(\lambda_3+2)} + \frac{\lambda_4}{(\lambda_4+1)(\lambda_4+2)}} \quad (3.14)$$

and

$$\tau_4 = \frac{\frac{\lambda_3(\lambda_3-1)(\lambda_3-2)}{(\lambda_3+1)(\lambda_3+2)(\lambda_3+3)(\lambda_3+4)} + \frac{\lambda_4(\lambda_4-1)(\lambda_4-2)}{(\lambda_4+1)(\lambda_4+2)(\lambda_4+3)(\lambda_4+4)}}{\frac{\lambda_3}{(\lambda_3+1)(\lambda_3+2)} + \frac{\lambda_4}{(\lambda_4+1)(\lambda_4+2)}}. \quad (3.15)$$

Karvanen & Nuutinen (2008) numerically calculated the boundaries of τ_3 and τ_4 for the GLD_{RS} . For the symmetric GLD_{RS} with $\lambda_3 = \lambda_4 = \lambda$, in effect, for Tukey's lambda distribution, they analytically derived these boundaries and showed that

$$\tau_3 = 0 \text{ and } \tau_4 = \frac{(\lambda-1)(\lambda-2)}{(\lambda+3)(\lambda+4)}.$$

The L -moment ratio diagrams of the GLD_{RS} in terms of Regions 3, 4, 5 and 6 are illustrated in Figure 3.6. These L -moment ratio diagrams are equivalent to the L -moment ratio diagrams obtained and presented by Karvanen & Nuutinen (2008). It is furthermore indicated in Figure 3.6 that the boundaries of τ_3 and τ_4 for Regions 3 and 4, obtained as $\lambda_3 \rightarrow 0$ or $\lambda_4 \rightarrow 0$, are given by the generalized Pareto and reflected generalized Pareto distributions.

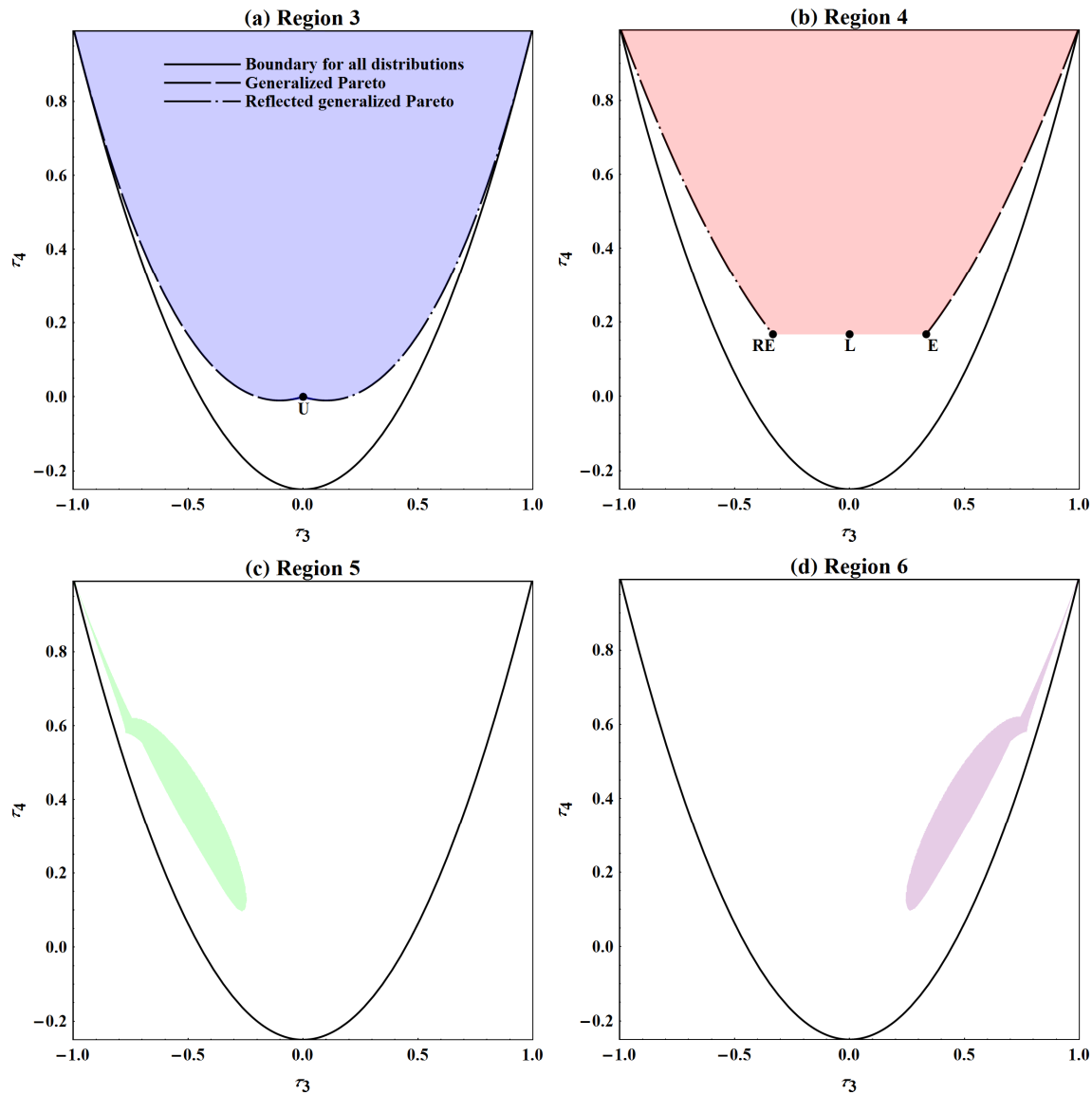


Figure 3.6: L -moment ratio diagrams for Regions 3, 4, 5 and 6 of the GLD_{RS} . The line types indicated in diagram (a) also apply to the other diagrams. The uniform, logistic, exponential and reflected exponential distributions are indicated by U, L, E and RE.

In contrast to the GLD_{RS} , the L -moments of the GLD_{FMKL} have not been studied in detail before in the literature – one study giving and using the L -moments of the GLD_{FMKL} is by Nair & Vineshkumar (2010). The expressions for the L -moments of the GLD_{FMKL} , derived in Section 3.17.2, are similar in form to those of the GLD_{RS} . If $\lambda_3 > -1$ and $\lambda_4 > -1$, then

$$L_1 = \lambda_1 - \frac{1}{\lambda_2} \left(\frac{1}{\lambda_3+1} - \frac{1}{\lambda_4+1} \right), \quad (3.16)$$

$$L_2 = \frac{1}{\lambda_2} \left(\frac{1}{(\lambda_3+1)(\lambda_3+2)} + \frac{1}{(\lambda_4+1)(\lambda_4+2)} \right) \quad (3.17)$$

and

$$L_r = \frac{1}{\lambda_2} \left(\frac{\prod_{k=1}^{r-2} (\lambda_3-k)}{\prod_{k=1}^r (\lambda_3+k)} + (-1)^r \frac{\prod_{k=1}^{r-2} (\lambda_4-k)}{\prod_{k=1}^r (\lambda_4+k)} \right), \quad r = 3, 4, 5, \dots \quad (3.18)$$

The L -skewness ratio and L -kurtosis ratio for the GLD_{FMKL} are

$$\tau_3 = \frac{\frac{\lambda_3-1}{(\lambda_3+1)(\lambda_3+2)(\lambda_3+3)} - \frac{\lambda_4-1}{(\lambda_4+1)(\lambda_4+2)(\lambda_4+3)}}{\frac{1}{(\lambda_3+1)(\lambda_3+2)} + \frac{1}{(\lambda_4+1)(\lambda_4+2)}} \quad (3.19)$$

and

$$\tau_4 = \frac{\frac{(\lambda_3-1)(\lambda_3-2)}{(\lambda_3+1)(\lambda_3+2)(\lambda_3+3)(\lambda_3+4)} + \frac{(\lambda_4-1)(\lambda_4-2)}{(\lambda_4+1)(\lambda_4+2)(\lambda_4+3)(\lambda_4+4)}}{\frac{1}{(\lambda_3+1)(\lambda_3+2)} + \frac{1}{(\lambda_4+1)(\lambda_4+2)}}. \quad (3.20)$$

L -moment ratio diagrams indicating the (τ_3, τ_4) spaces covered by the four regions of the GLD_{FMKL} are shown in Figure 3.7. It is evident from comparing Figures 3.6(a) and 3.7(b) that the (τ_3, τ_4) space covered by Regions 3 of the GLD_{RS} and the GLD_{FMKL} are the same.

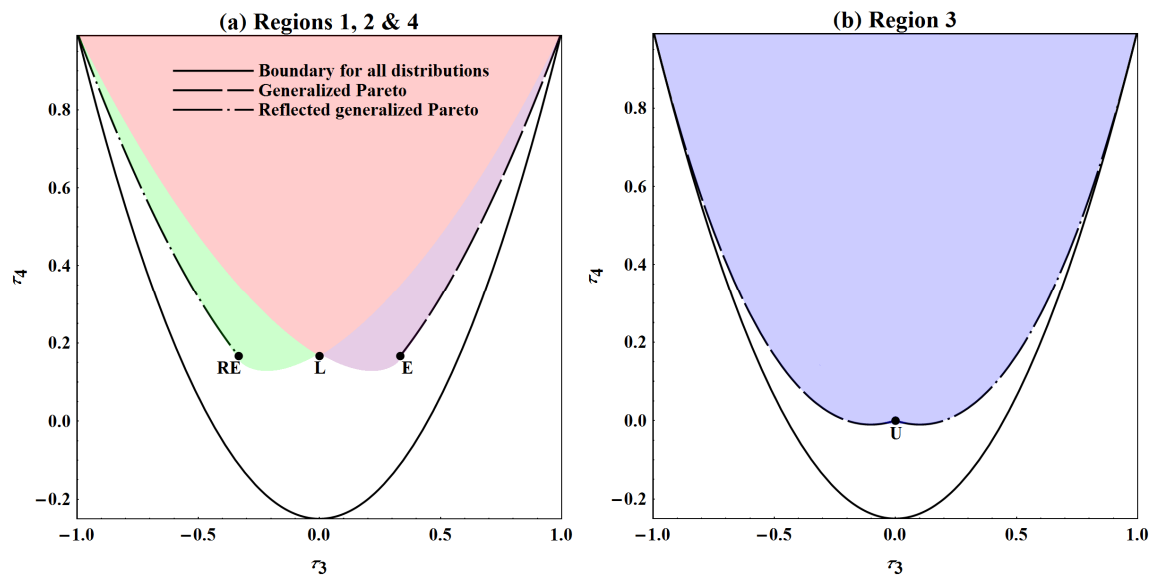


Figure 3.7: L -moment ratio diagrams for Regions 1, 2, 3 and 4 of the GLD_{FMKL} . The line types indicated in diagram (a) also apply to diagram (b). The uniform, logistic, exponential and reflected exponential distributions are indicated by U, L, E and RE. The green-shaded, purple-shaded and red-shaded areas in diagram (a) are the (τ_3, τ_4) spaces attained by Regions 1, 2 and 4.

Figure 3.8 depicts the L -moment ratio diagrams for Region 3(a) and Region 4 of the GLD_{RS} and for Class I of the GLD_{FMKL} , both with $\lambda_3 < 1$ and $\lambda_4 < 1$. As will be seen in Sections 3.11 and 3.12, these two regions of the GLD_{RS} and Class I of the GLD_{FMKL} provide the most useful distributional shapes. Note that, whereas the combined coverage of the (τ_3, τ_4) space by Regions 3(a) and 4 of the GLD_{RS} extends all the way towards the boundaries given by the generalized Pareto and the reflected generalized Pareto distributions, the coverage by Class I of the GLD_{FMKL} does not. The reason is that $\lambda_3 < 1$ and $\lambda_4 < 1$ in Class I, while the generalized Pareto and reflected generalized Pareto distributions are obtained from the GLD_{FMKL} when $\lambda_3 \rightarrow \infty$ or $\lambda_4 \rightarrow \infty$ in Classes II and II'.

It is clear from the L -moment ratio diagrams in Figures 3.6 to 3.8 that the GLD covers a substantial area of the (τ_3, τ_4) space, especially through Regions 3(a) and 4 of the GLD_{RS} and Class I of the GLD_{FMKL} . The area covered by the GLD is larger than the area covered by other popular four-parameter distributions, such as the Burr Type III and Burr Type XII distributions (see again Figure 2.10), highlighting the greater flexibility of the GLD with respect to distributional shape.

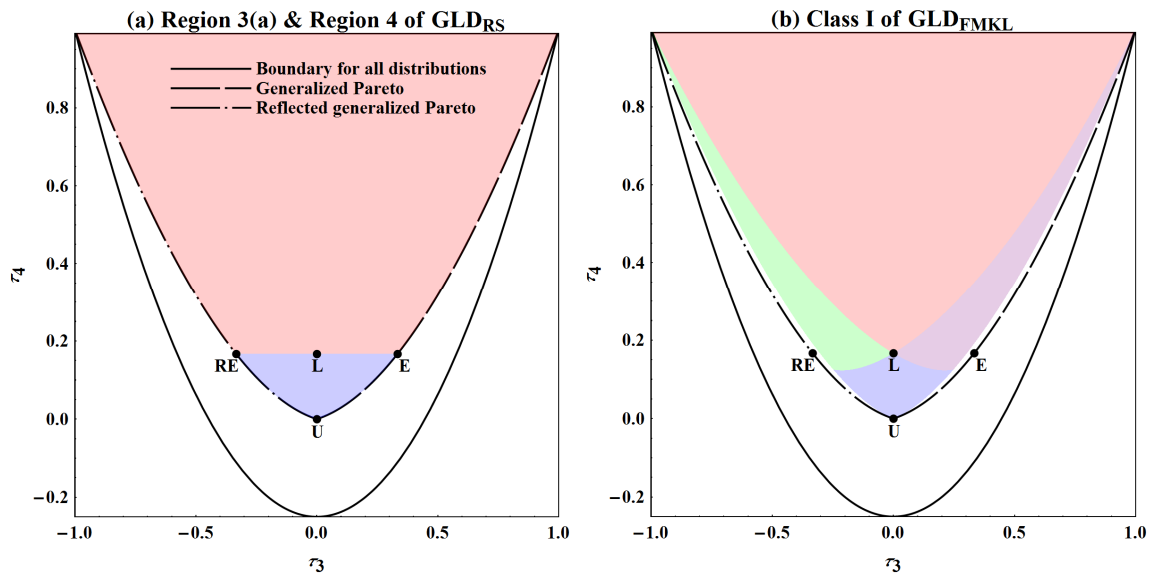


Figure 3.8: L -moment ratio diagrams for Region 3(a) and Region 4 of the GLD_{RS} and for Class I of the GLD_{FMKL} . The line types indicated in diagram (a) also apply to diagram (b). U, L, E and RE denote the uniform, logistic, exponential and reflected exponential distributions. In diagram (a), the blue-shaded area is the (τ_3, τ_4) space covered by Region 3(a), while the red-shaded area is the (τ_3, τ_4) space covered by Region 4. The green-shaded, purple-shaded, blue-shaded and red-shaded areas in diagram (b) indicate the coverage of the (τ_3, τ_4) spaces by Regions 1, 2, 3 and 4 of the GLD_{FMKL} with $\lambda_3 < 1$ and $\lambda_4 < 1$.

3.8 QUANTILE-BASED MEASURES OF LOCATION, SPREAD AND SHAPE

The non-existence of moments and L -moments for certain shape parameter values of the GLD is problematic in that the use of these measures in describing the location, spread and shape of the GLD_{RS} and GLD_{FMKL} for the affected regions and classes is constrained. In contrast, measures of location, spread and shape defined in terms of the quantiles of the GLD exist for all values of λ_3 and λ_4 . King (1999) and also King & MacGillivray (2007) gave the median, spread function, γ -functional, η -functional and ratio-of-spread functions for both the GLD_{RS} and the GLD_{FMKL} .

Let $\frac{1}{2} < v < u < 1$. Then the median and spread function of the GLD_{RS} are

$$me = \lambda_1 + \frac{1}{\lambda_2} \left(\left(\frac{1}{2} \right)^{\lambda_3} - \left(\frac{1}{2} \right)^{\lambda_4} \right) \quad (3.21)$$

and

$$S(u) = \frac{1}{\lambda_2} \left(u^{\lambda_3} - (1-u)^{\lambda_3} + u^{\lambda_4} - (1-u)^{\lambda_4} \right), \quad (3.22)$$

while the two skewness functionals and the ratio-of-spread functions for the GLD_{RS} are

$$\gamma(u) = \frac{u^{\lambda_3 + (1-u)^{\lambda_3}} - u^{\lambda_4} - (1-u)^{\lambda_4} - 2 \left(\left(\frac{1}{2} \right)^{\lambda_3} - \left(\frac{1}{2} \right)^{\lambda_4} \right)}{u^{\lambda_3} - (1-u)^{\lambda_3} + u^{\lambda_4} - (1-u)^{\lambda_4}},$$

$$\eta(u, v) = \frac{u^{\lambda_3 + (1-u)^{\lambda_3}} - v^{\lambda_3} - (1-v)^{\lambda_3} - u^{\lambda_4} - (1-u)^{\lambda_4} + v^{\lambda_4} + (1-v)^{\lambda_4}}{v^{\lambda_3} - (1-v)^{\lambda_3} + v^{\lambda_4} - (1-v)^{\lambda_4}}$$

and

$$R(u, v) = \frac{u^{\lambda_3} - (1-u)^{\lambda_3} + u^{\lambda_4} - (1-u)^{\lambda_4}}{v^{\lambda_3} - (1-v)^{\lambda_3} + v^{\lambda_4} - (1-v)^{\lambda_4}}.$$

The κ -functional, the bounded functional for kurtosis proposed in Section 2.6 of Chapter 2, is

$$\kappa(u, v) = \frac{u^{\lambda_3} - (1-u)^{\lambda_3} - v^{\lambda_3} + (1-v)^{\lambda_3} + u^{\lambda_4} - (1-u)^{\lambda_4} - v^{\lambda_4} + (1-v)^{\lambda_4}}{u^{\lambda_3} - (1-u)^{\lambda_3} + u^{\lambda_4} - (1-u)^{\lambda_4}}$$

for the GLD_{RS} .

Given $\frac{1}{2} < v < u < 1$, $j = 3, 4$ and $k = 3, 4$, the median and spread function of the GLD_{FMKL} are

$$me = \begin{cases} \lambda_1 + \frac{1}{\lambda_2} \left(\frac{(-1)^k}{\lambda_j} \left(\left(\frac{1}{2} \right)^{\lambda_j} - 1 \right) + \frac{(-1)^j}{\lambda_k} \left(\left(\frac{1}{2} \right)^{\lambda_k} - 1 \right) \right), & \lambda_j \neq 0, \lambda_k \neq 0, \lambda_j \neq \lambda_k, \\ \lambda_1 + \frac{1}{\lambda_2} \left(\frac{(-1)^k}{\lambda_j} \left(\left(\frac{1}{2} \right)^{\lambda_j} - 1 \right) + (-1)^j \log \left[\frac{1}{2} \right] \right), & \lambda_j \neq 0, \lambda_k = 0, \\ \lambda_1, & \lambda_j = \lambda_k, \end{cases} \quad (3.23)$$

and

$$S(u) = \begin{cases} \frac{1}{\lambda_2} \left(\frac{u^{\lambda_j} - (1-u)^{\lambda_j}}{\lambda_j} + \frac{u^{\lambda_k} - (1-u)^{\lambda_k}}{\lambda_k} \right), & \lambda_j \neq 0, \lambda_k \neq 0, \\ \frac{1}{\lambda_2} \left(\frac{u^{\lambda_j} - (1-u)^{\lambda_j}}{\lambda_j} + \log \left[\frac{u}{1-u} \right] \right), & \lambda_j \neq 0, \lambda_k = 0, \\ \frac{2}{\lambda_2} \log \left[\frac{u}{1-u} \right], & \lambda_j = \lambda_k = 0. \end{cases} \quad (3.24)$$

The shape functionals of the GLD_{FMKL} are

$$\gamma(u) = \begin{cases} \frac{\frac{(-1)^k}{\lambda_j} \left(u^{\lambda_j} + (1-u)^{\lambda_j} - 2 \left(\frac{1}{2} \right)^{\lambda_j} \right)}{\frac{u^{\lambda_j} - (1-u)^{\lambda_j}}{\lambda_j} + \frac{u^{\lambda_k} - (1-u)^{\lambda_k}}{\lambda_k}} \\ + \frac{\frac{(-1)^j}{\lambda_k} \left(u^{\lambda_k} + (1-u)^{\lambda_k} - 2 \left(\frac{1}{2} \right)^{\lambda_k} \right)}{\frac{u^{\lambda_j} - (1-u)^{\lambda_j}}{\lambda_j} + \frac{u^{\lambda_k} - (1-u)^{\lambda_k}}{\lambda_k}}, & \lambda_j \neq 0, \lambda_k \neq 0, \lambda_j \neq \lambda_k, \\ \frac{\frac{(-1)^k}{\lambda_j} \left(u^{\lambda_j} + (1-u)^{\lambda_j} - 2 \left(\frac{1}{2} \right)^{\lambda_j} \right) + (-1)^j \log[4u(1-u)]}{\frac{u^{\lambda_j} - (1-u)^{\lambda_j}}{\lambda_j} + \log \left[\frac{u}{1-u} \right]}, & \lambda_j \neq 0, \lambda_k = 0, \\ 0, & \lambda_j = \lambda_k, \end{cases}$$

$$\eta(u, v) = \begin{cases} \frac{\frac{(-1)^k}{\lambda_j} \left(u^{\lambda_j} + (1-u)^{\lambda_j} - v^{\lambda_j} - (1-v)^{\lambda_j} \right)}{\frac{v^{\lambda_j} - (1-v)^{\lambda_j}}{\lambda_j} + \frac{v^{\lambda_k} - (1-v)^{\lambda_k}}{\lambda_k}} \\ + \frac{\frac{(-1)^j}{\lambda_k} \left(u^{\lambda_k} + (1-u)^{\lambda_k} - v^{\lambda_k} - (1-v)^{\lambda_k} \right)}{\frac{v^{\lambda_j} - (1-v)^{\lambda_j}}{\lambda_j} + \frac{v^{\lambda_k} - (1-v)^{\lambda_k}}{\lambda_k}}, & \lambda_j \neq 0, \lambda_k \neq 0, \lambda_j \neq \lambda_k, \\ \frac{\frac{(-1)^k}{\lambda_j} \left(u^{\lambda_j} + (1-u)^{\lambda_j} - v^{\lambda_j} - (1-v)^{\lambda_j} \right)}{\frac{v^{\lambda_j} - (1-v)^{\lambda_j}}{\lambda_j} + \log\left[\frac{u}{1-u}\right]} \\ + \frac{(-1)^j \log\left[\frac{u(1-u)}{v(1-v)}\right]}{\frac{v^{\lambda_j} - (1-v)^{\lambda_j}}{\lambda_j} + \log\left[\frac{u}{1-u}\right]}, & \lambda_j \neq 0, \lambda_k = 0, \\ 0, & \lambda_j = \lambda_k, \end{cases}$$

$$R(u, v) = \begin{cases} \frac{\frac{u^{\lambda_j} - (1-u)^{\lambda_j}}{\lambda_j} + \frac{u^{\lambda_k} - (1-u)^{\lambda_k}}{\lambda_k}}{\frac{v^{\lambda_j} - (1-v)^{\lambda_j}}{\lambda_j} + \frac{v^{\lambda_k} - (1-v)^{\lambda_k}}{\lambda_k}}, & \lambda_j \neq 0, \lambda_k \neq 0, \\ \frac{\frac{u^{\lambda_j} - (1-u)^{\lambda_j}}{\lambda_j} + \log\left[\frac{u}{1-u}\right]}{\frac{v^{\lambda_j} - (1-v)^{\lambda_j}}{\lambda_j} + \log\left[\frac{v}{1-v}\right]}, & \lambda_j \neq 0, \lambda_k = 0, \\ \frac{\log\left[\frac{u}{1-u}\right]}{\log\left[\frac{v}{1-v}\right]}, & \lambda_j = \lambda_k = 0, \end{cases}$$

and

$$\kappa(u, v) = \begin{cases} \frac{\frac{u^{\lambda_j} - (1-u)^{\lambda_j} - v^{\lambda_j} + (1-v)^{\lambda_j}}{\lambda_j} + \frac{u^{\lambda_k} - (1-u)^{\lambda_k} - v^{\lambda_k} + (1-v)^{\lambda_k}}{\lambda_k}}{\frac{u^{\lambda_j} - (1-u)^{\lambda_j}}{\lambda_j} + \frac{u^{\lambda_k} - (1-u)^{\lambda_k}}{\lambda_k}}, & \lambda_j \neq 0, \lambda_k \neq 0, \\ \frac{\frac{u^{\lambda_j} - (1-u)^{\lambda_j} - v^{\lambda_j} + (1-v)^{\lambda_j}}{\lambda_j} + \log\left[\frac{u(1-v)}{(1-u)v}\right]}{\frac{u^{\lambda_j} - (1-u)^{\lambda_j}}{\lambda_j} + \log\left[\frac{u}{1-u}\right]}, & \lambda_j \neq 0, \lambda_k = 0, \\ \frac{\log\left[\frac{u(1-v)}{(1-u)v}\right]}{\log\left[\frac{u}{1-u}\right]}, & \lambda_j = \lambda_k = 0. \end{cases}$$

3.9 LOCATION AND SPREAD

The interpretation of the location and scale parameters of the GLD is straightforward. Holding the values of all the other parameters constant, an increase in the value of λ_1 leads to an increase in the location of the GLD. This follows immediately from the expressions for the mean in (3.6) and (3.8), the L -location in (3.12) and (3.16), and the median in (3.21) and (3.23) of the GLD_{RS} and GLD_{FMKL} respectively and is illustrated in Figure 3.9(a) for the GLD_{RS} .

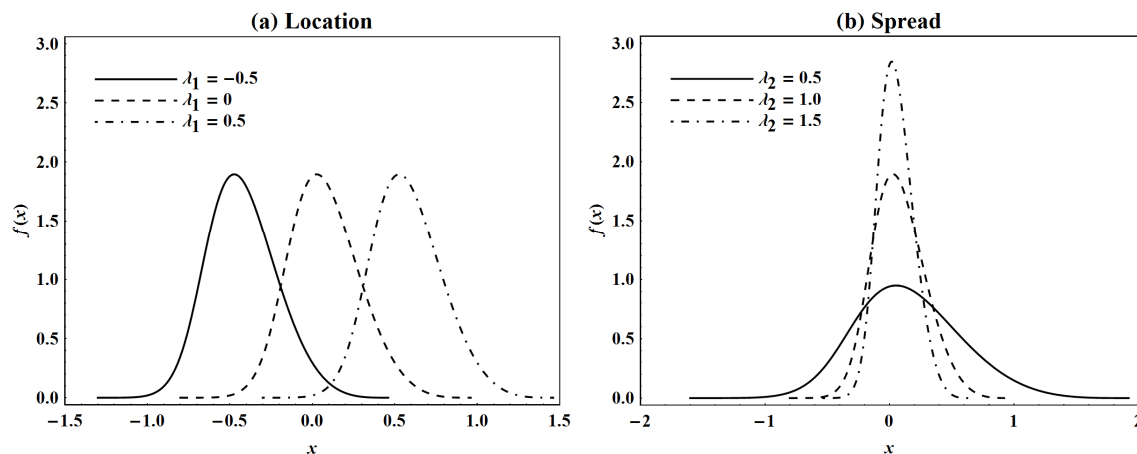


Figure 3.9: Probability density functions of members of the GLD_{RS} with varying location and spread. In graph (a), where $(\lambda_2, \lambda_3, \lambda_4) = (1, 0.1, 0.2)$, an increase in the value of λ_1 leads to an increase in the location of the GLD_{RS} , while in graph (b), where $\lambda_1 = 0$ and $(\lambda_3, \lambda_4) = (0.1, 0.2)$, an increase in the value of λ_2 leads to a decrease in the spread of the GLD_{RS} .

There is an inverse relation between the spread of the GLD and the value of λ_2 in that the spread of the GLD decreases when the value of λ_2 increases (holding the values of the other parameters constant). This inverse relation is evident from the expressions for the variance in (3.7), the L -scale in (3.13) and the spread function in (3.22) of the GLD_{RS} , as well as from the corresponding expressions in (3.9), (3.17) and (3.24) for the GLD_{FMKL} , and is demonstrated graphically in Figure 3.9(b) for the GLD_{RS} .

3.10 DISTRIBUTIONAL SHAPE

The GLD is highly flexible with respect to distributional shape. But this flexibility comes at a cost in that the relationship between the shape parameters of the GLD and the distributional shape is extremely complex, particularly with respect to skewness. This is especially true in Region 3 of both the GLD_{RS} and GLD_{FMKL} .

The shape properties of the GLD are discussed below. See MacGillivray (1982), Groeneveld (1986), Freimer *et al.* (1988), King (1999) and Karian & Dudewicz (2000, 2010) for in-depth analyses of the GLD's shape properties. Since the GLD_{RS} and GLD_{FMKL} share most of the intricacies and complexities with respect to distributional shape, the shape properties of the GLD are illustrated via the GLD_{RS} . Where necessary, main differences between shape properties of the GLD_{RS} and the GLD_{FMKL} are highlighted.

3.10.1 TAIL BEHAVIOR

As explained by King (1999), for certain combinations of values of the GLD's shape parameters in Regions 3 and 4, a change in the value of one of these parameters will affect one of the tails of the GLD. In Region 4 for $\lambda_3 < 0$ and $\lambda_4 < 0$ and in Region 3 for $0 < \lambda_3 < 2$ and $0 < \lambda_4 < 2$, the left tail of the GLD is affected by a change in the value of λ_3 , whereas the right tail is affected by a change in the value of λ_4 . When $\lambda_3 > 2$ and $\lambda_4 > 2$ in Region 3, a change in the value of λ_3 affects the right tail of the GLD while a change in the value of λ_4 affects the left tail. See Figure 3.10 for examples in terms of the GLD_{RS} . The tail behavior is not straightforward for other combinations of shape parameter values in Regions 3 and 4 and also not for the other regions of the GLD.

3.10.2 SKEWNESS AND KURTOSIS

As can be seen from the various measures of shape, the two shape parameters, λ_3 and λ_4 , jointly determine the skewness and the kurtosis of the GLD. For example, the L -skewness and L -kurtosis ratios of the GLD_{RS} in (3.14) and (3.15) and of the GLD_{FMKL} in (3.19) and (3.20) are functions of both λ_3 and λ_4 . This complicates not only the interpretation of the two shape parameters but also parameter estimation for the GLD discussed in Section 3.13.

Recall from Section 3.5 that the uniform distribution is obtained from the GLD_{RS} when $(\lambda_3, \lambda_4) = (1, 1)$, when $(\lambda_3, \lambda_4) = (2, 2)$, when $(\lambda_3, \lambda_4) = (1, 0)$ and when $(\lambda_3, \lambda_4) = (0, 1)$. The skewness and kurtosis moment ratios of the uniform distribution are $\alpha_3 = 0$ and $\alpha_4 = 1.8$ respectively. Thus four different pairs of values of λ_3 and λ_4 from the GLD_{RS} produce these values of α_3 and α_4 . This suggests that there does not exist a one-to-one correspondence between the shape parameters of the GLD and the skewness and kurtosis moment ratios.

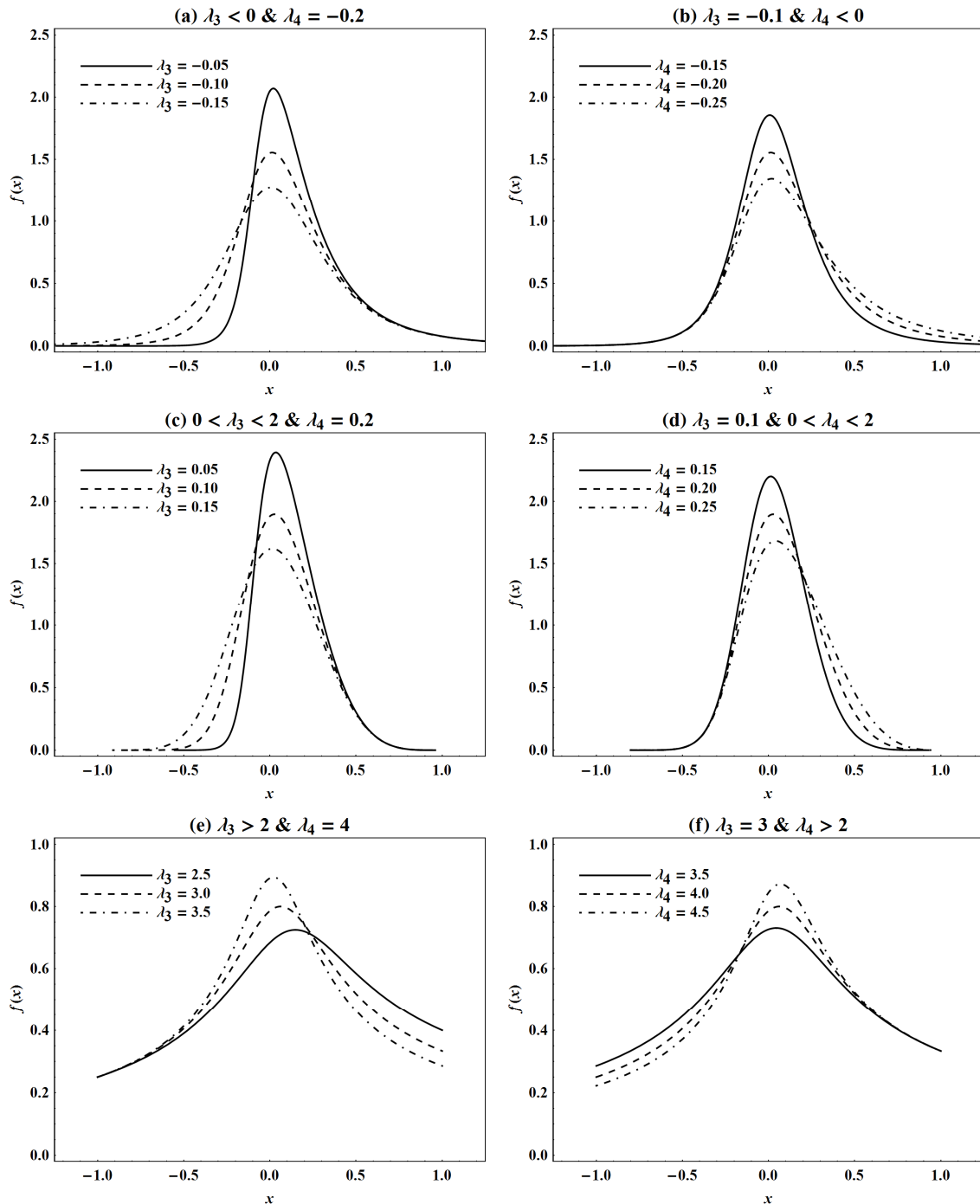


Figure 3.10: Probability density functions of members of the GLD_{RS} from Regions 3 and 4 illustrating tail behavior. In graphs (a) and (b), where $(\lambda_1, \lambda_2) = (0, -1)$, $\lambda_3 < 0$ and $\lambda_4 < 0$ from Region 4, and in graphs (c) and (d), where $(\lambda_1, \lambda_2) = (0, 1)$, $0 < \lambda_3 < 2$ and $0 < \lambda_4 < 2$ from Region 3, a change in the value of λ_3 affects the left tail, while a change in the value of λ_4 affects the right tail. In graphs (e) and (f), where $(\lambda_1, \lambda_2) = (0, 1)$, $\lambda_3 > 2$ and $\lambda_4 > 2$ from Region 3, a change in the value of λ_3 affects the right tail, while a change in the value of λ_4 affects the left tail.

Johnson (1980) pointed out that the correspondence is one-to-one for both the Pearson and the Johnson families of distributions and queried whether the same is true for the GLD. In response Ramberg *et al.* (1980) gave an example to show that the correspondence is indeed

not one-to-one for the GLD. Their example indicated that the three members of the GLD_{RS} with $(\lambda_3, \lambda_4) = (0.0742, 0.0742)$, $(\lambda_3, \lambda_4) = (6.026, 6.026)$ and $(\lambda_3, \lambda_4) = (35.498, 2.297)$, whose probability density functions are plotted in Figure 3.11, all have $\alpha_3 = 0$ and $\alpha_4 = 3.4$.

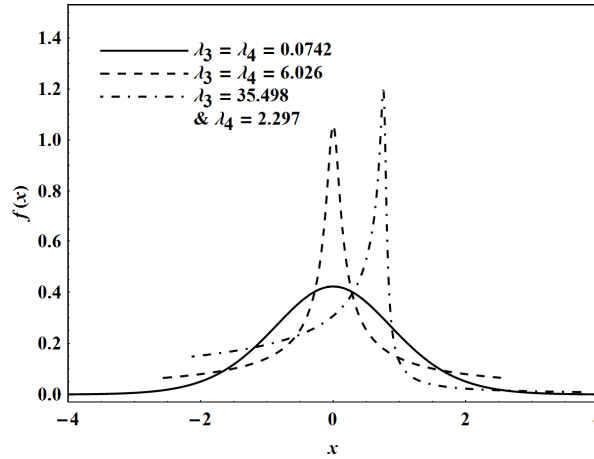


Figure 3.11: Probability density functions of three members of the GLD_{RS} , all with $\alpha_3 = 0$ and $\alpha_4 = 3.4$. Note that $\mu = 0$ and $\sigma^2 = 1$ for all three members of the GLD_{RS} , that is, all three members have zero mean and unit variance.

This undesirable characteristic of the GLD is not restricted to the skewness and kurtosis moment ratios. The same is true for other measures of shape such as the L -skewness and L -kurtosis ratios. For instance, $\tau_3 = \tau_4 = 0$ for the four different pairs of values of λ_3 and λ_4 from the GLD_{RS} which yield the uniform distribution. As another example, Figure 3.12 shows the probability density functions of three members of the GLD_{RS} with $(\lambda_3, \lambda_4) = (\frac{1}{2}, \frac{1}{2})$, $(\lambda_3, \lambda_4) = (3, 3)$ and $(\lambda_3, \lambda_4) = (84.1160, 1.2734)$, all yielding $\tau_3 = 0$ and $\tau_4 = \frac{1}{21} = 0.0476$.

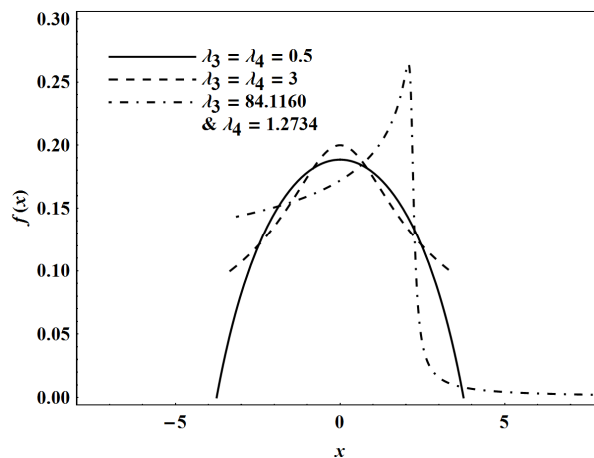


Figure 3.12: Probability density functions of three members of the GLD_{RS} , all with $\tau_3 = 0$ and $\tau_4 = \frac{1}{21}$. Note that $L_1 = 0$ and $L_2 = 1$ for all three members.

To complicate matters further, when one considers different pairs of values of λ_3 and λ_4 which have the same set of values for a certain set of shape measures, say τ_3 and τ_4 , then these different pairs of values of λ_3 and λ_4 will not necessarily have the same set of values for another set of shape measures, say α_3 and α_4 . For example, the three members of the GLD_{RS} with $(\lambda_3, \lambda_4) = (\frac{1}{2}, \frac{1}{2})$, $(\lambda_3, \lambda_4) = (3, 3)$ and $(\lambda_3, \lambda_4) = (84.1160, 1.2734)$ all have the same set of values for τ_3 and τ_4 . However, if $(\lambda_3, \lambda_4) = (\frac{1}{2}, \frac{1}{2})$, then $(\alpha_3, \alpha_4) = (0, 2.0817)$, if $(\lambda_3, \lambda_4) = (3, 3)$, then $(\alpha_3, \alpha_4) = (0, 2.0570)$, whereas if $(\lambda_3, \lambda_4) = (84.1160, 1.2734)$, then $(\alpha_3, \alpha_4) = (0.2697, 3.1305)$.

Figures 3.11 and 3.12 illustrate another interesting shape property of the GLD. There exist values of λ_3 and λ_4 for which the GLD is asymmetric, but which give $\alpha_3 = 0$ or $\tau_3 = 0$. Examples include the GLD_{RS} with $(\lambda_3, \lambda_4) = (35.498, 2.297)$ and $\alpha_3 = 0$ depicted in Figure 3.11 and the GLD_{RS} with $(\lambda_3, \lambda_4) = (84.1160, 1.2734)$ and $\tau_3 = 0$ depicted in Figure 3.12.

3.10.3 SHAPE OF THE DENSITY CURVE

When the values of λ_3 and λ_4 are interchanged, the shape of the GLD's probability density function is reflected. In effect, as demonstrated in Figure 3.13 with the probability density function of the GLD_{RS} , the GLD with parameters $(\lambda_1, \lambda_2, \lambda_3, \lambda_4)$ is the reflection of the GLD with parameters $(\lambda_1, \lambda_2, \lambda_4, \lambda_3)$ about the line $x = \lambda_1$.

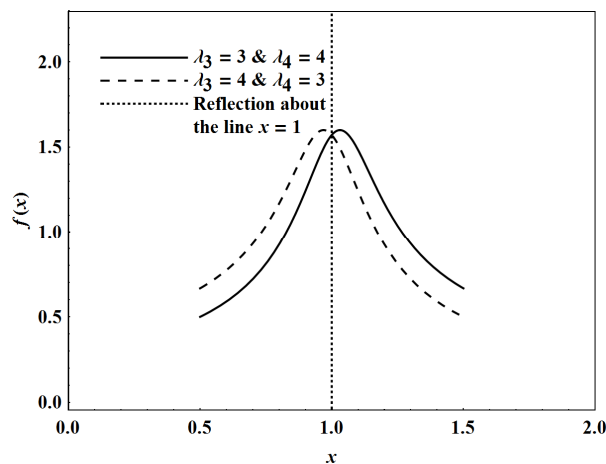


Figure 3.13: Probability density functions of two members of the GLD_{RS} illustrating the reflection in the shape of the density curve when the values of λ_3 and λ_4 are interchanged. The GLD_{RS} with parameters $(\lambda_1, \lambda_2, \lambda_3, \lambda_4) = (1, 2, 3, 4)$ is the reflection of the GLD_{RS} with parameters $(\lambda_1, \lambda_2, \lambda_3, \lambda_4) = (1, 2, 4, 3)$ about the line $x = \lambda_1 = 1$.

CHAPTER 3. THE GENERALIZED LAMBDA DISTRIBUTION (GLD)

Depending on the values of its shape parameters, the GLD's probability density function can exhibit zero, one or two relative extreme turning points – examples in terms of the GLD_{RS} are shown in Figure 3.14. The number of turning points with respect to the shape parameter values of the GLD_{RS} , derived by Karian & Dudewicz (2000, 2010), is shown in Figure 3.15 and summarized in Table 3.5. For the GLD_{FMKL} , the number of turning points exhibited by its probability density function is indicated graphically in Figure 3.16 and tabulated in Table 3.6.

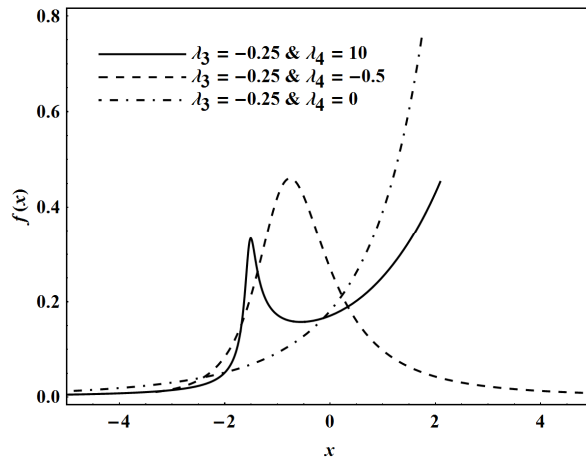


Figure 3.14: Probability density functions of three members of the GLD_{RS} with zero, one and two relative extreme turning points, all with $L_1 = 0$ and $L_2 = 1$. The density function with two turning points is from Region 5, while the unimodal and J-shaped density functions with one and zero turning points respectively are from Region 4.

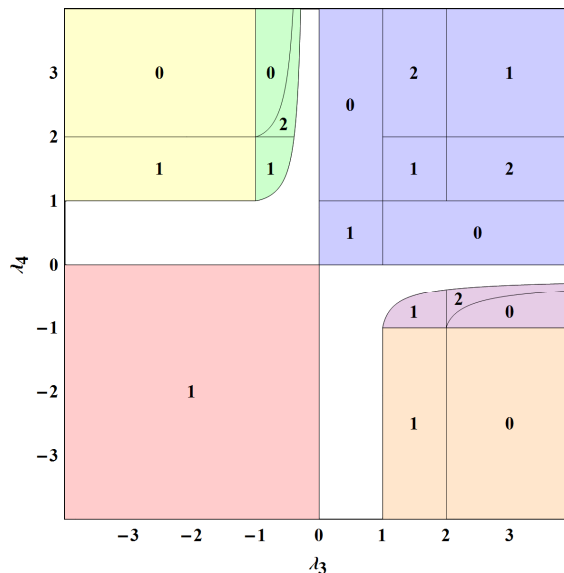


Figure 3.15: The number of relative extreme turning points of the probability density function of the GLD_{RS} in terms of the values of λ_3 and λ_4 . The yellow-shaded, orange-shaded, blue-shaded, red-shaded, green-shaded and purple-shaded areas indicate Regions 1, 2, 3, 4, 5 and 6 as shown in Figure 3.2.

CHAPTER 3. THE GENERALIZED LAMBDA DISTRIBUTION (GLD)

Table 3.5: Number of relative extreme turning points of the probability density function of the GLD_{RS} as depicted in Figure 3.15.

Region	Shape parameter values	Number of turning points
Region 1	$\lambda_3 < -1, 1 < \lambda_4 < 2$	1
	$\lambda_3 < -1, \lambda_4 \geq 2$	0
Region 2	$1 < \lambda_3 < 2, \lambda_4 < -1$	1
	$\lambda_3 \geq 2, \lambda_4 < -1$	0
Region 3	$\lambda_3 = 0, \lambda_4 > 0$	0
	$\lambda_3 > 0, \lambda_4 = 0$	0
	$0 < \lambda_3 < 1, 0 < \lambda_4 < 1$	1
	$0 < \lambda_3 < 1, \lambda_4 > 1$	0
	$\lambda_3 > 1, 0 < \lambda_4 < 1$	0
	$\lambda_3 = 1, \lambda_4 > 0$	0
	$\lambda_3 > 0, \lambda_4 = 1$	0
	$1 < \lambda_3 < 2, 1 < \lambda_4 < 2$	1
	$1 < \lambda_3 < 2, \lambda_4 = 2$	1
	$\lambda_3 = 2, 1 < \lambda_4 < 2$	1
	$\lambda_3 = \lambda_4 = 2$	0
	$1 < \lambda_3 < 2, \lambda_4 > 2$	2
	$\lambda_3 > 2, 1 < \lambda_4 < 2$	2
	$\lambda_3 > 2, \lambda_4 > 2$	1
$\lambda_3 = 2, \lambda_4 > 2$	1	
$\lambda_3 > 2, \lambda_4 = 2$	1	
Region 4	$\lambda_3 = 0, \lambda_4 < 0$	0
	$\lambda_3 < 0, \lambda_4 = 0$	0
	$\lambda_3 < 0, \lambda_4 < 0$	1
Region 5*	$-1 < \lambda_3 < 0, 1 < \lambda_4 \leq 2, u(\lambda_3, \lambda_4) < v(\lambda_3, \lambda_4)$	1
	$-1 < \lambda_3 < 0, \lambda_4 > 2, u(\lambda_3, \lambda_4) < v(\lambda_3, \lambda_4), U(\lambda_3, \lambda_4) < V(\lambda_3, \lambda_4)$	2
	$-1 < \lambda_3 < 0, \lambda_4 > 2, U(\lambda_3, \lambda_4) > V(\lambda_3, \lambda_4)$	0
Region 6*	$1 < \lambda_3 \leq 2, -1 < \lambda_4 < 0, u(\lambda_4, \lambda_3) < v(\lambda_4, \lambda_3)$	1
	$\lambda_3 > 2, -1 < \lambda_4 < 0, u(\lambda_4, \lambda_3) < v(\lambda_4, \lambda_3), U(\lambda_4, \lambda_3) < V(\lambda_4, \lambda_3)$	2
	$\lambda_3 > 2, -1 < \lambda_4 < 0, U(\lambda_4, \lambda_3) > V(\lambda_4, \lambda_3)$	0

$$* u(\lambda_i, \lambda_j) = \frac{(1 - \lambda_i)^{1 - \lambda_i} (\lambda_j - 1)^{\lambda_j - 1}}{(\lambda_j - \lambda_i)^{\lambda_j - \lambda_i}}, v(\lambda_i, \lambda_j) = -\frac{\lambda_i}{\lambda_j}, U(\lambda_i, \lambda_j) = \frac{(2 - \lambda_i)^{\lambda_i - 2} (\lambda_j - \lambda_i)^{\lambda_j - \lambda_i}}{(\lambda_j - 2)^{\lambda_j - 2}}, V(\lambda_i, \lambda_j) = \frac{\lambda_j (\lambda_j - 1)}{\lambda_i (\lambda_i - 1)}$$

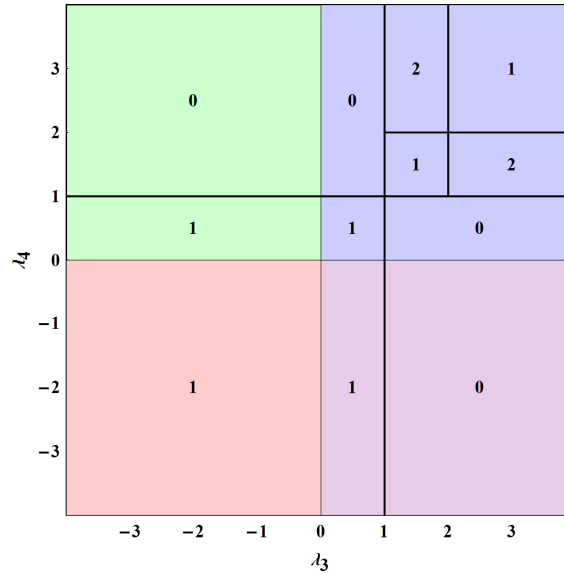


Figure 3.16: The number of relative extreme turning points of the probability density function of the GLD_{FMKL} in terms of the values of λ_3 and λ_4 . The green-shaded, purple-shaded, blue-shaded and red-shaded areas indicate Regions 1, 2, 3 and 4 as shown in Figure 3.4.

Table 3.6: Number of relative extreme turning points of the probability density function of the GLD_{FMKL} as depicted in Figure 3.16.

Class	Shape parameter values	Number of turning points
Class I	$\lambda_3 < 1, \lambda_4 < 1$	1
Class II	$\lambda_3 \geq 1, \lambda_4 \leq 1$	0
Class II'	$\lambda_3 \leq 1, \lambda_4 \geq 1$	0
Class III	$1 < \lambda_3 \leq 2, 1 < \lambda_4 \leq 2, \lambda_3 + \lambda_4 < 4$	1
	$\lambda_3 = \lambda_4 = 2$	0
Class IV	$\lambda_3 > 2, 1 < \lambda_4 < 2$	2
Class IV'	$1 < \lambda_3 < 2, \lambda_4 > 2$	2
Class V	$\lambda_3 \geq 2, \lambda_4 \geq 2, \lambda_3 + \lambda_4 > 4$	1

3.11 REGIONS OF THE GLD_{RS}

In Figures 3.17 to 3.24 the probability density functions of some examples of asymmetric members of the GLD_{RS} from Regions 1, 3, 4 and 5 are plotted (see Figure 3.1 for examples of symmetric members of the GLD_{RS} from Regions 3 and 4 with $\lambda_3 = \lambda_4 = \lambda$). The distributional shape and characteristics of the GLD_{RS} are briefly described below for each region. Since any GLD_{RS} from Region 2 is simply the reflection of the GLD_{RS} from Region 1 about the line $x = \lambda_1$, these two regions are considered together. For the same reason Regions 5 and 6 are also considered together.

3.1.1.1 REGIONS 1 AND 2

Region 1 with $\lambda_3 < -1$ and $\lambda_4 > 1$ and Region 2 with $\lambda_3 > 1$ and $\lambda_4 < -1$ contain asymmetric members of the GLD_{RS} with half-infinite support. In Region 1 the GLD_{RS} is negatively skewed, while in Region 2 it is positively skewed.

As shown in Figure 3.17(a), when $1 < \lambda_4 < 2$ in Region 1, the density curve of the GLD_{RS} has one turning point at the right tail. Figure 3.17(b) depicts J-shaped density curves from Region 1, occurring for $\lambda_4 \geq 2$. Similarly in Region 2, the density curve of the GLD_{RS} has a turning point at the left tail when $1 < \lambda_3 < 2$, while the density curve is J-shaped for $\lambda_3 \geq 2$.

Regions 1 and 2 are the only regions of the GLD_{RS} for which no moments or L -moments exist. As a result quantile-based measures of location, spread and shape must be used for these two regions.

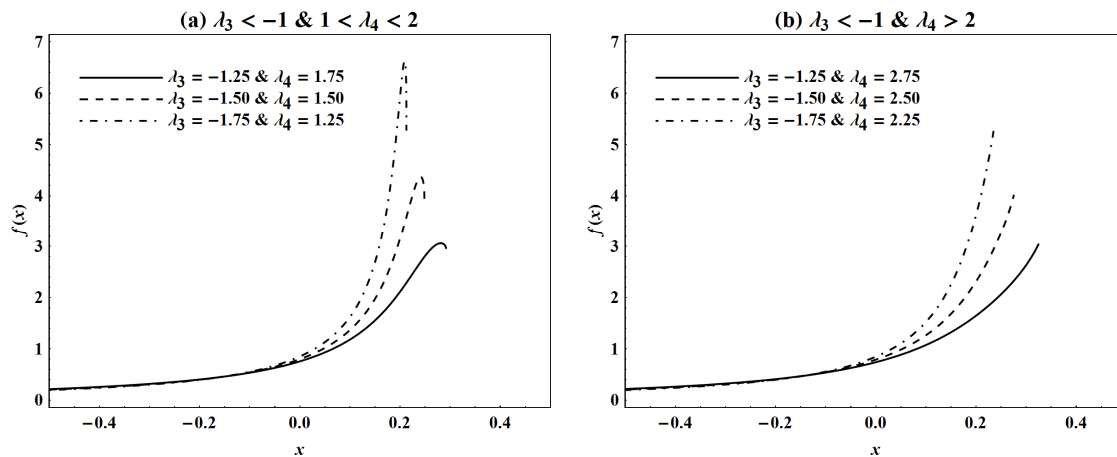


Figure 3.17: Probability density functions of members of the GLD_{RS} from Region 1, all with $me = 0$ and $IQR = SF(\frac{3}{4}) = 1$.

3.1.1.2 REGION 3

Region 3 of the GLD_{RS} is defined for $\lambda_3 \geq 0$, $\lambda_4 \geq 0$ and $\lambda_3 + \lambda_4 > 0$, with the third restriction ensuring that the two shape parameters cannot simultaneously be zero. The GLD_{RS} in Region 3 always possesses bounded support. In fact, Region 3 is the only region of the GLD_{RS} with bounded support.

Examples of symmetric members of the GLD_{RS} from Region 3 with $\lambda_3 = \lambda_4 = \lambda$ are given in Figure 3.1(b-d). Figures 3.18 to 3.22 present examples of asymmetric members of the GLD_{RS} from Region 3, all with $\lambda_3 < \lambda_4$. The reason for this restriction is that the shape of the GLD_{RS} will simply be reflected for $\lambda_3 > \lambda_4$ and hence the corresponding graphs are omitted.

Compared to the other five regions, Region 3 is the most flexible with respect to distributional shape, but, as a result, it is also by far the most complex region. For instance, as indicated in Figure 3.15 and Table 3.5, the density curve of the GLD_{RS} in Region 3 can exhibit zero, one or two relative extreme turning points.

In Region 3(a), if $0 < \lambda_3 < 1$ and $0 < \lambda_4 < 1$, the left and right tails of the density curve both approach zero and hence the GLD_{RS} is then unimodal with a single turning point. See Figures 3.18(b-d) for examples of these unimodal density curves. King (1999) proved that the slope of the density curve at the end-point of the left tail is zero for $0 < \lambda_3 < \frac{1}{2}$, non-zero but finite for $\lambda_3 = \frac{1}{2}$, and infinite for $\frac{1}{2} < \lambda_3 < 1$. The same results hold for the right tail in terms of the corresponding values of λ_4 . So the most useful unimodal members from the GLD_{RS} in Region 3(a) are obtained for $0 < \lambda_3 < \frac{1}{2}$ and $0 < \lambda_4 < \frac{1}{2}$. Examples of these members of the GLD_{RS} are shown in Figure 3.18(b).

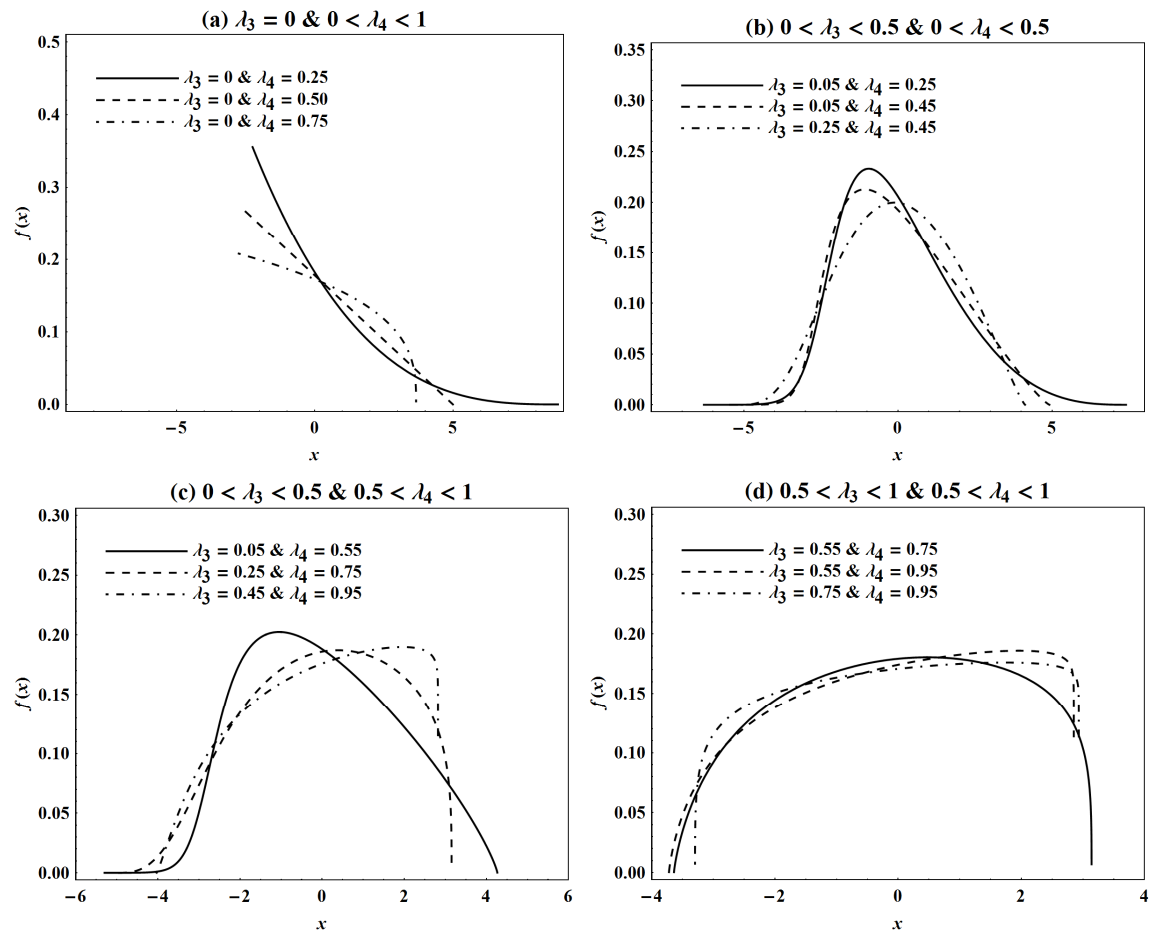


Figure 3.18: Probability density functions of members of the GLD_{RS} from Region 3(a), all with $L_1 = 0$ and $L_2 = 1$.

As illustrated by Karian & Dudewicz (2000, 2010), many of the well-known distributions can be approximated by the GLD_{RS} when $0 < \lambda_3 < \frac{1}{2}$ and $0 < \lambda_4 < \frac{1}{2}$. For instance, as pointed out in Section 3.5, the normal distribution is approximated by the GLD_{RS} with $\lambda_3 = \lambda_4 \approx 0.14$. Note that the normal distribution is an example of a mesokurtic distribution with $\alpha_4 = 3$. Distributions with $\alpha_4 < 3$ are called platykurtic (short-tailed), while distributions with $\alpha_4 > 3$ are said to be leptokurtic (heavy-tailed) – see Pearson (1905) and Student (1927) for details. The unimodal members of the GLD_{RS} in Region 3(a) can be platykurtic, mesokurtic or leptokurtic.

In Region 3(c) the density curve of the GLD_{RS} is U-shaped with a single turning point if both shape parameters are between one and two, or if one of the shape parameters is between one and two while the other shape parameter equals two. Examples of these U-shaped density curves from Region 3(c) are demonstrated in Figure 3.19.

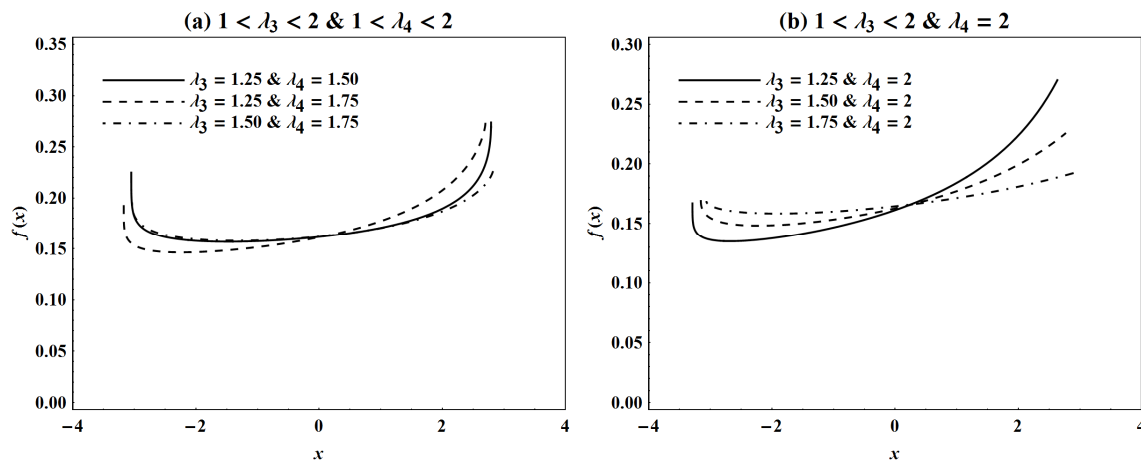


Figure 3.19: Probability density functions of members of the GLD_{RS} from Region 3(c), all with $L_1 = 0$ and $L_2 = 1$.

The density curve of the GLD_{RS} in Region 3 has no turning point when either of the two shape parameters is zero or one, when one of the two shape parameters is between zero and one with the other shape parameter greater than one, and when the shape parameters are both equal to two. The corresponding distributional shapes are uniform, monotone decreasing or monotone increasing. The uniform distribution is obtained in Region 3 for the four different pairs of values of λ_3 and λ_4 given Section 3.5. Monotone decreasing density curves are attained in Region 3(d) with $\lambda_3 \geq 1$ and $0 \leq \lambda_4 \leq 1$ and also, as shown in Figure 3.18(a), in Region 3(a) when $\lambda_3 = 0$ and $0 < \lambda_4 < 1$. Figure 3.20 presents examples from Region 3(e)

with $0 \leq \lambda_3 < 1$ and $\lambda_4 \geq 1$ where the density curve of the GLD_{RS} is monotone increasing. The density curve is also monotone increasing in Region 3(a) when $0 < \lambda_3 < 1$ and $\lambda_4 = 0$.

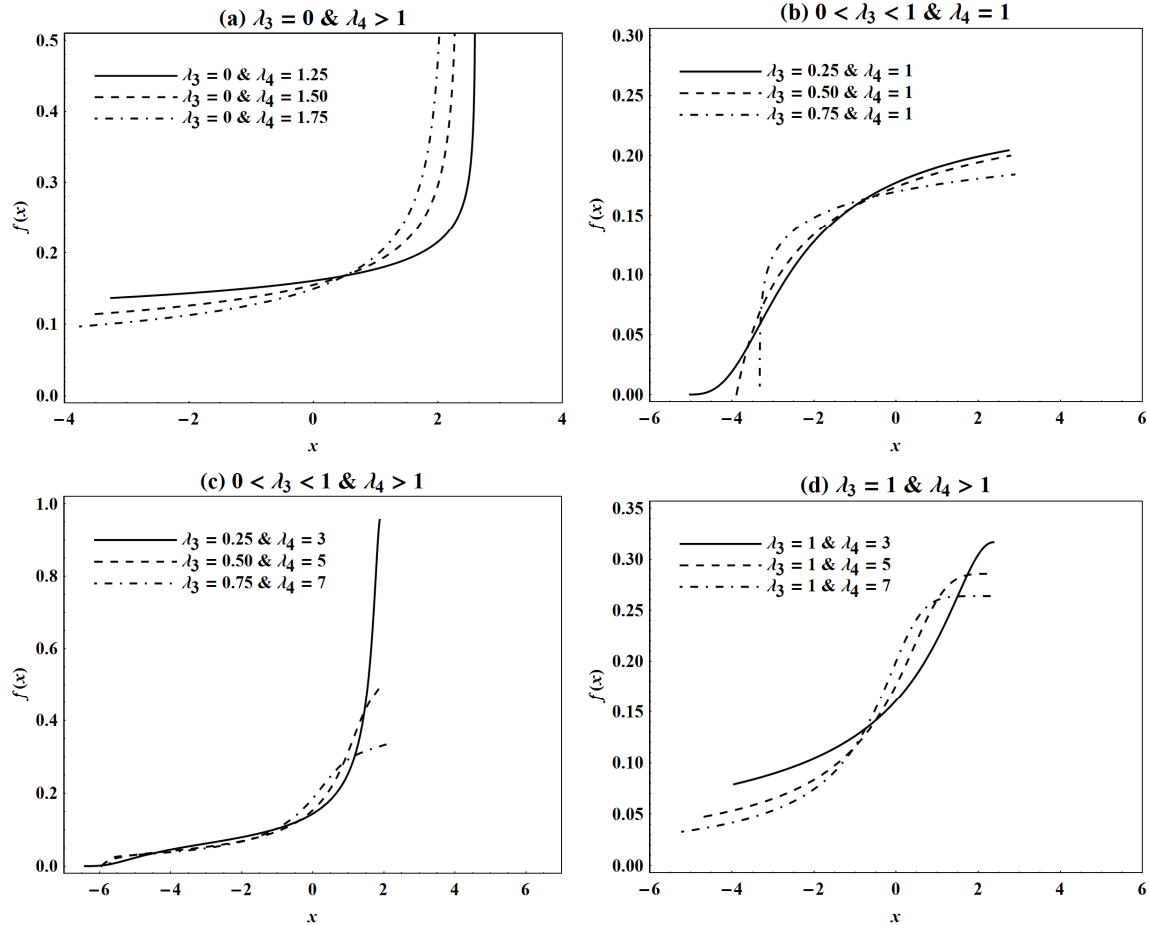


Figure 3.20: Probability density functions of members of the GLD_{RS} from Region 3(e), all with $L_1 = 0$ and $L_2 = 1$.

If the one shape parameter is between one and two and the other shape parameter is greater than two, the density curve is S-shaped with two turning points. These S-shaped density curves occur in Region 3(f) and Region 3(g), with examples from the latter sub-region given in Figure 3.21. The turning point at the right tail of the density curve in Region 3(f) and the turning point at the left tail of the density curve in Region 3(g) become less pronounced when the absolute difference between the values of λ_3 and λ_4 increases, and, as a result the S-shaped pattern of the density curve is then less apparent – Figure 3.21 illustrates this characteristic of the GLD_{RS} for Region 3(g).

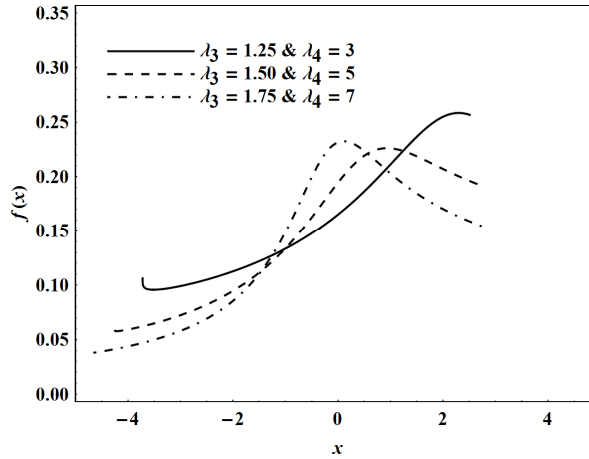


Figure 3.21: Probability density functions of members of the GLD_{RS} from Region 3(g), all with $L_1 = 0$ and $L_2 = 1$.

Region 3(h) is defined for $\lambda_3 \geq 2$, $\lambda_4 \geq 2$ and $\lambda_3 + \lambda_4 > 4$, where the third restriction ensures that the two shape parameters cannot simultaneously be equal to two, avoiding the uniform distribution with $\lambda_3 = \lambda_4 = 2$. Unimodal truncated density curves are obtained from this sub-region, examples of which are plotted in Figure 3.22.

Region 3 is the only region for which all the moments and the L -moments exist. But, as shown with the examples in Figure 3.11 and Figure 3.12, there does not exist a one-to-one correspondence between the shape parameters in Region 3 and the moments, and also not between the shape parameters in this region and the L -moments.

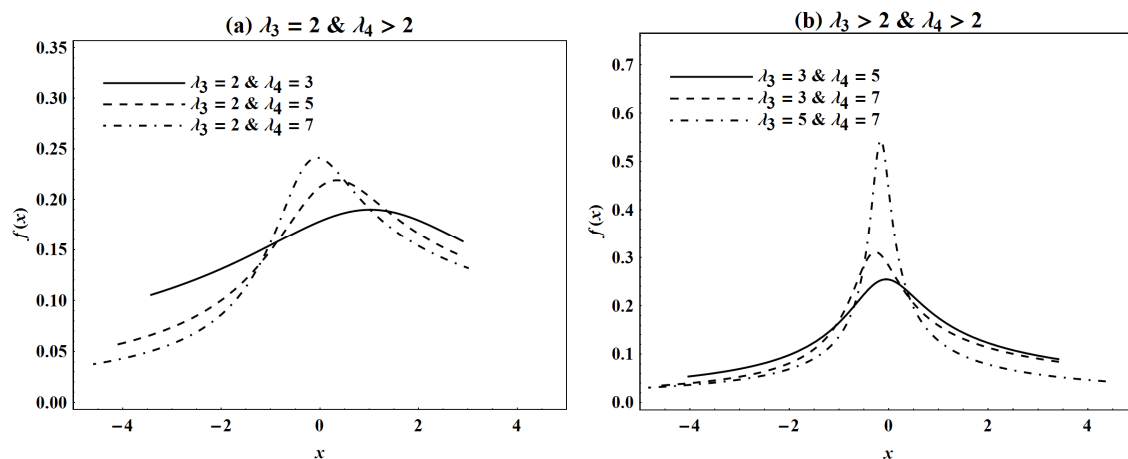


Figure 3.22: Probability density functions of members of the GLD_{RS} from Region 3(h), all with $L_1 = 0$ and $L_2 = 1$.

3.11.3 REGION 4

Along with Region 3(a), Region 4 presents the most useful members of the GLD_{RS} . When both $\lambda_3 < 0$ and $\lambda_4 < 0$ in Region 4, unimodal, leptokurtic members of the GLD_{RS} with

infinite support are obtained. Region 4 is the only region of the GLD_{RS} which produces members with infinite support. When either $\lambda_3 = 0$ or $\lambda_4 = 0$, the density curve of the GLD_{RS} in Region 4 is J-shaped with half-infinite support. The GLD_{RS} in Region 4 is positively skewed for $\lambda_3 > \lambda_4$ and negatively skewed for $\lambda_3 < \lambda_4$. Examples of positively skewed members of the GLD_{RS} are given in Figure 3.23, while examples of symmetric members with $\lambda_3 = \lambda_4 = \lambda$ are shown in Figure 3.1(a).

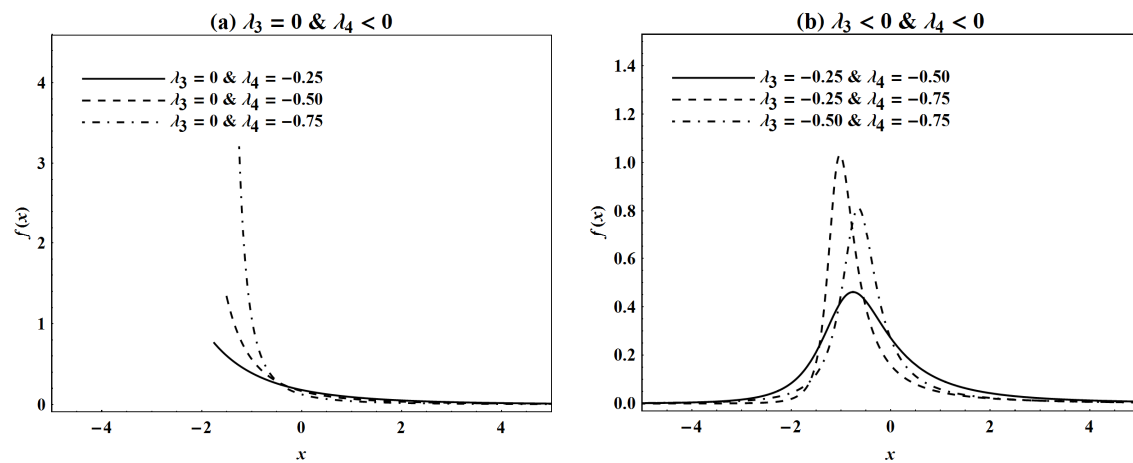


Figure 3.23: Probability density functions of members of the GLD_{RS} from Region 4, all with $L_1 = 0$ and $L_2 = 1$.

3.11.4 REGIONS 5 AND 6

The GLD_{RS} in Region 5 with $-1 < \lambda_3 < 0$ and $\lambda_4 > 1$ is positively skewed with half-infinite support. When $1 < \lambda_4 < 2$, the shape of the density curve, shown in Figure 3.24(a), is similar to the shape of the density curve in Region 1 for $\lambda_3 < -1$, shown in Figure 3.17(a), in that there is a turning point at the right tail. When $\lambda_4 > 2$, the density curve has no turning point (and is monotone increasing) or it has two turning points appearing close to the right tail – see Figure 3.24(b) for examples.

In Region 6 the GLD_{RS} is negatively skewed, also with half-infinite support. When $1 < \lambda_3 < 2$ and $-1 < \lambda_4 < 0$, the density curve has a single turning point at the left tail. If $\lambda_3 > 2$ and $-1 < \lambda_4 < 0$, the density curve has zero or two turning points.

For the majority of shape parameter values from Regions 5 and 6, moments are not available. However, the mean and hence all the L -moments exist for all shape parameter values from these two regions.

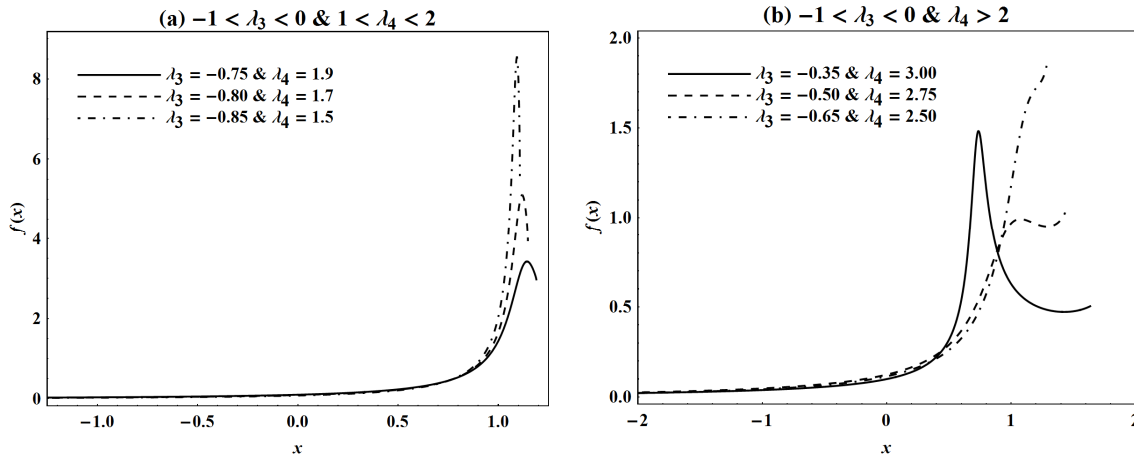


Figure 3.24: Probability density functions of members of the GLD_{RS} from Region 5, all with $L_1 = 0$ and $L_2 = 1$.

3.12 CLASSES OF THE GLD_{FMKL}

The distributional shape and properties of the seven classes of the GLD_{FMKL} are briefly discussed below, with Figures 3.25 to 3.32 showing the density curves of examples of asymmetric members from these classes (see again Figure 3.1 for density curves of examples of symmetric members). Note that $\lambda_3 > \lambda_4$ in all the graphs in Figures 3.25 to 3.32, because for $\lambda_3 < \lambda_4$ the shape of the GLD_{FMKL} is reflected about the line $x = \lambda_1$ and thus the corresponding graphs are omitted. Also, since they contain reflections of each other, Classes II and II' are considered together below, as are classes IV and IV'.

3.12.1 CLASS I

Akin to Region 3(a) of the GLD_{RS} , the two tails of the density curve of the GLD_{FMKL} in Class I with $\lambda_3 < 1$ and $\lambda_4 < 1$ both approach zero. As a result Class I contains unimodal distributions with half-infinite support in Regions 1 and 2 of Class I, with bounded support in Region 3 of Class I, and with infinite support in Region 4 of Class I, examples of which are shown in Figures 3.25 to 3.27. These unimodal members of the GLD_{FMKL} in Class I are platykurtic, mesokurtic (for instance, the approximation of the normal distribution by the GLD_{FMKL} with $\lambda_3 = \lambda_4 \approx 0.14$) or leptokurtic.

Freimer *et al.* (1988) proved that at the end-point of the left tail, the slope of the density curve is zero when $\lambda_3 < \frac{1}{2}$, non-zero but finite when $\lambda_3 = \frac{1}{2}$, and infinite when $\frac{1}{2} < \lambda_3 < 1$. Equivalent results hold for the right tail of the density curve based on the corresponding values of λ_4 .

All moments and L -moments exist in Region 3 of Class I. In Regions 1, 2 and 4 of Class I the first four moments only exist when both $\lambda_3 > -\frac{1}{4}$ and $\lambda_4 > -\frac{1}{4}$, while all L -moments exist when $\lambda_3 > -1$ and $\lambda_4 > -1$.

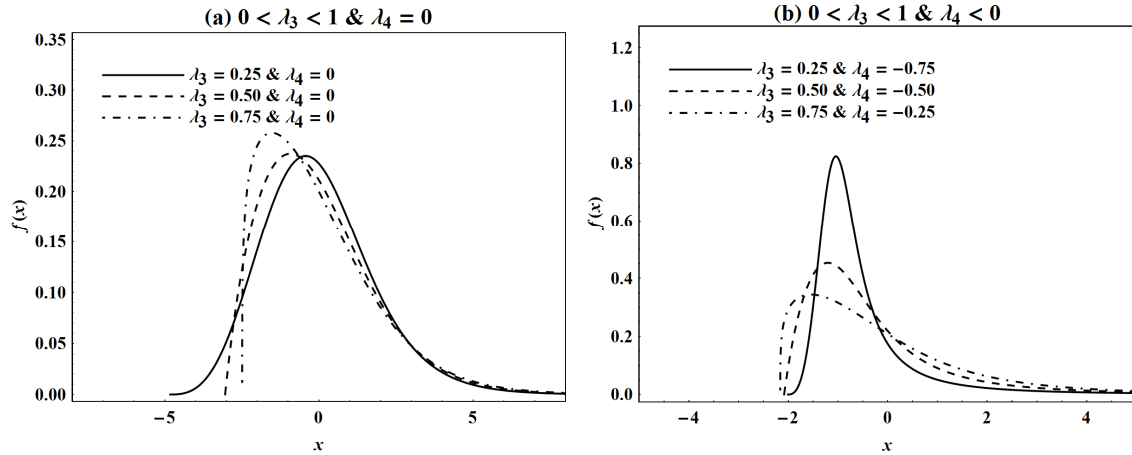


Figure 3.25: Probability density functions of members of the GLD_{FMKL} from Region 2 in Class I, all with $L_1 = 0$ and $L_2 = 1$.

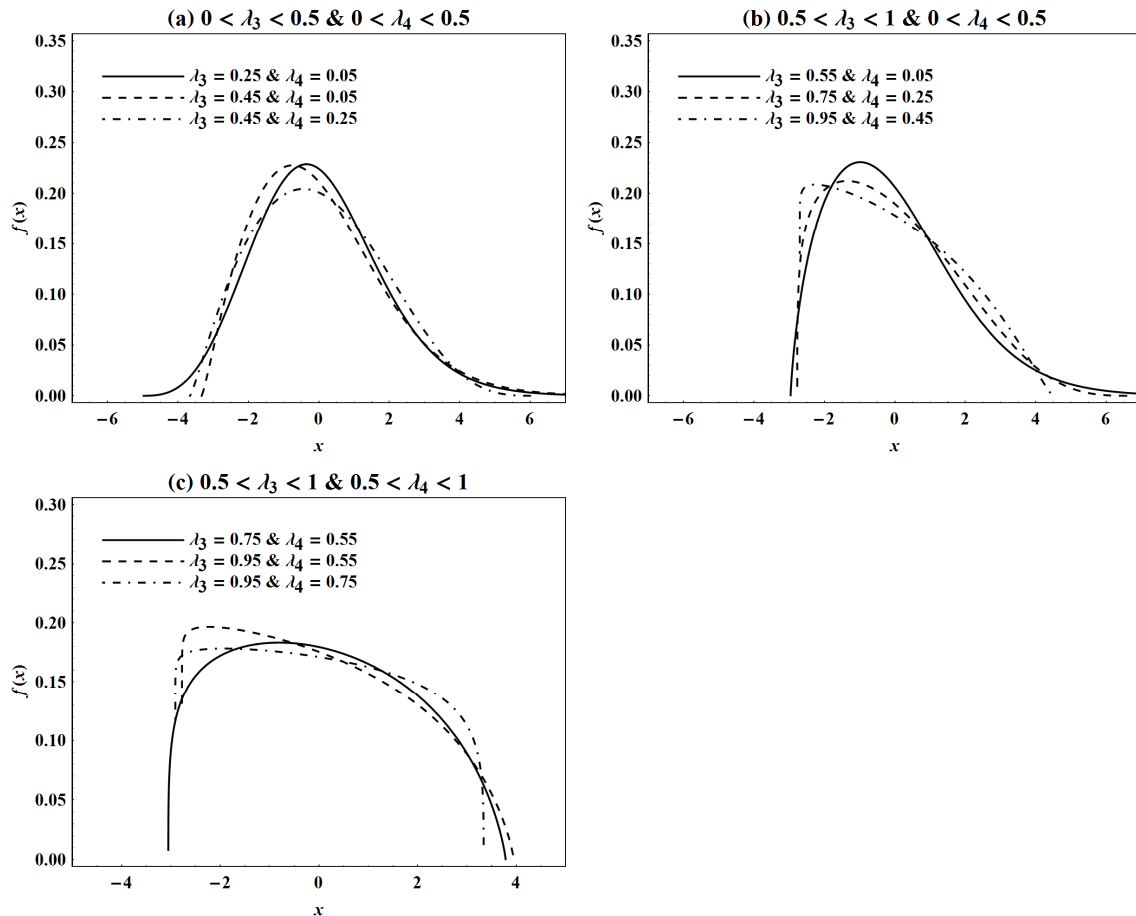


Figure 3.26: Probability density functions of members of the GLD_{FMKL} from Region 3 in Class I, all with $L_1 = 0$ and $L_2 = 1$.

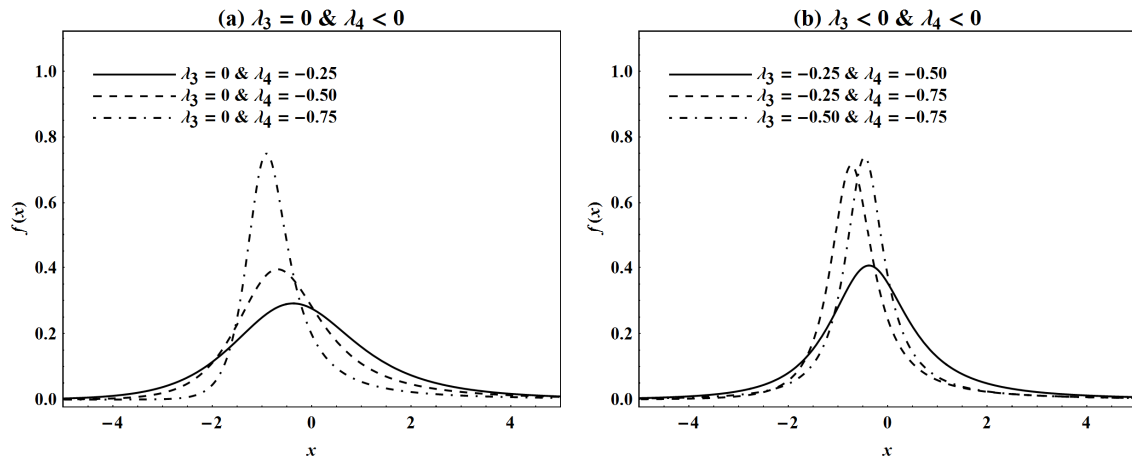


Figure 3.27: Probability density functions of members of the GLD_{FMKL} from Region 4 in Class I, all with $L_1 = 0$ and $L_2 = 1$.

3.12.2 CLASSES II AND II'

Based on its support, two regions, namely Region 2 with $\lambda_4 \leq 0$ and Region 3 with $0 < \lambda_4 \leq 1$, are included in Class II. Figure 3.28 presents examples of members from Region 2, where the support of the GLD_{FMKL} is half-infinite.

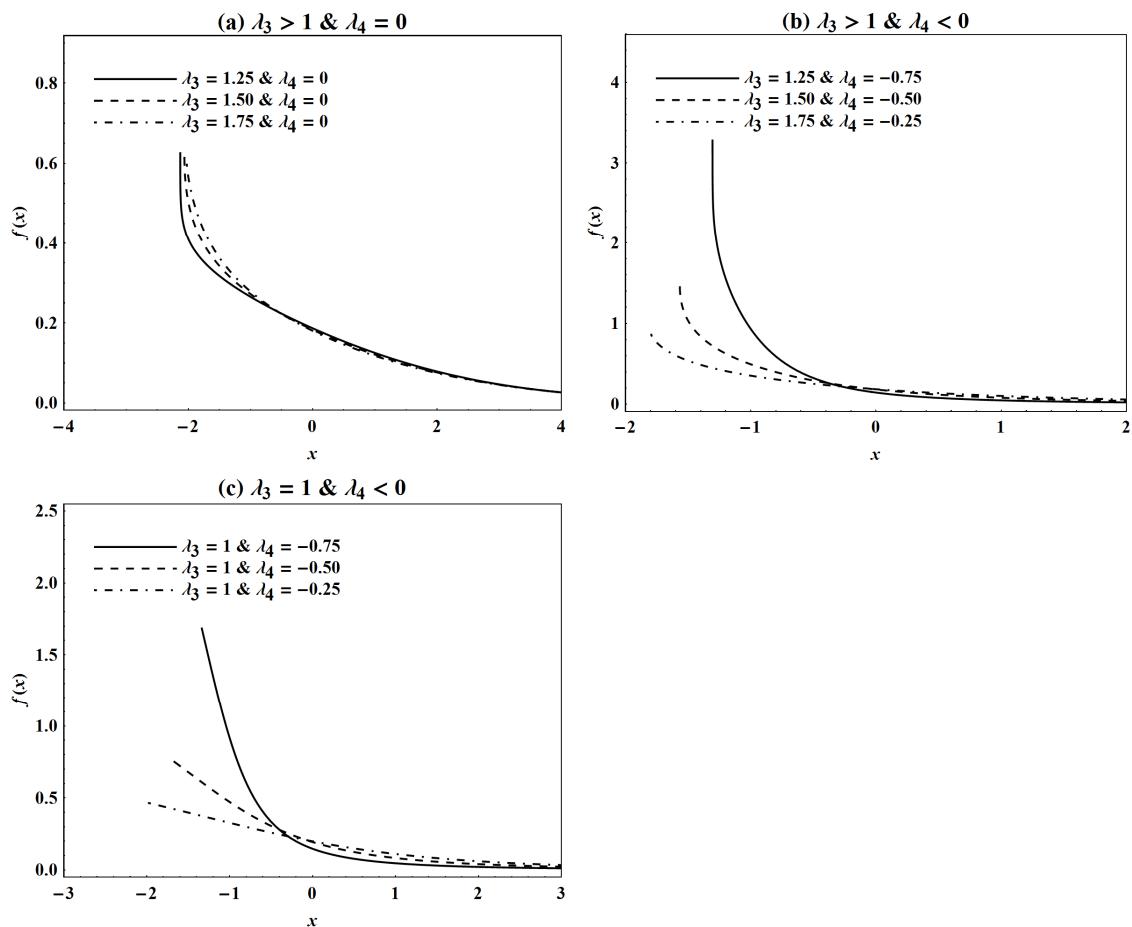


Figure 3.28: Probability density functions of members of the GLD_{FMKL} from Region 2 in Class II, all with $L_1 = 0$ and $L_2 = 1$.

In Region 3 of Class II the support of the GLD_{FMKL} is bounded, with examples shown in Figure 3.29. Likewise the support in Class II' is half-infinite in Region 1 with $\lambda_3 \leq 0$ and bounded in Region 3 with $0 < \lambda_3 \leq 1$.

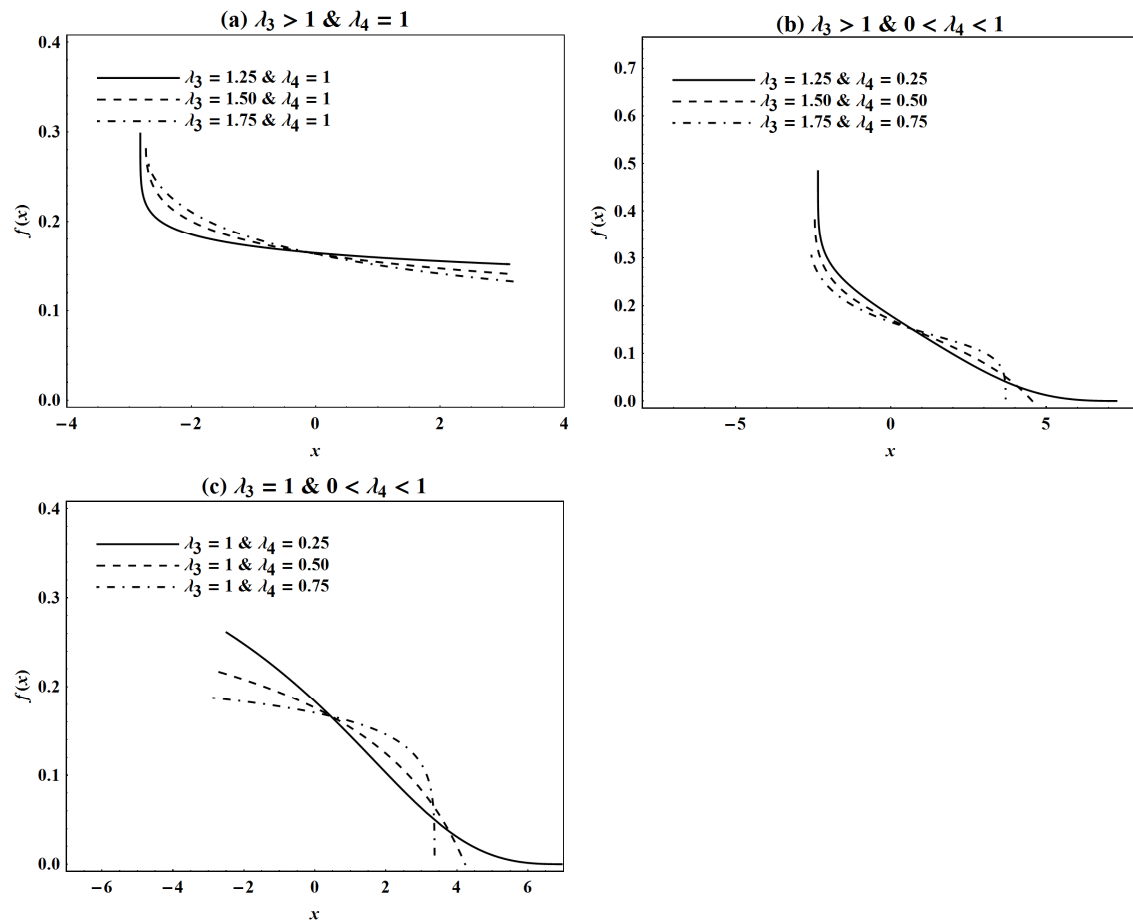


Figure 3.29: Probability density functions of members of the GLD_{FMKL} from Region 3 in Class II, all with $L_1 = 0$ and $L_2 = 1$.

As indicated in Figure 3.16, Classes II and II' are the only classes of the GLD_{FMKL} where the probability density function always exhibits no extreme turning point. In fact, the GLD_{FMKL} with $(\lambda_3, \lambda_4) = (2, 2)$ in Class III, which gives the uniform distribution, is the only member of the GLD_{FMKL} from outside Classes II and II' which has no turning point in the density curve. Three types of density curves are possible from Classes II and II'. The uniform distribution is obtained in these two classes when both shape parameters are equal to one, or when one of the shape parameters equals one while the other shape parameter tends to infinity. Monotone decreasing density curves are attained in Class II, while monotone increasing density curves occur in Class II'. As a result, apart from the shape parameter

values for which the uniform distribution is obtained, the GLD_{FMKL} is positively skewed in Class II and negatively skewed in Class II'.

As with Region 3 of Class I, all moments and L -moments exist for Region 3 of Classes II and II'. However, in Region 1 of Class II' and in Region 2 of Class II the first four moments only exist when $\lambda_3 > -\frac{1}{4}$ and $\lambda_4 > -\frac{1}{4}$, while all L -moments exist when $\lambda_3 > -1$ and $\lambda_4 > -1$.

3.1.2.3 CLASS III

Class III of the GLD_{FMKL} is defined for $1 < \lambda_3 \leq 2$ and $1 < \lambda_4 \leq 2$ and hence is equivalent to Region 3(c) of the GLD_{RS} with respect to parameter space. Furthermore, akin to Region 3(c) of the GLD_{RS} , the density curve of the GLD_{FMKL} in Class III is U-shaped for all pairs of values of λ_3 and λ_4 , except for $(\lambda_3, \lambda_4) = (2, 2)$ which produces the uniform distribution. Figure 3.30 presents examples of U-shaped density curves from Class III.

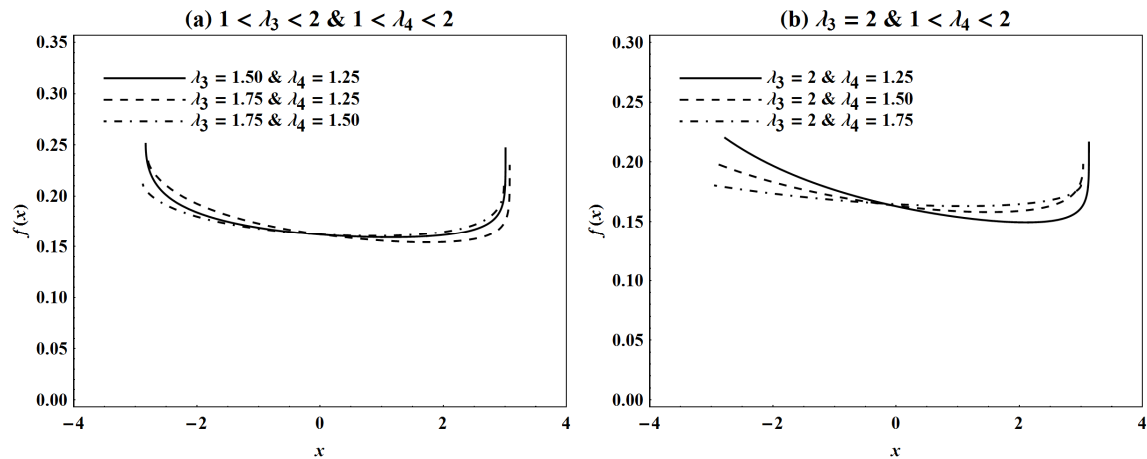


Figure 3.30: Probability density functions of members of the GLD_{FMKL} from Class III, all with $L_1 = 0$ and $L_2 = 1$.

3.1.2.4 CLASSES IV AND IV'

The GLD_{FMKL} only produces probability density functions with two turning points in a single region, that is, Region 3, whereas such density functions are obtained in Regions 3, 5 and 6 of the GLD_{RS} . In particular, these types of density functions occur in Classes IV and IV' of the GLD_{FMKL} and are S-shaped, similar to the density curves from Regions 3(f) and 3(g) of the GLD_{RS} . Examples of members of the GLD_{FMKL} from Class IV are depicted in Figure 3.31. It is noted again that the S-shaped pattern of the density curve becomes less visible as the absolute difference between the values of λ_3 and λ_4 increases.

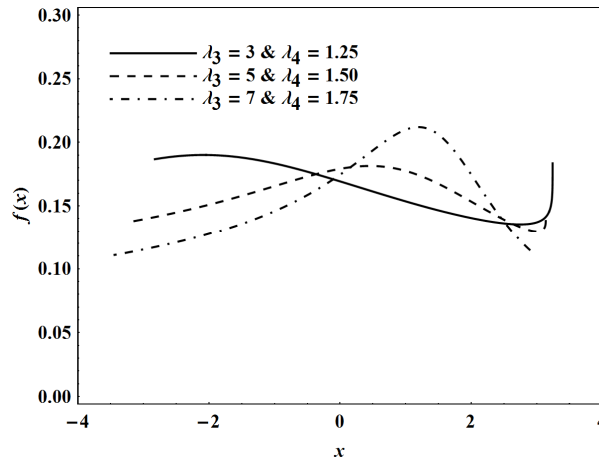


Figure 3.31: Probability density functions of members of the GLD_{FMKL} from Class IV, all with $L_1 = 0$ and $L_2 = 1$.

3.12.5 CLASS V

Class V of the GLD_{FMKL} , with $\lambda_3 \geq 2$, $\lambda_4 \geq 2$ and $\lambda_3 + \lambda_4 > 4$, where the third restriction is to prevent the uniform distribution with $\lambda_3 = \lambda_4 = 2$, is similar to Region 3(h) of the GLD_{RS} in that it possesses unimodal truncated density curves. Figure 3.32 demonstrates examples of these density curves.

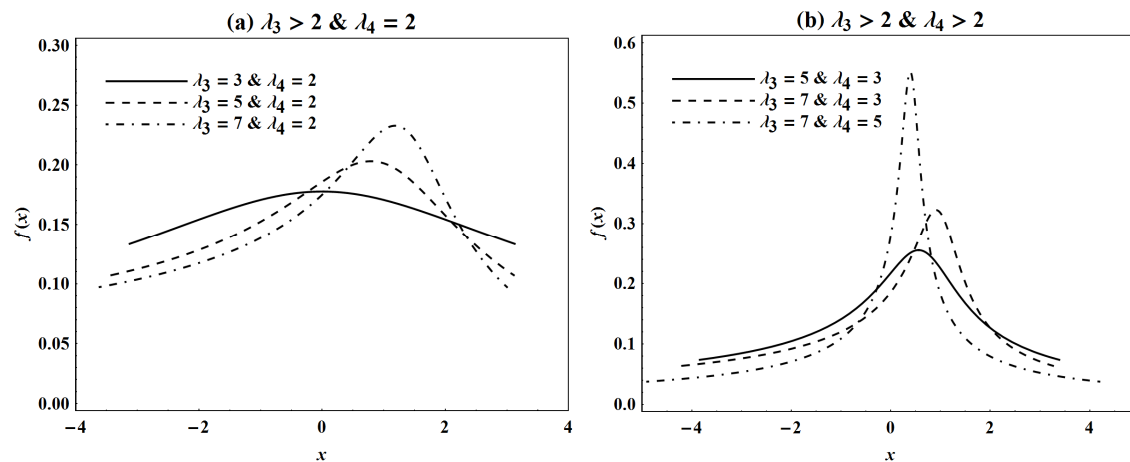


Figure 3.32: Probability density functions of members of the GLD_{FMKL} from Class V, all with $L_1 = 0$ and $L_2 = 1$.

3.13 PARAMETER ESTIMATION

A drawback of both the GLD_{RS} and the GLD_{FMKL} is that parameter estimation is computationally difficult. Various estimation methodologies have been proposed in the literature. All of them require numerical optimization techniques.

One approach is to apply an estimation method where four measures, namely a measure of location, a measure of spread and two measures of shape, are utilized. This approach

includes method of moments estimation (Ramberg *et al.*, 1979; Cooley, 1991; Dudewicz & Karian, 1996; Karian *et al.*, 1996), percentile-based methods (Mykytka & Ramberg, 1979; Cooley, 1991; Dudewicz & Karian, 1999; Karian & Dudewicz, 1999; Haritha *et al.*, 2008), the use of shape functionals (King, 1999; King & MacGillivray, 2007) and method of L -moments estimation (Mohan, 1994; Karian & Dudewicz, 2003; Asquith, 2007; Karvanen & Nuutinen 2008).

With all the above-mentioned estimation techniques, the four chosen population measures are equated to the corresponding sample statistics, resulting in four equations with four unknowns which must be solved simultaneously. Since no closed-form expressions exist for the shape parameter estimators of either the GLD_{RS} or the GLD_{FMKL} , numerical optimization techniques must be used. The reason is that λ_3 and λ_4 jointly account for the skewness and the kurtosis of the GLD, irrespective of the shape measures used. Another complication with some of the above-mentioned methods is that the corresponding population measures are not defined for all parameter values. In particular, as indicated in Figures 3.2 and 3.4, method of moments estimation is only applicable for $\lambda_3 > -\frac{1}{4}$ and $\lambda_4 > -\frac{1}{4}$, while method of L -moments estimation requires that $\lambda_3 > -1$ and $\lambda_4 > -1$.

Alternative approaches for parameter estimation for the GLD include a “least-squares” method by Öztürk & Dale (1985), the starship method by King (1999) and King & MacGillivray (1999), a discretized approach by Su (2005) and numerical maximum likelihood estimation by Su (2007b). These methods also require numerical optimization techniques. For a detailed discussion on the computational difficulties in fitting the GLD to a data set, see Karian & Dudewicz (2007).

3.14 MONTE CARLO SIMULATION

In the 1970s, thanks to advances in computational resources, Monte Carlo simulation studies had already become a central method in the evaluation and comparison of proposed inferential statistical techniques. However, a major difficulty encountered in the simulation studies was the generation of real-valued random variables from selected distributions due to the popular inverse transformation technique not being applicable for those distributions (such as the normal distribution) not possessing closed-form expressions for their quantile functions. The introduction of the GLD_{RS} in the literature, (Ramberg & Schmeiser, 1972, 1974), circumvented this difficulty, since the GLD_{RS} possesses a simple quantile function

given in (3.3) with a single functional form through which symmetric and asymmetric real-valued random variables can easily be generated via the inverse transformation technique. Hence, not surprisingly, the GLD_{RS} soon became the distribution of choice in the Monte Carlo simulations of numerous studies – see for instance Hogg *et al.* (1975), Hogg & Randles (1975), Broffitt *et al.* (1976), Randles *et al.* (1978), Moberg *et al.* (1978, 1980) and Randles *et al.* (1980). The GLD, and in particular the GLD_{RS} , remains a popular distribution for simulation studies. The selection of the members of the GLD to be used in a simulation study can be done in several ways.

3.14.1 DISTRIBUTIONAL SHAPE

One approach is to select members of the GLD possessing distributional shapes specifically required for the simulation study. For instance, to assess the performance of a test for symmetry, one would include symmetric members of the GLD with $\lambda_3 = \lambda_4$ as well as asymmetric members with $\lambda_3 \neq \lambda_4$ in the Monte Carlo simulation. This was for example done by Randles *et al.* (1980). In order to compare their proposed triples test for symmetry with other tests for symmetry in a simulation study, they selected six symmetric members of the GLD_{RS} , including the uniform distribution ($\lambda_3 = \lambda_4 = 1$) and the GLD_{RS} approximation of the normal distribution ($\lambda_3 = \lambda_4 \approx 0.14$), and eight asymmetric members of the GLD_{RS} . McWilliams (1990) used the same set of eight asymmetric members of the GLD_{RS} along with the GLD_{RS} approximation of the normal distribution to compare his proposed distribution-free test for symmetry with other distribution-free tests for symmetry in a Monte Carlo study. It has since become common practice in the literature to use this set of nine members of the GLD_{RS} in Monte Carlo simulation studies related to tests for symmetry – see Belaire-Franch & Contreras (2002), Baklizi (2003, 2007), Cheng & Balakrishnan (2004) and Thas *et al.* (2005) for recent examples.

3.14.2 MEASURES OF SHAPE

Another way of choosing the members of the GLD used in a Monte Carlo study is to select pairs of values for specific measures of skewness and kurtosis for the random variables in the study, and then compute the parameter values of the corresponding members of the GLD to be used in simulating these random variables. Examples of this approach include Wilcox (2002) and O’Gorman (2006, 2008), who selected pairs of values for the skewness and

kurtosis moment ratios, α_3 and α_4 , and then computed the parameter values of the members of the GLD_{RS} for their Monte Carlo studies based on these values of α_3 and α_4 .

3.1.4.3 APPROXIMATION OF DISTRIBUTIONS

The GLD's ability to accurately approximate many of the well-known probability distributions can be incorporated into Monte Carlo studies. This is done by selecting specific probability distributions and then, instead of simulating the random variables in the study from the chosen distributions themselves, simulating the random variables using the GLD approximations of these distributions. For instance, in the simulation study conducted by Bautista & Gómez (2007) to examine the robustness of the Mann-Whitney U test and two permutation tests (based respectively on the mean and the median) to the violation of equality of variances, the authors simulated samples with random variables from the GLD_{RS} approximations of the beta, logistic and Laplace distributions.

3.1.4.4 ISOTONES

Finally, the choice of GLD members in a simulation study can be based upon a graphical procedure proposed by Mudholkar *et al.* (1991). Their procedure, specifically designed for the GLD_{FMKL} , entails the construction of isotones, which are contours of equal p -values for the test under consideration, using a grid of shape parameter values from the GLD_{FMKL} . These isotones can be used to identify members of the GLD_{FMKL} which provide interesting alternatives to the null hypothesis and these members are then included in the simulation study. For instance, Thas & Ottoy (2004) used isotones to select members of the GLD_{FMKL} for a Monte Carlo study in which they compared an extended version of the k -sample Anderson–Darling test they developed with the Kruskal–Wallis test and the k -sample Kolmogorov–Smirnov test.

3.15 APPLICATIONS

Because of its high flexibility with respect to distributional shape, the GLD has been utilized in diverse fields of research. Apart from its use in Monte Carlo simulation studies, the most obvious application is the fitting of the GLD to data sets. The GLD has furthermore been incorporated into various models developed by researchers to address specific problems in their research fields. Examples of recent applications of the GLD appearing in the literature since 2001 are briefly listed below. Karian & Dudewicz (2000) and King (1999) can be

consulted for applications before 2001. It is evident from the provided applications that, in general, the GLD_{RS} has been favored over the GLD_{FMKL} . This can be attributed to the simpler form of the quantile function of the GLD_{RS} as well as the availability of tables in Karian & Dudewicz (2000, 2010) to assist in obtaining parameter estimates (or at least starting values for the optimization techniques) for the GLD_{RS} .

3.15.1 ACTUARIAL SCIENCE

Balasoorya & Low (2008) used the percentile-based estimation method of Karian & Dudewicz (1999) to fit the GLD_{RS} to medical claim amounts, taken from a database of the Society of Actuaries. For the complete data set considered, the authors compared the fit of the GLD_{RS} with the fit obtained through semiparametric transformed kernel density estimation and found both models fitted the data well. They also used the GLD_{RS} and transformed kernel to model exceedances above a threshold of \$200 000 and showed that, compared with the generalized Pareto distribution, a distribution typically used to model extreme observations in insurance claims data, these two models provided good fits to the extreme claim amounts.

3.15.2 BIOCHEMISTRY

In order to measure false discovery rates in peptide and protein identification by four tandem mass spectrometry database search engines, Ramos-Fernández *et al.* (2008) used the GLD_{RS} to model assignment score distributions from these search engines. The authors fitted the GLD_{RS} to the score distributions using the percentile-based estimation method of Karian & Dudewicz (1999).

3.15.3 BUSINESS, ECONOMICS AND FINANCE

Corrado (2001) considered the use of the GLD_{RS} in security pricing. Whereas the popular Black-Scholes methodology assumes a log-normal distribution for future security prices, the author derived pricing expressions for European call and put options based on the GLD_{RS} .

Several authors have considered the modeling of income data using the GLD. In order to fit the GLD_{RS} to a grouped income data set, Tarsitano (2004) proposed and used an extension of the “least-squares” method of Öztürk & Dale (1985). Pacáková & Sipková (2007) modeled income data from the Slovak Republic with the GLD_{RS} . They considered various estimation methods, including method of moments estimation and the percentile-based method of Karian & Dudewicz (1999). Haritha *et al.* (2008) used their proposed percentile-based method to fit the GLD_{FMKL} to an income data set taken from Arnold (1983).

3.15.4 COMPUTER SCIENCE

Au-Yeung *et al.* (2004) used the GLD_{FMKL} with method of moments estimation to approximate response times from a number of Markov and semi-Markov models in computer science. For each model considered, they compared the density and distribution functions of the approximation provided by the fitted GLD_{FMKL} with the theoretical density and distribution functions computed with an exact Laplace transform-based method. Based upon calculation time for computing the density and distribution functions, the GLD_{FMKL} outperformed the exact Laplace transform-based method.

Gautama & van Gemund (2006) presented an analytical model of the execution time distribution of N -ary and binary parallel compositions of stochastic tasks. In their model they utilized the GLD_{RS} with method of moments estimation to approximate execution time distributions.

Recently Lange *et al.* (2011) used the GLD_{RS} to model standard cell performance of integrated circuits. The authors showed that, using method of moments estimation, the GLD_{RS} is not applicable to raw leakage power data, but it does fit both timing data and dynamic power consumption data well.

3.15.5 EPIDEMIOLOGY

A group of researchers from the Department of Infectious Disease Epidemiology at Imperial College in London has used a modified form of the GLD_{RS} as part of their epidemiological models for the transmission dynamics of bovine spongiform encephalopathy (BSE) in sheep in Great Britain (Ferguson *et al.*, 2002) and of the variant Creutzfeldt–Jakob disease (vCJD) in Great Britain (Ghani *et al.*, 2003). In these studies, to calculate the probability that an individual develops clinical disease, the authors used the GLD_{RS} to model the incubation period distribution.

3.15.6 FORESTRY

The within-ring wood density distribution in clones of three coniferous species, namely Norway spruce, Douglas fir and maritime pine, was modeled with the GLD_{RS} by Ivković & Rozenberg (2004). For each of the three species, the authors then analyzed the relation between the parameter estimates of the fitted GLD_{RS} (as proxy of the within-ring wood density distribution) and the growth rate expressed through ring width.

3.15.7 INVENTORY MODELING

Lau *et al.* (2002) presented exact expressions for the average on-hand inventory level in the continuous-review order-quantity reorder-point (Q, R) system with backordering. The authors presented expressions for handling normally distributed as well as non-normal lead time demands in this system, where the beta distribution and the GLD_{RS} were considered for non-normal lead time demands.

In solving a multi-item inventory model, Achary & Geetha (2007) used the GLD_{RS} to approximate the lead time demand distribution. The authors found the values obtained through the GLD_{RS} approximations to be in close agreement with those given by a quadratic approximation procedure, with the added advantage of the GLD_{RS} approximations being applicable to different demand distributions through modification of the parameters of the GLD_{RS} .

3.15.8 QUEUING THEORY

Chou *et al.* (2001) proposed a better timer design for a pretimed traffic signal at an intersection located in Touliu, Taiwan. They described the interarrival times of approaching vehicles for the north and south bounds at the intersection with exponential distributions, while the interarrival times for the west and east bounds were described with members of the GLD_{RS} using method of moments estimation.

Robinson & Chen (2003) developed a closed-form heuristic policy for scheduling doctors' appointments. In examining the performance of their heuristic policy, the authors fitted the GLD_{RS} through maximum likelihood estimation to three data sets of patient service times.

3.15.9 SIGNAL PROCESSING

Karvanen *et al.* (2002) proposed adaptive score function models for maximum likelihood independent component analysis (ICA) methods in blind signal separation, where the source distributions in these models were based on the GLD_{RS} and on the Pearson family of distributions. The authors estimated the parameters of the GLD_{RS} with method of moments and method of L -moments estimation. They showed that, when skewness is the dominant property of the source distributions, the performance of their proposed ICA methods based on the GLD_{RS} and on the Pearson family of distributions is significantly better than the performance of other widely used ICA methods.

3.15.10 STATISTICAL PROCESS CONTROL

Pal (2005) considered the computation of generalized process capability indices for a non-normal process, where he modeled the process data with the GLD_{RS} using method of moments estimation. Fournier *et al.* (2006) and van Staden (2006) illustrated the use of the GLD_{RS} in the construction of statistical process control charts for non-normal data.

3.15.11 SUPPLY CHAIN PLANNING

Poojari *et al.* (2008) formulated a strategic supply chain planning problem having uncertain demand as a two-stage stochastic integer programming model. They used the GLD_{FMKL} to approximate the uncertain demand distribution, estimating its parameters with method of moments estimation.

3.16 CONCLUSION

Two popular types of the GLD, the Ramberg-Schmeiser Type (GLD_{RS}) and the Freimer-Mudholkar-Kollia-Lin Type (GLD_{FMKL}), were discussed in this chapter. Both these types are highly flexible with respect to distributional shape. However, the shape properties of the GLD_{RS} and the GLD_{FMKL} are extremely complex. In particular, both shape parameters jointly explain the skewness and the kurtosis. As a result, closed-form expressions do not exist for the shape parameter estimators of either the GLD_{RS} or the GLD_{FMKL} , causing parameter estimation to be computationally difficult in that numerical optimization techniques must be used.

In Chapter 4 a type of the GLD is developed which possesses skewness-invariant measures of kurtosis. Consequently parameter estimation will be straightforward for this type.

3.17 DERIVATIONS

Derivations for the GLD_{FMKL} which have not appeared before in the literature are presented here. Specifically formulae for the moments of the GLD_{FMKL} with $\lambda_3 = 0$ and $\lambda_4 \neq 0$ and with $\lambda_3 \neq 0$ and $\lambda_4 = 0$ are derived in Section 3.17.1, while expressions for the L -moments of the GLD_{FMKL} are derived in Section 3.17.2.

3.17.1 MOMENTS OF GLD_{FMKL}

Lemma 3.17.1

In the derivation of the formulae for the moments of the GLD_{FMKL} with $\lambda_3 = 0$ and $\lambda_4 \neq 0$, the integral

$$\Psi_{\lambda_4}(j, k) = \int_0^1 (\log[p])^j (1-p)^{k\lambda_4} dp$$

must be solved for $j = 1, 2, 3, 4$ and $k = 0, 1, 2, 3$. Likewise the integral

$$\Psi_{\lambda_3}(j, k) = \int_0^1 p^{k\lambda_3} (\log[1-p])^j dp$$

must be solved in order to obtain formulae for the moments of the GLD_{FMKL} with $\lambda_3 \neq 0$ and $\lambda_4 = 0$. The methodology presented in Lemma 2.13.1 in Chapter 2 can be used to obtain expressions for $\Psi_{\lambda_4}(j, k)$ and $\Psi_{\lambda_3}(j, k)$. In particular, since

$$\begin{aligned} \Psi_{\lambda_4}(j, k) &= \frac{\partial^j}{\partial u^j} \left(\int_0^1 p^u (1-p)^{k\lambda_4} dy \right) \Big|_{u=0} \\ &= \frac{\partial^j}{\partial u^j} (\mathbf{B}(u+1, k\lambda_4+1)) \Big|_{u=0} \end{aligned} \quad (3.25)$$

and

$$\begin{aligned} \Psi_{\lambda_3}(j, k) &= \frac{\partial^j}{\partial v^j} \left(\int_0^1 p^{k\lambda_3} (1-p)^v dy \right) \Big|_{v=0} \\ &= \frac{\partial^j}{\partial v^j} (\mathbf{B}(k\lambda_3+1, v+1)) \Big|_{v=0}, \end{aligned} \quad (3.26)$$

where $\mathbf{B}(a, b)$ is the beta function (see Section 2.14.1), it can be shown that, for $i = 3, 4$,

$$\Psi_{\lambda_i}(j, 0) = (-1)^j j!,$$

while, because $\mathbf{B}(a+1, 1) = \mathbf{B}(1, a+1) = \frac{1}{a+1}$ for $a > -1$,

$$\begin{aligned} \Psi_{\lambda_i}(1, k) &= -\mathbf{B}(1, k\lambda_i+1) \left(C + \psi(k\lambda_i+2) \right) \\ &= -\frac{1}{k\lambda_i+1} \left(C + \psi(k\lambda_i+2) \right), \end{aligned}$$

$$\begin{aligned}\Psi_{\lambda_i}(2, k) &= B(1, k\lambda_i + 1) \left(\frac{\pi^2}{6} + \left(C + \psi(k\lambda_i + 2) \right)^2 - \psi^{(1)}(k\lambda_i + 2) \right) \\ &= \frac{1}{k\lambda_i + 1} \left(\frac{\pi^2}{6} + \left(C + \psi(k\lambda_i + 2) \right)^2 - \psi^{(1)}(k\lambda_i + 2) \right)\end{aligned}$$

and

$$\begin{aligned}\Psi_{\lambda_i}(3, k) &= -B(1, k\lambda_i + 1) \left(3 \left(\frac{\pi^2}{6} - \psi^{(1)}(k\lambda_i + 2) \right) \left(C + \psi(k\lambda_i + 2) \right) \right. \\ &\quad \left. + \left(C + \psi(k\lambda_i + 2) \right)^3 + 2\zeta(3) + \psi^{(2)}(k\lambda_i + 2) \right) \\ &= -\frac{1}{k\lambda_i + 1} \left(3 \left(\frac{\pi^2}{6} - \psi^{(1)}(k\lambda_i + 2) \right) \left(C + \psi(k\lambda_i + 2) \right) \right. \\ &\quad \left. + \left(C + \psi(k\lambda_i + 2) \right)^3 + 2\zeta(3) + \psi^{(2)}(k\lambda_i + 2) \right),\end{aligned}$$

where C is Euler's constant, $\psi(a)$ is the psi function, $\psi^{(r)}(a)$ is the r^{th} derivative of the psi function and $\zeta(a)$ is Riemann's zeta function – see again Section 2.14.1. Note that the integrals in (3.25) and (3.26) only converge if $(k\lambda_i + 1) > 0$, that is, if $\lambda_i > -\frac{1}{k}$ for $i = 3, 4$.

■

Theorem 3.17.1

Let X be a real-valued random variable whose distribution is the FMKL Type of the GLD, denoted $X \sim \text{GLD}_{\text{FMKL}}(\lambda_1, \lambda_2, \lambda_3, \lambda_4)$, with λ_1 the location parameter, $\lambda_2 \neq 0$ the scale parameter and λ_3 and λ_4 the shape parameters. Assume that only one of the shape parameters is zero. The mean, variance, and skewness and kurtosis moment ratios of X are given by (3.8) to (3.11), where, if $\lambda_3 = 0$ and $\lambda_4 > -\frac{1}{4}$,

$$M_r = \begin{cases} -\frac{\lambda_4}{\lambda_4+1}, & r=1, \\ \frac{2(2\lambda_4^3+\lambda_4^2-\lambda_4-1)}{\lambda_4(\lambda_4+1)(2\lambda_4+1)} + \frac{2(C+\psi(\lambda_4+2))}{\lambda_4(\lambda_4+1)}, & r=2, \\ -\frac{3(12\lambda_4^5+10\lambda_4^4-4\lambda_4^3-\lambda_4^2+4\lambda_4+1)}{\lambda_4^2(\lambda_4+1)(2\lambda_4+1)(3\lambda_4+1)} + \frac{6(C+\psi(\lambda_4+2))}{\lambda_4^2(\lambda_4+1)} \\ -\frac{3(C+\psi(2\lambda_4+2))}{\lambda_4^2(2\lambda_4+1)} - \frac{3\left(\frac{\pi^2}{6}+(C+\psi(\lambda_4+2))^2-\psi^{(1)}(\lambda_4+2)\right)}{\lambda_4(\lambda_4+1)}, & r=3, \\ \frac{4(144\lambda_4^7+156\lambda_4^6-18\lambda_4^5-24\lambda_4^4+7\lambda_4^3-11\lambda_4^2-7\lambda_4-1)}{\lambda_4^3(\lambda_4+1)(2\lambda_4+1)(3\lambda_4+1)(4\lambda_4+1)} + \frac{12(C+\psi(\lambda_4+2))}{\lambda_4^3(\lambda_4+1)} \\ -\frac{12(C+\psi(2\lambda_4+2))}{\lambda_4^3(2\lambda_4+1)} + \frac{4(C+\psi(3\lambda_4+2))}{\lambda_4^3(3\lambda_4+1)} - \frac{12\left(\frac{\pi^2}{6}+(C+\psi(\lambda_4+2))^2-\psi^{(1)}(\lambda_4+2)\right)}{\lambda_4^2(\lambda_4+1)} \\ + \frac{6\left(\frac{\pi^2}{6}+(C+\psi(2\lambda_4+2))^2-\psi^{(1)}(2\lambda_4+2)\right)}{\lambda_4^2(2\lambda_4+1)} \\ + \frac{4\left(3\left(\frac{\pi^2}{6}-\psi^{(1)}(\lambda_4+2)\right)(C+\psi(\lambda_4+2))+(C+\psi(\lambda_4+2))^3+2\zeta(3)+\psi^{(2)}(\lambda_4+2)\right)}{\lambda_4(\lambda_4+1)} & r=4, \end{cases}$$

whereas, if $\lambda_3 > -\frac{1}{4}$ and $\lambda_4 = 0$, then

$$M_r = \begin{cases} \frac{\lambda_3}{\lambda_3+1}, & r=1, \\ \frac{2(2\lambda_3^3+\lambda_3^2-\lambda_3-1)}{\lambda_3(\lambda_3+1)(2\lambda_3+1)} + \frac{2(C+\psi(\lambda_3+2))}{\lambda_3(\lambda_3+1)}, & r=2, \\ \frac{3(12\lambda_3^5+10\lambda_3^4-4\lambda_3^3-\lambda_3^2+4\lambda_3+1)}{\lambda_3^2(\lambda_3+1)(2\lambda_3+1)(3\lambda_3+1)} - \frac{6(C+\psi(\lambda_3+2))}{\lambda_3^2(\lambda_3+1)} \\ + \frac{3(C+\psi(2\lambda_3+2))}{\lambda_3^2(2\lambda_3+1)} + \frac{3\left(\frac{\pi^2}{6}+(C+\psi(\lambda_3+2))^2-\psi^{(1)}(\lambda_3+2)\right)}{\lambda_3(\lambda_3+1)}, & r=3, \\ \frac{4(144\lambda_3^7+156\lambda_3^6-18\lambda_3^5-24\lambda_3^4+7\lambda_3^3-11\lambda_3^2-7\lambda_3-1)}{\lambda_3^3(\lambda_3+1)(2\lambda_3+1)(3\lambda_3+1)(4\lambda_3+1)} + \frac{12(C+\psi(\lambda_3+2))}{\lambda_3^3(\lambda_3+1)} \\ -\frac{12(C+\psi(2\lambda_3+2))}{\lambda_3^3(2\lambda_3+1)} + \frac{4(C+\psi(3\lambda_3+2))}{\lambda_3^3(3\lambda_3+1)} - \frac{12\left(\frac{\pi^2}{6}+(C+\psi(\lambda_3+2))^2-\psi^{(1)}(\lambda_3+2)\right)}{\lambda_3^2(\lambda_3+1)} \\ + \frac{6\left(\frac{\pi^2}{6}+(C+\psi(2\lambda_3+2))^2-\psi^{(1)}(2\lambda_3+2)\right)}{\lambda_3^2(2\lambda_3+1)} \\ + \frac{4\left(3\left(\frac{\pi^2}{6}-\psi^{(1)}(\lambda_3+2)\right)(C+\psi(\lambda_3+2))+(C+\psi(\lambda_3+2))^3+2\zeta(3)+\psi^{(2)}(\lambda_3+2)\right)}{\lambda_3(\lambda_3+1)} & r=4. \end{cases}$$

Proof

Assume, without loss of generality, that $\lambda_1 = 0$ and $\lambda_2 = 1$ so that $X \sim \text{GLD}_{\text{FMKL}}(0, 1, \lambda_3, \lambda_4)$.

If $\lambda_3 = 0$ and $\lambda_4 > -\frac{1}{4}$, then, for example,

$$\begin{aligned}
 M_4 &= \int_0^1 \left(\log[p] - \frac{(1-p)^{\lambda_4} - 1}{\lambda_4} \right)^4 dp \\
 &= \frac{1}{\lambda_4^4} \int_0^1 \left(1 - 4(1-p)^{\lambda_4} + 6(1-p)^{2\lambda_4} - 4(1-p)^{3\lambda_4} + (1-p)^{4\lambda_4} \right) dp \\
 &\quad + \frac{1}{\lambda_4^3} \int_0^1 \left(4 - 12(1-p)^{\lambda_4} + 12(1-p)^{2\lambda_4} - 4(1-p)^{3\lambda_4} \right) \log[p] dp \\
 &\quad + \frac{1}{\lambda_4^2} \int_0^1 \left(6 - 12(1-p)^{\lambda_4} + 6(1-p)^{2\lambda_4} \right) (\log[p])^2 dp \\
 &\quad + \frac{1}{\lambda_4} \int_0^1 \left(4 - 4(1-p)^{\lambda_4} \right) (\log[p])^3 dp + \int_0^1 (\log[p])^4 dp \\
 &= \frac{1}{\lambda_4^4} \left(1 - \frac{4}{\lambda_4 + 1} + \frac{6}{2\lambda_4 + 1} - \frac{4}{3\lambda_4 + 1} + \frac{1}{4\lambda_4 + 1} \right) \\
 &\quad + \frac{1}{\lambda_4^3} \left(4\Psi_{\lambda_4}(1, 0) - 12\Psi_{\lambda_4}(1, 1) + 12\Psi_{\lambda_4}(1, 2) - 4\Psi_{\lambda_4}(1, 3) \right) \\
 &\quad + \frac{1}{\lambda_4^2} \left(6\Psi_{\lambda_4}(2, 0) - 12\Psi_{\lambda_4}(2, 1) + 6\Psi_{\lambda_4}(2, 2) \right) \\
 &\quad + \frac{1}{\lambda_4} \left(4\Psi_{\lambda_4}(3, 0) - 4\Psi_{\lambda_4}(3, 1) \right) + \Psi_{\lambda_4}(4, 0),
 \end{aligned}$$

where the restriction $\lambda_4 > -\frac{1}{4}$ is needed for convergence of the integrals. Likewise it can be shown that

$$M_1 = \frac{1}{\lambda_4} \left(1 - \frac{1}{\lambda_4 + 1} \right) + \Psi_{\lambda_4}(1, 0),$$

$$M_2 = \frac{1}{\lambda_4^2} \left(1 - \frac{2}{\lambda_4 + 1} + \frac{1}{2\lambda_4 + 1} \right) + \frac{1}{\lambda_4} \left(2\Psi_{\lambda_4}(1, 0) - 2\Psi_{\lambda_4}(1, 1) \right) + \Psi_{\lambda_4}(2, 0)$$

and

$$\begin{aligned}
 M_3 &= \frac{1}{\lambda_4^3} \left(1 - \frac{3}{\lambda_4 + 1} + \frac{3}{2\lambda_4 + 1} - \frac{1}{3\lambda_4 + 1} \right) + \frac{1}{\lambda_4^2} \left(3\Psi_{\lambda_4}(1, 0) - 6\Psi_{\lambda_4}(1, 1) + 3\Psi_{\lambda_4}(1, 2) \right) \\
 &\quad + \frac{1}{\lambda_4} \left(3\Psi_{\lambda_4}(2, 0) - 3\Psi_{\lambda_4}(2, 1) \right) + \Psi_{\lambda_4}(3, 0).
 \end{aligned}$$

The final expressions for M_1 to M_4 are obtained by substituting the expressions for $\Psi_{\lambda_4}(j, k)$ in Lemma 3.17.1 and simplifying. Expressions for M_1 to M_4 when $\lambda_3 > -\frac{1}{4}$ and $\lambda_4 = 0$ are obtained in a similar manner.

■

3.17.2 L-MOMENTS OF GLD_{FMKL}

Theorem 3.17.2

Suppose X is a real-valued random variable whose distribution is the FMKL Type of the GLD, denoted $X \sim \text{GLD}_{\text{FMKL}}(\lambda_1, \lambda_2, \lambda_3, \lambda_4)$, where λ_1 is the location parameter, $\lambda_2 \neq 0$ is the scale parameter and λ_3 and λ_4 are the shape parameters. If $\lambda_3 > -1$ and $\lambda_4 > -1$, the L -location and L -scale of X are given by (3.16) and (3.17), while the r^{th} order L -moment for $r > 2$ is given by (3.18).

Proof

To simplify the derivation of the L -moments of the GLD_{FMKL} , it is convenient to rewrite its quantile function, given in (3.4), as

$$Q(p) = \lambda_1 - \frac{1}{\lambda_2} \left(\frac{1}{\lambda_3} - \frac{1}{\lambda_4} \right) + \frac{1}{\lambda_2} \left(\frac{p^{\lambda_3}}{\lambda_3} - \frac{(1-p)^{\lambda_4}}{\lambda_4} \right). \quad (3.27)$$

Then, since $P_0^*(p) = 1$ as indicated in (2.89) in Section 2.14.2, the L -location is

$$\begin{aligned} L_1 &= \int_0^1 Q(p) dp \\ &= \lambda_1 - \frac{1}{\lambda_2} \left(\frac{1}{\lambda_3} - \frac{1}{\lambda_4} \right) + \frac{1}{\lambda_2} \left(\frac{1}{\lambda_3} \int_0^1 p^{\lambda_3} dp - \frac{1}{\lambda_4} \int_0^1 (1-p)^{\lambda_4} dp \right) \\ &= \lambda_1 - \frac{1}{\lambda_2} \left(\frac{1}{\lambda_3} - \frac{1}{\lambda_4} \right) + \frac{1}{\lambda_2} \left(\frac{1}{\lambda_3(\lambda_3+1)} - \frac{1}{\lambda_4(\lambda_4+1)} \right), \end{aligned} \quad (3.28)$$

which can be simplified to obtain the expression given in (3.16). Note that the integrals in (3.28) only converge if $\lambda_3 > -1$ and $\lambda_4 > -1$.

Substituting (3.27) into (2.23) from Section 2.5 in Chapter 2 and using (2.93) and (2.94) from Section 2.14.2 in Chapter 2, the r^{th} order L -moment for $r > 1$ can be written as

$$\begin{aligned}
 L_r &= \int_0^1 Q(p) P_{r-1}^*(p) dp \\
 &= \frac{1}{\lambda_2} \left(\frac{1}{\lambda_3} \int_0^1 p^{\lambda_3} P_{r-1}^*(p) dp - \frac{1}{\lambda_4} \int_0^1 (1-p)^{\lambda_4} P_{r-1}^*(p) dp \right) \\
 &= \frac{1}{\lambda_2} \left(\frac{1}{\lambda_3} \int_0^1 p^{\lambda_3} P_{r-1}^*(p) dp - \frac{(-1)^{r-1}}{\lambda_4} \int_0^1 (1-p)^{\lambda_4} P_{r-1}^*(1-p) dp \right) \\
 &= \frac{1}{\lambda_2} \left(\frac{1}{\lambda_3} \int_0^1 p^{\lambda_3} P_{r-1}^*(p) dp + \frac{(-1)^r}{\lambda_4} \int_0^1 p^{\lambda_4} P_{r-1}^*(p) dp \right) \\
 &= \frac{1}{\lambda_2} \left(\frac{1}{\lambda_3} \sum_{k=0}^{r-1} \binom{r-1}{k} \binom{r+k-1}{k} \int_0^1 p^{\lambda_3+k} dp \right) \\
 &\quad + \frac{(-1)^r}{\lambda_4} \sum_{k=0}^{r-1} \binom{r-1}{k} \binom{r+k-1}{k} \int_0^1 p^{\lambda_4+k} dp \Bigg) \\
 &= \frac{1}{\lambda_2} \sum_{k=0}^{r-1} \binom{r-1}{k} \binom{r+k-1}{k} \left(\frac{1}{\lambda_3(\lambda_3+k+1)} + \frac{(-1)^r}{\lambda_4(\lambda_4+k+1)} \right),
 \end{aligned}$$

provided that $\lambda_3 > -1$ and $\lambda_4 > -1$ in order for the integrals to converge. Now, for example, if

$r = 4$, then, for $i = 3, 4$,

$$\begin{aligned}
 \sum_{k=0}^3 \left(\binom{3}{k} \binom{k+3}{k} \left(\frac{(-1)^{3-k}}{\lambda_i(\lambda_i+k+1)} \right) \right) &= -\frac{1}{\lambda_i(\lambda_i+1)} + \frac{12}{\lambda_i(\lambda_i+2)} - \frac{30}{\lambda_i(\lambda_i+3)} + \frac{20}{\lambda_i(\lambda_i+4)} \\
 &= \frac{(\lambda_i-1)(\lambda_i-2)}{(\lambda_i+1)(\lambda_i+2)(\lambda_i+3)(\lambda_i+4)}.
 \end{aligned}$$

In general it can be shown that for $i = 3, 4$,

$$\sum_{k=0}^{r-1} \left(\binom{r-1}{k} \binom{r+k-1}{k} \left(\frac{(-1)^{r-k-1}}{\lambda_i(\lambda_i+k+1)} \right) \right) = \begin{cases} \frac{1}{(\lambda_i+1)(\lambda_i+2)}, & r = 2, \\ \frac{\prod_{k=1}^{r-2} (\lambda_i-k)}{\prod_{k=1}^r (\lambda_i+k)}, & r > 2, \end{cases}$$

from which the expressions for the L -scale in (3.17) and the r^{th} order L -moment for $r > 2$ in (3.18) are obtained.

■

4. A GLD TYPE WITH SKEWNESS–INVARIANT MEASURES OF KURTOSIS

4.1 INTRODUCTION

This chapter introduces a new type of the generalized lambda distribution (GLD) with separate skewness and kurtosis parameters and a simple relationship between its parameters and L -moments. Consequently closed-form expressions are available for the method of L -moments estimators of this proposed type, as well as for the standard errors of these estimators.

The new type is specified in terms of its quantile function, given in Definition 4.2.1 in Section 4.2. Its quantile function is constructed by applying the methodology of Proposition 2.8.1 from Chapter 2. With this methodology, the quantile function of a generalized quantile-based distribution is obtained by taking the weighted sum of the quantile function of an asymmetric distribution and the quantile function of the reflection of this asymmetric distribution.

The quantile function of any asymmetric distribution on bounded or half-infinite support can be used as the basic building block. In this chapter the quantile function of the generalized Pareto distribution (GPD) is used as the basic building block. The resulting new type of the GLD is therefore called the GPD Type of the GLD and denoted by GLD_{GPD} .

Similar to the GLD_{RS} and GLD_{FMKL} , the GLD_{GPD} is highly flexible with respect to distributional shape, able to attain uniform, unimodal, U-shaped, monotone increasing and monotone decreasing (including J-shaped) as well as truncated density curves, with infinite, half-infinite or bounded support. Based on the distributional shapes and the support achievable by the GLD_{GPD} , its parameter space is divided in four distinct classes, presented in Section 4.3 and explored in detail in Section 4.4.

A comprehensive analysis of the characterization of the GLD_{GPD} through its L -moments is presented in Section 4.6, specifically with respect to its coverage of the L -skewness and L -kurtosis ratios (τ_3 and τ_4). The coverage of the (τ_3, τ_4) space by the GLD_{GPD} is equivalent

to the coverage by the GLD_{RS} and GLD_{FMKL} . However, the relation between the shape parameters and the L -skewness and L -kurtosis ratios of the GLD_{GPD} is noticeably simpler compared to the corresponding relations for the GLD_{RS} and the GLD_{FMKL} . In particular the L -kurtosis ratio of the GLD_{GPD} is a skewness-invariant measure of kurtosis.

The main benefit arising from the skewness-invariance of the L -kurtosis ratio is the existence of closed-form expressions for the method of L -moments estimators of the parameters of the GLD_{GPD} . An estimation algorithm for computing the method of L -moments estimates is outlined in Section 4.9. Closed-form expressions are furthermore also available for the elements of the covariance matrix of the method of L -moments estimators and thus for these estimators' asymptotic standard errors. Although these expressions, derived in Section 4.13.3, are extremely complex, it should be remembered that no such expressions are available for either the GLD_{RS} and GLD_{FMKL} .

Probability distributions are typically characterized by their conventional moments. Formulae for the mean, variance, skewness moment ratio and kurtosis moment ratio of the GLD_{GPD} are therefore presented in Section 4.5, with the derivation thereof performed in Section 4.13.1. However, due to the complex structure of these moments' formulae for the GLD_{GPD} , their use in description, estimation and inference is unappealing.

Akin to the L -kurtosis ratio, the kurtosis functionals of the GLD_{GPD} are also skewness-invariant. Expressions for these functionals are given in Section 4.7 along with expressions for the median, spread function and skewness functionals of the GLD_{GPD} . The main advantage of these quantile-based measures compared to the moments and L -moments is that they exist for all valid parameter values of the GLD_{GPD} . The relation between the shape parameters of the GLD_{GPD} and its skewness, kurtosis, and tail behavior is explored in Section 4.8. Whereas the two shape parameters of the GLD_{RS} and GLD_{FMKL} jointly account for these GLD Types' skewness and kurtosis, the skewness-invariance of the L -kurtosis ratio and kurtosis functionals of the GLD_{GPD} allows one to describe the kurtosis of the GLD_{GPD} with one of its shape parameters, while the second shape parameter controls the level of skewness.

In Sections 4.10 and 4.11 the fitting of the GLD_{GPD} to data sets and the approximation of probability distributions by the GLD_{GPD} , using method of L -moments estimation, are illustrated and described. Conclusions are given in Section 4.12, before Chapter 4 ends with the derivations in Section 4.13.

4.2 GENESIS AND SPECIAL CASES

The quantile function of the generalized Pareto distribution (GPD) is used as the basic building block in the derivation of the alternative type of the GLD. The GPD was introduced by Pickands (1975) and is a cornerstone distribution in extreme value modeling – see for instance Hosking & Wallis (1987), Coles (2001) and Castillo *et al.* (2005). The quantile function of the standard GPD is given by

$$Q_0(p) = \begin{cases} -\frac{1}{\lambda} \left((1-p)^\lambda - 1 \right) & , \lambda \neq 0, \\ -\ln[1-p] & , \lambda = 0, \end{cases} \quad (4.1)$$

where λ is the shape parameter. The limiting case, $\lambda = 0$ in (4.1), obtained by L'Hôpital's rule (de l'Hôpital, 1696), is the quantile function of the standard exponential distribution. Note furthermore that setting $\lambda = 1$ in (4.1) gives the quantile function of the standard uniform distribution with support $[0, 1]$. In general the support of the standard GPD is $[0, \infty)$ if $\lambda \leq 0$ and $[0, \lambda^{-1}]$ if $\lambda > 0$. Thus, depending on the value of λ , the standard GPD has half-infinite or bounded support.

Applying the reflection rule, presented in Section 2.3.2, gives the quantile function of the standard reflected GPD,

$$Q_0(p) = \begin{cases} \frac{1}{\lambda} \left(p^\lambda - 1 \right) & , \lambda \neq 0, \\ \ln[p] & , \lambda = 0, \end{cases} \quad (4.2)$$

where the limiting case, $\lambda = 0$, again obtained by L'Hôpital's rule, is the quantile function of the standard reflected exponential distribution. The probability density functions of the standard GPD and the standard reflected GPD are shown in Figure 4.1 for various values of λ . It can be seen in Figure 4.1 that the standard reflected GPD is the reflection of the standard GPD about the line $x = 0$.

In Example 2.3.3 in Chapter 2 it was shown that the sum of the quantile functions of the standard exponential and standard reflected exponential distributions is the quantile function of the standard logistic distribution, given in (2.12). Adding the quantile functions of the standard GPD and standard reflected GPD in (4.1) and (4.2) gives

$$Q_0(p) = \begin{cases} \frac{1}{\lambda} \left(p^\lambda - (1-p)^\lambda \right), & \lambda \neq 0, \\ \log \left[\frac{p}{1-p} \right], & \lambda = 0, \end{cases} \quad (4.3)$$

the quantile function of the standard form of Tukey's lambda distribution, given in (3.1).

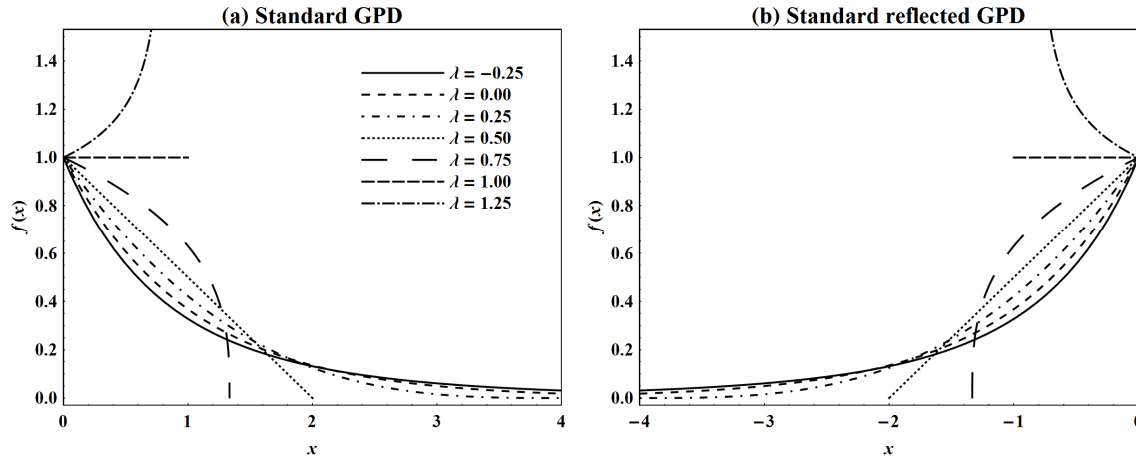


Figure 4.1: Probability density functions of the standard GPD and the standard reflected GPD for various values of λ . The line types indicated in graph (a) also apply to graph (b).

As explained in Section 2.3.3 and shown in (2.11), the sum of the quantile function of an asymmetric distribution on bounded or half-infinite support and the quantile function of the reflection of this distribution is the quantile function of a symmetric distribution. It was furthermore explained in Section 2.3.4 that skewness can be introduced using the transformation in (2.13), where the weighted sum of the quantile function of an asymmetric distribution on bounded or half-infinite support and the quantile function of the reflection of this distribution is taken, with $0 \leq \delta \leq 1$ the weight parameter. In Definition 4.2.1 below a type of the GLD, the GLD_{GPD} , is defined whose quantile function is given by the weighted sum of the quantile functions of the standard GPD and standard reflected GPD.

Definition 4.2.1

A real-valued random variable X is said to have the GPD Type of the GLD, denoted $X \sim \text{GLD}_{\text{GPD}}(\alpha, \beta, \delta, \lambda)$, if its quantile function is given by

$$Q(p) = \begin{cases} \alpha + \beta \left((1 - \delta) \left(\frac{p^\lambda - 1}{\lambda} \right) - \delta \left(\frac{(1-p)^\lambda - 1}{\lambda} \right) \right), & \lambda \neq 0, \\ \alpha + \beta \left((1 - \delta) \log[p] - \delta \log[1 - p] \right), & \lambda = 0, \end{cases} \quad (4.4)$$

where α is a location parameter, $\beta > 0$ is a scale parameter and $0 \leq \delta \leq 1$ and λ are shape parameters.

■

CHAPTER 4. A GLD TYPE WITH SKEWNESS-INVARIANT MEASURES OF KURTOSIS

In (4.4) the limiting case, $\lambda = 0$, is the quantile function of the skew logistic distribution (SLD), considered in Chapter 2. Akin to the SLD, the GLD_{GPD} is symmetric for $\delta = \frac{1}{2}$ and asymmetric for $\delta \neq \frac{1}{2}$. The shape properties of the GLD_{GPD} , including its skewness properties, will be discussed in more detail in Section 4.8.

The GLD_{GPD} contains various other well-known distributions as special cases, listed in Table 4.1. It follows from the quantile function of the GLD_{GPD} in (4.4) that the GPD and the reflected GPD are respectively obtained for $\delta = 1$ and for $\delta = 0$. From the intermediate rule, presented in Section 2.3.4 of Chapter 2, we have that the quantile function of the GLD_{GPD} is bounded by the quantile functions of these two distributions.

Table 4.1: Shape parameter values for distributions contained by the GLD_{GPD} .

Distribution	Shape parameter values
Exponential	$\delta = 1, \lambda = 0$
Reflected exponential	$\delta = 0, \lambda = 0$
Generalized Pareto	$\delta = 1, -\infty < \lambda < \infty$
Reflected generalized Pareto	$\delta = 0, -\infty < \lambda < \infty$
Logistic	$\delta = \frac{1}{2}, \lambda = 0$
Skew logistic	$0 \leq \delta \leq 1, \lambda = 0$
Tukey's lambda	$\delta = \frac{1}{2}, -\infty < \lambda < \infty$
Uniform	$0 \leq \delta \leq 1, \lambda = 1$ and $\delta = \frac{1}{2}, \lambda = 2$

As with the GLD_{RS} and the GLD_{FMKL} , the uniform distribution is obtained from the GLD_{GPD} for more than one set of values of the shape parameters. Firstly, when $\lambda = 1$, the uniform distribution is found for any $0 \leq \delta \leq 1$. Secondly, when $\lambda = 2$, the uniform distribution is attained only for $\delta = \frac{1}{2}$.

Similar to the GLD_{RS} and the GLD_{FMKL} , no closed-form expressions exists for the cumulative distribution function and the probability density function of the GLD_{GPD} , except of course for the special cases of the GLD_{GPD} listed in Table 4.1 (excluding Tukey's lambda distribution and the SLD). The quantile density function of the GLD_{GPD} is

$$q(p) = \beta \left((1 - \delta)p^{\lambda-1} + \delta(1-p)^{\lambda-1} \right), \quad (4.5)$$

and its density quantile function is

$$f_p(p) = \frac{1}{\beta \left((1-\delta)p^{\lambda-1} + \delta(1-p)^{\lambda-1} \right)}. \quad (4.6)$$

4.3 PARAMETER SPACE AND SUPPORT

In Section 3.5 it was shown how the parameter spaces of the GLD_{RS} and GLD_{FMKL} are divided into regions or classes. Likewise the parameter space of the GLD_{GPD} is divided into four classes based on the distributional shapes and the support attainable in each class. As indicated in Table 4.2, this division is controlled by the values of the shape parameter λ . In Section 4.4 the characteristics of the GLD_{GPD} are described for each class.

Table 4.2: Parameter space and support of the GLD_{GPD} in terms of Classes I, II, III and IV.

Class	Shape parameter values	Support
Class I	$\delta = 0, \lambda \leq 0$	$(-\infty, \alpha]$
	$0 < \delta < 1, \lambda \leq 0$	$(-\infty, \infty)$
	$\delta = 1, \lambda \leq 0$	$[\alpha, \infty)$
Class II	$0 \leq \delta \leq 1, 0 < \lambda < 1$	$\left[\alpha - \frac{(1-\delta)\beta}{\lambda}, \alpha + \frac{\delta\beta}{\lambda} \right]$
Class III	$0 \leq \delta \leq 1, 1 \leq \lambda \leq 2$	$\left[\alpha - \frac{(1-\delta)\beta}{\lambda}, \alpha + \frac{\delta\beta}{\lambda} \right]$
Class IV	$0 \leq \delta \leq 1, \lambda > 2$	$\left[\alpha - \frac{(1-\delta)\beta}{\lambda}, \alpha + \frac{\delta\beta}{\lambda} \right]$

4.4 CLASSES OF THE GLD_{GPD}

The probability density functions of some examples of members of the GLD_{GPD} are illustrated in Figures 4.2 to 4.5 for the four classes of the GLD_{GPD} . In each given plot a symmetric member of the GLD_{GPD} with $\delta = \frac{1}{2}$ is shown along with asymmetric members of the GLD_{GPD} for two selected values of $\delta > \frac{1}{2}$. For $\delta < \frac{1}{2}$, the asymmetric GLD_{GPD} is reflected about the line $x = \alpha$ (see for instance again Figure 2.7(d) in Chapter 2 for the density curves of the standard SLD with $\lambda = 0$, where the reflection is about the line $x = \alpha = 0$). Hence the plots for $\delta < \frac{1}{2}$ are omitted. To enable comparisons for different shape parameter values, the L -location and L -scale are set to zero and unity ($L_1 = 0$ and $L_2 = 1$) for all plots in Figures 4.2 to 4.5. The expressions for the L -moments, including the L -location and L -scale, will be given in Section 4.6.

4.4.1 CLASS I

Figure 4.2 illustrates the distributional shapes attained by the GLD_{GPD} in Class I with $\lambda \leq 0$. These shapes correspond to the shapes attained in Region 4 of the GLD_{RS} and in Region 4 of Class I of the GLD_{FMKL} with $\lambda_3 \leq 0$ and $\lambda_4 \leq 0$. The SLD with $\lambda = 0$ is a special case in Class 1 of the GLD_{GPD} .

When $0 < \delta < 1$, Class I contains unimodal, leptokurtic members of the GLD_{GPD} with infinite support. For $\delta = 0$ and $\delta = 1$, the density curve of the GLD_{GPD} is J-shaped with half-infinite support. Class I is the only class of the GLD_{GPD} producing members with infinite and half-infinite support.

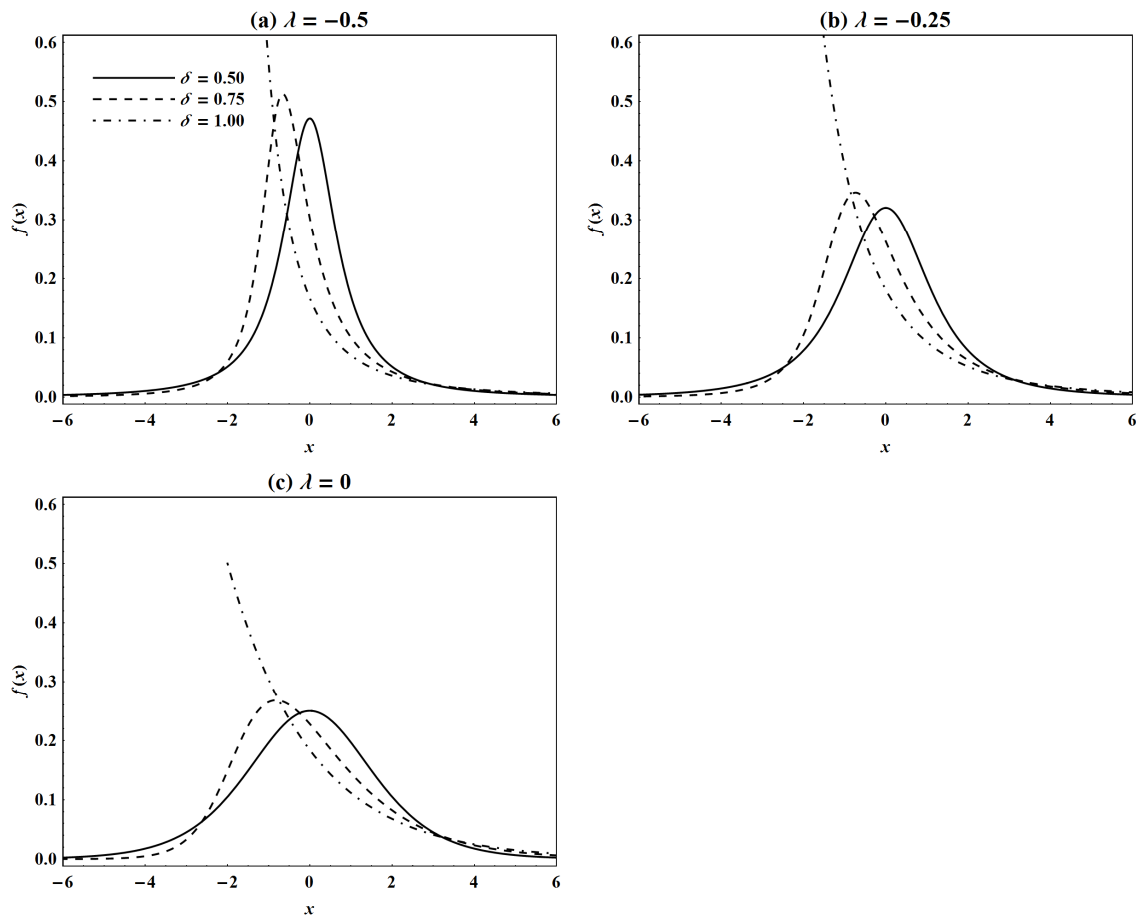


Figure 4.2: Probability density functions of members of the GLD_{GPD} from Class I, all with $L_1 = 0$ and $L_2 = 1$. The line types indicated in graph (a) also apply to graphs (b) and (c).

4.4.2 CLASS II

Platykurtic, mesokurtic and leptokurtic members of the GLD_{GPD} with bounded support are found in Class II with $0 < \lambda < 1$. Along with Class I, Class II provides the most useful distributional shapes for the GLD_{GPD} , examples of which are shown in Figure 4.3. The

density curve in Class II is unimodal for $0 < \delta < 1$, monotone increasing for $\delta = 0$, while it is monotone decreasing for $\delta = 1$. As $\lambda \uparrow 1$, the GLD_{GPD} tends to the uniform distribution.

When $0 < \lambda < \frac{1}{2}$ and $0 < \delta < 1$, the GLD_{GPD} in Class II yields density curve shapes equivalent to those in Region 3(a) of the GLD_{RS} and in Region 3 of Class I of the GLD_{FMKL} with $0 < \lambda_3 < \frac{1}{2}$ and $0 < \lambda_4 < \frac{1}{2}$. For $\frac{1}{2} < \lambda < 1$ and $0 < \delta < 1$, the shapes produced in Class II of the GLD_{GPD} resemble the shapes produced in Region 3(a) of the GLD_{RS} and in Region 3 of Class I of GLD_{FMKL} with $\frac{1}{2} < \lambda_3 < 1$ and $\frac{1}{2} < \lambda_4 < 1$.

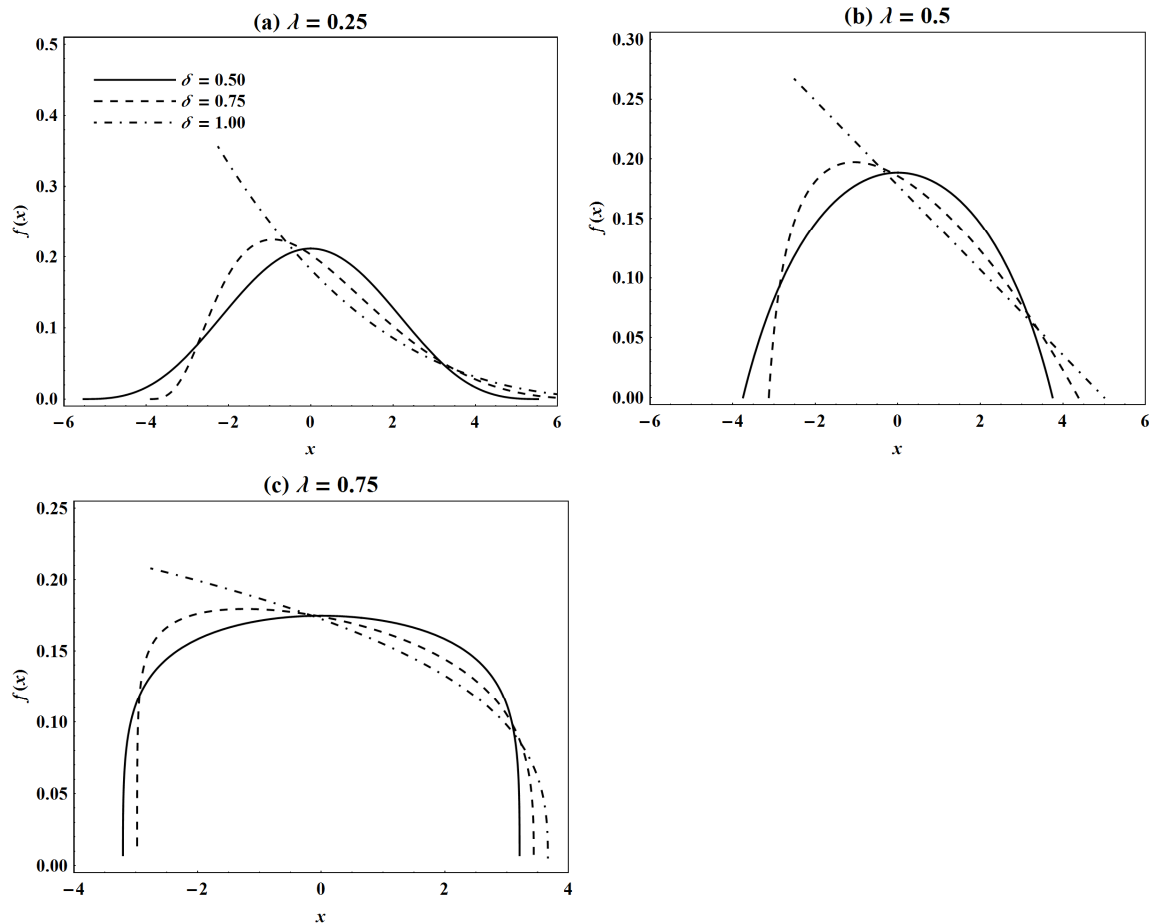


Figure 4.3: Probability density functions of members of the GLD_{GPD} from Class II, all with $L_1 = 0$ and $L_2 = 1$. The line types indicated in graph (a) also apply to graphs (b) and (c).

4.4.3 CLASS III

Examples of members of the GLD_{GPD} from Class III with bounded support are depicted in Figure 4.4. In terms of λ , Class III of the GLD_{GPD} covers the values $1 \leq \lambda \leq 2$. The uniform distribution is obtained for $\lambda = 1$, irrespective of the value of δ . When $1 < \lambda < 2$, the density curve of the GLD_{GPD} is U-shaped for $0 < \delta < 1$ and J-shaped for $\delta = 0$ and $\delta = 1$. If $\lambda = 2$,

the density curve is J-shaped for all $\delta \neq \frac{1}{2}$ and uniform for $\delta = \frac{1}{2}$. The U-shaped density curves from Class III of the GLD_{GPD} are similar to the U-shaped density curves from Region 3(c) of the GLD_{RS} and from Class III of the GLD_{FMKL} .

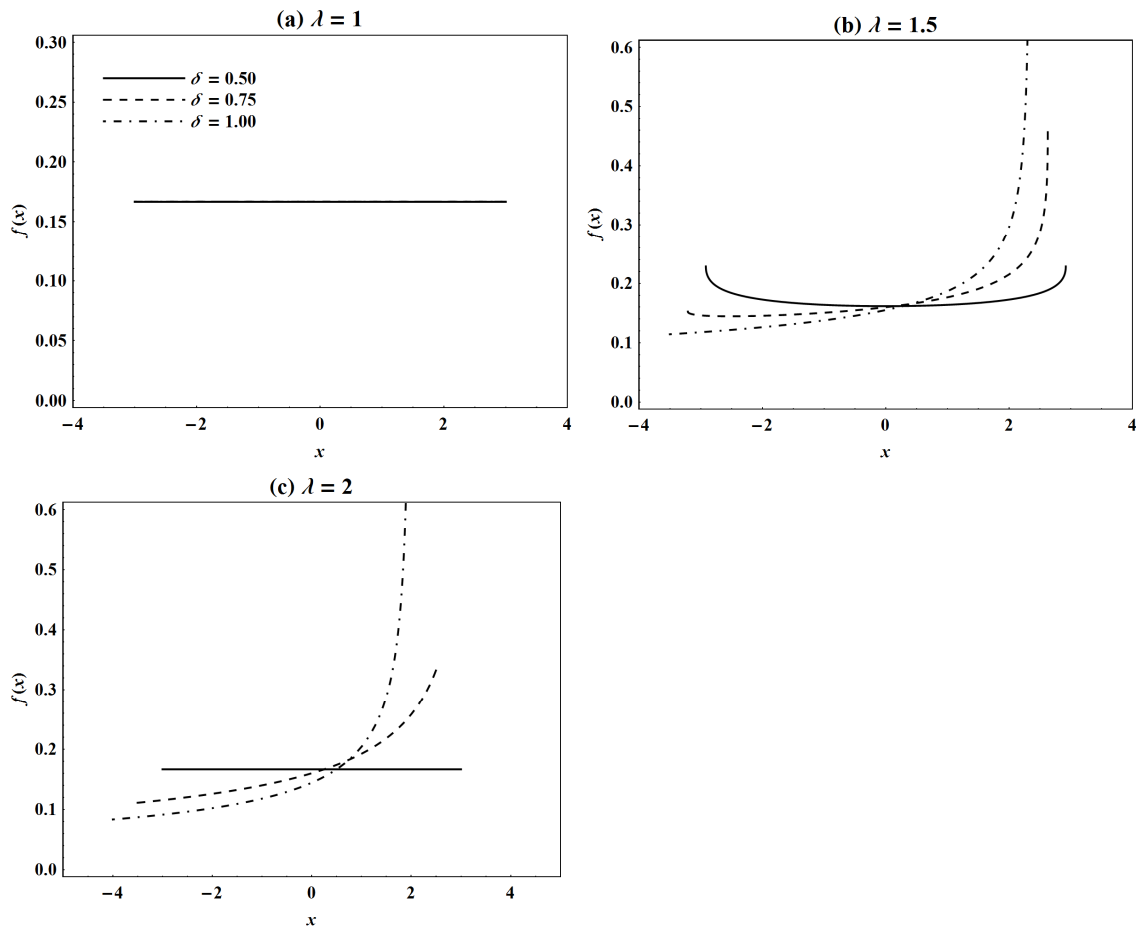


Figure 4.4: Probability density functions of members of the GLD_{GPD} from Class III, all with $L_1 = 0$ and $L_2 = 1$. The line types indicated in graph (a) also apply to graphs (b) and (c). For $\lambda = 1$ in graph (a), the GLD_{GPD} reduces to the uniform distribution, irrespective of the value of δ , and hence the three density curves for the different values of δ plot on top of each other.

4.4.4 CLASS IV

In Class IV with $\lambda > 2$, the members of the GLD_{GPD} are truncated with bounded support and correspond to the truncated members of the GLD_{RS} from Region 3(h) and of the GLD_{FMKL} from Class V. The density curve of the GLD_{GPD} in Class IV is unimodal for $0 < \delta < 1$ and J-shaped for $\delta = 0$ and $\delta = 1$. Examples are presented in Figure 4.5.

CHAPTER 4. A GLD TYPE WITH SKEWNESS-INVARIANT MEASURES OF KURTOSIS

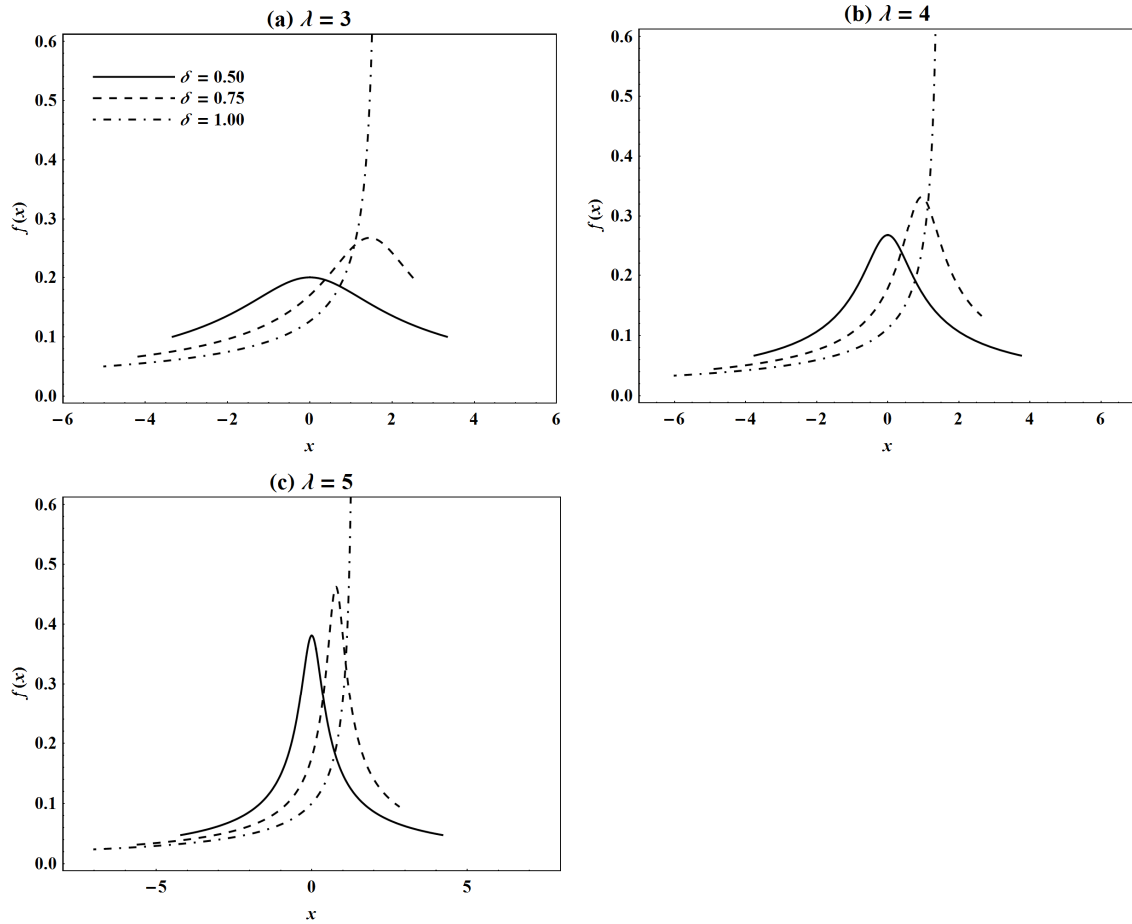


Figure 4.5: Probability density functions of members of the GLD_{GPD} from Class IV, all with $L_1 = 0$ and $L_2 = 1$. The line types indicated in graph (a) also apply to graphs (b) and (c).

4.5 MOMENTS

The r^{th} order moment of the GLD_{GPD} only exists if $\lambda > -\frac{1}{r}$. In particular, if $\lambda > -\frac{1}{4}$, then the mean, variance, skewness moment ratio and kurtosis moment ratio of the GLD_{GPD} are

$$\mu = \alpha - \beta\phi_1, \quad (4.7)$$

$$\sigma^2 = \begin{cases} \frac{\beta^2}{\lambda^2} \left(\phi_2 - \phi_1^2 - 2\omega B(\lambda + 1, \lambda + 1) \right), & \lambda \neq 0, \\ \beta^2 \left(\phi_1^2 + \frac{\pi^2}{3} \omega \right), & \lambda = 0, \end{cases} \quad (4.8)$$

$$\alpha_3 = \begin{cases} \frac{\beta^3}{(\lambda\sigma)^3} \left(\phi_3 + 2\phi_1^3 - 3\phi_1 \left(\phi_2 - \omega \left(2B(\lambda+1, \lambda+1) \right. \right. \right. \\ \left. \left. \left. - (\lambda+1)B(2\lambda+1, \lambda+1) \right) \right) \right), \lambda \neq 0, & (4.9) \\ \frac{\beta^3}{\sigma^3} \left(2\phi_1 \left(\omega \left(4 - 3\zeta(3) \right) - 1 \right) \right), \lambda = 0, \end{cases}$$

and

$$\alpha_4 = \begin{cases} \frac{\beta^4}{(\lambda\sigma)^4} \left(\phi_4 - 3\phi_1^4 + 6\phi_1^2 \left(\phi_2 - 2\omega B(\lambda+1, \lambda+1) \right) \right. \\ \left. - 4\phi_1 \left(\phi_3 - 3\omega\phi_1(\lambda+1)B(2\lambda+1, \lambda+1) \right) \right. \\ \left. - \omega \left(4\phi_2(2\lambda+1)B(3\lambda+1, \lambda+1) \right. \right. \\ \left. \left. - 6\omega B(2\lambda+1, 2\lambda+1) \right) \right), \lambda \neq 0, & (4.10) \\ \frac{\beta^4}{\sigma^4} \left(9 + \omega \left(2 \left(\phi_1^2 \pi^2 - 4 \right) + (9\omega - 4) \left(16 - \frac{\pi^4}{15} \right) \right) \right), \lambda = 0, \end{cases}$$

where $B(a, b)$ and $\zeta(a)$ are the beta and Riemann's zeta functions (see Section 2.14.1 in Chapter 2 for details), $\omega = \delta(1 - \delta)$ and $\phi_k = \frac{(1-\delta)^k + (-1)^k \delta^k}{k\lambda+1}$ for $k = 1, 2, 3, 4$. The formulae for $\lambda = 0$ in (4.7) to (4.10), that is, for the SLD, were derived in Section 2.13.1 in Chapter 2. The formulae for $\lambda \neq 0$ are derived in Section 4.13.1 of this chapter.

Since the r^{th} order moment of the GLD_{GPD} exists if $\lambda > -\frac{1}{r}$, it follows that the mean, the variance and the skewness and kurtosis moment ratios of the GLD_{GPD} exist for all values of λ in Classes II, III and IV. But in Class I these first four moments only exist when $\lambda > -\frac{1}{4}$.

Similar to the formulae for the conventional moments of the GLD_{RS} and GLD_{FMKL} , given in Section 3.6, the formulae in (4.7) to (4.10) for the GLD_{GPD} are complex. Also, both α_3 and α_4 depend on the two shape parameters. It is therefore not ideal to characterize the GLD_{GPD} with conventional moments. As will be seen in Sections 4.6 and 4.7, formulae for L -moments and for quantile-based measures of location, spread and shape of the GLD_{GPD} are substantially simpler.

4.6 L-MOMENTS

The expressions for the L -moments of the GLD_{GPD} are determined using Proposition 2.8.1 in Chapter 2. Suppose X has a standard GPD. If $\lambda > -1$, then, as shown by Hosking (1986), the L -location, L -scale, L -skewness ratio and L -kurtosis ratio of the standard GPD are

$$L_{X;1} = \frac{1}{\lambda+1},$$

$$L_{X;2} = \frac{1}{(\lambda+1)(\lambda+2)},$$

$$\tau_{X;3} = \frac{1-\lambda}{\lambda+3}$$

and

$$\tau_{X;4} = \frac{(\lambda-1)(\lambda-2)}{(\lambda+3)(\lambda+4)},$$

while, in general, the r^{th} order L -moment of the standard GPD is given by

$$L_{X;r} = \frac{\Gamma(1+\lambda)\Gamma(r-1-\lambda)}{\Gamma(1-\lambda)\Gamma(r+1+\lambda)} = (-1)^r \frac{\prod_{k=1}^{r-2} (\lambda-k)}{\prod_{k=1}^r (\lambda+k)}, \quad r > 1,$$

and its r^{th} order L -moment ratio is

$$\tau_{X;r} = \frac{\Gamma(3+\lambda)\Gamma(r-1-\lambda)}{\Gamma(1-\lambda)\Gamma(r+1+\lambda)} = (-1)^r \frac{\prod_{k=1}^{r-2} (\lambda-k)}{\prod_{k=3}^r (\lambda+k)}, \quad r > 2.$$

Using (2.52), (2.53) and (2.54) in Proposition 2.8.1(a), the GLD_{GPD} then has

$$L_1 = \alpha + \frac{\beta(2\delta-1)}{\lambda+1}, \tag{4.11}$$

$$L_r = \beta(2\delta-1)^{r \bmod 2} (-1)^r \frac{\prod_{k=1}^{r-2} (\lambda-k)}{\prod_{k=1}^r (\lambda+k)}, \quad r > 1, \tag{4.12}$$

and

$$\tau_r = (2\delta-1)^{r \bmod 2} (-1)^r \frac{\prod_{k=1}^{r-2} (\lambda-k)}{\prod_{k=3}^r (\lambda+k)}, \quad r > 2. \tag{4.13}$$

The L -location of the GLD_{GPD} in (4.11) is of course the mean, μ , given in (4.7). The L -scale, L -skewness ratio and L -kurtosis ratio of the GLD_{GPD} are

$$L_2 = \frac{\beta}{(\lambda+1)(\lambda+2)}, \tag{4.14}$$

$$\tau_3 = \frac{(2\delta-1)(1-\lambda)}{\lambda+3} \tag{4.15}$$

and

$$\tau_4 = \frac{(\lambda-1)(\lambda-2)}{(\lambda+3)(\lambda+4)}. \quad (4.16)$$

The expressions for the first four L -moments of the GLD_{GPD} in (4.11), (4.14), (4.15) and (4.16) are considerably simpler than the expressions for the first four conventional moments of the GLD_{GPD} in (4.7) to (4.10). Furthermore, there are simple general expressions for the r^{th} order L -moment and for the r^{th} order L -moment ratio of the GLD_{GPD} , given in (4.12) and (4.13). No simple general expression exists for the r^{th} order moment of the GLD_{GPD} . Hence it is more convenient to characterize the GLD_{GPD} with its L -moments than with its conventional moments.

Comparing the expressions of τ_3 and τ_4 in (4.15) and (4.16) with those of the GLD_{RS} in (3.14) and (3.15) and the GLD_{FMKL} in (3.19) and (3.20), a major advantage of the GLD_{GPD} over the GLD_{RS} and GLD_{FMKL} emerges. With the GLD_{RS} and the GLD_{FMKL} , both shape parameters, λ_3 and λ_4 , simultaneously control the L -skewness ratio and the L -kurtosis ratio. With the GLD_{GPD} , only λ influences the L -kurtosis ratio, while the L -skewness ratio depends on both δ and λ . In effect, as is the case with the SLD (that is, the GLD_{GPD} with $\lambda = 0$), the L -kurtosis ratio of the GLD_{GPD} is skewness-invariant. As will become evident in Section 4.9, this significantly simplifies parameter estimation for the GLD_{GPD} using L -moments.

As with the GPD, the r^{th} order L -moment and the r^{th} order L -moment ratio of the GLD_{GPD} exist if $\lambda > -1$. Thus, all the L -moments exist for Classes II, III and IV of the GLD_{GPD} , while in Class I all the L -moments exist when $\lambda > -1$. The (τ_3, τ_4) space covered by the four classes of the GLD_{GPD} is shown in the L -moment ratio diagrams in Figure 4.6. In Figure 4.6(a) the combined coverage of the (τ_3, τ_4) space by Classes I and II of the GLD_{GPD} (which are the two classes with the most useful distributional shapes) is equivalent to the combined coverage of the (τ_3, τ_4) space by Regions 3(a) and 4 of the GLD_{RS} in Figure 3.8(a) and the coverage of the (τ_3, τ_4) space by Class I of the GLD_{FMKL} in Figure 3.8(b).

In Section 4.13.2 it is proved that the minimum value of τ_4 for the GLD_{GPD} is given by

$$\tau_4^{\min} = \frac{12-5\sqrt{6}}{12+5\sqrt{6}} = -0.0102, \quad (4.17)$$

obtained for

$$\tilde{\lambda} = \sqrt{6} - 1 = 1.4495. \quad (4.18)$$

As indicated by Karvanen & Nuutinen (2008), this is also the minimum value of τ_4 for the symmetric GLD_{RS} , that is, for Tukey's lambda distribution. But, because the L -kurtosis ratio of the GLD_{GPD} is skewness-invariant, the minimum value of τ_4 in (4.17) is obtained for the

CHAPTER 4. A GLD TYPE WITH SKEWNESS-INVARIANT MEASURES OF KURTOSIS

symmetric and the asymmetric GLD_{GPD} , in effect, for any value of δ . In Figure 4.7 the L -kurtosis ratio of the GLD_{GPD} is plotted as a function of λ . Karvanen & Nuutinen (2008) gave a similar plot for the symmetric GLD_{RS} . Because of the skewness-invariance of τ_4 for the GLD_{GPD} , the plot in Figure 4.7 is applicable to both the symmetric and asymmetric GLD_{GPD} .

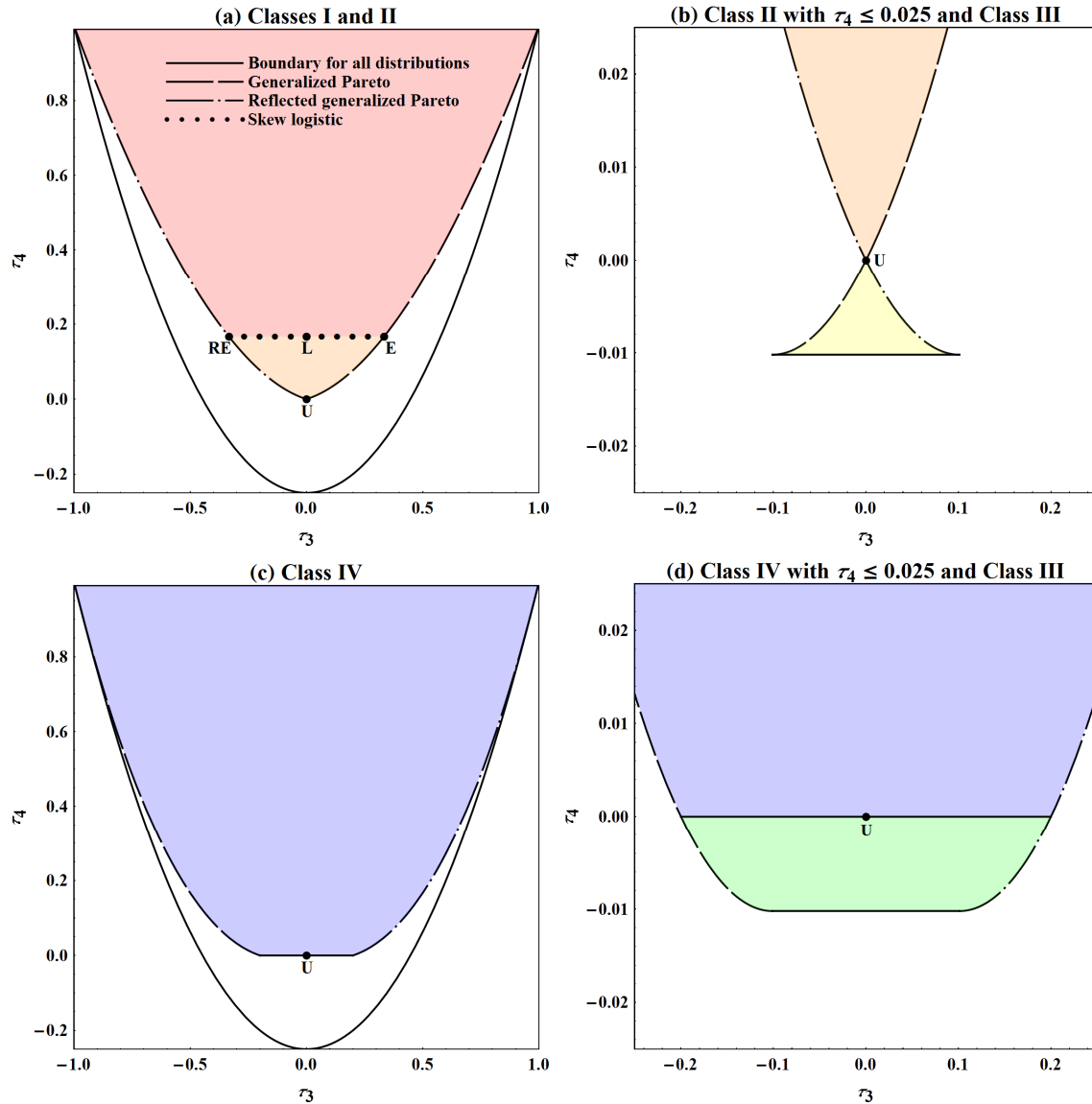


Figure 4.6: L -moment ratio diagrams for Classes I, II, III and IV of the GLD_{GPD} . The line types indicated in diagram (a) also apply to the other diagrams. The uniform, logistic, exponential and reflected exponential distributions are indicated by U, L, E and RE. The red-shaded, orange-shaded and blue-shaded areas are the (τ_3, τ_4) spaces attained by Classes I, II and IV. The small yellow-shaded area in diagram (b) and the small green-shaded area in diagram (d) are the (τ_3, τ_4) spaces attained by Class III.

CHAPTER 4. A GLD TYPE WITH SKEWNESS-INVARIANT MEASURES OF KURTOSIS

We note from Figure 4.7 that there does not exist a one-to-one relation between the value of λ and the value of τ_4 for the GLD_{GPD} . Therefore, as indicated in Table 4.3, the parameter space of the GLD_{GPD} can be divided into two broad regions, labeled Region A and Region B, based upon the values of λ and τ_4 assigned to each of these regions. In Region A with $-1 < \lambda < \tilde{\lambda}$, the value of τ_4 decreases from one to τ_4^{\min} as the value of λ increases. The L -moment ratio diagram for Region A of the GLD_{GPD} is depicted in Figure 4.8(a). In Region B with $\lambda \geq \tilde{\lambda}$, an increase in the value of λ results in an increase in the value of τ_4 from τ_4^{\min} to one. Figure 4.8(b) presents the L -moment ratio diagram for Region B.

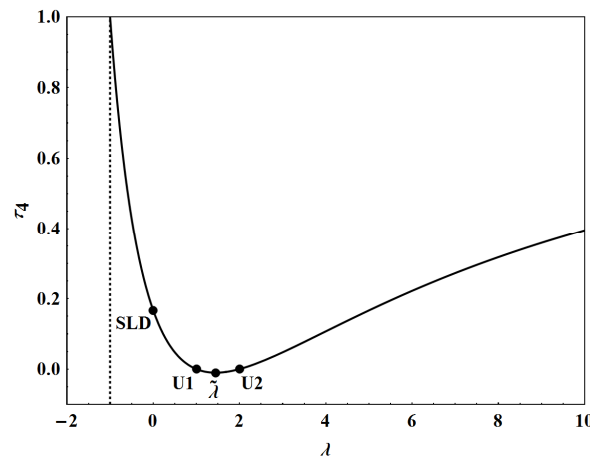


Figure 4.7: Plot of τ_4 for the GLD_{GPD} as a function of λ . The dotted line at $\lambda = -1$ is the lower limit for λ in order for the L -moments to exist. U1 and U2 denote the uniform distribution with $(\lambda, \tau_4) = (1, 0)$ and $(\lambda, \tau_4) = (2, 0)$ respectively, while SLD indicates $(\lambda, \tau_4) = (0, \frac{1}{6})$. The minimum value for τ_4 , $\tau_4^{\min} = -0.0102$, occurs at $\tilde{\lambda} = 1.4495$.

Table 4.3: L -kurtosis ratio values for the GLD_{GPD} in terms of Regions A and B and Classes I, II, III and IV.

Region	Class	Values of λ	Values of τ_4
Region A	Class I	$-1 < \lambda \leq 0$	$\frac{1}{6} \leq \tau_4 < 1$
	Class II	$0 < \lambda < 1$	$0 < \tau_4 < \frac{1}{6}$
	Class III	$1 \leq \lambda < \tilde{\lambda}$	$\tau_4^{\min} < \tau_4 \leq 0$
Region B	Class III	$\tilde{\lambda} \leq \lambda \leq 2$	$\tau_4^{\min} \leq \tau_4 \leq 0$
	Class IV	$\lambda > 2$	$0 < \tau_4 < 1$

CHAPTER 4. A GLD TYPE WITH SKEWNESS-INVARIANT MEASURES OF KURTOSIS

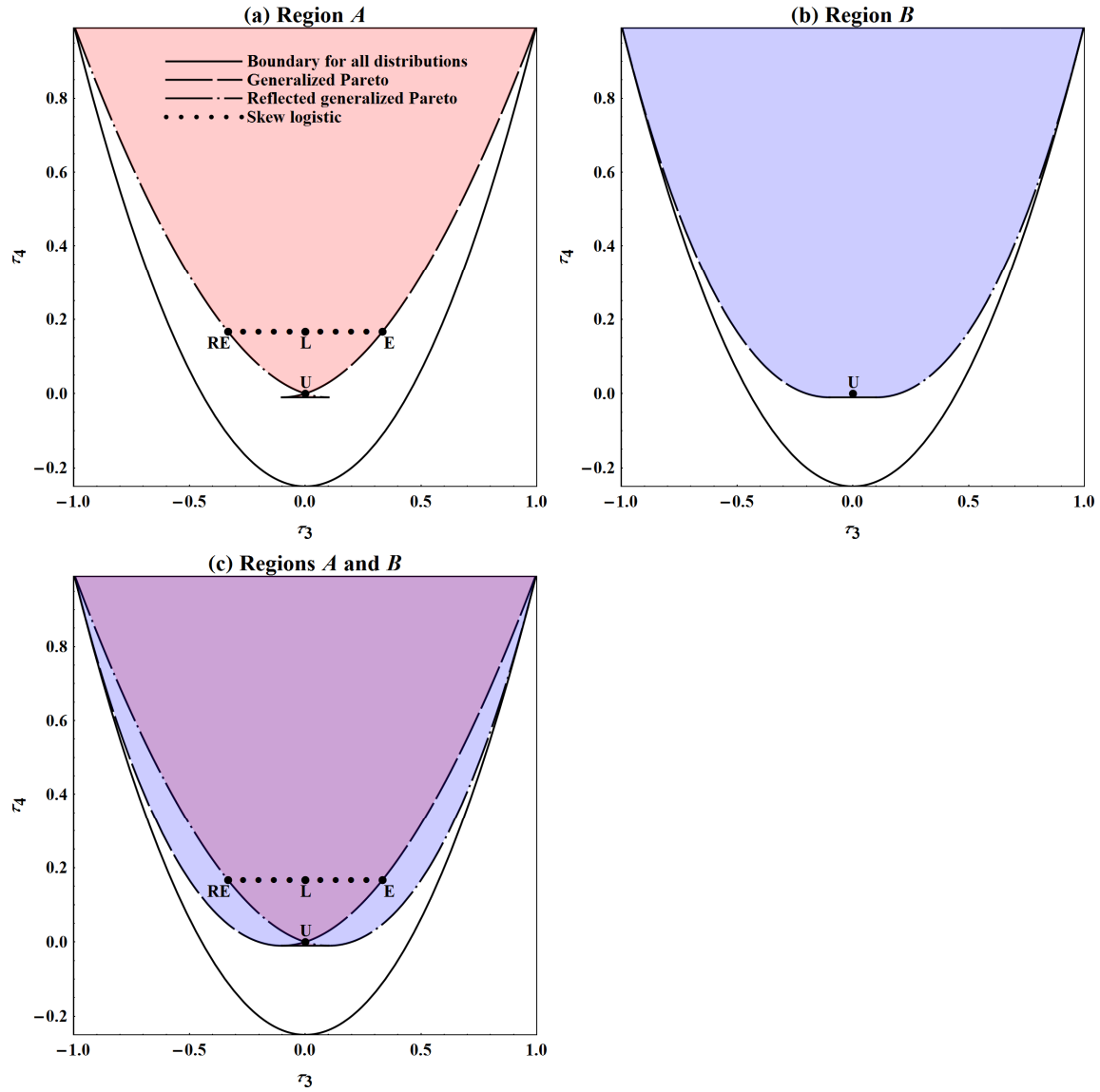


Figure 4.8: L -moment ratio diagrams for Regions A and B of the GLD_{GPD} . The line types indicated in diagram (a) also apply to the other diagrams. The uniform, logistic, exponential and reflected exponential distributions are indicated by U , L , E and RE .

The complete (τ_3, τ_4) space covered by the GLD_{GPD} is shown in Figure 4.8(c) and is equivalent to the coverage of the (τ_3, τ_4) space by the GLD_{RS} (see Figure 3.6) and the GLD_{RS} (see Figure 3.7). In the purple-shaded area in Figure 4.8(c), the same set of values for τ_3 and τ_4 is obtained by two members of the GLD_{GPD} possessing different pairs of values for δ and λ , where the first member of the GLD_{GPD} is from Region A and the second member is from Region B . In effect, as illustrated by Figure 4.9, for a given set of values for τ_3 and τ_4 from the purple-shaded area in Figure 4.8(c), two members of the GLD_{GPD} with different distributional shapes are attainable. Specifically, if $\frac{1}{6} \leq \tau_4 < 1$ and $0 < \delta < 1$, the first member of the GLD_{GPD} is from Class I in Region A and hence is unimodal with infinite support, while

the second member of the GLD_{GPD} , from Class IV in Region B , is also unimodal, but truncated with bounded support – see Figure 4.9(a). When $0 < \tau_4 < \frac{1}{6}$ and $0 < \delta < 1$, both members of the GLD_{GPD} are unimodal with bounded support, where the first member of the GLD_{GPD} is from Class II in Region A , while the second member is again from Class IV in Region B and thus truncated – see Figure 4.9(b). If $\tau_4^{\min} < \tau_4 \leq 0$ and $0 < \delta < 1$, both members of the GLD_{GPD} are from Class III (the first from Region A and the second from Region B) and consequently the density curves of both members are U-shaped with bounded support – see Figure 4.9(c).

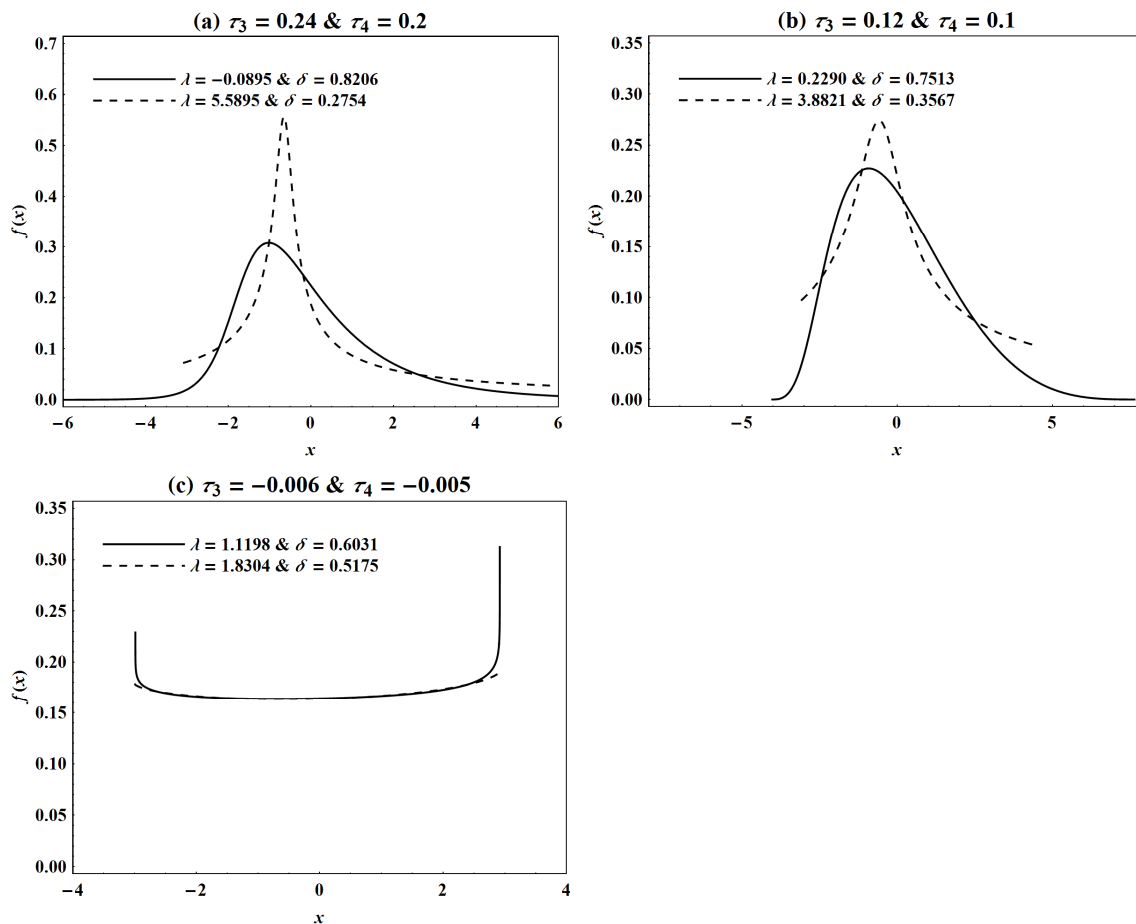


Figure 4.9: Probability density functions of members of the GLD_{GPD} from Regions A and B possessing the same set of values for τ_3 and τ_4 . In graphs (a) and (b) the solid lines indicate members of the GLD_{GPD} from Classes I and II in Region A respectively, while the dashed lines indicate members of the GLD_{GPD} from Class IV in Region B . In graph (c) the solid and dashed lines depict members of the GLD_{GPD} from Class III in Region A and in Region B respectively. Note that $L_1 = 0$ and $L_2 = 1$ for all the members of the GLD_{GPD} .

4.7 QUANTILE-BASED MEASURES OF LOCATION, SPREAD AND SHAPE

Unlike the moments and L -moments of the GLD_{GPD} , the existence of the quantile-based measures of location, spread and shape is not restricted by the value of λ . The formulae for these quantile-based measures are obtained by substituting the quantile function of the GLD_{GPD} , given in (4.4), into the expressions for the median in (2.34), the spread function in (2.35), the γ -functional and the η -functional in (2.37) and (2.38), and the ratio-of-spread functions and the κ -functional in (2.43) and (2.44), and simplifying. The formulae for the GLD_{GPD} are then

$$\begin{aligned}
 me &= \begin{cases} \alpha - \frac{\beta(2\delta-1)}{\lambda} \left(\left(\frac{1}{2} \right)^\lambda - 1 \right), & \lambda \neq 0, \\ \alpha + \beta(2\delta-1) \log[2], & \lambda = 0, \end{cases} \\
 S(u) &= \begin{cases} \frac{\beta}{\lambda} \left(u^\lambda - (1-u)^\lambda \right), & \lambda \neq 0, \\ \beta \log \left[\frac{u}{1-u} \right], & \lambda = 0, \end{cases} \\
 \gamma(u) &= \begin{cases} - \frac{(2\delta-1) \left(u^\lambda + (1-u)^\lambda - 2 \left(\frac{1}{2} \right)^\lambda \right)}{u^\lambda - (1-u)^\lambda}, & \lambda \neq 0, \\ - \frac{(2\delta-1) \log[4u(1-u)]}{\log \left[\frac{u}{1-u} \right]}, & \lambda = 0, \end{cases} \\
 \eta(u, v) &= \begin{cases} - \frac{(2\delta-1) \left(u^\lambda + (1-u)^\lambda - v^\lambda - (1-v)^\lambda \right)}{v^\lambda - (1-v)^\lambda}, & \lambda \neq 0, \\ - \frac{(2\delta-1) \log \left[\frac{u(1-u)}{v(1-v)} \right]}{\log \left[\frac{v}{1-v} \right]}, & \lambda = 0, \end{cases} \\
 R(u, v) &= \begin{cases} \frac{u^\lambda - (1-u)^\lambda}{v^\lambda - (1-v)^\lambda}, & \lambda \neq 0, \\ \frac{\log \left[\frac{u}{1-u} \right]}{\log \left[\frac{v}{1-v} \right]}, & \lambda = 0, \end{cases} \tag{4.19}
 \end{aligned}$$

and

$$\kappa(u, v) = \begin{cases} 1 - \frac{v^\lambda - (1-v)^\lambda}{u^\lambda - (1-u)^\lambda}, & \lambda \neq 0, \\ \frac{\log\left[\frac{u(1-v)}{v(1-u)}\right]}{\log\left[\frac{u}{1-u}\right]}, & \lambda = 0, \end{cases} \quad (4.20)$$

where $\frac{1}{2} < v < u < 1$. Note that, as with the moments in (4.7) to (4.10), the formulae for $\lambda = 0$ are for the SLD, given before in Section 2.6 in Chapter 2. All the shape functionals of the GLD_{GPD} are location- and scale-invariant and, more importantly, the two kurtosis functionals are skewness-invariant. The kurtosis of the GLD_{GPD} is described in more detail in Section 4.8.2.

4.8 DISTRIBUTIONAL SHAPE

As indicated in Section 4.4, the important distributional shapes attained by the GLD_{RS} and GLD_{FMKL} in their Regions 3 and 4, are also attained by the GLD_{GPD} . The main difference between the GLD_{GPD} and the GLD_{RS} and GLD_{FMKL} is in terms of the way in which each type's shape characteristics, that is, skewness, kurtosis and tail behavior, are related to and explained by their shape parameters. With the GLD_{RS} and the GLD_{FMKL} , their two shape parameters, λ_3 and λ_4 , jointly account for the skewness and the kurtosis (see Section 3.10.2), while for certain combinations of values of λ_3 and λ_4 in Regions 3 and 4, each shape parameter controls one of the two tails of the density curve (see Section 3.10.1). As will be explained in Sections 4.8.1 and 4.8.2 below, for a given value of the shape parameter λ , the skewness of the GLD_{GPD} is controlled by the second shape parameter, δ , while, when measured by the L -kurtosis ratio or the kurtosis functionals, the kurtosis of the GLD_{GPD} only depends on λ . The tail behavior of the density curve of the GLD_{GPD} , discussed in Section 4.8.3, is explained by both δ and λ .

4.8.1 SKEWNESS

As pointed out before in Section 4.2, the GLD_{GPD} is symmetric for $\delta = \frac{1}{2}$ and asymmetric for $\delta \neq \frac{1}{2}$. In particular, for $\lambda < 1$, in effect, for Classes I and II, the GLD_{GPD} is negatively skewed when $\delta < \frac{1}{2}$ and positively skewed when $\delta > \frac{1}{2}$. Conversely, in Classes III and IV with $\lambda > 1$ the GLD_{GPD} is positively skewed when $\delta < \frac{1}{2}$ and negatively skewed when

$\delta > \frac{1}{2}$. Recall that the GLD_{GPD} reduces to the uniform distribution for $\lambda = 1$, irrespective of the value of δ . The GLD_{GPD} at $\lambda = 1$ is therefore always symmetric.

4.8.2 KURTOSIS

It was seen in Sections 4.6 and 4.7 that the L -kurtosis ratio and the kurtosis functionals of the GLD_{GPD} are all invariant to the value of the weight parameter, δ , and are thus skewness-invariant kurtosis measures. The skewness-invariance of these kurtosis measures follows directly from Proposition 2.8.1, since the quantile function of the GLD_{GPD} , presented in (4.4) in Definition 4.2.1, is of the form (2.51).

Figure 4.7 in Section 4.6 illustrated the relation between the values of λ and τ_4 . Similar plots can be drawn for the two kurtosis functionals of the GLD_{GPD} for selected values of u and v . This is done in Figure 4.10 for the ratio-of-spread functions and the κ -functional for $(u, v) = (0.9, 0.6)$ and for $(u, v) = (0.9, 0.75)$. As with the L -kurtosis ratio of the GLD_{GPD} , there do not exist one-to-one relations between the value of λ and the values of $R(u, v)$ or $\kappa(u, v)$.

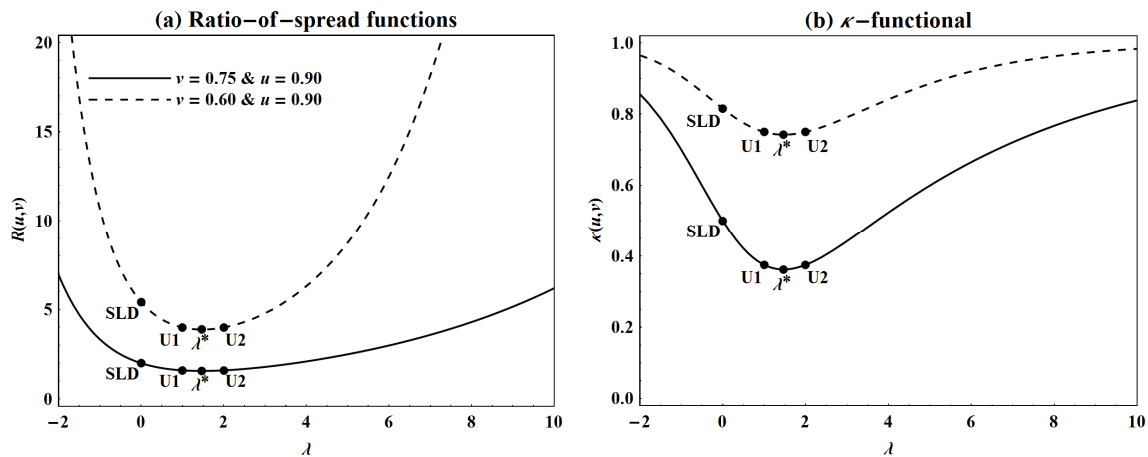


Figure 4.10: Plots of the kurtosis functionals for the GLD_{GPD} as functions of λ . The line types indicated in graph (a) also apply to graph (b). U1 and U2 denote the uniform distribution with $\lambda = 1$ and $\lambda = 2$ respectively, while SLD indicates $\lambda = 0$. The minimum kurtosis for the kurtosis functionals occur at $\lambda^* = 1.4696$ for $u = 0.9$ and $v = 0.75$, and at $\lambda^* = 1.4766$ for $u = 0.9$ and $v = 0.6$.

However, in Classes I and II, where $\lambda < 1$, a strictly inverse relation exists between the value of λ and the kurtosis of the GLD_{GPD} , with the kurtosis increasing in these two classes as the value of λ decreases. This is illustrated by Figure 4.11(a) in which the spread-spread plot for the GLD_{GPD} is concave, indicating the greater kurtosis for $\lambda = -0.5$ compared to

$\lambda = 0.5$. In Class IV with $\lambda > 2$, the kurtosis of the GLD_{GPD} becomes larger as the value of λ increases. For instance, in Figure 4.11(b) the spread-spread plot for the GLD_{GPD} is convex with greater kurtosis for $\lambda = 5$ than for $\lambda = 3$. Thus in Classes I and II and also in Class IV, the GLD_{GPD} is completely ordered by \leq_S , the kurtosis ordering presented in Section 2.6.

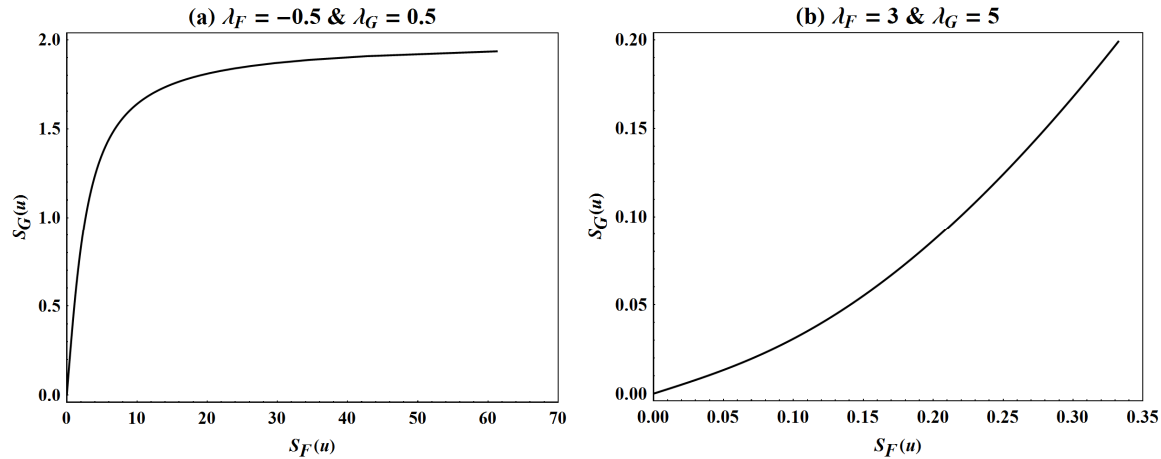


Figure 4.11: Spread-spread plots for members of the GLD_{GPD} . In plot (a) the GLD_{GPD} with $\lambda_F = -0.5$ from Class I, which is leptokurtic, has greater kurtosis than the GLD_{GPD} with $\lambda_G = 0.5$ from Class II, which is platykurtic. In plot (b) the GLD_{GPD} with $\lambda_G = 5$ has greater kurtosis than the GLD_{GPD} with $\lambda_F = 3$, where both these members of the GLD_{GPD} are from Class IV. For all members of the GLD_{GPD} the value of β is set to one in their respective spread functions.

In contrast to the other three classes of the GLD_{GPD} , the relation between the value of λ and the kurtosis of the GLD_{GPD} is not so simple in Class III where $1 \leq \lambda \leq 2$. As shown in Figures 4.7 and 4.10, the minimum kurtosis of the GLD_{GPD} occurs in this class. But the value of λ at which the minimum kurtosis is observed is not the same for the different kurtosis measures. As proven in Section 4.13.2, the minimum value for the L -kurtosis ratio is obtained for $\tilde{\lambda} = 1.4495$. With the kurtosis functionals, the minimum kurtosis attainable depends on the values of u and v . Let λ^* denote the value of λ at which the kurtosis functionals reach their minima. Then, for example, as shown in Figure 4.10, if $u = 0.9$ and $v = 0.75$, the minimum kurtosis for the kurtosis functionals occurs at $\lambda^* = 1.4696$, whereas for $u = 0.9$ and $v = 0.6$ the minimum kurtosis occurs at $\lambda^* = 1.4766$. Figure 4.12 shows the various values of λ^* for $\frac{1}{2} < v < u < 1$. Predominantly the values of λ^* are in the interval $1.4 < \lambda^* < 1.5$. In particular, when both $u \downarrow 0.5$ and $v \downarrow 0.5$, then $\lambda^* \uparrow 1.5$, while $\lambda^* \downarrow 1.1$ if both $u \uparrow 1$ and $v \uparrow 1$. If $u \uparrow 1$ and $v \downarrow 0.5$ so that $(u - v) \uparrow 0.5$, then $\lambda^* \downarrow 1.4427$.

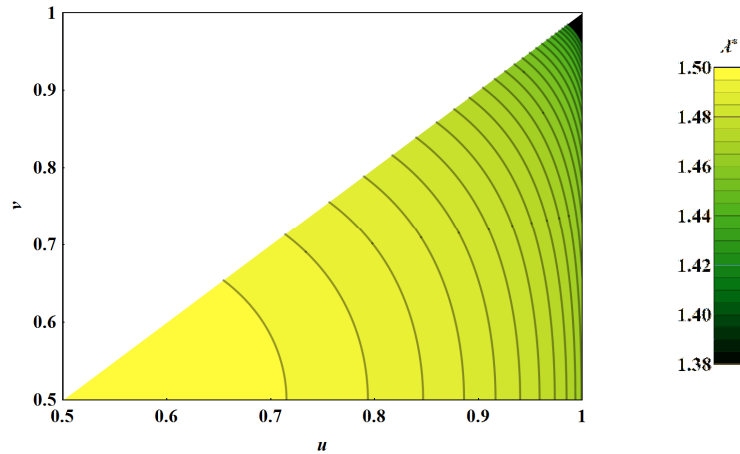


Figure 4.12: The values of λ^* in Class III of the GLD_{GPD} at which the minimum kurtosis of the kurtosis functionals is obtained for $\frac{1}{2} < v < u < 1$.

4.8.3 TAIL BEHAVIOR

As was explained in Section 2.11 of Chapter 2, the tail behavior of the density curve of a quantile-based distribution is studied through its density quantile function, $f_p(p)$, as well as the function $\xi(p)$, given in (2.71), which represents the derivative of the density curve. The density quantile function of the GLD_{GPD} is given in (4.6), while

$$\xi(p) = -\frac{(\lambda-1)\left((1-\delta)p^{\lambda-2} - \delta(1-p)^{\lambda-2}\right)}{\beta^2\left((1-\delta)p^{\lambda-1} + \delta(1-p)^{\lambda-1}\right)}.$$

Table 4.4 presents the tail behavior of the GLD_{GPD} . Note that the values given for $\delta = 1$ and $\delta = 0$ are respectively for the GPD and the reflected GPD, while the values for $\lambda = 0$ are for the SLD, considered before in Example 2.11.1 in Chapter 2.

The interpretation of $f(p)$ and the values obtained when computing $\lim_{p \rightarrow 0} f_p(p)$ and $\lim_{p \rightarrow 1} f_p(p)$ are straightforward for the GLD_{GPD} , with three broad scenarios occurring based on the value of λ . Firstly, if $\lambda < 1$, thus for Classes I and II of the GLD_{GPD} , the left tail of the density curve approaches zero for $\delta < 1$ and $\frac{1}{\beta}$ for $\delta = 1$, whereas the right tail of the density curve approaches $\frac{1}{\beta}$ for $\delta = 0$ and zero for $\delta > 0$. Consequently unimodal density curves are obtained for the GLD_{GPD} when $\lambda < 1$ and $0 < \delta < 1$, while monotone increasing and monotone decreasing density curves are obtained for $\delta = 0$ and for $\delta = 1$ respectively (see again Sections 4.4.1 and 4.4.2). Secondly, when $\lambda = 1$, the density curve of the GLD_{GPD} is uniform at $\frac{1}{\beta}$ for all values of δ and hence both tails are equal to $\frac{1}{\beta}$. Finally, in Classes III

CHAPTER 4. A GLD TYPE WITH SKEWNESS-INVARIANT MEASURES OF KURTOSIS

and IV of the GLD_{GPD} with $\lambda > 1$, the left tail of the density curve tends to infinity for $\delta = 0$ and approaches $\frac{1}{\beta\delta}$ for $\delta > 0$, while the right tail tends to infinity for $\delta = 1$ and approaches $\frac{1}{\beta(1-\delta)}$ for $\delta < 1$. As a result, when $0 < \delta < 1$, the density curves of the GLD_{GPD} are U-shaped in Class III and truncated in Class IV, and when $\delta = 0$ or $\delta = 1$, the density curves of the GLD_{GPD} in Classes III and IV are J-shaped (see again Sections 4.4.3 and 4.4.4).

Table 4.4: The values approached by the density curve and the slope of the density curve of the GLD_{GPD} at the end-points of the tails.

Class	Shape parameter values	Density curve		Slope of density curve	
		Left tail	Right tail	Left tail	Right tail
Class I	$\delta = 0, \lambda \leq 0$	0	$\frac{1}{\beta}$	0	$-\frac{\lambda-1}{\beta^2}$
	$0 < \delta < 1, \lambda \leq 0$	0	0	0	0
	$\delta = 1, \lambda \leq 0$	$\frac{1}{\beta}$	0	$\frac{\lambda-1}{\beta^2}$	0
Class II	$\delta = 0, 0 < \lambda < 0.5$	0	$\frac{1}{\beta}$	0	$-\frac{\lambda-1}{\beta^2}$
	$0 < \delta < 1, 0 < \lambda < 0.5$	0	0	0	0
	$\delta = 1, 0 < \lambda < 0.5$	$\frac{1}{\beta}$	0	$\frac{\lambda-1}{\beta^2}$	0
	$\delta = 0, \lambda = 0.5$	0	$\frac{1}{\beta}$	$\frac{1}{2\beta^2}$	$\frac{1}{2\beta^2}$
	$0 < \delta < 1, \lambda = 0.5$	0	0	$\frac{1}{2\beta^2(1-\delta)^2}$	$\frac{1}{2\beta^2\delta^2}$
	$\delta = 1, \lambda = 0.5$	$\frac{1}{\beta}$	0	$-\frac{1}{2\beta^2}$	$-\frac{1}{2\beta^2}$
	$\delta = 0, 0.5 < \lambda < 1$	0	$\frac{1}{\beta}$	∞	$-\frac{\lambda-1}{\beta^2}$
	$0 < \delta < 1, 0.5 < \lambda < 1$	0	0	∞	$-\infty$
	$\delta = 1, 0.5 < \lambda < 1$	$\frac{1}{\beta}$	0	$\frac{\lambda-1}{\beta^2}$	$-\infty$
Class III	$0 \leq \delta \leq 1, \lambda = 1$	$\frac{1}{\beta}$	$\frac{1}{\beta}$	0	0
	$\delta = 0, 1 < \lambda \leq 2$	∞	$\frac{1}{\beta}$	$-\infty$	$-\frac{\lambda-1}{\beta^2}$
	$0 < \delta < 1, 1 < \lambda < 2$	$\frac{1}{\beta\delta}$	$\frac{1}{\beta(1-\delta)}$	$-\infty$	∞
	$0 < \delta < 1, \lambda = 2$	$\frac{1}{\beta\delta}$	$\frac{1}{\beta(1-\delta)}$	$\frac{2\delta-1}{\beta^2\delta^3}$	$\frac{2\delta-1}{\beta^2(1-\delta)^3}$
	$\delta = 1, 1 < \lambda \leq 2$	$\frac{1}{\beta}$	∞	$\frac{\lambda-1}{\beta^2}$	∞
Class IV	$\delta = 0, \lambda > 2$	∞	$\frac{1}{\beta}$	$-\infty$	$-\frac{\lambda-1}{\beta^2}$
	$0 < \delta < 1, \lambda > 2$	$\frac{1}{\beta\delta}$	$\frac{1}{\beta(1-\delta)}$	$\frac{\lambda-1}{\beta^2\delta^2}$	$-\frac{\lambda-1}{\beta^2(1-\delta)^2}$
	$\delta = 1, \lambda > 2$	$\frac{1}{\beta}$	∞	$\frac{\lambda-1}{\beta^2}$	∞

Compared to $f_p(p)$, the interpretation of the function $\xi(p)$ for the GLD_{GPD} is more complex, since the values obtained when computing $\lim_{p \rightarrow 0} \xi(p)$ and $\lim_{p \rightarrow 1} \xi(p)$ for the GLD_{GPD}

are much more diverse than the values obtained when computing $\lim_{p \rightarrow 0} f(p)$ and $\lim_{p \rightarrow 1} f(p)$.

General results are only obtained for the special cases $\delta = 1$ and $\delta = 0$, in effect for the GPD and the reflected GPD. When $\delta = 1$, the slope of the left tail of the density curve always approaches $\frac{\lambda-1}{\beta^2}$. If $\delta = 0$, the slope of the density curve's right tail always approaches $-\frac{\lambda-1}{\beta^2}$.

Finally, it is noted from Table 4.4 that, for $0 < \delta < 1$, the tail behavior of the GLD_{GPD} is consistent across the left and right tails. This is as a result of the way in which the GLD_{GPD} is constructed.

4.9 METHOD OF *L*-MOMENTS ESTIMATION

In order to fit the GLD_{GPD} to an observed data set, the four parameters of the GLD_{GPD} , α , β , δ and λ , must be estimated. This can be done using an estimation method where four measures, namely a measure of location, a measure of spread and two measures of shape, are utilized. Now, because the skewness and kurtosis moment ratios of the GLD_{GPD} , given in (4.9) and (4.10), are dependent on both its shape parameters, δ and λ , closed-form expressions are not available for method of moments estimators for δ and λ , making this estimation method computationally difficult and impractical.

In contrast to the kurtosis moment ratio of the GLD_{GPD} in (4.10), the *L*-kurtosis ratio of the GLD_{GPD} in (4.16) as well as its two kurtosis functionals in (4.19) and (4.20) only depend on one of the shape parameters, λ . This suggest that, with estimation methods using either *L*-moments or quantile-based measures, λ can first be estimated using an expression written as a function of the corresponding kurtosis measure (in effect, the *L*-kurtosis ratio or one of the two kurtosis functionals), whereafter δ , β and α can be estimated sequentially. Unfortunately it is not mathematically possible to obtain a closed-form expression for λ as a function of either the ratio-of-spread functions or the κ -functional. But, as will be seen in the estimation algorithm presented below, λ can be expressed as a function of the *L*-kurtosis ratio and consequently closed-form expressions are available for method of *L*-moments estimators. Furthermore, although extremely complex, closed-form expressions are also available for these estimators' asymptotic standard errors. Method of *L*-moments estimation is therefore the preferred estimation method for the GLD_{GPD} . The estimation algorithm for computing the method of *L*-moments estimates as well as their asymptotic standard errors is described below:

Step 1

Use (2.30) to (2.33) to calculate the first four sample L -moments, l_1 , l_2 , l_3 and l_4 , and then (2.29) to calculate the sample L -skewness and L -kurtosis ratios, t_3 and t_4 . Verify whether the values of t_3 and t_4 lie within the (τ_3, τ_4) space of the GLD_{GPD} in Figure 4.8(c). If so, proceed with Step 2. If not, the GLD_{GPD} cannot be fitted to the data.

Step 2

Since the L -kurtosis ratio only depends on λ , this shape parameter is estimated first. Inverting (4.16) leads to two possible estimators for λ ,

$$\hat{\lambda}_A = \frac{3+7t_4 - \sqrt{t_4^2 + 98t_4 + 1}}{2(1-t_4)}$$

and

$$\hat{\lambda}_B = \frac{3+7t_4 + \sqrt{t_4^2 + 98t_4 + 1}}{2(1-t_4)},$$

where $-1 < \hat{\lambda}_A < \tilde{\lambda}$ is from Region A and $\hat{\lambda}_B \geq \tilde{\lambda}$ is from Region B . Next the other shape parameter, δ , is estimated with

$$\hat{\delta}_A = \begin{cases} \frac{1}{2} \left(1 - \frac{t_3(\hat{\lambda}_A + 3)}{\hat{\lambda}_A - 1} \right), & \hat{\lambda}_A \neq 1, \\ \frac{1}{2}, & \hat{\lambda}_A = 1, \end{cases} \quad (4.21)$$

and

$$\hat{\delta}_B = \frac{1}{2} \left(1 - \frac{t_3(\hat{\lambda}_B + 3)}{\hat{\lambda}_B - 1} \right),$$

with these expressions derived from (4.15). Finally the scale and location parameters, β and α , are estimated sequentially using

$$\hat{\beta}_h = \ell_2(\hat{\lambda}_h + 1)(\hat{\lambda}_h + 2), \quad h = A, B \quad (4.22)$$

and

$$\hat{\alpha}_h = \ell_1 - \frac{\hat{\beta}_h(2\hat{\delta}_h - 1)}{\hat{\lambda}_h + 1}, \quad h = A, B, \quad (4.23)$$

derived from (4.14) and (4.11) respectively.

If $\hat{\lambda}_A = 0$ so that the GLD_{GPD} reduces to the SLD, the estimators for the other three parameters in (4.21), (4.22) and (4.23) simplifies to the estimators given in (2.64), (2.65) and

(2.66). Also, when $\hat{\lambda}_A = 1$, the uniform distribution is obtained and, because the uniform distribution is symmetric, we can set $\hat{\delta}_A = \frac{1}{2}$.

Let $T = \sqrt{t_4^2 + 98t_4 + 1}$. Then, in terms of l_1 , l_2 , l_3 and l_4 , the method of L -moments estimators from Region A are

$$\hat{\alpha}_A = l_1 + \frac{\ell_3 \left(2\ell_4^2 - 3\ell_2^2(1+T) + \ell_2\ell_4(51-2T) \right)}{10(\ell_2 - \ell_4)\ell_4}, \quad (4.24)$$

$$\hat{\beta}_A = \frac{\ell_2 \left(4\ell_4^2 + \ell_2^2(9-3T) + \ell_2\ell_4(37-2T) \right)}{(\ell_2 - \ell_4)^2}, \quad (4.25)$$

$$\hat{\delta}_A = \frac{1}{2} + \frac{1}{20} \left(\frac{\ell_3}{\ell_4} (1+T) - \frac{\ell_3}{\ell_2} \right) \quad (4.26)$$

and

$$\hat{\lambda}_A = \frac{3 + 7\frac{\ell_4}{\ell_2} - T}{2 \left(1 - \frac{\ell_4}{\ell_2} \right)}, \quad (4.27)$$

while the method of L -moments estimators from Region B are

$$\hat{\alpha}_B = l_1 + \frac{\ell_3 \left(2\ell_4^2 - 3\ell_2^2(1-T) + \ell_2\ell_4(51+2T) \right)}{10(\ell_2 - \ell_4)\ell_4}, \quad (4.28)$$

$$\hat{\beta}_B = \frac{\ell_2 \left(4\ell_4^2 + \ell_2^2(9+3T) + \ell_2\ell_4(37+2T) \right)}{(\ell_2 - \ell_4)^2}, \quad (4.29)$$

$$\hat{\delta}_B = \frac{1}{2} + \frac{1}{20} \left(\frac{\ell_3}{\ell_4} (1-T) - \frac{\ell_3}{\ell_2} \right) \quad (4.30)$$

and

$$\hat{\lambda}_B = \frac{3 + 7\frac{\ell_4}{\ell_2} + T}{2 \left(1 - \frac{\ell_4}{\ell_2} \right)}. \quad (4.31)$$

Step 3

Expressions for the asymptotic standard errors of the method of L -moments estimators only exist if the variance of the GLD_{GPD} is finite, thus only if $\lambda > -\frac{1}{2}$. So in Region A the standard errors' expressions exist for $-\frac{1}{2} < \hat{\lambda}_A < \tilde{\lambda}$, while in Region B they exist for all $\hat{\lambda}_B > \tilde{\lambda}$. If $\hat{\lambda}_A \leq -\frac{1}{2}$ in Region A, the standard errors can be determined with the parametric bootstrap.

Because the expressions for the standard errors are the same for the estimators of both regions, the subscripts of the estimators are omitted in these expressions given below. Nonetheless, these expressions, derived in Section 4.13.3, are unfortunately extremely complex. The standard errors are

$$\begin{aligned} \text{s.e.}[\hat{\alpha}] &= \beta \sqrt{\frac{1}{n(\lambda-1)^2(\lambda+2)\vartheta_1}} \\ &\quad \times \sqrt{\vartheta_2 - \frac{\omega}{\lambda(\lambda+1)} \left(\left(\frac{1}{4}\vartheta_3 - \omega\vartheta_4\vartheta_5 \right) \mathbf{B}(\lambda, \lambda) + \vartheta_6 \left(\vartheta_7 - 4\omega\vartheta_4\vartheta_8 \right) \right)}, \end{aligned} \quad (4.32)$$

$$\text{s.e.}[\hat{\beta}] = \beta \sqrt{\frac{1}{n(\lambda+2)\vartheta_1} \left(\vartheta_9 - \frac{\omega}{\lambda(\lambda+1)} \left(\frac{1}{4}\vartheta_{10} \mathbf{B}(\lambda, \lambda) + \vartheta_6\vartheta_{11} \right) \right)}, \quad (4.33)$$

$$\begin{aligned} \text{s.e.}[\hat{\delta}] &= \sqrt{\frac{(\lambda+1)(\lambda+2)(\lambda+3)}{n(\lambda-1)^2\vartheta_1}} \\ &\quad \times \sqrt{\vartheta_{12} - \frac{\omega}{\lambda} \left(\frac{1}{4} \left(\vartheta_{13} - 12\omega\vartheta_{14} \right) \mathbf{B}(\lambda, \lambda) - \frac{\vartheta_6}{\lambda+3} \left(3\vartheta_{15} + \omega\vartheta_{16} \right) \right)} \end{aligned} \quad (4.34)$$

and

$$\text{s.e.}[\hat{\lambda}] = \sqrt{\frac{(\lambda+1)(\lambda+2)(\lambda+3)^2(\lambda+4)^2}{n\vartheta_1} \left(\vartheta_{17} - \frac{\omega}{\lambda} \left(\frac{1}{4}\vartheta_5 \mathbf{B}(\lambda, \lambda) + \vartheta_6\vartheta_8 \right) \right)}, \quad (4.35)$$

where $\mathbf{B}(a, b)$ is the beta function (see Section 2.14.1 in Chapter 2 for details), $\omega = \delta(1 - \delta)$,

$$\vartheta_1 = (2\lambda + 1)(2\lambda + 3)(2\lambda + 5)(2\lambda + 7)(\lambda^2 + 2\lambda - 5)^2,$$

$$\begin{aligned} \vartheta_2 &= 4\lambda^{10} + 32\lambda^9 + 51\lambda^8 - 104\lambda^7 - 43\lambda^6 + 735\lambda^5 + 995\lambda^4 + 6418\lambda^3 + 22611\lambda^2 \\ &\quad + 27911\lambda + 13966, \end{aligned}$$

$$\begin{aligned} \vartheta_3 &= (\lambda + 3)(\lambda^{13} + 17\lambda^{12} + 99\lambda^{11} + 255\lambda^{10} + 667\lambda^9 + 3595\lambda^8 + 8745\lambda^7 - 17879\lambda^6 \\ &\quad - 149808\lambda^5 - 312756\lambda^4 - 103684\lambda^3 + 432056\lambda^2 + 215458\lambda \\ &\quad - 367080), \end{aligned}$$

$$\vartheta_4 = (\lambda + 4)^2(\lambda^2 - 2\lambda - 11)^2,$$

$$\vartheta_5 = \lambda^8 + 8\lambda^7 + 12\lambda^6 - 84\lambda^5 - 405\lambda^4 - 492\lambda^3 + 548\lambda^2 + 964\lambda - 840,$$

$$\vartheta_6 = \frac{2}{\lambda(\lambda+1)(\lambda+2)},$$

$$\begin{aligned} \vartheta_7 &= 4\lambda^{15} + 52\lambda^{14} + 243\lambda^{13} + 167\lambda^{12} - 2343\lambda^{11} - 3244\lambda^{10} + 27697\lambda^9 + 74517\lambda^8 \\ &\quad + 8739\lambda^7 + 244921\lambda^6 + 1532136\lambda^5 + 1771024\lambda^4 + 923048\lambda^3 - 1541641\lambda^2 \\ &\quad + 686268\lambda + 550620, \end{aligned}$$

$$\vartheta_8 = 4\lambda^9 + 32\lambda^8 + 35\lambda^7 - 216\lambda^6 - 159\lambda^5 + 1053\lambda^4 + 350\lambda^3 - 1451\lambda^2 + 148\lambda + 420,$$

$$\vartheta_9 = 8\lambda^{10} + 124\lambda^9 + 822\lambda^8 + 3133\lambda^7 + 7894\lambda^6 + 14519\lambda^5 + 22236\lambda^4 + 35026\lambda^3 \\ + 53894\lambda^2 + 54316\lambda + 22696,$$

$$\vartheta_{10} = 4\lambda^{14} + 84\lambda^{13} + 757\lambda^{12} + 3614\lambda^{11} + 7369\lambda^{10} - 18988\lambda^9 - 199465\lambda^8 - 747082\lambda^7 \\ - 1606417\lambda^6 - 1893644\lambda^5 - 580072\lambda^4 + 1264048\lambda^3 + 1118160\lambda^2 \\ - 396656\lambda - 567840,$$

$$\vartheta_{11} = 8\lambda^{15} + 172\lambda^{14} + 1742\lambda^{13} + 10633\lambda^{12} + 39856\lambda^{11} + 79701\lambda^{10} + 31792\lambda^9 \\ - 125933\lambda^8 + 172824\lambda^7 + 1449179\lambda^6 + 2083778\lambda^5 + 200988\lambda^4 \\ - 1588440\lambda^3 - 552332\lambda^2 + 624208\lambda - 283920,$$

$$\vartheta_{12} = 18(\lambda + 1)(\lambda + 3)(2\lambda^2 + 3\lambda + 2),$$

$$\vartheta_{13} = 2\lambda^{10} + 29\lambda^9 + 149\lambda^8 + 253\lambda^7 - 575\lambda^6 - 3857\lambda^5 - 8701\lambda^4 - 6229\lambda^3 + 11573\lambda^2 \\ + 14412\lambda - 15120,$$

$$\vartheta_{14} = 29\lambda^7 + 206\lambda^6 - 119\lambda^5 - 3822\lambda^4 - 7189\lambda^3 + 5506\lambda^2 + 13279\lambda - 10290,$$

$$\vartheta_{15} = 4\lambda^{11} + 28\lambda^{10} - 49\lambda^9 - 699\lambda^8 - 1280\lambda^7 - 1601\lambda^6 - 11409\lambda^5 - 22185\lambda^4 + 5456\lambda^3 \\ + 23485\lambda^2 - 6654\lambda - 7560,$$

$$\vartheta_{16} = 8\lambda^{13} + 44\lambda^{12} - 282\lambda^{11} - 1699\lambda^{10} + 4418\lambda^9 + 32076\lambda^8 - 1094\lambda^7 - 164198\lambda^6 \\ + 24618\lambda^5 + 557596\lambda^4 - 7256\lambda^3 - 643599\lambda^2 + 100548\lambda + 185220$$

and

$$\vartheta_{17} = 4\lambda^5 + 4\lambda^4 - 17\lambda^3 + 43\lambda^2 - 14\lambda + 16.$$

□

It follows from the above algorithm that two possible GLD_{GPD} fits may be obtained for a data set, one fit from Region A and the second fit from Region B. These two fits are obtained if the values of t_3 and t_4 calculated for the data set lie within the purple-shaded area in the L -moment ratio diagram of the GLD_{GPD} in Figure 4.8(c). For $t_4 \in (0, 1)$, the first fit will be from Class I of Region A if $t_4 \geq \frac{1}{6}$ and from Class II of Region A if $t_4 < \frac{1}{6}$, whereas the second fit will be from Class IV of Region B. If $t_4 \in [\tau_4^{\min}, 0]$, then the two fits will both be from Class III, one from Region A and the other from Region B. A single fit is obtained if the values of t_3 and t_4 fall in the blue-shaded area in the L -moment ratio diagram of the GLD_{GPD} in Figure 4.8(c). This fit will be from Class III of Region B if $t_4 \in [\tau_4^{\min}, 0]$ and from Class IV of Region B if $t_4 \in (0, 1)$.

If one is interested in modeling exceedances in a data set above a threshold, the GPD (that is, the GLD_{GPD} with $\delta = 1$) is used. Method of L -moments estimation for the GPD has been presented in the literature (Hosking, 1986; Hosking & Wallis, 1987, 1997) and will hence not be discussed here. But it should be noted that to fit the GPD to exceedances, the threshold must be selected and the GPD's parameter estimates will depend on the choice of threshold.

Once members of the GLD_{GPD} have been fitted to a data set, the goodness of these fits can be assessed using the tests and graphical displays discussed in Section 2.10 of Chapter 2. In situations where two GLD_{GPD} fits are obtained, the fit with the lowest average scaled absolute error (ASAE) value can typically be regarded as the best fit. However, it is important to verify whether the chosen fit adequately explains the complete data set. That is, one should check whether the support of the fitted GLD_{GPD} covers the range of values observed in the data set. Unfortunately, as will be seen in the examples presented in Section 4.10, the bounded support of the truncated members of the GLD_{GPD} from Class IV in Region B often does not cover all the data values observed. But this problem can occur for any distribution with bounded support, including the GLD_{GPD} from Class II in Region A .

4.10 FITTING OF THE GLD_{GPD} TO DATA

Illustrative examples are presented in this section in which the fit of the GLD_{GPD} to various data sets with diverse characteristics is examined. The sample sizes, sample L -moment and L -moment ratio values and the data ranges for these data sets are given in Table 4.5. Table 4.6 presents the parameter estimates with asymptotic standard errors of the GLD_{GPD} fits along with these fitted distributions' support. The test statistic values and p -values of the Kolmogorov-Smirnov, Anderson-Darling and Cramér-von Mises goodness-of-fit tests as well as the ASAE values for the GLD_{GPD} fits are compared in Table 4.7. Note that N_V in Table 4.7 denotes the number of valid bootstrap samples (out of $N = 10\,000$ simulated bootstrap samples) used in determining the p -values of the goodness-of-fit tests.

Table 4.5: Sample sizes, sample L -moment values and data ranges for the data sets in Section 4.10.

Data set	n	ℓ_1	ℓ_2	t_3	t_4	Data range
Toxic gas concentrations	100	7.9384	1.8432	0.1293	0.1451	[1.701, 16.910]
Venice sea-levels	51	119.6078	10.9341	0.1220	0.2132	[78, 194]
McAlpha ages at death	54	67.4444	11.3969	-0.2902	0.1435	[9, 95]
CHD patients' ages	100	44.3800	6.7774	-0.0022	0.0305	[20, 69]

CHAPTER 4. A GLD TYPE WITH SKEWNESS–INVARIANT MEASURES OF KURTOSIS

Table 4.6: Parameter estimates with asymptotic standard errors* and support for the GLD_{GPD} fitted to the data sets in Section 4.10.

Data set	Class of GLD_{GPD}	$\hat{\alpha}$	$\hat{\beta}$	$\hat{\delta}$	$\hat{\lambda}$	Support
Toxic gas concentrations	II	6.3240 (0.6026)	4.0557 (0.7013)	0.7120 (0.0694)	0.0654 (0.1076)	$[-11.5405, 50.4980]$
	IV	11.2597 (0.9429)	68.8412 (9.4305)	0.3641 (0.0322)	4.6318 (0.5479)	$[1.8092, 16.6719]$
Venice sea-levels	I	113.1792 (4.2316)	18.0359 (4.3744)	0.6565 (0.1170)	-0.1218 (0.1536)	$(-\infty, \infty)$
	IV	138.7045 (10.4960)	585.0591 (110.9265)	0.3885 (0.0483)	5.8320 (0.9268)	$[77.3592, 177.6786]$
McAlpha ages at death	II	90.0580 (5.6500)	25.2549 (6.9240)	0.0208 (0.0766)	0.0703 (0.1746)	$[-261.5536, 97.5289]$
	IV	21.3614 (8.9046)	422.0286 (95.9283)	0.8061 (0.0359)	4.6057 (0.9218)	$[3.5902, 95.2212]$
CHD patients' ages	II	44.7678 (7.4973)	28.9643 (6.9921)	0.4891 (0.1859)	0.6269 (0.2047)	$[21.1631, 67.3660]$
	IV	44.1401 (3.2489)	117.1769 (22.7403)	0.5038 (0.0629)	2.6880 (0.4732)	$[22.5084, 66.1009]$

* Standard errors given in parentheses.

Table 4.7: Goodness-of-fit statistics with p -values* as well as average scaled absolute error (ASAE) values for the GLD_{GPD} fitted to the data sets in Section 4.10.

Data set	Class of GLD_{GPD}	D_n	A_n	W_n	N_V	ASAE
Toxic gas concentrations	II	0.4987 (0.2744)	0.2527 (0.3495)	0.0387 (0.2968)	9 996	0.0148
	IV	0.4362 (0.5971)	0.2999 (0.5050)	0.0223 (0.8088)	10 000	0.0108
Venice sea-levels	I	0.5081 (0.2249)	0.2166 (0.5214)	0.0376 (0.3680)	9 987	0.0144
	IV	0.5415 (0.4729)	0.5452 (0.2204)	0.0617 (0.3520)	10 000	0.0224
McAlpha ages at death	II	0.4946 (0.2586)	1.0902 (0.0030)	0.0585 (0.1052)	5 599	0.0223
	IV	0.3119 (0.9250)	0.1156 (0.9906)	0.0161 (0.9689)	9 971	0.0113
CHD patients' ages	II	0.4055 (0.5520)	0.3253 (0.3231)	0.0241 (0.6504)	8 475	0.0116
	IV	0.4140 (0.4882)	0.3537 (0.3590)	0.0267 (0.5323)	9 495	0.0127

* p -values given in parentheses.

Where applicable, other distributions fitted to the data sets in the literature will also be presented. It is important to note that it is not the purpose of the examples to show that the GLD_{GPD} provides better fits than these distributions. The examples in Section 4.10 are presented to illustrate the flexibility of the GLD_{GPD} .

4.10.1 TOXIC GAS PEAK CONCENTRATIONS

Consider again the data set consisting of toxic gas peak concentrations (Hall, 1991) to which the SLD, in effect, the GLD_{GPD} with $\lambda = 0$, was fitted in Section 2.9 in Chapter 2. This data set's sample L -skewness and L -kurtosis ratio values, $(t_3, t_4) = (0.1293, 0.1451)$, lie in Class II of Region A and in Class IV of Region B of the GLD_{GPD} . So fits from these two classes of the GLD_{GPD} are obtained. Figure 4.13 shows a histogram of the data set along with the density curves of the two GLD_{GPD} fits, while $Q-Q$ plots for these two fits are given in Figure 4.14 – see Figures 2.16 and 2.17 for the density curves and $Q-Q$ plots of the fitted SLD as well as the fitted Davies distribution (Hankin & Lee, 2006).

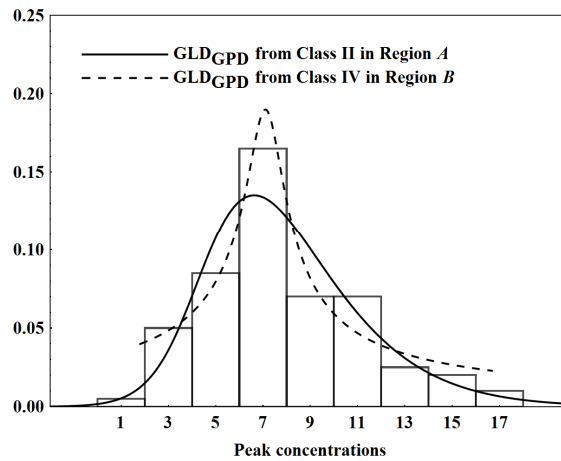


Figure 4.13: Histogram of the peak concentrations (in percent) of toxic gas together with the probability density functions of the fitted GLD_{GPD} .

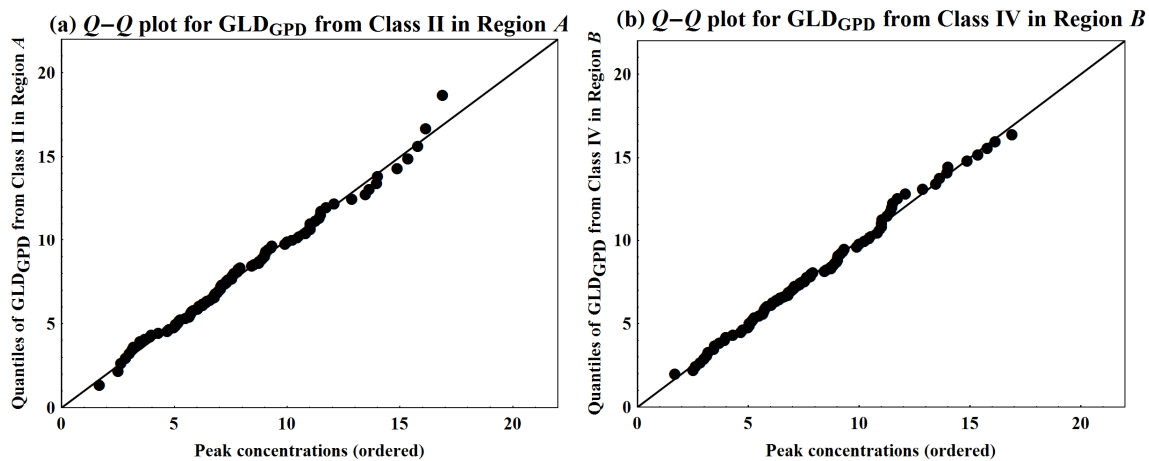


Figure 4.14: $Q-Q$ plots for the GLD_{GPD} fitted to the peak concentrations (in percent) of toxic gas.

Comparing the $Q-Q$ plot for the fitted GLD_{GPD} from Class II in Figure 4.14(a) with the SLD's $Q-Q$ plot in Figure 2.17(a), it is noted that the fit of the GLD_{GPD} from Class II is

similar but slightly better than the SLD's fit, especially at the lower tail. Also, the ASAE value of 0.0148 for the GLD_{GPD} from Class II is marginally lower than the SLD's ASAE value of 0.0154. But the parameter estimate for λ in Class II of the GLD_{GPD} , $\hat{\lambda}_A = 0.0654$, is close to zero with a relatively large standard error (0.1076), indicating that this additional shape parameter of the GLD_{GPD} in Class II is not significantly different from zero. That is, the GLD_{GPD} from Class II simplifies to the SLD with $\lambda = 0$.

Turning to the fitted GLD_{GPD} from Class IV, this distribution's density curve very closely corresponds to the histogram of the data in Figure 4.13, suggesting an excellent fit, which is confirmed by its $Q-Q$ plot in Figure 4.14(b). Furthermore, the fitted GLD_{GPD} from Class IV has a very low ASAE value of 0.0108, which is smaller than the ASAE values of the GLD_{GPD} from Class II and the SLD. So it seems that the GLD_{GPD} from Class IV provides the best fit for the data set. But this distribution's bounded support of $[1.8092, 16.6719]$ does not cover the complete data set in that both the minimum and maximum values in the data, 1.701 and 16.91, lie outside the support. This is due to the truncated form of the GLD_{GPD} in Class IV.

4.10.2 VENICE MAXIMUM SEA-LEVELS

Smith (1986) and Coles (2001) both considered the sea-levels in Venice within the context of extreme value modeling. The data set contains the 10 largest sea-levels (in centimeters), measured annually in Venice from 1931 to 1981, apart from 1935, for which only the six largest sea-levels are available. Here the annual maximum sea-level is considered, giving $n = 51$ measurements, graphically presented in the histograms in Figure 4.15. The generalized extreme value (GEV) distribution is implied by extreme value theory for data like this. Here we consider the GLD_{GPD} to illustrate its flexibility. The data possesses heavy tails, so the GLD_{GPD} yields fits from Class I in Region A and Class IV in Region B. Coles (2001) fitted the GEV distribution to the data set using maximum likelihood estimation. The fitted density curves of the GLD_{GPD} and the GEV distribution are superimposed on the histograms in Figure 4.15, while $Q-Q$ plots for these fitted distributions are given in Figure 4.16.

The GLD_{GPD} from Class I with infinite support provides a very good fit, which, when comparing their ASAE values in Table 4.7 and $Q-Q$ plots in Figures 4.16(a) and 4.16(b), is much better than the fit of the GLD_{GPD} from Class IV. Although not rejected by any of the goodness-of-fit tests (Table 4.7), the GLD_{GPD} from Class IV does not provide a good fit in that the center part of its density curve rises too high compared to the data's histogram – see again Figure 4.15(a). Furthermore, because of its truncated form, the support of the fitted

GLD_{GPD} from Class IV does not cover the data range, resulting in poor fits at the tails, especially in the upper tail for maximum sea-levels above 140 centimeters.

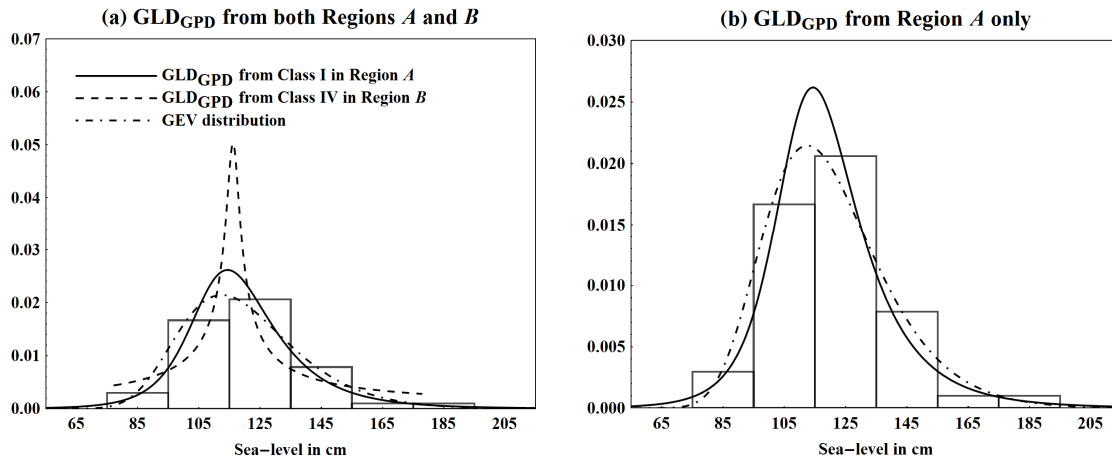


Figure 4.15: Histograms of the annual maximum sea-levels (in centimeters) in Venice together with the probability density functions of the fitted GLD_{GPD} and generalized extreme value (GEV) distribution. The line types indicated in graph (a) also apply to graph (b).

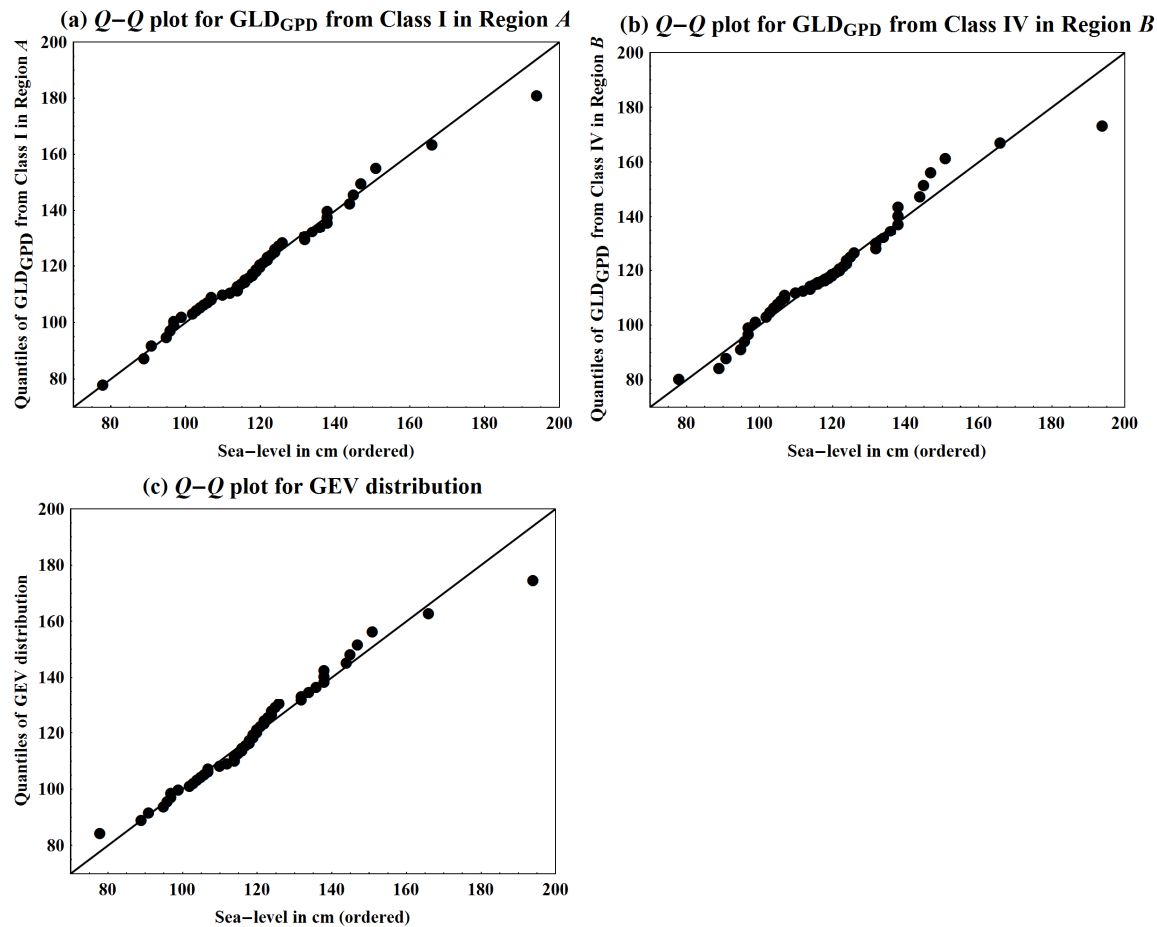


Figure 4.16: $Q-Q$ plots for the GLD_{GPD} and the generalized extreme value (GEV) distribution fitted to the annual maximum sea-levels (in centimeters) in Venice.

The GEV distribution fitted by Coles (2001) has an ASAE value of 0.0189, which is larger than the ASAE value for the fitted GLD_{GPD} from Class I. But this is not surprising, since the GLD_{GPD} has two shape parameters, whereas the GEV distribution has a single shape parameter. Also, as indicated before, the GEV distribution is the correct distribution to be used for modeling maximum values.

4.10.3 MCALPHA CLAN AGES AT DEATH

In their book on applied nonparametric statistics, Sprent & Smeeton (2007) presented the age at death (in completed years) of male members of four Scottish clans, obtained from the burial ground at Badenscallie in Scotland. Of these, the McAlpha clan has the largest sample size and will hence be used in this example. The nature of the data renders it useful for survival analysis. For instance, recently Cooray & Ananda (2010) used this data set to illustrate the applicability of the Gompertz-sinh family of distributions in survival analysis.

A histogram of the age at death for the males from the McAlpha clan is shown in Figure 4.17. The slightly higher frequency for deaths under age five, compared to the frequencies for adjacent age intervals, is notable. In this example the age at death excluding under-age-five mortality is used. In effect, the data set is truncated with respect to the lower tail by excluding the five males with age at death of less than five years.

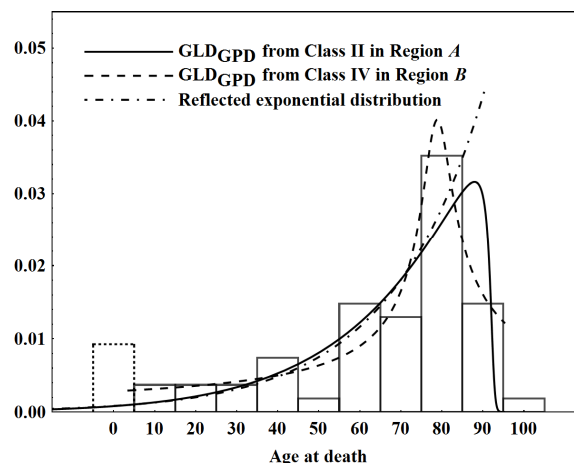


Figure 4.17: Histogram of the age at death (in completed years) of male members of the McAlpha clan together with the probability density functions of the fitted GLD_{GPD} and reflected exponential distribution. The dotted bar in the histogram represents five males with age at death of less than five years. These five observations are neither considered in the fitting of the distributions, nor in the model validation of these fits.

Fitting the GLD_{GPD} to this truncated data set of $n = 54$ observations yields fits from Class II of Region A and Class IV of Region B. The density curves of these fits are shown in Figure

4.17, while their Q - Q plots are given in Figure 4.18. The GLD_{GPD} from Class IV provides an excellent fit as indicated by the high p -values for its goodness-of-fit tests and its low ASAE value in Table 4.7, as well as its Q - Q plot in Figure 4.18(b). The excellent fit is partly due to the inherent truncated form of the GLD_{GPD} in Class IV, which captures the truncation applied to the data. Note that, in contrast to the previous two examples (Sections 4.10.1 and 4.10.2), the support of the fitted GLD_{GPD} from Class IV, $[3.5902, 95.2212]$, covers the data range of the truncated data set, $[9, 95]$.

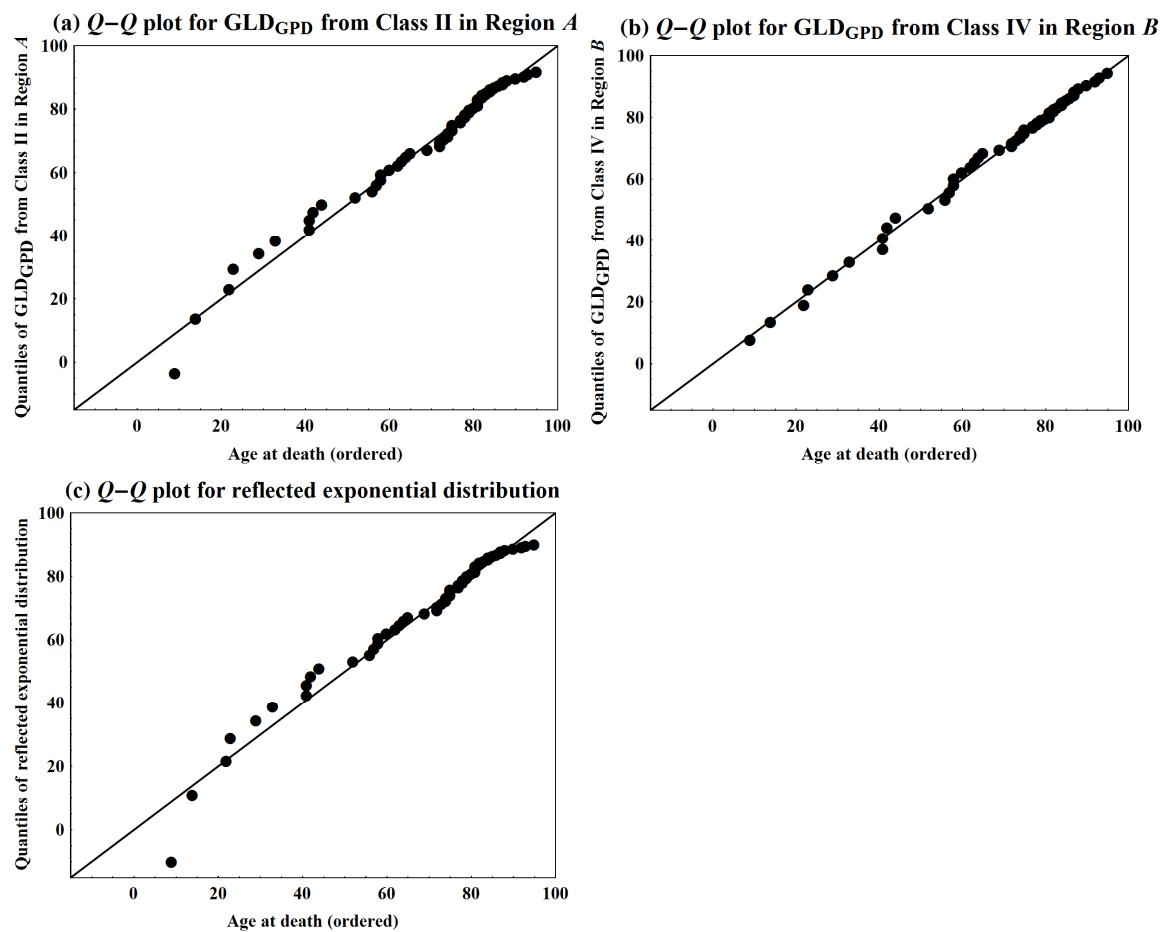


Figure 4.18: Q - Q plots for the GLD_{GPD} and the reflected exponential distribution fitted to the age at death (in completed years) of male members of the McAlpha clan, excluding under-age-five mortality.

The fit of the GLD_{GPD} from Class II is substantially worse, especially with respect to males with age of death less than 50 years – see the Q - Q plot in Figure 4.18(a). It is interesting to note that neither of the shape parameters of the GLD_{GPD} from Class II differs significantly from zero, suggesting a simplification to the reflected exponential distribution with $\delta = \lambda = 0$. The density curve of this fitted distribution, with method of L -moments estimates $\hat{\alpha} = \ell_1 + 2\ell_2 = 90.2383$ and $\hat{\beta} = 2\ell_2 = 22.7939$ for the location parameter (upper

endpoint of the distribution) and the scale parameter, is shown in Figure 4.17, while the corresponding $Q-Q$ plot is shown in Figure 4.18(c). Not surprisingly the fit of the reflected exponential distribution is similar to but worse than the fit of the GLD_{GPD} from Class II.

4.10.4 CORONARY HEART DISEASE (CHD) PATIENTS' AGES

The coronary heart disease (CHD) data set in Hosmer & Lemeshow (2000) contains the age (in completed years) of $n = 100$ subjects, assumed to have a logistic distribution in a logistic regression framework. A histogram of the data is given in Figure 4.19 and suggests that the data is approximately symmetric, but that it has tails shorter than the logistic distribution. These visual deductions are confirmed by the sample L -moment ratio values, given in Table 4.5, in that $t_3 = -0.0022$ is very close to zero, while $t_4 = 0.0305$ is less than $\tau_4 = \frac{1}{6}$, the L -kurtosis ratio for the logistic distribution – also see the logistic distribution's $Q-Q$ plot in Figure 4.20(c).

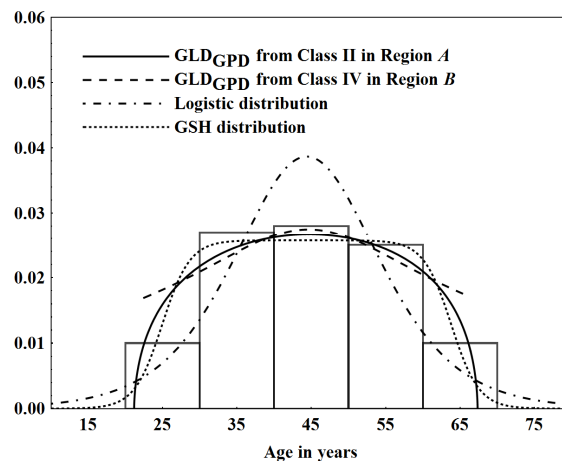


Figure 4.19: Histogram of the age (in completed years) of patients in a coronary heart disease (CHD) study together with the probability density functions of the fitted GLD_{GPD} , logistic distribution and generalized secant hyperbolic (GSH) distribution.

Given the data set's values for t_3 and t_4 , platykurtic members of the GLD_{GPD} from Class II of Region A and from Class IV of Region B are fitted to the data. Because of the symmetry of the data, the estimates for δ of both fits of the GLD_{GPD} are close to $\frac{1}{2}$ ($\hat{\delta}_A = 0.4981$ and $\hat{\delta}_B = 0.5038$). The fitted GLD_{GPD} from Class II has a slightly lower ASAE value than the fitted GLD_{GPD} from Class IV (0.0116 compared to 0.0127) and their $Q-Q$ plots in Figures 4.20(a) and 4.20(b) indicate very good fits, apart from the minimum and maximum values in the data set which are not covered by the bounded support of the two fits.

Another symmetric distribution, the generalized secant hyperbolic (GSH) distribution, was fitted to the data by Vaughan (2002). The GSH distribution exhibits short or heavy tails, depending on the value of its kurtosis parameter (Vaughan, 2002; Klein & Fisher, 2008; van Staden & Loots, 2009b). Because the GSH distribution possesses infinite support, it provides a better fit to the data compared to the GLD_{GPD} as can be seen from its $Q-Q$ plot in Figure 4.20(d). Note also that the GSH distribution's fit has an ASAE value of 0.0104 which is marginally smaller than the ASAE values of the two GLD_{GPD} fits.

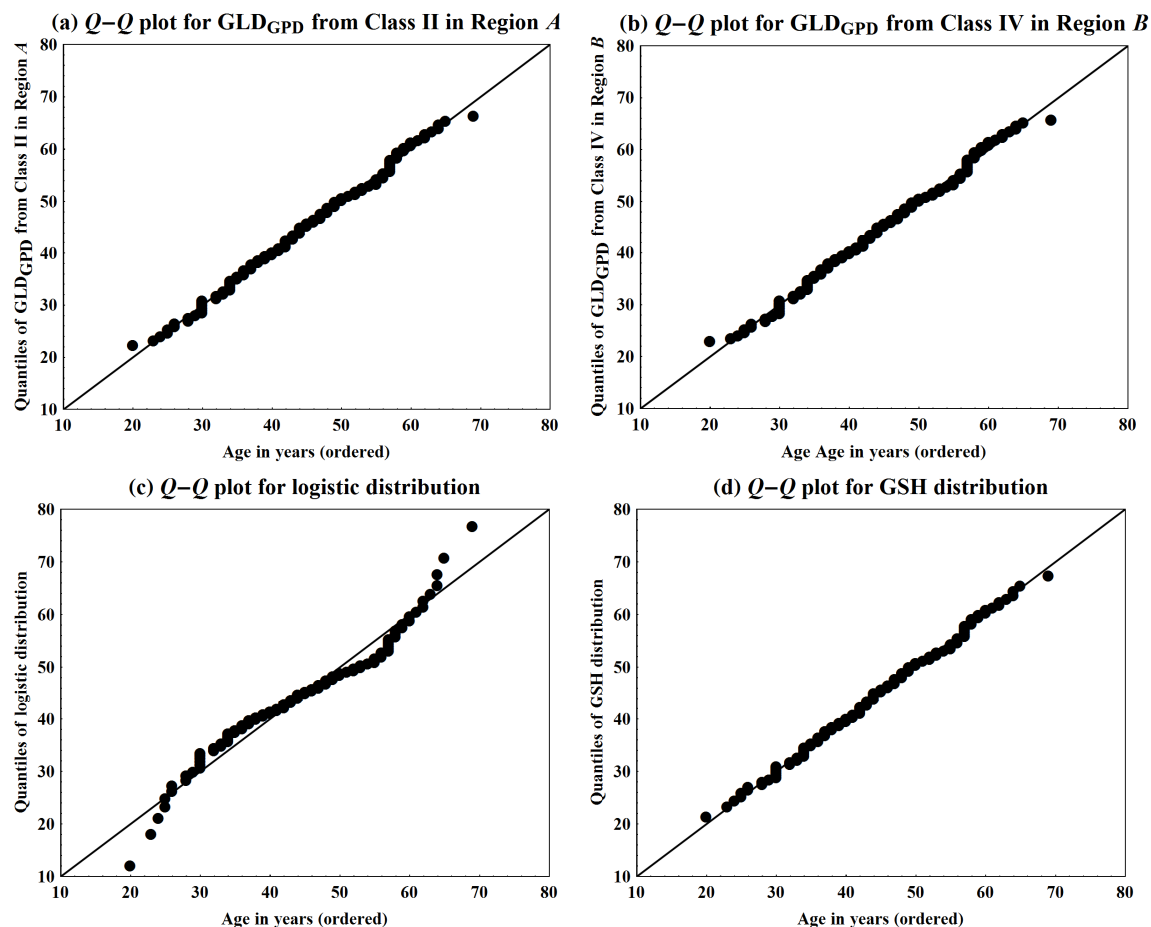


Figure 4.20: $Q-Q$ plots for the GLD_{GPD} , the logistic distribution and the generalized secant hyperbolic (GSH) distribution fitted to the age (in completed years) of patients in a coronary heart disease (CHD) study.

4.11 GLD_{GPD} APPROXIMATION OF DISTRIBUTIONS

The flexibility of the GLD_{GPD} is further highlighted in this section by showing its ability to approximate a variety of different probability distributions through the matching of theoretical L -moments. Any distribution whose values of τ_3 and τ_4 fall within the (τ_3, τ_4) space of the GLD_{GPD} in Figure 4.8(c) can be approximated by the GLD_{GPD} . But, since a detailed analysis is beyond the scope of this thesis, the focus in this section will be on well-

known distributions such as the normal, Student's t , gamma and log-normal distributions. Distributions popular in various statistical disciplines, for example survival analysis and extreme value theory, as well as distributions with specific properties, for instance the cosine distribution which is platykurtic, will also be considered.

A distribution can be approximated by the GLD_{GPD} with the following steps:

Step 1

For the distribution under consideration, select values for its location parameter, scale parameter and, if present, shape parameter(s). Calculate the distribution's L -moments and L -moment ratios, in effect, L_1 , L_2 , τ_3 and τ_4 . This approach is followed if one wants to approximate a specific distribution, say for example a standard normal distribution with zero mean and unit variance.

Alternatively, choose values for the distribution's L -moments and L -moment ratios and calculate the corresponding parameter values. This is for example done when one wants to compare the GLD_{GPD} approximations for different distributions with equivalent measures of location, spread and shape, say for the gamma and log-normal distributions with $L_1 = 0$, $L_2 = 1$ and $\tau_3 = 0.2$.

Step 2

Check whether the distribution's values of τ_3 and τ_4 lie within the (τ_3, τ_4) space of the GLD_{GPD} in Figure 4.8(c). If so, proceed with Step 3. If not, the distribution cannot be approximated by the GLD_{GPD} for the selected parameter values.

Step 3

Use the estimation algorithm given in Section 4.9 to estimate the parameters of the GLD_{GPD} by determining $\hat{\alpha}_h$, $\hat{\beta}_h$, $\hat{\delta}_h$ and $\hat{\lambda}_h$ for $h = A, B$.

□

Given the distributional shapes obtained by the GLD_{GPD} in its four classes, it provides the best approximations for unimodal distributions, and these GLD_{GPD} approximations are achieved from Classes I and II in Region A. The truncated distributions from Region B seldom produce adequate approximations. Thus, in Step 2 above, it is usually only necessary

to consider the (τ_3, τ_4) space of Classes I and II in Region A of the GLD_{GPD} in Figure 4.6(a). This is true for all the distributions considered here and hence the subscripts for the parameter estimates of the GLD_{GPD} approximations are dropped.

Table 4.8 presents the values for the parameters and L -moments of the distributions considered as well as the parameter estimates of their GLD_{GPD} approximations. See Tables 2.10 to 2.14 in Section 2.14.3 for details regarding the properties and functions of the selected distributions. Note though that in this section, to avoid confusion with the parameters of the GLD_{GPD} , the location, scale and shape parameters of the distributions are denoted by a , b and c respectively.

Also, to simplify comparisons between the various distributions, $L_1 = 0$ and $L_2 = 1$ and, where applicable, $\tau_3 = 0.2$. In Figures 4.21 to 4.24 the probability density function, $f(x)$, of each distribution is presented along with the probability density function, $\hat{f}(x)$, of the corresponding GLD_{GPD} approximation.

Various methods exist for validating the quality of an approximation. In this thesis, as a first check, the closeness between the probability density functions is determined by approximating

$$S = \sup | \hat{f}(x) - f(x) |$$

with

$$\hat{S} = \max_{1 \leq i \leq n} | \hat{f}(x_{i:n}) - f(x_{i:n}) |,$$

where $\hat{f}(x_{i:n})$ is the empirical probability density function of the GLD_{GPD} approximation. For a second check, the ASAE between $Q(p_{i:n})$, the quantile function of the approximated distribution, and $\hat{Q}(p_{i:n})$, the empirical quantile function of the GLD_{GPD} approximation, is calculated. That is,

$$\text{ASAE} = \frac{1}{n} \sum_{i=1}^n \frac{|Q(p_{i:n}) - \hat{Q}(p_{i:n})|}{Q(p_{n:n}) - Q(p_{1:n})}$$

with $p_{i:n}$ given by (2.70), is calculated. For both \hat{S} and ASAE, $n = 9\,999$ is used.

CHAPTER 4. A GLD TYPE WITH SKEWNESS-INVARIANT MEASURES OF KURTOSIS

Table 4.8: Parameter and L -moment values of various distributions, parameter estimates of these distributions' GLD_{GPD} approximations, and values for validating the quality of the GLD_{GPD} approximations.

Distribution	a	b	c	τ_3	τ_4	$\hat{\alpha}$	$\hat{\beta}$	$\hat{\delta}$	$\hat{\lambda}$	\hat{S}	ASAE
Symmetric distributions											
Cosine	-4	8	-	0	0.0625	0	3.3956	0.5	0.4093	0.0045	0.0004
Normal	0	1.7725	-	0	0.1226	0	2.4449	0.5	0.1416	0.0005	0.0002
Secant hyperbolic	0	1.1729	-	0	0.1940	0	1.7829	0.5	-0.0742	0.0050	0.0007
Student's $t(2)$	0	0.9003	-	0	0.3750	0	0.9069	0.5	-0.4244	0.0181	0.0002
Extreme value distributions											
Fréchet	-0.8624	1.3798	-0.0463	0.2	0.1629	-1.2242	2.0328	0.8044	0.0109	0.0129	0.0012
Gumbel	-0.8327	1.4427	-	0.1699	0.1504	-1.1157	2.1486	0.7723	0.0487	0.0091	0.0011
Rayleigh	-3.4142	2.7241	-	0.1140	0.1054	-1.0173	2.6641	0.7305	0.2071	0.0145	0.0019
Weibull	-2.6582	2.9367	0.6808	0.2	0.1190	-1.6085	2.4882	0.8732	0.1548	0.0491	0.0017
Gamma and log-normal distributions											
Gamma	-3.0661	1.1222	0.3660	0.2	0.1358	-1.4346	2.2960	0.8423	0.0956	0.0198	0.0014
Log-normal	-4.3504	3.9944	0.4132	0.2	0.1541	-1.2854	2.1131	0.8155	0.0372	0.0145	0.0013
Generalized exponential and logistic distributions											
Generalized exponential	-3.7471	1.5312	0.1672	0.2	0.1500	-1.3162	2.1523	0.8210	0.0499	0.0147	0.0012
Generalized logistic	-0.3226	0.9355	-0.2000	0.2	0.2000	-1.0208	1.7396	0.7672	-0.0895	0.0225	0.0016

4.1.1.1 SYMMETRIC DISTRIBUTIONS

Figure 4.21 presents the density curves of four symmetric distributions, namely the cosine, normal, secant hyperbolic and Student's $t(2)$ distribution, along with the density curves of their GLD_{GPD} approximations. The cosine distribution, a special symmetric case of the complementary beta distribution proposed by Jones (2002b), is a platykurtic distribution. Hence its GLD_{GPD} approximation is from Class II. So too is the GLD_{GPD} approximation of the normal distribution, a mesokurtic distribution. Both the secant hyperbolic distribution (Vaughan, 2002) and Student's $t(2)$ distribution (Jones, 2002a) are leptokurtic distributions and therefore they are approximated by the GLD_{GPD} from Class I.

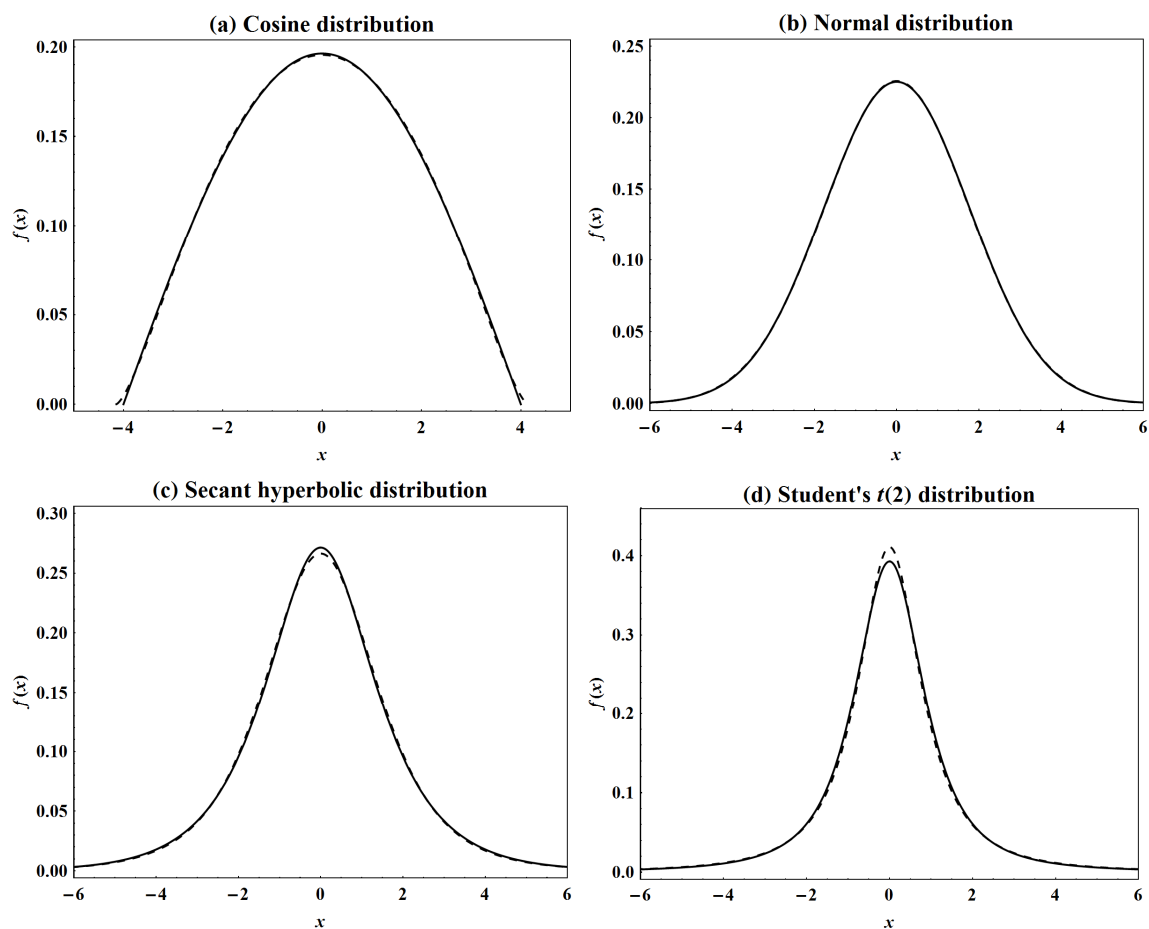


Figure 4.21: Probability density functions of various symmetric distributions, indicated by the solid lines, along with the probability density functions of their GLD_{GPD} approximations, indicated by the dashed lines.

The GLD_{GPD} approximations of all the symmetric distributions considered are excellent, as is evident from their low values for \hat{S} and ASAE in Table 4.8. This is especially true for the normal distribution, with no visible difference between the density curves depicted in Figure 4.21(b). The only slight concern, which in fact also occurs for the corresponding

approximations of the normal distribution by the GLD_{RS} and the GLD_{FMKL} , is that the support of the GLD_{GPD} approximation is finite – when $L_1 = 0$ and $L_2 = 1$, the support of the normal distribution's GLD_{GPD} approximation is $[-8.6323, 8.6323]$.

4.1.1.2 EXTREME VALUE DISTRIBUTIONS

The generalized extreme value (GEV) distribution combines into a single family the extreme value distributions of Types 1, 2 and 3. It contains as a special limiting case the Gumbel distribution for $c = 0$, while the Fréchet and the reflected Weibull distributions are obtained for $c < 0$ and $c > 0$ respectively. All L -moments of the GEV distribution exist for $c > -1$. For $-1 < c \leq -0.0589$, the GLD_{GPD} approximation is from Class I, while the GLD_{GPD} approximation is from Class II for $-0.0589 < c < 1$. When $c = 1$, the GEV distribution reduces to the reflected exponential distribution (in effect, the GLD_{GPD} with $\delta = \lambda = 0$). When $c > 1$, no GLD_{GPD} approximation is possible from either Class I or II.

Turning to specific members from the GEV distribution, if $\tau_3 = 0.2$, then $c = -0.0463$ and the Fréchet distribution is obtained. Its density curve is depicted in Figure 4.22(a), while the density curve of the Gumbel distribution, for which $\tau_3 \approx 0.17$, is given in Figure 4.22(b). When $\tau_3 = -0.2$, the shape parameter value is $c = 0.6808$ and, because $c > 0$, the GEV distribution reduces to the reflected Weibull distribution. Figure 4.22(d) shows the density curve of the corresponding Weibull distribution with $\tau_3 = 0.2$. The Rayleigh distribution is a special case of the Weibull distribution, obtained when the value of the Weibull distribution's shape parameter is $c = 0.5$. The Rayleigh distribution's density curve is shown in Figure 4.22(c).

To simplify interpretation, all four members taken from the GEV distribution are positively skewed. The parameter estimates of the GLD_{GPD} approximations for these four members from the GEV distribution are given in Table 4.8. These approximations' density curves are plotted in Figure 4.22 along with the density curves of the distributions being approximated. It is noted that, in general, the GLD_{GPD} approximation of the right tail of each distribution is very good. Given the difference in the tail behavior of the Weibull and GLD_{GPD} distributions, the GLD_{GPD} approximation in the left tail of the Weibull distribution is not good. This is specifically the case when the Weibull distribution is positively skewed with $\tau_3 > 0$.

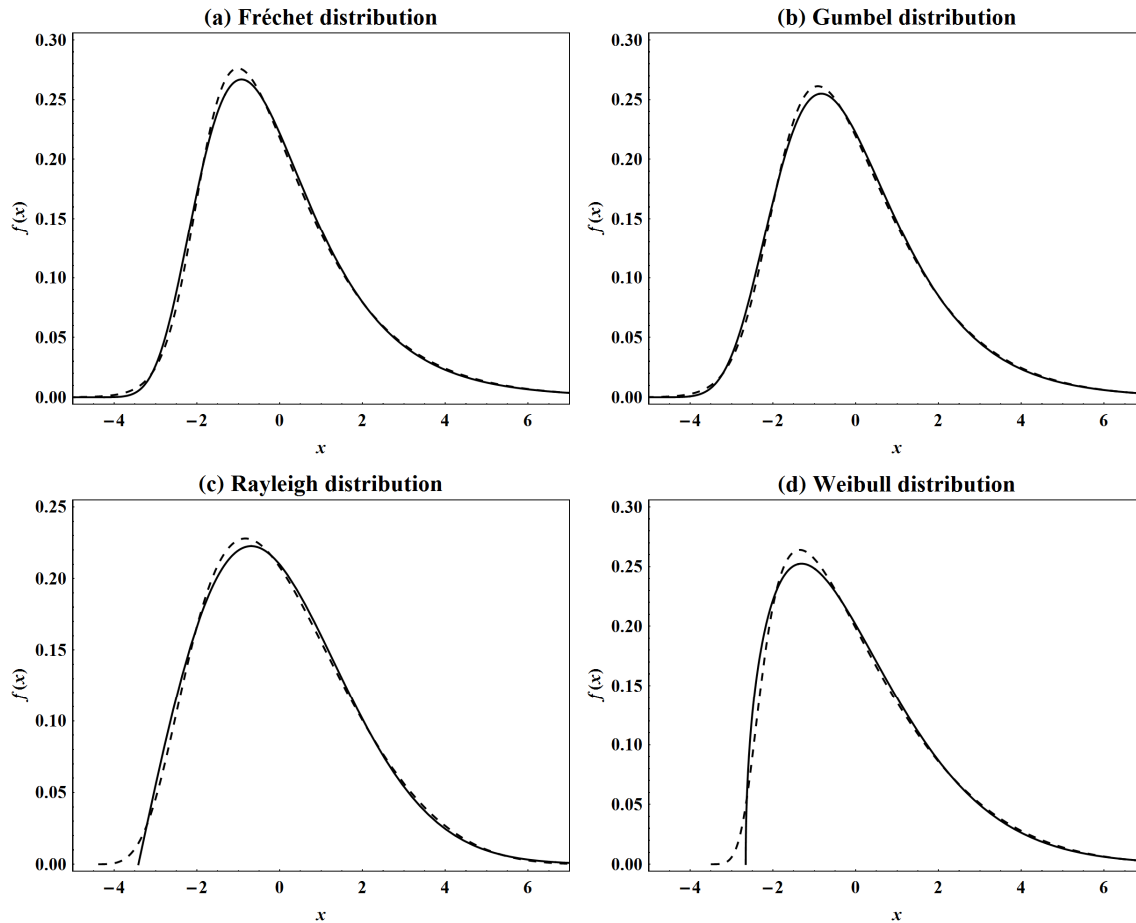


Figure 4.22: Probability density functions of various extreme value distributions, indicated by the solid lines, along with the probability density functions of their GLD_{GPD} approximations, indicated by the dashed lines.

4.11.3 GAMMA AND LOG-NORMAL DISTRIBUTIONS

For the gamma and log-normal distributions, no simple expressions exist for either τ_3 or τ_4 . For given parameter values, the values for τ_3 and τ_4 can be calculated using the rational-function approximations given by Hosking & Wallis (1997), or through numerical integration, which is done here.

The gamma distribution is approximated by the GLD_{GPD} from Class II when $0 < c < 1$, corresponding to $0 < \tau_3 < \frac{1}{3}$. The case $\tau_3 = 0.2$ is shown in Figure 4.23(a) and given in Table 4.8. The gamma distribution approaches the normal distribution as $c \downarrow 0$, while the exponential distribution (GLD_{GPD} with $\delta = 1$ and $\lambda = 0$) is obtained for $c = 1$. For $c > 1$ no GLD_{GPD} approximation is possible from Class II.

The log-normal distribution also approaches the normal distribution as $c \downarrow 0$. For $0 < c < 0.4903$ the GLD_{GPD} approximation is from Class II, as is for instance the GLD_{GPD} approximation presented in Table 4.8 and illustrated in Figure 4.23(b) for the case $\tau_3 = 0.2$.

The GLD_{GPD} approximation is from Class I for $0.4903 \leq c \leq 1.1429$, while no GLD_{GPD} approximation is possible from either Class I or Class II if $c > 1.1429$.

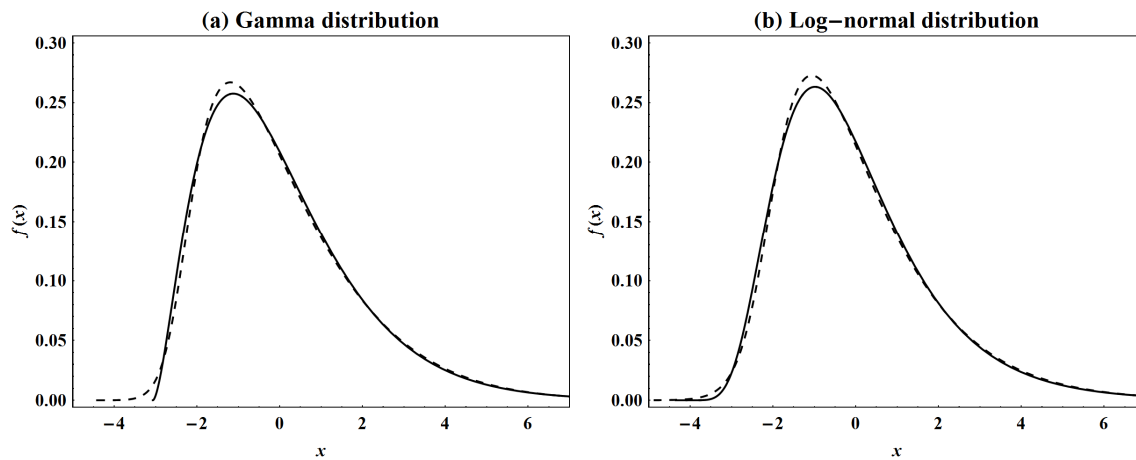


Figure 4.23: Probability density functions of the gamma and log-normal distributions, indicated by the solid lines, along with the probability density functions of their GLD_{GPD} approximations, indicated by the dashed lines.

4.1.1.4 GENERALIZED EXPONENTIAL AND LOGISTIC DISTRIBUTIONS

The generalized exponential distribution with shape parameter $c > 0$, analyzed by Gupta & Kundu (1999, 2007), is approximated by the GLD_{GPD} from Class II for $0 < c < 1$. When $c \rightarrow 0$, the generalized exponential distribution approaches the Gumbel distribution, while it reduces to the exponential distribution for $c = 1$. When $c > 1$, no GLD_{GPD} approximation is available from either Class I or Class II of the GLD_{GPD} . In Figure 4.24(a) the GLD_{GPD} approximation for $\tau_3 = 0.2$ and $\tau_4 = 0.15$ is illustrated, attained for $c = 0.1672$.

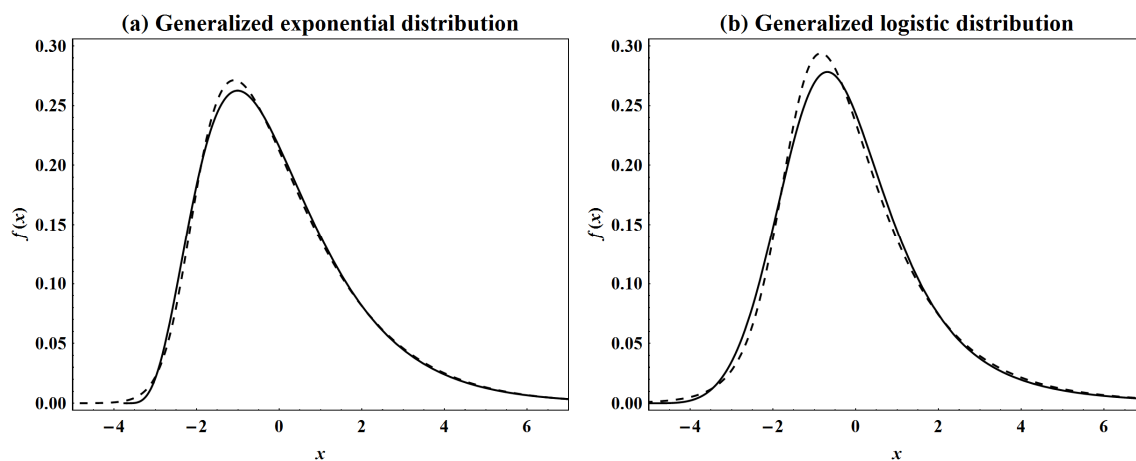


Figure 4.24: Probability density functions of the generalized exponential and logistic distributions, indicated by the solid lines, along with the probability density functions of their GLD_{GPD} approximations, indicated by the dashed lines.

The generalized logistic distribution, introduced by Hosking (1986), is a reparameterized version of the log-logistic distribution. It approaches the logistic distribution as $c \rightarrow 0$. The L -moments of the generalized logistic distribution only exist for $|c| < 1$. The distribution is leptokurtic for all values of c and is hence approximated by the GLD_{GPD} from Class I. Figure 4.24(b) shows the case $\tau_3 = \tau_4 = 0.2$ obtained for $c = -0.2$.

4.12 CONCLUSION

Using the quantile function of the GPD with shape parameter λ as the basic building block, the methodology presented in Proposition 2.8.1 in Chapter 2 was applied in this chapter to develop a four-parameter quantile-based distribution through the inclusion of a second shape parameter, $0 \leq \delta \leq 1$, which controls the level of skewness. The proposed quantile-based distribution, specified in terms of its quantile function in Definition 4.2.1, is a skewed generalization of Tukey's lambda distribution and hence a type of the GLD, referred to as the GPD Type and denoted GLD_{GPD} . The GLD_{GPD} can also be viewed as a generalization of the SLD, studied in Chapter 2 and attained from the GLD_{GPD} for $\lambda = 0$, with the parameter λ controlling the level of kurtosis.

The distributional properties and shape characteristics of the GLD_{GPD} were explored in detail, emphasizing similarities and differences between the GLD_{GPD} and the two types of the GLD presented in Chapter 3, the GLD_{RS} and GLD_{FMKL} . Compared to these two types, the GLD_{GPD} possesses tractability advantages with respect to skewness and kurtosis. In particular, the L -kurtosis ratio as well as the quantile-based kurtosis measures of the GLD_{GPD} are skewness-invariant. As a result, parameter estimation for the GLD_{GPD} is straightforward. Closed-form expressions exist for the method of L -moments estimators of the parameters of the GLD_{GPD} , as well as for these estimators' asymptotic standard errors. This is not the case for any estimation method of either the GLD_{RS} or the GLD_{FMKL} .

4.13 DERIVATIONS

This section contains derivations for the GLD_{GPD} , specifically for $\lambda \neq 0$. The equivalent derivations for $\lambda = 0$, that is, for the SLD, were done in Section 2.13 in Chapter 2. Formulae for the mean, the variance and the skewness and kurtosis moment ratios of the GLD_{GPD} are derived in Section 4.13.1. In Section 4.13.2 the minimum value of the L -kurtosis ratio for the

GLD_{GPD} is obtained. The derivation of the covariance matrix for the method of L -moments estimators of the GLD_{GPD} is done in Section 4.13.2.

4.13.1 MOMENTS OF GLD_{GPD}

Theorem 4.13.1

Let X be a real-valued random variable with distribution given by the GPD Type of the GLD, denoted $X \sim \text{GLD}_{\text{GPD}}(\alpha, \beta, \delta, \lambda)$, where α is a location parameter, $\beta > 0$ is a scale parameter and $0 \leq \delta \leq 1$ and λ are shape parameters. The mean, variance, skewness moment ratio and kurtosis moment ratio of X are given by (4.7) to (4.10).

Proof

The mean, variance, skewness moment ratio and kurtosis moment ratio for the GLD_{GPD} with $\lambda = 0$, in effect, the SLD, were derived in Section 2.13.1 of Chapter 2. So here only the derivation of the moments for $\lambda \neq 0$ is done.

The quantile function of the GLD_{GPD} with $\lambda \neq 0$, given in (4.4), can be rewritten as

$$\begin{aligned} Q_X(p) &= \alpha + \beta \left((1 - \delta) \left(\frac{p^\lambda - 1}{\lambda} \right) - \delta \left(\frac{(1-p)^\lambda - 1}{\lambda} \right) \right) \\ &= \alpha + \frac{\beta}{\lambda} (2\delta - 1) + \frac{\beta}{\lambda} (1 - \delta) p^\lambda - \frac{\beta}{\lambda} \delta (1 - p)^\lambda \\ &= \tilde{\alpha} + \tilde{\beta} \left((1 - \delta) p^\lambda - \delta (1 - p)^\lambda \right). \end{aligned}$$

Let $Z = \frac{X - \tilde{\alpha}}{\tilde{\beta}}$ with

$$\tilde{\alpha} = \alpha + \frac{\beta}{\lambda} (2\delta - 1) \quad (4.36)$$

and

$$\tilde{\beta} = \frac{\beta}{\lambda}. \quad (4.37)$$

Then the quantile function of Z is

$$Q_Z(p) = (1 - \delta) p^\lambda - \delta (1 - p)^\lambda.$$

The r^{th} order uncorrected moment of Z is given by

$$\begin{aligned} E[Z^r] &= \int_0^1 (Q_Z(p))^r dp \\ &= \int_0^1 \left((1 - \delta) p^\lambda - \delta (1 - p)^\lambda \right)^r dp. \end{aligned}$$

Using the binomial series, $(a+b)^r = \sum_{k=0}^r \binom{r}{k} a^{r-k} b^k$, Gradshteyn & Ryzhik (2007, 1.111), and the beta function, $B(a,b)$, (see Section 2.14.1 in Chapter 2 for details),

$$\begin{aligned} E[Z^r] &= \int_0^1 \sum_{k=0}^r \binom{r}{k} \left((1-\delta)p^\lambda \right)^{r-k} \left(-\delta(1-p)^\lambda \right)^k dp \\ &= \sum_{k=0}^r (-1)^k \binom{r}{k} (1-\delta)^{r-k} \delta^k \int_0^1 p^{\lambda(r-k)} (1-p)^{\lambda k} dp \\ &= \sum_{k=0}^r (-1)^k \binom{r}{k} (1-\delta)^{r-k} \delta^k B(\lambda(r-k)+1, \lambda k+1). \end{aligned}$$

But $B(a,b)$ converges if and only if $a > 0$ and $b > 0$, so $E[Z^r]$ exists if and only if $\lambda(r-k)+1 > 0$ and $\lambda k+1 > 0$ for $k=0,1,\dots,r$. In effect, $E[Z^r]$ and hence the r^{th} order uncorrected moment as well as the r^{th} order corrected moment of the GLD_{GPD} exist if and only if $\lambda > -\frac{1}{r}$.

In particular, using $B(a+1,1) = B(1,a+1) = \frac{1}{a+1}$ for $a > -1$, the first four uncorrected moments of Z are

$$\begin{aligned} E[Z] &= (1-\delta)B(\lambda+1,1) - \delta B(1,\lambda+1) \\ &= \phi_1, \quad \lambda > -1, \end{aligned}$$

$$\begin{aligned} E[Z^2] &= (1-\delta)^2 B(2\lambda+1,1) - 2(1-\delta)\delta B(\lambda+1,\lambda+1) + \delta^2 B(1,2\lambda+1) \\ &= \phi_2 - 2\omega B(\lambda+1,\lambda+1), \quad \lambda > -\frac{1}{2}, \end{aligned}$$

$$\begin{aligned} E[Z^3] &= (1-\delta)^3 B(3\lambda+1,1) - 3(1-\delta)^2 \delta B(2\lambda+1,\lambda+1) \\ &\quad + 3(1-\delta)\delta^2 B(\lambda+1,2\lambda+1) - \delta^3 B(1,3\lambda+1) \\ &= \phi_3 + 3\omega(2\delta-1)B(2\lambda+1,\lambda+1), \quad \lambda > -\frac{1}{3}, \end{aligned}$$

and

$$\begin{aligned} E[Z^4] &= (1-\delta)^4 B(4\lambda+1,1) - 4(1-\delta)^3 \delta B(3\lambda+1,\lambda+1) \\ &\quad + 6(1-\delta)^2 \delta^2 B(2\lambda+1,2\lambda+1) \\ &\quad - 4(1-\delta)\delta^3 B(\lambda+1,3\lambda+1) + \delta^4 B(1,4\lambda+1) \\ &= \phi_4 - 4\omega \left((1-\delta)^2 + \delta^2 \right) B(3\lambda+1,\lambda+1) + 6\omega^2 B(2\lambda+1,2\lambda+1), \quad \lambda > -\frac{1}{4}, \end{aligned}$$

where $\omega = \delta(1-\delta)$ and $\phi_k = \frac{(1-\delta)^k + (-1)^k \delta^k}{k\lambda+1}$.

Since $X = \tilde{\alpha} + \tilde{\beta}Z$, with $\tilde{\alpha}$ and $\tilde{\beta}$ given in (4.36) and (4.37) respectively, the first four uncorrected moments of X are

$$\begin{aligned}
 \mu'_1 &= E[X] \\
 &= \tilde{\alpha} + \tilde{\beta}E[Z] \\
 &= \alpha - \beta\phi_1, \quad \lambda > -1,
 \end{aligned} \tag{4.38}$$

$$\begin{aligned}
 \mu'_2 &= E[X^2] \\
 &= \tilde{\alpha}^2 + 2\tilde{\alpha}\tilde{\beta}E[Z] + \tilde{\beta}^2E[Z^2] \\
 &= \left(\alpha + \frac{\beta}{\lambda}(2\delta - 1)\right)^2 + 2\left(\alpha + \frac{\beta}{\lambda}(2\delta - 1)\right)\frac{\beta}{\lambda}\phi_1 \\
 &\quad + \frac{\beta^2}{\lambda^2}\left(\phi_2 - 2\omega B(\lambda + 1, \lambda + 1)\right), \quad \lambda > -\frac{1}{2},
 \end{aligned}$$

$$\begin{aligned}
 \mu'_3 &= E[X^3] \\
 &= \tilde{\alpha}^3 + 3\tilde{\alpha}^2\tilde{\beta}E[Z] + 3\tilde{\alpha}\tilde{\beta}^2E[Z^2] + \tilde{\beta}^3E[Z^3] \\
 &= \left(\alpha + \frac{\beta}{\lambda}(2\delta - 1)\right)^3 + 3\left(\alpha + \frac{\beta}{\lambda}(2\delta - 1)\right)^2\frac{\beta}{\lambda}\phi_1 \\
 &\quad + 3\left(\alpha + \frac{\beta}{\lambda}(2\delta - 1)\right)\frac{\beta^2}{\lambda^2}\left(\phi_2 - 2\omega B(\lambda + 1, \lambda + 1)\right) \\
 &\quad + \frac{\beta^3}{\lambda^3}\left(\phi_3 + 3\omega(2\delta - 1)B(2\lambda + 1, \lambda + 1)\right), \quad \lambda > -\frac{1}{3},
 \end{aligned}$$

and

$$\begin{aligned}
 \mu'_4 &= E[X^4] \\
 &= \tilde{\alpha}^4 + 4\tilde{\alpha}^3\tilde{\beta}E[Z] + 6\tilde{\alpha}^2\tilde{\beta}^2E[Z^2] + 4\tilde{\alpha}\tilde{\beta}^3E[Z^3] + \tilde{\beta}^4E[Z^4] \\
 &= \left(\alpha + \frac{\beta}{\lambda}(2\delta - 1)\right)^4 + 4\left(\alpha + \frac{\beta}{\lambda}(2\delta - 1)\right)^3\frac{\beta}{\lambda}\phi_1 \\
 &\quad + 6\left(\alpha + \frac{\beta}{\lambda}(2\delta - 1)\right)^2\frac{\beta^2}{\lambda^2}\left(\phi_2 - 2\omega B(\lambda + 1, \lambda + 1)\right) \\
 &\quad + 4\left(\alpha + \frac{\beta}{\lambda}(2\delta - 1)\right)\frac{\beta^3}{\lambda^3}\left(\phi_3 + 3\omega(2\delta - 1)B(2\lambda + 1, \lambda + 1)\right) \\
 &\quad + \frac{\beta^4}{\lambda^4}\left(\phi_4 - 4\omega\left((1 - \delta)^2 + \delta^2\right)B(3\lambda + 1, \lambda + 1)\right. \\
 &\quad \left.+ 6\omega^2B(2\lambda + 1, 2\lambda + 1)\right), \quad \lambda > -\frac{1}{4}.
 \end{aligned}$$

The first four corrected moments of X are then

$$\mu_1 = E[X - E[X]] = 0,$$

$$\begin{aligned}
 \mu_2 &= E[(X - E[X])^2] \\
 &= \mu'_2 - (\mu'_1)^2 \\
 &= \frac{\beta^2}{\lambda^2} \left(\phi_2 - \phi_1^2 - 2\omega B(\lambda + 1, \lambda + 1) \right), \quad \lambda > -\frac{1}{2},
 \end{aligned} \tag{4.39}$$

$$\begin{aligned}
 \mu_3 &= E[(X - E[X])^3] \\
 &= \mu'_3 - 3\mu'_2\mu'_1 + 2(\mu'_1)^3 \\
 &= \frac{\beta^3}{\lambda^3} \left(\phi_3 + 2\phi_1^3 - 3\phi_1 \left(\phi_2 - \omega \left(2B(\lambda + 1, \lambda + 1) \right. \right. \right. \\
 &\quad \left. \left. \left. - (\lambda + 1)B(2\lambda + 1, \lambda + 1) \right) \right) \right), \quad \lambda > -\frac{1}{3},
 \end{aligned} \tag{4.40}$$

and

$$\begin{aligned}
 \mu_4 &= E[(X - E[X])^4] \\
 &= \mu'_4 - 4\mu'_3\mu'_1 + 6\mu'_2(\mu'_1)^2 - 3(\mu'_1)^4 \\
 &= \frac{\beta^4}{\lambda^4} \left(\phi_4 - 3\phi_1^4 + 6\phi_1^2 \left(\phi_2 - 2\omega B(\lambda + 1, \lambda + 1) \right) \right. \\
 &\quad \left. - 4\phi_1 \left(\phi_3 - 3\omega\phi_1(\lambda + 1)B(2\lambda + 1, \lambda + 1) \right) \right. \\
 &\quad \left. - \omega \left(4\phi_2(2\lambda + 1)B(3\lambda + 1, \lambda + 1) \right. \right. \\
 &\quad \left. \left. - 6\omega B(2\lambda + 1, 2\lambda + 1) \right) \right), \quad \lambda > -\frac{1}{4},
 \end{aligned} \tag{4.41}$$

where each moment's final expression is found after substantial simplification. The mean and variance of X for $\lambda \neq 0$ in (4.7) and (4.8) are given by $\mu = \mu'_1$ in (4.38) and $\sigma^2 = \mu_2$ in (4.39) respectively, and the skewness and kurtosis moment ratios of X for $\lambda \neq 0$ in (4.9) and (4.10) are obtained by substituting the expressions for μ_3 in (4.40) and μ_4 in (4.41) into (2.18).

■

4.13.2 MINIMUM VALUE OF L -KURTOSIS RATIO FOR GLD_{GPD}

Theorem 4.13.2

Suppose X is a real-valued random variable whose distribution is the GPD Type of the GLD, denoted $X \sim GLD_{GPD}(\alpha, \beta, \delta, \lambda)$, where α is a location parameter, $\beta > 0$ is a scale

parameter and $0 \leq \delta \leq 1$ and λ are shape parameters. The minimum value of the L -kurtosis ratio for the GLD_{GPD} is given by τ_4^{\min} in (4.17) for $\tilde{\lambda}$ in (4.18).

Proof

The derivative of the expression for the L -kurtosis ratio for the GLD_{GPD} , given in (4.16), with respect to λ is

$$\frac{d\tau_4}{d\lambda} = \frac{30}{(\lambda+4)^2} - \frac{20}{(\lambda+3)^2}. \quad (4.42)$$

Setting (4.42) equal to zero and simplifying gives

$$\lambda^2 + 2\lambda - 5 = 0.$$

Solving then for λ gives

$$\lambda = -1 \pm \sqrt{6},$$

but, since τ_4 only exists for $\lambda > -1$, it follows that the minimum value of τ_4 is obtained for $\tilde{\lambda}$ given in (4.18). This minimum value, τ_4^{\min} , is calculated by substituting (4.18) into (4.16).

■

4.1.3.3 COVARIANCE MATRIX FOR METHOD OF L -MOMENTS ESTIMATORS OF GLD_{GPD}

Lemma 4.13.1

The derivation of the covariance matrix for the method of L -moments estimators of the GLD_{GPD} requires the solving of the double integral

$$\begin{aligned} \Xi_t(j, k) &= \int_0^1 v^{t\lambda+k} (1-v)^{(1-t)\lambda} \int_0^v u^{j-1} (1-u)^{\lambda-1} du dv \\ &= \int_0^1 v^{t\lambda+k} (1-v)^{(1-t)\lambda} B_v(j, \lambda) dv, \end{aligned} \quad (4.43)$$

for $j = 2, 3, 4, 5$, $k = -1, 0, 1, 2, 3$ and $t = 0, 1$, where $B_z(a, b)$ is the incomplete beta function (see Section 2.14.1). Following Gradshteyn & Ryzhik (2007, 8.391),

$$B_v(j, \lambda) = \frac{v^j}{j} F(j, 1-\lambda; j+1; v), \quad (4.44)$$

where $F(a, b; c; z)$ is the hypergeometric series (see Section 2.14.1 in Chapter 2). Since

$$F(j, 1-\lambda; j+1; v) = (1-v)^\lambda F(1, \lambda+j; j+1; v)$$

from Gradshteyn & Ryzhik (2007, 9.131.1), the incomplete beta function in (4.44) can be rewritten as

$$B_v(j, \lambda) = \frac{v^j(1-v)^\lambda}{j} F(1, \lambda + j; j + 1; v). \quad (4.45)$$

Because the first argument of the hypergeometric series in (4.45) is one, this function can be written as the sum of the ratios of gamma functions. That is,

$$F(1, \lambda + j; j + 1; v) = \sum_{i=0}^{\infty} \frac{\Gamma(\lambda+i+j)\Gamma(j+1)v^i}{\Gamma(\lambda+j)\Gamma(i+j+1)},$$

where $\Gamma(a)$ is the gamma function (see Section 2.14.1 in Chapter 2). Thus,

$$B_v(j, \lambda) = (1-v)^\lambda \frac{\Gamma(j)}{\Gamma(\lambda+j)} \sum_{i=0}^{\infty} \frac{\Gamma(\lambda+i+j)v^{i+j}}{\Gamma(i+j+1)}. \quad (4.46)$$

Setting $m = i + j$ in (4.46) and simplifying gives

$$\begin{aligned} B_v(j, \lambda) &= (1-v)^\lambda \frac{\Gamma(j)}{\Gamma(\lambda+j)} \sum_{m=j}^{\infty} \frac{\Gamma(\lambda+m)v^m}{\Gamma(m+1)} \\ &= (1-v)^\lambda \frac{\Gamma(j)}{\Gamma(\lambda+j)} \left(\sum_{m=0}^{\infty} \frac{\Gamma(\lambda+m)v^m}{\Gamma(m+1)} - \sum_{m=0}^{j-1} \frac{\Gamma(\lambda+m)v^m}{\Gamma(m+1)} \right) \\ &= (1-v)^\lambda \frac{\Gamma(j)}{\Gamma(\lambda+j)} \left(\sum_{m=0}^{\infty} \frac{\Gamma(\lambda+m)v^m}{\Gamma(m+1)} - \left(\Gamma(\lambda) + \sum_{m=1}^{j-1} \frac{\Gamma(\lambda+m)v^m}{\Gamma(m+1)} \right) \right) \\ &= (1-v)^\lambda \frac{\Gamma(\lambda)\Gamma(j)}{\Gamma(\lambda+j)} \left(F(1, \lambda; 1; v) - \left(1 + \frac{1}{\Gamma(\lambda)} \sum_{m=1}^{j-1} \frac{\Gamma(\lambda+m)v^m}{\Gamma(m+1)} \right) \right) \\ &= (1-v)^\lambda \frac{\Gamma(\lambda)\Gamma(j)}{\Gamma(\lambda+j)} \left((1-v)^{-\lambda} - \left(1 + \sum_{m=1}^{j-1} \frac{\Gamma(\lambda+m)v^m}{m\Gamma(\lambda)\Gamma(m)} \right) \right), \end{aligned} \quad (4.47)$$

where Gradshteyn & Ryzhik (2007, 9.121.1) is used in the final result in (4.47). Therefore,

$$B_v(j, \lambda) = B(j, \lambda) \left(1 - (1-v)^\lambda \left(1 + \sum_{m=1}^{j-1} \frac{v^m}{mB(m, \lambda)} \right) \right), \quad (4.48)$$

where $B(a, b) = \frac{\Gamma(a)\Gamma(b)}{\Gamma(a+b)}$ is the beta function (see again Section 2.14.1). In effect, the incomplete beta function can be expressed in terms of beta functions.

Substituting (4.48) into (4.43) gives

$$\begin{aligned}
 \Xi_t(j, k) &= \int_0^1 v^{t\lambda+k} (1-v)^{(1-t)\lambda} \left(B(j, \lambda) \left(1 - (1-v)^\lambda \left(1 + \sum_{m=1}^{j-1} \frac{v^m}{mB(m, \lambda)} \right) \right) \right) dv \\
 &= B(j, \lambda) \left(\int_0^1 v^{t\lambda+k} (1-v)^{(1-t)\lambda} dv - \int_0^1 v^{t\lambda+k} (1-v)^{(2-t)\lambda} dv \right. \\
 &\quad \left. - \sum_{m=1}^{j-1} \left(\frac{1}{mB(m, \lambda)} \int_0^1 v^{t\lambda+k+m} (1-v)^{(2-t)\lambda} dv \right) \right) \quad (4.49) \\
 &= B(j, \lambda) \left(B(t\lambda+k+1, (1-t)\lambda+1) - B(t\lambda+k+1, (2-t)\lambda+1) \right. \\
 &\quad \left. - \sum_{m=1}^{j-1} \frac{B(t\lambda+k+m+1, (2-t)\lambda+1)}{mB(m, \lambda)} \right).
 \end{aligned}$$

Specifically

$$\Xi_0(j, k) = B(j, \lambda) \left(B(k+1, \lambda+1) - B(k+1, 2\lambda+1) - \sum_{m=1}^{j-1} \frac{B(k+m+1, 2\lambda+1)}{mB(m, \lambda)} \right)$$

and, because $B(a+1, 1) = B(1, a+1) = \frac{1}{a+1}$,

$$\begin{aligned}
 \Xi_1(j, k) &= B(j, \lambda) \left(\frac{1}{\lambda+k+1} - B(\lambda+k+1, \lambda+1) - \sum_{m=1}^{j-1} \frac{B(\lambda+k+m+1, \lambda+1)}{mB(m, \lambda)} \right) \\
 &= \frac{B(j, \lambda) - B(\lambda+j+k+1, \lambda)}{\lambda+k+1}.
 \end{aligned}$$

■

Theorem 4.13.3

Let X be a real-valued random variable which has the GPD Type of the GLD, denoted $X \sim \text{GLD}_{\text{GPD}}(\alpha, \beta, \delta, \lambda)$, with method of L -moments estimators for the location parameter, α , scale parameter, $\beta > 0$, and shape parameters, $0 \leq \delta \leq 1$ and λ , given by $\hat{\alpha}_A$ in (4.24), $\hat{\beta}_A$ in (4.25), $\hat{\delta}_A$ in (4.26) and $\hat{\lambda}_A$ in (4.27) for Region A of the GLD_{GPD} , and by $\hat{\alpha}_B$ in (4.28), $\hat{\beta}_B$ in (4.29), $\hat{\delta}_B$ in (4.30) and $\hat{\lambda}_B$ in (4.31) for Region B of the GLD_{GPD} . Given that the variance of the GLD_{GPD} is finite, in effect, given $\lambda > -\frac{1}{2}$, the asymptotic standard errors of $\hat{\alpha}_h$, $\hat{\beta}_h$, $\hat{\delta}_h$ and $\hat{\lambda}_h$ for $h = A, B$ are given by (4.32), (4.33), (4.34) and (4.35).

Proof

The asymptotic variances of $\hat{\alpha}_h$, $\hat{\beta}_h$, $\hat{\delta}_h$ and $\hat{\lambda}_h$ for $h = A, B$ are obtained with

$$n \operatorname{var} \begin{bmatrix} \hat{\alpha}_h \\ \hat{\beta}_h \\ \hat{\delta}_h \\ \hat{\lambda}_h \end{bmatrix} \approx \begin{bmatrix} \Theta_{1,1} & \Theta_{1,2} & \Theta_{1,3} & \Theta_{1,4} \\ \Theta_{2,1} & \Theta_{2,2} & \Theta_{2,3} & \Theta_{2,4} \\ \Theta_{3,1} & \Theta_{3,2} & \Theta_{3,3} & \Theta_{3,4} \\ \Theta_{4,1} & \Theta_{4,2} & \Theta_{4,3} & \Theta_{4,4} \end{bmatrix},$$

that is, by determining the elements of the covariance matrix $\Theta = G\Lambda G^T$. The elements of the symmetric matrix

$$\Lambda = \begin{bmatrix} \Lambda_{1,1} & \Lambda_{1,2} & \Lambda_{1,3} & \Lambda_{1,4} \\ \Lambda_{2,1} & \Lambda_{2,2} & \Lambda_{2,3} & \Lambda_{2,4} \\ \Lambda_{3,1} & \Lambda_{3,2} & \Lambda_{3,3} & \Lambda_{3,4} \\ \Lambda_{4,1} & \Lambda_{4,2} & \Lambda_{4,3} & \Lambda_{4,4} \end{bmatrix}$$

are derived with (2.62), using the quantile density function of the GLD_{GPD} in (4.5) and the shifted Legendre polynomials $P_0^*(x)$, $P_1^*(x)$, $P_2^*(x)$ and $P_3^*(x)$ given in (2.89) to (2.92). For example,

$$\begin{aligned}
 \Lambda_{2,2} &= \int_0^1 \int_0^v \left(P_1^*(u)P_1^*(v) + P_1^*(u)P_1^*(v) \right) u(1-v)q(u)q(v)dudv \\
 &= 2 \int_0^1 \int_0^v (2u-1)(2v-1)u(1-v) \\
 &\quad \times \beta\left((1-\delta)u^{\lambda-1} + \delta(1-u)^{\lambda-1} \right) \beta\left((1-\delta)v^{\lambda-1} + \delta(1-v)^{\lambda-1} \right) dudv \\
 &= 2\beta^2 \int_0^1 \left((1-\delta) \left(-2v^{\lambda+1} + 3v^\lambda - v^{\lambda-1} \right) + \delta(2v-1)(1-v)^\lambda \right) \\
 &\quad \times \int_0^v \left((1-\delta) \left(2u^{\lambda+1} - u^\lambda \right) + \delta \left(2u^2 - u \right) (1-u)^{\lambda-1} du \right) dv \\
 &= 2\beta^2 \int_0^1 \left((1-\delta) \left(-2v^{\lambda+1} + 3v^\lambda - v^{\lambda-1} \right) + \delta(2v-1)(1-v)^\lambda \right) \\
 &\quad \times \left((1-\delta) \left(\frac{2}{\lambda+2} v^{\lambda+2} - \frac{1}{\lambda+1} v^{\lambda+1} \right) + \delta \left(2B_v(3, \lambda) - B_v(2, \lambda) \right) \right) dv \\
 &= 2\beta^2 \left((1-\delta)^2 \frac{2\lambda(\lambda-1)(\lambda+1) - (\lambda-2)(\lambda+2)}{2(\lambda+1)^2(\lambda+2)^2(2\lambda+1)(2\lambda+3)} \right. \\
 &\quad + \omega \left(\frac{4}{\lambda+2} B(\lambda+4, \lambda+1) - \frac{2(2\lambda+3)}{(\lambda+1)(\lambda+2)} B(\lambda+3, \lambda+1) + \frac{1}{\lambda+1} B(\lambda+2, \lambda+1) \right) \\
 &\quad + \omega \left(-4\Xi_1(3,1) + 6\Xi_1(3,0) - 2\Xi_1(3,-1) \right. \\
 &\quad \quad \left. + 2\Xi_1(2,1) - 3\Xi_1(2,0) + \Xi_1(2,-1) \right) \\
 &\quad \left. + \delta^2 \left(4\Xi_0(3,1) - 2\Xi_0(3,0) - 2\Xi_0(2,1) + \Xi_0(2,0) \right) \right) \\
 &= \frac{\beta^2}{(\lambda+1)(2\lambda+1)(2\lambda+3)} \left(\frac{2\lambda(\lambda-1)(\lambda+1) - (\lambda-2)(\lambda+2)}{(\lambda+1)(\lambda+2)^2} - \frac{\omega}{\lambda} \left(\frac{2(2\lambda^3 - 5\lambda^2 + 2\lambda + 3)}{\lambda(\lambda+1)} + (\lambda-3)B(\lambda, \lambda) \right) \right),
 \end{aligned}$$

where $\omega = \delta(1-\delta)$ and with the final result found after substantial simplification. Similarly it can be shown that

$$\Lambda_{1,1} = \frac{\beta^2}{(2\lambda+1)} \left(\frac{1}{(\lambda+1)^2} - \frac{\omega}{\lambda} \left(\frac{2(\lambda^2 - 2\lambda - 1)}{\lambda(\lambda+1)^2} + B(\lambda, \lambda) \right) \right),$$

$$\Lambda_{3,3} = \frac{\beta^2}{(\lambda+1)(\lambda+2)(2\lambda+1)(2\lambda+3)(2\lambda+5)} \times \left(\frac{4\lambda^6 - 16\lambda^5 - 13\lambda^4 + 184\lambda^3 + 123\lambda^2 - 66\lambda + 72}{(\lambda+1)(\lambda+2)(\lambda+3)^2} - \frac{\omega}{\lambda} \left(\frac{2(4\lambda^8 - 24\lambda^7 + 63\lambda^6 + 154\lambda^5 - 772\lambda^4 + 74\lambda^3 + 1725\lambda^2 - 396\lambda - 540)}{\lambda(\lambda+1)(\lambda+2)(\lambda+3)^2} + (\lambda-2)(\lambda^3 + 6\lambda^2 + 14\lambda - 15)B(\lambda, \lambda) \right) \right),$$

$$\Lambda_{4,4} = \frac{\beta^2}{(\lambda+1)(\lambda+2)(\lambda+3)(2\lambda+1)(2\lambda+3)(2\lambda+5)(2\lambda+7)} \times \left(\frac{8\lambda^9 - 84\lambda^8 + 78\lambda^7 + 2601\lambda^6 + 1536\lambda^5 - 4887\lambda^4 + 10684\lambda^3 + 12360\lambda^2 - 5016\lambda + 4320}{(\lambda+1)(\lambda+2)(\lambda+3)(\lambda+4)^2} - \frac{\omega}{\lambda} \left(\frac{2(8\lambda^9 - 132\lambda^8 + 654\lambda^7 + 801\lambda^6 - 5784\lambda^5 + 4218\lambda^4 + 11422\lambda^3 - 12915\lambda^2 - 1188\lambda + 3780)}{\lambda(\lambda+1)(\lambda+2)(\lambda+3)} + 3(3\lambda^5 + 9\lambda^4 - 46\lambda^3 - 231\lambda^2 + 451\lambda - 210)B(\lambda, \lambda) \right) \right),$$

$$\Lambda_{1,2} = \Lambda_{2,1} = -\beta^2 \left(\frac{(2\delta-1)(\lambda-1)}{(\lambda+1)^2(\lambda+2)(2\lambda+1)} \right),$$

$$\Lambda_{1,3} = \Lambda_{3,1} = \frac{\beta^2}{(\lambda+1)(2\lambda+1)(2\lambda+3)} \times \left(\frac{2\lambda^3 - 5\lambda^2 - 12\lambda + 3}{(\lambda+1)(\lambda+2)(\lambda+3)} - \frac{\omega}{\lambda} \left(\frac{2(2\lambda^5 - 9\lambda^4 + 8\lambda^3 + 32\lambda^2 - 27\lambda - 18)}{\lambda(\lambda+1)(\lambda+2)(\lambda+3)} - (\lambda^2 + \lambda - 3)B(\lambda, \lambda) \right) \right),$$

$$\Lambda_{1,4} = \Lambda_{4,1} = -\beta^2 \left(\frac{(2\delta-1)(\lambda-1)(2\lambda^3 - 13\lambda^2 - 30\lambda + 6)}{(\lambda+1)^2(\lambda+2)(\lambda+3)(\lambda+4)(2\lambda+1)(2\lambda+3)} \right),$$

$$\Lambda_{2,3} = \Lambda_{3,2} = -\beta^2 \left(\frac{(2\delta-1)(\lambda-1)(2\lambda^3 - 5\lambda^2 - 6\lambda + 6)}{(\lambda+1)^2(\lambda+2)^2(\lambda+3)(2\lambda+1)(2\lambda+3)} \right),$$

$$\Lambda_{2,4} = \Lambda_{4,2} = \frac{\beta^2}{(\lambda+1)(\lambda+2)(2\lambda+1)(2\lambda+3)(2\lambda+5)} \times \left(\frac{4\lambda^6 - 24\lambda^5 - 65\lambda^4 + 96\lambda^3 - 17\lambda^2 - 234\lambda + 60}{(\lambda+1)(\lambda+2)(\lambda+3)(\lambda+4)} - \frac{\omega}{\lambda} \left(\frac{2(4\lambda^7 - 32\lambda^6 - 37\lambda^5 + 222\lambda^4 - 24\lambda^3 - 481\lambda^2 + 132\lambda + 180)}{\lambda(\lambda+1)(\lambda+2)(\lambda+3)^2} - 3(\lambda^3 - \lambda^2 - 11\lambda + 10)B(\lambda, \lambda) \right) \right)$$

and

$$\Lambda_{3,4} = \Lambda_{4,3} = -\beta^2 \left(\frac{(2\delta-1)(\lambda-1)(4\lambda^6 - 32\lambda^5 + 11\lambda^4 + 368\lambda^3 + 135\lambda^2 - 186\lambda + 180)}{(\lambda+1)^2(\lambda+2)^2(\lambda+3)^3(\lambda+4)(2\lambda+1)(2\lambda+3)(2\lambda+5)} \right).$$

The matrix G is given by

$$G = \begin{bmatrix} \frac{\partial \alpha}{\partial L_1} & \frac{\partial \alpha}{\partial L_2} & \frac{\partial \alpha}{\partial L_3} & \frac{\partial \alpha}{\partial L_4} \\ \frac{\partial \beta}{\partial L_1} & \frac{\partial \beta}{\partial L_2} & \frac{\partial \beta}{\partial L_3} & \frac{\partial \beta}{\partial L_4} \\ \frac{\partial \delta}{\partial L_1} & \frac{\partial \delta}{\partial L_2} & \frac{\partial \delta}{\partial L_3} & \frac{\partial \delta}{\partial L_4} \\ \frac{\partial \lambda}{\partial L_1} & \frac{\partial \lambda}{\partial L_2} & \frac{\partial \lambda}{\partial L_3} & \frac{\partial \lambda}{\partial L_4} \end{bmatrix},$$

where

$$\begin{aligned} \frac{\partial \alpha}{\partial L_1} &= 1, \\ \frac{\partial \alpha}{\partial L_2} &= \begin{cases} \frac{L_3 \left(103L_4^3 + L_2L_4^2(541-53T) - 3L_2^2L_4(47-2T) - 3L_2^3(1+T) \right)}{10L_2L_4(L_2-L_4)^2T} & , h = A, \\ -\frac{L_3 \left(103L_4^3 + L_2L_4^2(541+53T) - 3L_2^2L_4(47+2T) - 3L_2^3(1-T) \right)}{10L_2L_4(L_2-L_4)^2T} & , h = B, \end{cases} \\ &= \frac{(2\delta-1)(\lambda-2)(\lambda+4) \left(\lambda^2 - 2\lambda - 11 \right)}{10 \left(\lambda^2 + 2\lambda - 5 \right)}, \\ \frac{\partial \alpha}{\partial L_3} &= \begin{cases} \frac{2L_4^2 + L_2L_4(51-2T) - 3L_2^2(1+T)}{10L_4(L_2-L_4)} & , h = A, \\ \frac{2L_4^2 + L_2L_4(51+2T) - 3L_2^2(1-T)}{10L_4(L_2-L_4)} & , h = B, \end{cases} \\ &= \frac{(\lambda+2)(\lambda+3)}{\lambda-1}, \\ \frac{\partial \alpha}{\partial L_4} &= \begin{cases} -\frac{L_3 \left(103L_4^3 + L_2L_4^2(541-53T) - 3L_2^2L_4(47-2T) - 3L_2^3(1+T) \right)}{10L_4^2(L_2-L_4)^2T} & , h = A, \\ \frac{L_3 \left(103L_4^3 + L_2L_4^2(541+53T) - 3L_2^2L_4(47+2T) - 3L_2^3(1-T) \right)}{10L_4^2(L_2-L_4)^2T} & , h = B, \end{cases} \\ &= -\frac{(2\delta-1)(\lambda+3)(\lambda+4)^2 \left(\lambda^2 - 2\lambda - 11 \right)}{10(\lambda-1) \left(\lambda^2 + 2\lambda - 5 \right)}, \\ \frac{\partial \beta}{\partial L_1} &= 0, \end{aligned}$$

CHAPTER 4. A GLD TYPE WITH SKEWNESS-INVARIANT MEASURES OF KURTOSIS

$$\frac{\partial \beta}{\partial L_2} = \begin{cases} \frac{2L_4^4 + 2L_2L_4^3(151-2T) + 3L_2^2L_4^2(279-26T) - 3L_2^3L_4(46+9T) - L_2^4(3-9T)}{L_2(L_2-L_4)^3T}, & h = A, \\ -\frac{2L_4^4 + 2L_2L_4^3(151+2T) + 3L_2^2L_4^2(279+26T) - 3L_2^3L_4(46-9T) - L_2^4(3+9T)}{L_2(L_2-L_4)^3T}, & h = B, \end{cases}$$

$$= -\frac{2\lambda^5 + \lambda^4 - 52\lambda^3 - 95\lambda^2 + 92\lambda + 172}{10(\lambda^2 + 2\lambda - 5)},$$

$$\frac{\partial \beta}{\partial L_3} = 0,$$

$$\frac{\partial \beta}{\partial L_4} = \begin{cases} -\frac{5L_2(21L_4^2 + L_2L_4(148-9T) + L_2^2(31-11T))}{(L_2-L_4)^3T}, & h = A, \\ \frac{5L_2(21L_4^2 + L_2L_4(148+9T) + L_2^2(31+11T))}{(L_2-L_4)^3T}, & h = B, \end{cases}$$

$$= \frac{(\lambda+3)^2(\lambda+4)^2(2\lambda+3)}{10(\lambda^2 + 2\lambda - 5)},$$

$$\frac{\partial \delta}{\partial L_1} = 0,$$

$$\frac{\partial \delta}{\partial L_2} = \begin{cases} -\frac{L_3(L_4 + L_2(49-T))}{20L_2^3T}, & h = A, \\ \frac{L_3(L_4 + L_2(49+T))}{20L_2^3T}, & h = B, \end{cases}$$

$$= -\frac{3(2\delta-1)(\lambda-1)(\lambda+1)(\lambda+2)(\lambda+3)}{10\beta(\lambda^2 + 2\lambda - 5)},$$

$$\frac{\partial \delta}{\partial L_3} = \begin{cases} -\frac{L_4 - L_2(1+T)}{20L_2L_4}, & h = A, \\ -\frac{L_4 - L_2(1-T)}{20L_2L_4}, & h = B, \end{cases}$$

$$= -\frac{(\lambda+1)(\lambda+2)(\lambda+3)}{2\beta(\lambda-1)},$$

$$\frac{\partial \delta}{\partial L_4} = \begin{cases} -\frac{L_3(49L_4 + L_2(1+T))}{20L_2L_4^2T}, & h = A, \\ \frac{L_3(49L_4 + L_2(1-T))}{20L_2L_4^2T}, & h = B, \end{cases}$$

$$= -\frac{(2\delta-1)(\lambda+1)(\lambda+2)(\lambda+3)(\lambda+4)^2}{5\beta(\lambda-1)(\lambda^2 + 2\lambda - 5)},$$

$$\frac{\partial \lambda}{\partial L_1} = 0,$$

$$\frac{\partial \lambda}{\partial L_2} = \begin{cases} \frac{5L_4(5L_4 + L_2(5-T))}{L_2(L_2 - L_4)^2 T}, & h = A, \\ -\frac{5L_4(5L_4 + L_2(5+T))}{L_2(L_2 - L_4)^2 T}, & h = B, \end{cases}$$

$$= -\frac{(\lambda-1)(\lambda-2)(\lambda+1)(\lambda+2)(\lambda+3)(\lambda+4)}{10\beta(\lambda^2 + 2\lambda - 5)},$$

$$\frac{\partial \lambda}{\partial L_3} = 0$$

and

$$\frac{\partial \lambda}{\partial L_4} = \begin{cases} -\frac{5(5L_4 + L_2(5-T))}{(L_2 - L_4)^2 T}, & h = A, \\ \frac{5(5L_4 + L_2(5+T))}{(L_2 - L_4)^2 T}, & h = B, \end{cases}$$

$$= \frac{(\lambda+1)(\lambda+2)(\lambda+3)^2(\lambda+4)^2}{10\beta(\lambda^2 + 2\lambda - 5)},$$

with $T = \sqrt{t_4^2 + 98t_4 + 1}$ and where the final result of each non-constant partial derivative is obtained using (4.14), (4.15) and (4.16) and simplifying. We note that the partial derivatives, and therefore the matrix G , are the same for Regions A and B , even though the expressions for the method of L -moments estimators in the two regions differ – compare (4.24) to (4.27) for Region A with (4.28) to (4.31) for Region B . As a result, the asymptotic variances of the estimators are the same for both regions.

Finally expressions for the elements of the covariance matrix Θ can be determined by solving $\Theta = G\Lambda G^T$. Unfortunately these expressions are extremely complex and are hence not presented here in full. See (4.32), (4.33), (4.34) and (4.35) for the expressions of the asymptotic standard errors of the method of L -moments estimators in both regions.

It is important to verify the parameter values of the GLD_{GPD} for which the covariance matrix Θ is valid. Firstly, the variance of the GLD_{GPD} must be finite, thus $\lambda > -\frac{1}{2}$. Note though that convergence of the integrals in (4.49) in Lemma 4.13.1 requires that $\iota\lambda + k + 1 > 0$ for $\iota = 0, 1$ and $k \geq -1$, in effect, that $\lambda > 0$. However, the expressions obtained for the elements of Λ are analytic functions for all $\lambda > -\frac{1}{2}$. Thus, by analytic continuation, the expressions for the elements of Λ are valid solutions of (2.62) for $\lambda > -\frac{1}{2}$.

See Gradshteyn & Ryzhik (2007, 9.154) for details regarding analytic continuation by means of the hypergeometric series, and Hosking *et al.* (1985) who utilized analytic continuation with respect to the derivation of Λ and Θ for the generalized extreme value distribution.

Recall that the GLD_{GPD} simplifies to the SLD for $\lambda = 0$. The covariance matrix Θ for this limiting case was derived in Section 2.13.2 in Chapter 2.

In the matrix G , the partial derivatives of α and δ with respect to L_3 and L_4 only exist for $\lambda \neq 1$. Consequently all the elements of Θ , apart from $\Theta_{2,2}$, $\Theta_{2,4} = \Theta_{4,2}$ and $\Theta_{4,4}$, only exist for $\lambda \neq 1$. In particular, the standard errors of the method of L -moments estimators of α and δ in (4.34) and (4.36) require that $\lambda \neq 1$. But, when $\lambda = 1$, the uniform distribution is obtained from the GLD_{GPD} . Hosking (1986) can be consulted regarding results for the uniform distribution.

Finally, the partial derivatives of α , β , δ and λ with respect to L_2 and L_4 in the matrix G only exist if $\lambda^2 + 2\lambda - 5 \neq 0$. As shown in Section 4.13.2, $\lambda^2 + 2\lambda - 5 = 0$ for $\lambda = \tilde{\lambda}$ in (4.18). So, for the GLD_{GPD} with $\lambda = \tilde{\lambda}$, expressions for the elements of the covariance matrix Θ do not exist.

■

5. CONCLUSION

This thesis presented techniques, functions and measures to develop and fit distributions in the quantile statistical universe. While the bulk of the thesis is centered on a new type of the generalized lambda distribution (GLD), the application of the method used to derive it, extends much broader than the GLD.

5.1 CONSTRUCTION OF QUANTILE-BASED FAMILIES OF DISTRIBUTIONS

Chapter 2 of the thesis showed that new distributions can be created through the transformation of quantile functions. Specifically a methodology was proposed for the construction of quantile-based families of distributions. The benefit of this methodology, proved in Proposition 2.8.1, is that it generates distributions with skewness-invariant measures of kurtosis. Therefore the skewness and kurtosis can be identified and analyzed separately. Furthermore, parameter estimation is straightforward in that closed-form expressions are available for the parameter estimators.

5.2 CONSTRUCTION OF THE GPD TYPE OF THE GLD

The quantile function of any asymmetric distribution on bounded or half-infinite support can be employed as the basic building block in the application of the methodology of Proposition 2.8.1. In Chapter 4, the quantile function of the generalized Pareto distribution (GPD) was used as the basic building block. The resulting quantile-based distribution is a new type of the GLD, labeled the GPD Type.

Akin to the Ramberg-Schmeiser (RS) and Freimer-Mudholkar-Kollia-Lin (FMKL) Types of the GLD, described in detail in Chapter 3, the GPD Type of the GLD is a four-parameter generalization of Tukey's lambda distribution, possessing, apart from location and scale parameters, two shape parameters. The main difference between the GPD Type and the RS and FMKL Types is in terms of the way in which each type's skewness and kurtosis are described by their shape parameters. Whereas the two shape parameters of the other types jointly explain the skewness and kurtosis, irrespective of the shape measures considered, the

kurtosis of the GPD Type, when measured by its L -kurtosis ratio or its quantile-based kurtosis measures (including its kurtosis functionals), is fully described by just one of the two shape parameters. That is, the L -kurtosis ratio as well as the quantile-based kurtosis measures of the GPD Type are skewness-invariant.

Chapter 4 showed that it is convenient to characterize the GPD Type through its L -moments. Furthermore, as a result of the L -kurtosis ratio's skewness-invariance, the method of L -moments estimators for the parameters of the GPD Type have closed-form expressions. The asymptotic standard errors of these estimators also have closed-form expressions. Neither the RS nor the FMKL Type of the GLD possesses closed-form expressions for the estimators of any of their estimation methods.

5.3 THEORETICAL DEVELOPMENT AND PRACTICAL UTILIZATION

The simple relationship between the parameters and the L -moments of the GPD Type and the ease with which its parameters can be estimated using method of L -moments estimation, ensure that this new type of the GLD is a valuable addition to Tukey's lambda family of distributions with respect to theoretical development in quantile modeling as well as practical utilization.

For instance, quantile-based reliability analysis has become a popular alternative to the classical approach of using distribution functions in reliability theory. See for example the recent book by Nair *et al.* (2013a) as well as the articles by Sunoj & Sankaran (2012), Sunoj *et al.* (2013) and Nair *et al.* (2013b, 2013c). The GPD Type of the GLD is one of the quantile-based distributions included and considered in Nair *et al.* (2013a, 2013b, 2013c).

Note that the GPD Type is named the van Staden-Loots distribution by these authors, citing van Staden & Loots (2009a), and that they denote its parameters by λ_1 , λ_2 , λ_3 and λ_4 instead of α , β , δ and λ . However, given that, compared to the shape parameters of the RS and FMKL Types, the shape parameters of the GPD Type relate in a completely different way to the GLD's shape, it is preferable to denote its parameters as done in this thesis.

Turning to practical utilization, Chapter 4 showed how, using method of L -moments estimation, the GPD Type of the GLD can be fitted to data sets and be used to approximate probability distributions. Another important application of the GLD is the generation of random variables in Monte Carlo simulation studies (Section 3.14). Recall from Section 3.14.3 that the GLD's ability to approximate probability distributions provides one way of selecting the members of the GLD to be used in the simulation study. Therefore, in

evaluating the ability of LULU smoothers for signals to remove different noise types, Fabris-Rotelli *et al.* (2010) used the GPD Type of the GLD to simulate noise from eight selected distributions.

5.4 FUTURE RESEARCH

The focus of this thesis was on Tukey's lambda family of distributions and the development of the GPD Type of the GLD. Obviously the methodology presented in Proposition 2.8.1 allows for the construction of other generalized families of quantile-based distributions. The only restrictions are that the support of the asymmetric distribution, whose quantile function is used as the building block, must be bounded or half-infinite, and that the quantile function of this chosen asymmetric distribution should have a simple closed-form expression. It is furthermore beneficial for parameter estimation if the expressions for this asymmetric distribution's L -moments are also of a simple form.

Given that the method of L -moments estimators for the GPD Type have closed-form expressions, method of L -moments estimation is the preferred estimation method. Recall though that, as with the RS and FMKL Types, the L -moments of the GPD Type do not exist for all parameter values. The development of other estimation methods for the GPD Type, which do not place restrictions on the parameter values, would be worth consideration. This includes the use of shape functionals and the starship method.

Since the GPD was used as the building block for the construction of the GPD Type of the GLD, it would be of interest to investigate the application of this type of the GLD in extreme event analysis. This analysis would include the modeling of exceedances above a threshold and hence the modeling of high quantiles.

Turning to model validation, in this thesis goodness-of-fit tests based on the empirical distribution function were used. Because expressions for the cumulative distribution functions of quantile-based distributions are not available in closed form, one has to compute the empirical distribution function numerically. This computational problem can be circumvented by utilizing tests based on the empirical quantile function, briefly presented in Chapter 5 of Thas (2010). Alternatively, smooth tests for goodness-of-fit, discussed in detail by Rayner *et al.* (2009), can be used.

As commented in Chapter 3, parameter estimation for the RS and FMKL Types of the GLD is computationally demanding, requiring the use of numerical optimization techniques. Therefore, to fit either the RS or FMKL Types to data, one must have the programming skills

to program the necessary software code oneself, or alternatively have access to statistical software packages containing the code needed, such as the **gld** (King, 2013) and **GLDEX** (Su, 2007a, 2012) packages in R. In contrast, because of the existence of closed-form expressions for the estimators and their asymptotic standard errors, the estimation algorithm for estimating the parameters of the GPD Type is extremely simple to apply and can be done with any standard software package, including spreadsheets. Nonetheless, the inclusion of the GPD Type into the **gld** package in R is an important priority.

REFERENCES

- Achary, K.K., & Geetha, K.K. (2007). On solving multi-item inventory model using GLD approximation, *International Journal of Information and Management Sciences*, 18(2), 147–156.
- Ahsanullah, M., & Hamedani G.G. (2010). *Exponential Distribution: Theory and Methods*, Nova Science Publishers, Inc., New York.
- Arnold, B.C. (1983). *Pareto distributions*, International Co-operative Publishing House, Fairland, Maryland.
- Asquith, W.H. (2007). *L*-moments and *TL*-moments of the generalized lambda distribution, *Computational Statistics & Data Analysis*, 51(9), 4484–4496.
- Au-Yeung, S.W.M., Dingle, N.J., & Knottenbelt, W.J. (2004). Efficient approximation of response time densities and quantiles in stochastic models, *ACM SIGSOFT Software Engineering Notes*, 29(1), 151–155.
- Azzalini, A. (1985). A class of distributions which includes the normal ones, *Scandinavian Journal of Statistics*, 12(2), 171–178.
- Azzalini, A. (1986). Further results on a class of distributions which includes the normal ones, *Rivista Statistica*, 46(2), 199–208.
- Bain, L.J., & Engelhardt, M. (1992). *Introduction to Probability and Mathematical Statistics* (2nd ed.), Duxbury Press, Belmont, California.
- Baklizi, A. (2003). A conditional distribution free runs test for symmetry, *Nonparametric Statistics*, 15(6), 713–718.
- Baklizi, A. (2007). Testing symmetry using a trimmed longest run statistic, *Australian & New Zealand Journal of Statistics*, 49(4), 339–347.
- Balakrishnan, N. (ed.) (1992). *Handbook of the Logistic Distribution*, Marcel Dekker, Inc., New York.
- Balakrishnan, N., & Basu, A.P. (eds.) (1995). *The Exponential Distribution: Theory, Methods and Applications*, Gordon & Breach Science Publishers, Newark, New Jersey.
- Balakrishnan, N., & Nevzorov, V.B. (2003), *A Primer on Statistical Distributions*, John Wiley & Sons, Inc., Hoboken, New Jersey.

- Balanda, K.P., & MacGillivray, H.L. (1990). Kurtosis and spread, *The Canadian Journal of Statistics*, 18(1), 17–30.
- Balasoorya, U., & Low, C.-K. (2008). Modeling insurance claims with extreme observations: Transformed kernel density and generalized lambda distribution, *North American Actuarial Journal*, 12(2), 129–142.
- Bautista, F., & Gómez, E. (2007). Una exploración de robustez de tres pruebas: Dos de permutación y la de Mann-Whitney, *Revista Colombiana de Estadística*, 30(2), 177–185.
- Belaire-Franch, J., & Contreras, D. (2002). A Pearson's test for symmetry with an application to the Spanish business cycle, *Spanish Economic Review*, 4(3), 221–238.
- Bergevin, R.J. (1993). An analysis of the generalized lambda distribution, *Master's Thesis, Air Force Institute of Technology, Wright-Patterson Air Force Base, Ohio*.
- Blom, G. (1958). *Statistical Estimates and Transformed Beta-Variables*, Wiley, New York.
- Bowley, A.L. (1902). *Elements of Statistics* (2nd ed.), P. S. King, London.
- Broffitt, J.D., Randles, R.H., & Hogg, R.V. (1976). Distribution-free partial discriminant analysis, *Journal of the American Statistical Association*, 71(356), 934–939.
- Burr, I.W. (1942). Cumulative frequency functions, *The Annals of Mathematical Statistics*, 13(2), 215–232.
- Burr, I.W. (1968). On a general system of distributions, III: The sample range, *Journal of the American Statistical Association*, 63(322), 636–643.
- Burr, I.W., & Cislak, P.J. (1968). On a general system of distributions, I: Its curve-shape characteristics, II: The sample median, *Journal of the American Statistical Association*, 63(322), 627–635.
- Castillo, E., & Hadi, A.S. (1997). Fitting the generalized Pareto distribution to data, *Journal of the American Statistical Association*, 92(440), 1609–1620.
- Castillo, E., Hadi, A.S., Balakrishnan, N., & Sarabia, J.M. (2005). *Extreme Value and Related Models with Applications in Engineering and Science*, John Wiley & Sons, Inc., Hoboken, New Jersey.
- Cauchy, A.L. (1853). Sur les résultats moyens d'observations de même nature, et sur les résultats les plus probables, *Comptes Rendus Hebdomadaires des Seances de l'Académie des Sciences de Paris*, 37, 198–206.
- Chan, L.K. (1967). On a characterization of distributions by expected values of extreme order statistics, *The American Mathematical Monthly*, 74(8), 950–951.
- Cheng, W.-H., & Balakrishnan, N. (2004). A modified sign test for symmetry, *Communications in Statistics: Simulation and Computation*, 33(3), 703–709.

- Chernoff, H., Gastwirth, J.L., & Johns Jr., M.V. (1967). Asymptotic distribution of linear combinations of functions of order statistics with applications to estimation, *The Annals of Mathematical Statistics*, 38(1), 52–72.
- Chou, C.-Y., Chen, C.-H., & Li, M.-H.C. (2001). Application of computer simulation to the design of a traffic signal timer, *Computers & Industrial Engineering*, 39(1–2), 81–94.
- Coles, S. (2001). *An Introduction to Statistical Modeling of Extreme Values*, Springer-Verlag, London.
- Cooley, C.A. (1991). The generalized lambda distribution: Applications and parameter estimation, *Honors Project, Denison University, Granville, Ohio*.
- Cooray, K., & Ananda, M.A. (2010). Analyzing survival data with highly negatively skewed distribution: The Gompertz-sinh family, *Journal of Applied Statistics*, 37(1), 1–11.
- Corrado, C.J. (2001). Option pricing based on the generalized lambda distribution, *The Journal of Futures Markets*, 21(3), 213–236.
- Crow, E.L., & Shimizu, K. (eds.) (1988). *Lognormal Distributions: Theory and Applications*, Marcel Dekker, Inc., New York.
- David, F.N., & Johnson, N.L. (1956). Some tests of significance with ordered variables, *Journal of the Royal Statistical Society, Series B (Methodological)*, 18(1), 1–20.
- de l'Hôpital, G.F.A. (1696). *Analyse Des Infiniment Petits, Pour L'intelligence Des Lignes Courbes*.
- Downton, F. (1966). Linear estimates with polynomial coefficients, *Biometrika*, 53(1–2), 129–141.
- Dudewicz, E.J., & Karian, Z.A. (1996). The extended generalized lambda distribution (EGLD) system for fitting distributions to data with moments, II: Tables, *American Journal of Mathematical and Management Sciences*, 16(3–4), 271–332.
- Dudewicz, E.J., & Karian, Z.A. (1999). Fitting the generalized lambda distribution (GLD) system by a method of percentiles, II: Tables, *American Journal of Mathematical and Management Sciences*, 19(1–2), 1–73.
- Fabris-Rotelli, I.N., van Oldenmark, K., & van Staden, P.J. (2010). Evaluation of noise removal in signals by LULU operators, In *Proceedings of the 52nd Annual Conference of the South African Statistical Association for 2010 (SASA 2010)*, North-West University, Potchefstroom, South Africa, 44–51.
- Ferguson, N.M., Ghani, A.C., Donnelly, C.A., Hagenaars, T.J., & Anderson, R.M. (2002). Estimating the human health risk from possible BSE infection of the British sheep flock, *Nature*, 415(6870), 420–424.

- Fournier, B., Rupin, N., Bigerelle, M., Najjar, D., & Iost, A. (2006). Application of the generalized lambda distributions in a statistical process control methodology, *Journal of Process Control*, 16(10), 1087–1098.
- Fréchet, M. (1927). Sur la loi de probabilité de l'écart maximum, *Annales de la Société Polonaise de Mathématique, Cracovie*, 6, 93–116.
- Freimer, M., Mudholkar, G.S., Kollia, G., & Lin, C.T. (1988). A study of the generalized Tukey lambda family, *Communications in Statistics: Theory and Methods*, 17(10), 3547–3567.
- Galton, F. (1881). Report of the Anthropometric Committee, *Report of the 51st Meeting of the British Association for the Advancement of Science*, 245–260.
- Gauss, C.F. (1809). *Theoria Motus Corporum Coelestium in Sectionibus Conicis Solem Ambientium*, Perthes & Besser, Hamburg.
- Gauss, C.F. (1816). Bestimmung der Genauigkeit der Beobachtungen, *Zeitschrift Astronomi*, 1, 185–197.
- Gautama, H., & van Gemund, A.J.C. (2006). Low-cost static performance prediction of parallel stochastic task compositions, *IEEE Transactions on Parallel and Distributed Systems*, 17(1), 78–91.
- Ghani, A.C., Ferguson, N.M., Donnelly, C.A., & Anderson, R.M. (2003). Factors determining the pattern of the variant Creutzfeldt–Jakob disease (vCJD) epidemic in the UK, *Proceedings of the Royal Society of London, Series B (Biological Sciences)*, 270(1516), 689–698.
- Gilchrist, W.G. (2000). *Statistical Modelling with Quantile Functions*, Chapman & Hall / CRC Press, Boca Raton, Florida.
- Gini, C. (1913–1914). Sulla misura della concentrazione e della variabilità dei caratteri, *Atti del Reale Istituto Veneto di Scienze, Lettere ed Arti*, 73(2), 1203–1248.
- Gompertz, B. (1825). On the nature of the function expressive of the law of human mortality, and on a new mode of determining the value of life contingencies, *Philosophical Transactions of the Royal Society of London*, 115, 513–583.
- Gradshteyn, I. S., & Ryzhik, I. M. (2007). *Table of Integrals, Series and Products* (7th ed.), eds. A. Jeffrey & D. Zwillinger, Academic Press, Burlington, Massachusetts.
- Greenwood, J.A., Landwehr, J.M., Matalas, N.C., & Wallis, J.R. (1979). Probability weighted moments: Definition and relation to parameters of several distributions expressible in inverse form, *Water Resources Research*, 15(5), 1049–1054.

- Groeneveld, R.A. (1986). Measurement of skewness and kurtosis for the generalized Tukey lambda distributions, *Communications in Statistics: Theory and Methods*, 15(2), 329–343.
- Gumbel, E.J. (1954). *Statistical Theory of Extreme Values and Some Practical Applications*, National Bureau of Standards, Applied Mathematics Series, Vol. 33, United States Government Printing Office, Washington DC.
- Gumbel, E.J. (1958). *Statistics of Extremes*, Columbia University Press, New York.
- Gupta, R.D., & Kundu, D. (1999). Generalized exponential distributions, *Australian & New Zealand Journal of Statistics*, 41(2), 173–188.
- Gupta, R.D., & Kundu, D. (2001). Generalized exponential distributions: Different methods of estimation, *Journal of Statistical Computation and Simulation*, 69(4), 315–337.
- Gupta, R.D., & Kundu, D. (2007). Generalized exponential distribution: Existing results and some recent developments, *Journal of Statistical Planning and Inference*, 137(11), 3537–3547.
- Hall, D.J. (1991). Repeat variability in instantaneously released heavy gas clouds – some wind tunnel experiments, *Technical report LR 804 (PA)*, Warren Spring Laboratory, Stevenage, Hertfordshire.
- Hankin, R.K.S., & Lee, A. (2006). A new family of non-negative distributions, *Australian & New Zealand Journal of Statistics*, 48(1), 67–78.
- Haritha, H.N., Nair, N.U., & Nair, K.R.M. (2008). Modelling income using the generalised lambda distribution, *Journal of Income Distribution*, 17(2), 37–51.
- Hastings Jr., C., Mosteller, F., Tukey, J.W., & Winsor, C.P. (1947). Low moments for small samples: A comparative study of order statistics, *The Annals of Mathematical Statistics*, 18(3), 413–426.
- Hoaglin, D.C. (1983). Letter values: A set of selected order statistics, in *Understanding Robust and Explanatory Data Analysis*, eds. D.C. Hoaglin, F. Mosteller, & J.W. Tukey, John Wiley & Sons, Inc., New York, 33–57.
- Hoeffding, W. (1948). A class of statistics with asymptotically normal distribution, *The Annals of Mathematical Statistics*, 19(3), 293–325.
- Hogg, R.V., Fisher, D.M., & Randles, R.H. (1975). A two-sample adaptive distribution-free test, *Journal of the American Statistical Association*, 70(351), 656–661.
- Hogg, R.V., & Randles, R.H. (1975). Adaptive distribution-free regression methods and their applications, *Technometrics*, 17(4), 399–407.

- Hosking, J.R.M. (1986). The theory of probability weighted moments, *Research Report RC12210, IBM Research, Yorktown Heights*.
- Hosking, J.R.M. (1990). *L*-moments: Analysis and estimation of distributions using linear combinations of order statistics, *Journal of the Royal Statistical Society, Series B (Methodological)*, 52(1), 105–124.
- Hosking, J.R.M. (1992). Moments or *L* moments? An example comparing two measures of distributional shape, *The American Statistician*, 46(3), 186–189.
- Hosking, J.R.M. (1994). The four-parameter kappa distribution, *IBM Journal of Research and Development*, 38(3), 251–258.
- Hosking, J.R.M., & Wallis, J.R. (1987). Parameter and quantile estimation for the generalized Pareto distribution, *Technometrics*, 27(3), 339–349.
- Hosking, J.R.M., & Wallis, J.R. (1997). *Regional Frequency Analysis: An Approach Based on L-Moments*, Cambridge University Press, Cambridge, United Kingdom.
- Hosking, J.R.M., Wallis, J.R., & Wood, E.F. (1985). Estimation of the generalized extreme-value distribution by the method of probability-weighted moments, *Technometrics*, 27(3), 251–261.
- Hosmer, D.W., & Lemeshow, S. (2000). *Applied Logistic Regression* (2nd ed.), John Wiley & Sons, Inc., New York.
- Ivkovic, M., & Rozenberg, P. (2004). A method for describing and modelling of within-ring wood density distribution in clones of three coniferous species, *Annals of Forest Science*, 61(8), 759–769.
- Jenkinson, A.F. (1955). The frequency distribution of the annual maximum (or minimum) of meteorological elements, *Quarterly Journal of the Royal Meteorological Society*, 81(348), 158–171.
- Johnson, N.L. (1949). Systems of frequency curves generated by methods of translation, *Biometrika*, 36(1–2), 149–176.
- Johnson, N.L. (1954). Systems of frequency curves derived from the first law of Laplace, *Trabajos de Estadística*, 5(3), 283–291.
- Johnson, N.L. (1980). Letters to the editor, *Technometrics*, 22(1), 135.
- Johnson, N.L., Kotz, S., & Balakrishnan, N. (1994). *Continuous Univariate Distributions* (Vol. 1, 2nd ed.), John Wiley & Sons, Inc., New York.
- Johnson, N.L., Kotz, S., & Balakrishnan, N. (1995). *Continuous Univariate Distributions* (Vol. 2, 2nd ed.), John Wiley & Sons, Inc., New York.

- Jones, M.C. (2002a). Student's simplest distribution, *Journal of the Royal Statistical Society, Series D (The Statistician)*, 51(1), 41–49.
- Jones, M.C. (2002b). The complementary beta distribution, *Journal of Statistical Planning and Inference*, 104(2), 329–337.
- Jones, M.C. (2004). On some expressions for variance, covariance, skewness and L -moments, *Journal of Statistical Planning and Inference*, 126(1), 97–106.
- Jones, M.C. (2009). Kumaraswamy's distribution: A beta-type distribution with some tractability advantages, *Statistical Methodology*, 6(1), 70–81.
- Jones, M.C., Rosco, J.F., & Pewsey, A. (2011). Skewness-invariant measures of kurtosis, *The American Statistician*, 65(2), 89–95.
- Karian, Z.A., & Dudewicz, E.J. (1999). Fitting the generalized lambda distribution to data: A method based on percentiles, *Communications in Statistics: Simulation and Computation*, 28(3), 793–819.
- Karian, Z.A., & Dudewicz, E.J. (2000). *Fitting Statistical Distributions: The Generalized Lambda Distribution and Generalized Bootstrap Methods*, Chapman & Hall / CRC Press, Boca Raton, Florida.
- Karian, Z.A., & Dudewicz, E.J. (2003). Comparison of GLD fitting methods: Superiority of percentile fits to moments in L^2 norm, *Journal of the Iranian Statistical Society*, 2(2), 171–187.
- Karian, Z.A., & Dudewicz, E.J. (2007). Computational issues in fitting statistical distributions to data, *American Journal of Mathematical and Management Sciences*, 27(3–4), 319–349.
- Karian, Z.A., & Dudewicz, E.J. (2010). *Handbook of Fitting Statistical Distributions with R*, Chapman & Hall / CRC Press, Boca Raton, Florida.
- Karian, Z.A., Dudewicz, E.J., & McDonald, P. (1996). The extended generalized lambda distribution system for fitting distributions to data: History, completion of theory, tables, applications, the “final word” on moment fits, *Communications in Statistics: Simulation and Computation*, 25(3), 611–642.
- Karvanen, J., Eriksson, J., & Koivunen, V. (2002). Adaptive score functions for maximum likelihood ICA, *Journal of VLSI Signal Processing*, 32(1–2), 83–92.
- Karvanen, J., & Nuutinen, A. (2008). Characterizing the generalized lambda distribution by L -moments, *Computational Statistics & Data Analysis*, 52(4), 1971–1983.

- Kelley, T.L. (1921). A new measure of dispersion, *Quarterly Publications of the American Statistical Association*, 17(134), 743–749.
- King, R.A.R. (1999). New distributional fitting methods applied to the generalised λ distribution, *PhD Thesis, Queensland University of Technology, Queensland, Australia*.
- King R.A.R. (2013). **gld**: Estimation and use of the generalised (Tukey) lambda distribution. R package version 2.0.1, URL <http://CRAN.R-project.org/>.
- King, R.A.R., & MacGillivray, H.L. (1999). A starship estimation method for the generalized λ distributions, *Australian & New Zealand Journal of Statistics*, 41(3), 353–374.
- King, R.A.R., & MacGillivray, H.L. (2007). Fitting the generalized lambda distribution with location and scale-free shape functionals, *American Journal of Mathematical and Management Sciences*, 27(3–4), 441–460.
- Kleiber, C., & Kotz, S. (2003). *Statistical Size Distributions in Economics and Actuarial Sciences*, John Wiley & Sons, Inc., Hoboken, New Jersey.
- Klein, I., & Fischer, M. (2008). A note on the kurtosis ordering of the generalized secant hyperbolic distribution, *Communications in Statistics: Theory and Methods*, 37(1), 1–7.
- Konheim, A.G. (1971). A note on order statistics, *The American Mathematical Monthly*, 78(5), 524.
- Kotz, S., Kozabowski, T.J., & Podgórski, K. (2001). *The Laplace Distribution and Generalizations: A Revisit with Applications to Communications, Economics, Engineering, and Finance*, Birkhäuser, Boston.
- Kotz, S., & Seier, E. (2008). Visualizing peak and tails to introduce kurtosis, *The American Statistician*, 62(4), 348–354.
- Kumaraswamy, P. (1980). A generalized probability density function for double-bounded random processes, *Journal of Hydrology*, 46(1–2), 79–88.
- Lakhany, A., & Mausser, H. (2000). Estimating the parameters of the generalized lambda distribution, *ALGO Research Quarterly*, 3(3), 47–58.
- Lampasi, D.A. (2008). An alternative approach to measurement based on quantile functions, *Measurement*, 41(9), 994–1013.
- Lan, Y., & Leemis, L.M. (2008). The logistic-exponential survival distribution, *Naval Research Logistics*, 55(3), 252–264.
- Lange, A., Haase, J., & Mau, H.T. (2011). Fitting standard cell performance to generalized lambda distributions, In *Proceedings of the 21st ACM Great Lakes Symposium on VLSI (GLSVLSI'11), Lausanne, Switzerland*, 259–264.

- Laplace, P.S. (1774). Mémoire sur la probabilité des causes par les évènements, *Mémoires de Mathématique et de Physique, Presentes à l'Académie Royale des Sciences, par divers Savans et lûs dans ses Assemblées*, 6, 621–656.
- Lau, A.H.-L., Lau, H.-S., & Robinson, L.W. (2002). Convenient expressions for computing the exact annual cost of continuous-review (Q, R) system with backordering, *Journal of the Operational Research Society*, 53(6), 655–663.
- Lomax, K.S. (1954). Business failures: Another example of the analysis of failure data, *Journal of the American Statistical Association*, 49(268), 847–852.
- Loots, M.T. (2008). The theory and application of L -moments, *Honors Essay, Department of Statistics, University of Pretoria, Pretoria, South Africa*.
- MacGillivray, H.L. (1982). Skewness properties of asymmetric forms of Tukey lambda distributions, *Communications in Statistics: Theory and Methods*, 11(20), 2239–2248.
- MacGillivray, H.L. (1986). Skewness and asymmetry: Measures and orderings, *The Annals of Statistics*, 14(3), 994–1011.
- MacGillivray, H.L. (1992). Shape properties of the g -and- h and Johnson families, *Communications in Statistics: Theory and Methods*, 21(5), 1233–1250.
- MacGillivray, H.L., & Balanda, K.P. (1988). The relationships between skewness and kurtosis, *Australian Journal of Statistics*, 30(3), 319–337.
- Mallows, C.L. (1973). Bounds on distribution functions in terms of expectations of order-statistics, *The Annals of Probability*, 1(2), 297–303.
- McWilliams, T.P. (1990). A distribution-free test for symmetry based on a runs statistic, *Journal of the American Statistical Association*, 85(412), 1130–1133.
- Mielke Jr., P.W. (1973). Another family of distributions for describing and analyzing precipitation data, *Journal of Applied Meteorology*, 12(2), 275–280.
- Moberg, T.F., Ramberg, J.S., & Randles, R.H. (1978). An adaptive M -estimator and its application to a selection problem, *Technometrics*, 20(3), 255–263.
- Moberg, T.F., Ramberg, J.S., & Randles, R.H. (1980). An adaptive multiple regression procedure based on M -estimators, *Technometrics*, 22(2), 213–224.
- Mohan, R.B. (1994). The use of L -moments to fit the generalized lambda distribution to sample data, *Master's Thesis, Air Force Institute of Technology, Wright-Patterson Air Force Base, Ohio*.
- Moore, D.S. (1968). An elementary proof of asymptotic normality of linear functions of order statistics, *The Annals of Mathematical Statistics*, 39(1), 263–265.

- Moors, J.J.A. (1988). A quantile alternative for kurtosis, *Journal of the Royal Statistical Society, Series D (The Statistician)*, 37(1), 25–32.
- Moors, J.J.A., Wagemakers, R.Th.A., Coenen, V.M.J., Heuts, R.M.J., & Janssens, M.J.B.T. (1996). Characterizing systems of distributions by quantile measures, *Statistica Neerlandica*, 50(3), 417–430.
- Mudholkar, G.S., Kollia, G.D., Lin, C.T., & Patel, K.R. (1991). A graphical procedure for comparing goodness-of-fit tests, *Journal of the Royal Statistical Society, Series B (Methodological)*, 53(1), 221–232.
- Mykytka, E.F., & Ramberg, J.S. (1979). Fitting a distribution to data using an alternative to moments, In *Proceedings of the 11th IEEE Winter Simulation Conference (WSC'79), San Diego, California*, Vol. 2, 361–374.
- Nadarajah, S. (2009). The skew logistic distribution, *AStA Advances in Statistical Analysis*, 93(2), 187–203.
- Nair, N.U., Sankaran, P.G., & Balakrishnan, N. (2013a). *Quantile-Based Reliability Analysis*, Springer, New York.
- Nair, N.U., Sankaran, P.G., & Sunoj, S.M. (2013b). Quantile based reliability aspects of partial moments, *Journal of the Korean Statistical Society*, 42(3), 329–342.
- Nair, N.U., Sankaran, P.G., & Sunoj, S.M. (2013c). Quantile based stop-loss transform and its applications, *Statistical Methods & Applications*, 22(2), 167–182.
- Nair, N.U., & Vineshkumar, B. (2010). *L*-moments of residual life, *Journal of Statistical Planning and Inference*, 140(9), 2618–2631.
- O’Gorman, T.W. (2006). An adaptive test of a subset of regression coefficients using permutations of residuals, *Journal of Statistical Computation and Simulation*, 76(12), 1095–1105.
- O’Gorman, T.W. (2008). An adaptive method of variable selection in regression, *Communications in Statistics: Simulation and Computation*, 37(6), 1129–1142.
- Öztürk, A., & Dale, R.F. (1985). Least squares estimation of the parameters of the generalized lambda distribution, *Technometrics*, 27(1), 81–84.
- Pacáková V., & Sipková, L. (2007). Generalized lambda distributions of household’s incomes, *E a M: Ekonomie a Management*, 10(1), 98–107.
- Pal, S. (2005). Evaluation of non-normal process capability indices using generalized lambda distribution, *Quality Engineering*, 17(1), 77–85.
- Pareto, V. (1896). *Cours d’Économie Politique. Professe a l’Université de Lausanne*, Vol. 1.
- Pareto, V. (1897). *Cours d’Économie Politique. Professe a l’Université de Lausanne*, Vol. 2.

- Parzen, E. (1979). Nonparametric statistical data modeling, *Journal of the American Statistical Association*, 74(365), 105–121.
- Patel, J.K., & Read, C.B. (1997). *Handbook of the Normal Distribution* (2nd ed.), Marcel Dekker, Inc., New York.
- Pearson, K. (1894). Contributions to the mathematical theory of evolution, *Philosophical Transactions of the Royal Society of London, Series A*, 185, 71–110.
- Pearson, K. (1895). Contributions to the mathematical theory of evolution. II. Skew variation in homogeneous material, *Philosophical Transactions of the Royal Society of London, Series A*, 186, 343–414.
- Pearson, K. (1905) ‘Das Fehlergesetz und Seine Verallgemeinerungen Durch Fechner und Pearson.’ A rejoinder, *Biometrika*, 4(1–2), 169–212.
- Pickands III, J. (1975). Statistical inference using extreme order statistics, *The Annals of Statistics*, 3(1), 119–131.
- Poojari, C.A., Lucas, C., & Mitra, G. (2008). Robust solutions and risk measures for a supply chain planning problem under uncertainty, *Journal of the Operational Research Society*, 59(1), 2–12.
- Ramberg, J.S., & Schmeiser, B.W. (1972). An approximate method for generating symmetric random variables, *Communications of the Association for Computing Machinery*, 15(11), 987–990.
- Ramberg, J.S., & Schmeiser, B.W. (1974). An approximate method for generating asymmetric random variables, *Communications of the Association for Computing Machinery*, 17(2), 78–82.
- Ramberg, J.S., Tadikamalla, P.R., Dudewicz, E.J., & Mykytka, E.F. (1979). A probability distribution and its uses in fitting data, *Technometrics*, 21(2), 201–214.
- Ramberg, J.S., Tadikamalla, P.R., Dudewicz, E.J., & Mykytka, E.F. (1980). Letters to the editor, *Technometrics*, 22(1), 135.
- Ramos-Fernández, A., Paradela, A., Navajas, R., & Albar, J.P. (2008). Generalized method for probability-based peptide and protein identification from tandem mass spectrometry data and sequence database searching, *Molecular & Cellular Proteomics*, 7(9), 1748–1754.
- Randles, R.H., Broffitt, J.D., Ramberg, J.S., & Hogg, R.V. (1978). Discriminant analysis based on ranks, *Journal of the American Statistical Association*, 73(362), 379–384.

- Randles, R.H., Fligner, M.A., Policello II, G.E., & Wolfe, D.A. (1980). An asymptotically distribution-free test for symmetry versus asymmetry, *Journal of the American Statistical Association*, 75(369) 168–172.
- Rayleigh, J.W.S. (1880). On the resultant of a large number of vibrations of the same pitch and of arbitrary phase, *Philosophical Magazine*, 5th Series, 10, 73–78.
- Rayleigh, J.W.S. (1919). On the problem of random vibrations, and of random flights in one, two, or three dimensions, *Philosophical Magazine*, 6th Series, 37, 321–347.
- Rayner, J.C.W., Thas, O., & Best, D.J. (2009). *Smooth Tests of Goodness of Fit* (2nd ed.), John Wiley & Sons (Asia) Pte. Ltd., Singapore.
- Rinne, H. (2009). *The Weibull Distribution: A Handbook*, Chapman & Hall / CRC Press, Boca Raton, Florida.
- Robinson, L.W., & Chen, R.R. (2003). Scheduling doctors' appointments: Optimal and empirically-based heuristic policies, *IIE Transactions*, 35(3), 295–307.
- Rodriguez, R.N. (1977). A guide to the Burr type XII distributions, *Biometrika*, 64(1), 129–134.
- Schmeiser, B.W., & Deutsch, S.J. (1977). A versatile four parameter family of probability distributions suitable for simulation, *AIIE Transactions*, 9(2), 176–182.
- Seier, E., & Bonett, D. (2003). Two families of kurtosis measures, *Metrika*, 58(1), 59–70.
- Sillitto, G.P. (1951). Interrelations between certain linear systematic statistics of samples from any continuous population, *Biometrika*, 38(3–4), 377–382.
- Sillitto, G.P. (1964). Some relations between expectations of order statistics in samples of different sizes, *Biometrika*, 51(1–2), 259–262.
- Sillitto, G.P. (1969). Derivation of approximants to the inverse distribution function of a continuous univariate population from the order statistics of a sample, *Biometrika*, 56(3), 641–650.
- Smith, R.L. (1986). Extreme value theory based on the r largest annual events, *Journal of Hydrology*, 86(1–2), 27–43.
- Sprent, P., & Smeeton, N.C. (2007). *Applied Nonparametric Statistical Methods* (4th ed.), Chapman & Hall / CRC Press, Boca Raton, Florida.
- Stigler, S.M. (1974). Linear functions of order statistics with smooth weight functions, *The Annals of Statistics*, 2(4), 676–693.
- Stigler, S.M. (1979). Note: Correction to linear functions of order statistics with smooth weight functions, *The Annals of Statistics*, 7(2), 466.

- Stuart, A., & Ord, J.K. (1994). *Kendall's Advanced Theory of Statistics* (Vol. 1, 6th ed.), Halsted Press, New York.
- Student. (1908). The probable error of a mean, *Biometrika*, 6(1), 1–25.
- Student. (1927). Errors of routine analysis, *Biometrika*, 19(1–2), 151–164.
- Su, S. (2005). A discretized approach to flexibly fit generalized lambda distributions to data, *Journal of Modern Applied Statistical Methods*, 4(2), 408–424.
- Su, S. (2007a). Fitting single and mixture of generalized lambda distributions to data via discretized and maximum likelihood methods: GLDEX in R, *Journal of Statistical Software*, 21(9), 1–17.
- Su, S. (2007b). Numerical maximum log likelihood estimation for generalized lambda distributions, *Computational Statistics & Data Analysis*, 51(8), 3983–3998.
- Su, S. (2012). **GLDEX**: Fitting single and mixture of generalized lambda distributions (RS and FMKL) using discretized and maximum likelihood methods. R package version 1.0.4.4, URL <http://CRAN.R-project.org/>.
- Sunoj, S.M., & Sankaran, P.G. (2012). Quantile based entropy function, *Statistics and Probability Letters*, 82(6), 1049–1053.
- Sunoj, S.M., Sankaran, P.G., & Nanda, A.K. (2013). Quantile based entropy function in past lifetime, *Statistics and Probability Letters*, 83(1), 366–372.
- Tadikamalla, P.R. (1980). A look at the Burr and related distributions, *International Statistical Review*, 48(3), 337–344.
- Tadikamalla, P.R., & Johnson, N.L. (1982). Systems of frequency curves generated by transformations of logistic variables, *Biometrika*, 69(2), 461–465.
- Thas, O. (2010). *Comparing Distributions*, Springer, New York.
- Thas, O., & Ottoy, J.-P. (2004). An extension of the Anderson-Darling k -sample test to arbitrary sample space partition sizes, *Journal of Statistical Computation and Simulation*, 74(9), 651–665.
- Thas, O., Rayner, J.C.W., & Best, D.J. (2005). Tests for symmetry based on the one-sample Wilcoxon signed rank statistic, *Communications in Statistics: Simulation and Computation*, 34(4), 957–973.
- Tukey, J.W. (1960). The practical relationship between the common transformations of percentages of counts and of amounts, *Technical Report 36, Statistical Techniques Research Group, Princeton University*.
- Tukey, J.W. (1962). The future of data analysis, *The Annals of Mathematical Statistics*, 33(1), 1–67.

- Tukey, J.W. (1965). Which part of the sample contains the information?, *Proceedings of the National Academy of Sciences*, 53(1), 127–134.
- Tukey, J.W. (1977). *Exploratory Data Analysis*, Addison-Wesley Publishing Co., Reading, Massachusetts.
- Tukey, J.W., & McLaughlin, D.H. (1963). Less vulnerable confidence and significance procedures for location based on a single sample: Trimming/Winsorization 1, *Sankhyā: The Indian Journal of Statistics, Series A*, 25(3), 331–352.
- van Staden, P.J. (2006). An individuals control chart based upon the generalized lambda distribution, *Technical Report 06/02, Department of Statistics, University of Pretoria, Pretoria, South Africa*.
- van Staden, P.J., & Loots, M.T. (2009a), Method of *L*-moment estimation for the generalized lambda distribution, In *Proceedings of the Third Annual Applied Statistics Education and Research Collaboration (ASEARC) Research Conference, University of Newcastle, Australia*.
- van Staden, P.J., & Loots, M.T. (2009b). Teaching the concept of kurtosis in introductory statistics courses using *Mathematica*: Searching for platypuses and kangaroos beneath the cloth of Table Mountain, In *Proceedings of the Seventh Southern Right Delta Conference on the Teaching and Learning of Undergraduate Mathematics and Statistics, Gordon's Bay, South Africa*, 244–256.
- van Zwet, W.R. (1964a). *Convex Transformations of Random Variables*, Mathematical Centre Tracts, No. 7, Mathematisch Centrum, Amsterdam.
- van Zwet, W.R. (1964b). Convex transformations: A new approach to skewness and kurtosis, *Statistica Neerlandica*, 18(4), 433–441.
- Vaughan, D.C. (2002). The generalized secant hyperbolic distribution and its properties, *Communications in Statistics: Theory and Methods*, 31(2), 219–238.
- Voit, E.O. (1992). The *S*-distribution: A tool for approximation and classification of univariate, unimodal probability distributions. *Biometrical Journal*, 34(7), 855–878.
- Wahed, A.S., & Ali, M.M. (2001). The skew-logistic distribution. *Journal of Statistical Research*, 35(2), 71–80.
- Weibull, W. (1939a). *A Statistical Theory of the Strength of Materials*, Ingeniörs Vetenskaps Adademiens Handlingar, No. 151, Stockholm.
- Weibull, W. (1939b). *The Phenomenon of Rupture in Solids*, Ingeniörs Vetenskaps Adademiens Handlingar, No. 153, Stockholm.

- Wilcox, R.R. (2002). Comparing the variances of two independent groups, *British Journal of Mathematical and Statistical Psychology*, 55(1), 169–175.
- Yu, K., & Zhang, J. (2005). A three-parameter asymmetric Laplace distribution and its extension, *Communications in Statistics: Theory and Methods*, 34(9–10), 1867–1879.